Year : 2019

CHARACTERIZATION OF BRACHYPODIUM DISTACHYON ROOT DEVELOPMENT

Van Der Schuren Alja

Van Der Schuren Alja, 2019, CHARACTERIZATION OF BRACHYPODIUM DISTACHYON ROOT DEVELOPMENT

Originally published at : Thesis, University of Lausanne

Posted at the University of Lausanne Open Archive http://serval.unil.ch
Document URN : urn:nbn:ch:serval-BIB_9493436ADAFB5

UNIL | Université de Lausanne
Faculté de biologie
et de médecine

Département de Biologie Moléculaire Végétale

CHARACTERIZATION OF *BRACHYPODIUM DISTACHYON* ROOT DEVELOPMENT

Thèse de doctorat ès sciences de la vie (PhD)

présentée à la

Faculté de biologie et de médecine
de l'Université de Lausanne

par

Alja VAN DER SCHUREN

Master Biotechnology de Wageningen University and Research

Jury

Prof. Paul FRANKEN, Président
Prof. Christian S. HARDTKE, Directeur de thèse
Prof. Julia SANTIAGO CUELLAR, expert
Prof. Lars ØSTERGAARD, expert

Lausanne 2019

UNIL | Université de Lausanne
Faculté de biologie
et de médecine

Département de Biologie Moléculaire Végétale

CHARACTERIZATION OF *BRACHYPODIUM DISTACHYON* ROOT DEVELOPMENT

Thèse de doctorat ès sciences de la vie (PhD)

présentée à la

Faculté de biologie et de médecine
de l'Université de Lausanne

par

Alja VAN DER SCHUREN

Master Biotechnology de Wageningen University and Research

Jury

Prof. Paul FRANKEN, Président
Prof. Christian S. HARDTKE, Directeur de thèse
Prof. Julia SANTIAGO CUELLAR, expert
Prof. Lars ØSTERGAARD, expert

Lausanne 2019

UNIL | Université de Lausanne
Faculté de biologie
et de médecine

Ecole Doctorale
Doctorat ès sciences de la vie

Imprimatur

Vu le rapport présenté par le jury d'examen, composé de

Président·e	Monsieur	Prof.	Paul	**Franken**
Directeur·rice de thèse	Monsieur	Prof.	Christian	**Hardtke**
Experts·es	Madame	Prof.	Julia	**Santiago Cuellar**
	Monsieur	Prof.	Lars	**Østergaard**

le Conseil de Faculté autorise l'impression de la thèse de

Madame Alja van der Schuren

Master Biotechnology, Wageningen University and Research, Pays-Bas

intitulée

Characterization of *Brachypodium distachyon* root development

Lausanne, le 10 mai 2019

pour le Doyen
de la Faculté de biologie et de médecine

Prof. Paul Franken

Table of Contents

Acknowledgements

I would like to thank Professor Christian S. Hardtke for the opportunity to do my PhD in his laboratory. Also the other Hardtke members for their support, the great atmosphere and the helpful discussions. Especially Amelia Amiguet Vercher for her help in working with *Brachypodium distachyon*. Also Dr. Pauline Anne and Dr. Mortiz Graeff for their excellent comments on my thesis report. Special thanks to Amandine Masson, Matthieu Leclerc and my family for mental support. Many thanks to Chulmin Kim and the Dolan laboratory for teaching me how to perform crosses in *Brachypodium* and Zhongjuan Zhang and Cecilia Aliaga for their input in *in situ* hybridizations. Furthermore I would like to thank our collaborators in the Karin Ljung laboratory and Markus Pauly laboratory and last but not least, the thesis committee for taking the time to read this report and commenting on my work.

Abstract

Crops like maize, rice and wheat are economically of high importance, however current yield will not sustain the world's demands in the long run. Plant roots are crucial for uptake and transport of minerals, hormones and water via their vasculature and are therefore of interest for yield improvement. Unfortunately, root development is not yet completely understood and the research that has been performed to date has mainly focused on the dicotyledon (dicot) model system *Arabidopsis thaliana* (*Arabidopsis*). Dicots differ substantially from most crops, the majority of which are monocotyledons (monocots). for which *Brachypodium distachyon* (*Brachypodium*) was recently proposed as a good model system. It is closely related to wheat and barley, and more distantly to rice, with a smaller genome and simplified growth conditions that make it suitable for research. My thesis has therefore focused on transferring knowledge from *Arabidopsis* root development into *Brachypodium* in order to determine to what degree research in dicots can be applied to monocot root development. The first gene that I studied was *AUX1* which is coding for an auxin importer. Mutations in *Arabidopsis AUX1* only resulted in mild root phenotypes whereas in monocots, including *Brachypodium*, the phenotypes also include shoot dwarfism and even sterility. Furthermore *Brachypodium aux1* mutant displays increased root cell elongation and reduced cell diameter. Other genes that were further investigated during this thesis are *OCTOPUS* (*OPS*)*, BREVIS RADIX* (*BRX*)*, CLAVATA3/EMBRYO SURROUNDING REGION 45, BARELY ANY MERISTEM 3* and *BRASSINOSTEROID INSENSITIVE 1*. All of them affect protophloem development in *Arabidopsis* and mutations in *OPS* and *BRX* result in small roots due to undifferentiated cells within the protophloem. In order to analyze these gene families in *Brachypodium*, we developed a CRISPR-Cas9 genome editing system to create the corresponding mutants. We discovered that most *Brachypodium* homologs were part of bigger gene families and therefore multiple members may have to be mutated in order to observe putative phenotypes. This project is still ongoing, however preliminary data suggests that indeed for *BRX* family members, single, double and triple mutants do not induce phenotypes.

Also preliminary results for double *ops* family member mutants, indicate the lack of root phenotypes. As for *AUX1*, these preliminary results differ from the phenotypes observed in *Arabidopsis* and underlines the importance of research in a monocot model plant in order to understand crop development better and hopefully improve yield on the long term.

Résumé

Le maïs, le riz et le blé jouent une grande importance économique. Toutefois, les rendements actuels ne permettront pas de répondre à la demande mondiale à long terme et doivent être améliorés. Comme les racines des plantes assurent le transport de l'eau, des minéraux et de certaines molecules de signalisation, elles sont d'un grand intérêt pour l'amélioration des rendements. À ce jour, les recherches sur le développement des racines ont principalement porté sur l'étude de la plante modèle dicotylédone (dicot) *Arabidopsis thaliana* (*Arabidopsis*). Les dicots diffèrent substantiellement des cultures monocotylédones (monocots) mentionnées précédemment, pour lesquelles *Brachypodium distachyon* (*Brachypodium*) a récemment été proposé comme bon model d'étude. Ma thèse a donc porté sur le transfert des connaissances d'*Arabidopsis* en termes de développement racinaire vers *Brachypodium*, le but étant de déterminer dans quelle mesure la recherche sur les dicots peut être appliquée au développement des racines des grandes cultures. En premier lieu, j'ai étudié la function du gène *AUXIN RESISTANT 1 (AUX1)*, qui importe l'auxine dans la cellule. Chez *Arabidopsis* le mutant *aux1* ne présente que des phénotypes discrets au niveau de la racine. En revanche, chez les monocots, y compris chez *Brachypodium*, lorsque la function d'AUX1 est affectée, les plantes sont aussi naines et stériles. De plus, le mutant *aux1* chez *Brachypodium* présente une augmentation de l'élongation cellulaires au niveau de la racine ainsi qu'un diamètre cellulaire réduit. D'autres gènes, impliqués dans le développement du protophloème chez *Arabidopsis*, ont été étudiés au cours de cette thèse: *OCTOPUS* (*OPS*), *BREVIS RADIX* (*BRX*), *CLAVATA3/EMBRYO SURROUNDING REGION 45*, *BARELY ANY MERISTEM 3* et *BRASSINOSTEROID INSENSITIVE 1*. Chez *Arabidopsis* la perte de fonction des gènes *OPS* et *BRX* provoque à l'échelle macroscopique une reduction de la croissance racinaire ainsi qu'une différentation stochastique du protophloème. A l'échelle microscopique certaine cellules au sein de la fille cellulaire phloèmienne présentent des caractéristiques de cellulues indifférenciées. Afin d'étudier ces familles multigéniques chez *Brachypodium*, j'ai adopté le système CRISPR-Cas9

pour *Brachypodium* et édité son génome en conséquence. Afin de s'affranchir d'une putative redondance fonctionelle, il sera peut-être nécessaire de muter plusieurs membres d'une même famille. Les données préliminaires de ce projet suggèrent que pour les membres de la famille de *BREVIS RADIX*, les mutants simples, doubles et triples n'induisent pas de phénotypes. Les résultats préliminaires concernant les doubles mutants au sein de la famille *OPS* ne presentment pas de phénotypes macroscopique au niveau de la racine. Quant à *AUX1*, il diffère des phénotypes observés chez *Arabidopsis* et ce qui souligne l'importance de la recherche sur une plante modèle tel que *Brachypodium* et l'intérêt majeur d'étudier les monocotylédones afin de mieux comprendre le développement des cultures et ainsi d'améliorer leurs rendements à long terme.

Traduit avec l'aide de Dr. Pauline Anne

Résumé vulgarisé - Caractérisation du développement racinaire chez *Brachypodium distachyon*

Alja van der Schuren – Hardtke Lab, DBMV UniL

À long terme, nous consommerons beaucoup plus de nourriture que nous ne pouvons en produire actuellement. Il est donc urgent d'améliorer les rendements agricoles. Chez les plantes, les racines sont responsables de l'absorption de l'eau et du transport des minéraux et des hormones, ainsi l'amélioration du système racinaire pourrait être une solution. Malheureusement, les céréales comme le blé et le riz, qui constitue la base de notre alimentation, sont difficiles à cultiver en laboratoire. C'est pourquoi la petite adventice (mauvaise herbe) *Arabidopsis thaliana* (*Arabidopsis*) est largement étudiée, mais elle est encore assez différente des cultures. Par conséquent, une nouvelle espèce modèle a récemment été suggérée: *Brachypodium distachyon* (*Brachypodium*). Au cours de ma thèse, j'ai donc déterminé dans quelle mesure les recherches déjà effectuées chez *Arabidopsis* pourraient être transposées chez *Brachypodium*. J'ai étudié AUX1, une protéine qui transporte une hormone végétale appelée auxine. Une version non fonctionnelle de ce transporteur chez *Arabidopsis* fait perdre aux racines leur sens de l'orientation. La même mutation chez les céréales et *Brachypodium* a des effets supplémentaires : les pousses sont naines et parfois les plantes sont stériles. J'ai également étudié les gènes impliqués dans le développement du système vasculaire de la racine. Lorsque les gènes *OCTOPUS (OPS)* et *BREVIS RADIX (BRX)* ne sont pas fonctionnels chez *Arabidopsis*, ce système ne s'établit pas correctement et les racines restent courtes. J'ai créé un système permettant de muter ces gènes chez *Brachypodium* afin de déterminer leur fonction. Pour le moment, je n'ai pas pu isoler de combinaison de mutants ayant entraîné des racines courtes chez *Brachypodium*. Tous ces résultats montrent à quel point il est primordial d'étudier des espèces davantage similaires aux grandes cultures si nous voulons les améliorer.

Traduit avec l'aide de Dr. Pauline Anne et Matthieu Leclerc

1. Introduction

The world has more than fifty thousand edible plants, however only major crops like rice, maize and wheat provide for almost sixty percent of the world food energy intake. World cereal production reaches more than two and a half million tons per year and wheat alone makes up thirty-one percent of it (Food Agriculture Organization of the United Nations 2018). However its current yield increase will not sustain worlds demand on the long term (Chochois, Vogel, and Watt 2012). It is predicted that crop yield must almost double by 2050 in order to sustain current the world's needs (Hsia et al. 2017). A fundamental understanding of how these plants grow and develop is therefore crucial to address challenges for cereal breeding.

1.1 An introduction to plant development

Plant development starts with the fertilization of an egg cell by a male gamete (Alberts 2002). A root-shoot axis is established when a well-controlled and oriented division takes place to produce an embryo proper and a suspensor. More rounds of divisions take place and embryonic cells close to the suspensor develop into the root, while the opposite end of the embryo produces one or two cotyledons that will form the seedling shoot. Groups of stem cells embedded in the growth regions at the end of the shoot and the root, the so-called meristems, ensure that the plant can keep growing by continuously creating new cells. The position of shoot and root apical meristems is already determined at the embryonic stage. From the meristem, cells go through three orderly phases: division, elongation and differentiation from where they will not develop any further (Alberts 2002; Ivanov and Dubrovsky 2013).

Plants derived from embryos with one cotyledon (monocotyledons or monocots), differ substantially from plants grown from embryos with two cotyledons (dicotyledons or dicots). Apart from differences in the amount of cotyledons, they also display differences in vascular tissue organization in the leaf and in root growth (McSteen 2010; Pacheco-Villalobos and Hardtke 2012). This often-invisible part of plants, the root system, is as

important as the shoot. It provides an anchor into the soil, ensures nutrient and water up-take, functions in defense against pathogens and is important in the transport and synthesis of hormones (Aiken and Smucker 1996; Osmont, Sibout, and Hardtke 2007; Lucas et al. 2013). In order to improve crops in terms of the use of water, fertilizers or necessary land area, understanding the root system and its development plays a crucial part (Chochois, Vogel, and Watt 2012; Coudert et al. 2010).

1.2 Dicotyledon versus monocotyledon root development

A good example of a dicot root system is seen in the model plant *Arabidopsis thaliana* (*Arabidopsis*). It develops one primary root with several branched (lateral) roots. The primary root consists of several single-celled layers, from outside to inside: epidermis, cortex, endodermis, pericycle and the stele (Peret et al. 2009; Anne and Hardtke 2018) (Figure 1A,C,D). The stele contains the vasculature (xylem, phloem and cambium) that ensures the transport between root and shoot.

The root system of monocots is much more complex than dicot root systems. Apart from the primary root with lateral roots, some monocots develop additional embryonic roots, also called seminal roots. Later on, all monocots develop shoot-borne roots (crown roots) that eventually take over the function of the embryonic root system (Draper et al. 2001; Hochholdinger et al. 2004; Pacheco-Villalobos and Hardtke 2012) (Figure 1A, B). An example of a monocot root system can be seen in Figure 1B (Pacheco-Villalobos and Hardtke 2012, unpublished data). In this case the primary root consists of a single layer of epidermal cells, three to five cortical layers, one endodermal cell layer and the vasculature (Coudert et al. 2010; Pacheco-Villalobos and Hardtke 2012) (Figure 1E,F). The central vascular cylinder consists of one or sometimes two large central metaxylem cell files with eight peripheral xylem tracheary elements in a circle around it (Coudert et al. 2010; Pacheco-Villalobos and Hardtke 2012, unpublished data). The latter are alternating with phloem that is composed of a protophloem sieve tube associated with two companion cells and the metaphloem (Pacheco-Villalobos et al. 2013) (Figure 1F).

This stele arrangement with closed polyarch vasculature of alternating xylem and phloem around the central pith is typical for monocotyledons; in dicots xylem is arranged in a diarch to hexarch shape with phloem in between the extensions of xylem (Scarpella and Meijer 2004; Coudert et al. 2010; Pacheco-Villalobos and Hardtke 2012; Chochois, Vogel, and Watt 2012). Furthermore, cambium is not present in monocotyledon roots while in dicots it is important in a process called secondary growth (Scarpella and Meijer 2004; Chochois, Vogel, and Watt 2012). Roots undergo radial growth from the cambium, whose initials originate from procambium within vascular bundles or from parenchyma cells between vascular bundles (Scarpella and Meijer 2004). Several other differences, like the development of root hairs, origin of lateral roots, origin of epidermis and the existence of rhizosheats are not the focus of this thesis and will therefore not be discussed in detail here (Hochholdinger et al. 2004; Dinneny and Yanofsky 2004; Scarpella and Meijer 2004; Coudert et al. 2010; McSteen 2010; Pacheco-Villalobos and Hardtke 2012; Lucas et al. 2013; Kirschner et al. 2017).

1.3 *Brachypodium distachyon* as a monocotyledon model species

It has become clear that monocotyledons that include important crops like maize (*Zea mays L.)*, rice (*Oryza sativa*), wheat (*Triticum Aestivium*) and barley (*Hordeum vulgare L.*) differ from dicotyledons in many aspects. Due to these differences, it is difficult to transfer knowledge directly from the dicot *Arabidopsis* to these economically important crops (Draper et al. 2001; Hsia et al. 2017). Direct research on crops has been challenging owing to the requirement of special growth conditions; crops are in general larger and are therefore difficult to maintain in a growth chamber, especially rice needs well-adjusted growth conditions (Vogel, Garvin, et al. 2006; Scholthof et al. 2018). Furthermore, crops have longer generation times and a greater genome size that includes genome duplications and in the case of wheat even hexaploidy (Keller and Feuillet 2000; Pacheco-Villalobos and Hardtke 2012; Tao et al. 2016).

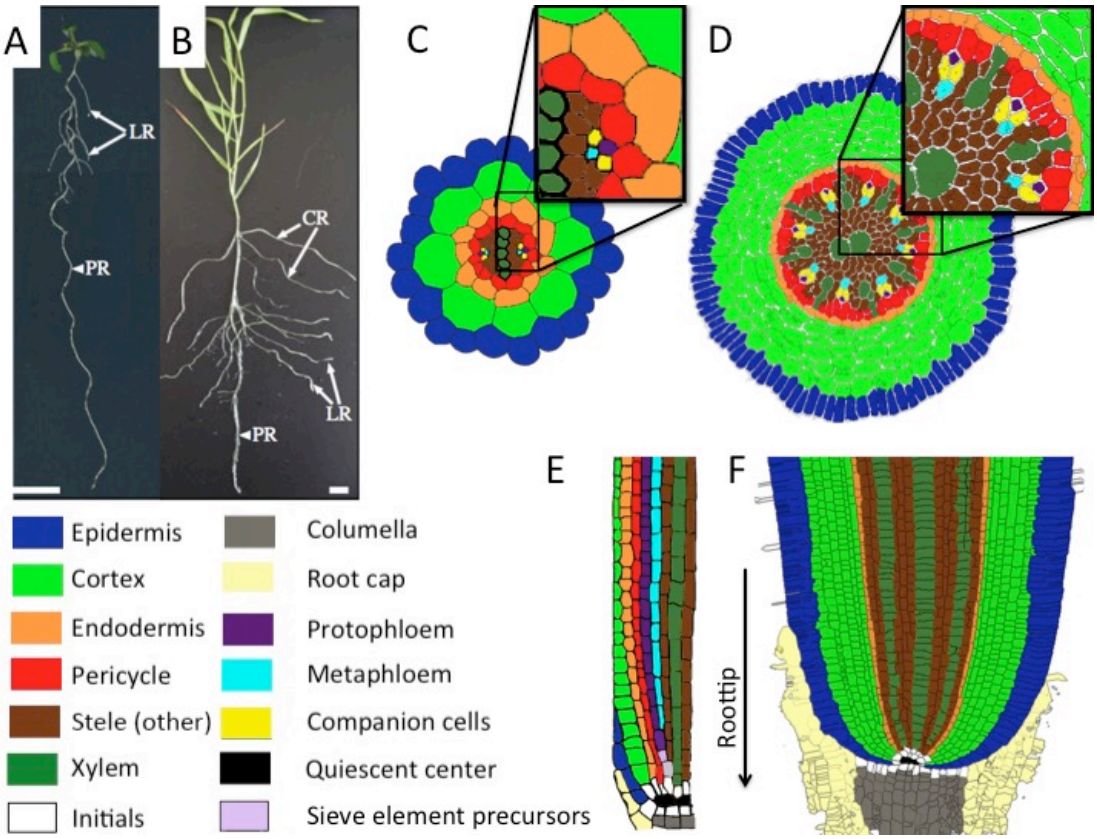

*Figure 1: Representation of root growth of dicot (*Arabidopsis*: A,C,E) versus monocot (*Brachypodium*: B,D,F). A&B) Pictures of root systems, taken from Pacheco-Villalobos et al 2012. A) Typical dicotyledon root system architecture in 10-day-old* Arabidopsis thaliana *plants.* Arabidopsis *forms only one primary root during its development, which branches out through lateral roots. (B) Typical monocotyledon root system architecture in a 30-day-old* Brachypodium distachyon *plant, composed of a primary root, crown roots and lateral roots. PR, primary root; LR, lateral root; CR, crown root. Scale bars represent 1 cm. C-F) Schematic representations of roots, different cell types are annotated in different colors. C) Cross-section of* Arabidopsis *root elongation zone, showing the diarch shape with phloem in between extensions of xylem. Image adjusted from Vaughan-Hirsch et al. 2018. D) Cross-section of* Brachypodium *root elongation zone, showing the closed polyarch structure of alternating xylem and phloem around a central pith. Image is based on real photo obtained during this thesis. E) Median longitudinal section of* Arabidopsis *root tip, showing development of phloem. Picture adjusted from Anne et al 2018. F) Median longitudinal section of* Brachypodium *root tip, image is based on real photo obtained during this thesis.*

In order to perform routine research on a plant, it requires specific characteristics: a relatively small genome size, simple growth conditions, fast regeneration time and self-pollination. Furthermore the existence of T-DNA libraries, BAC-libraries and yeast-two-hybrid libraries are beneficial to speed up research (Scholthof et al. 2018). Recently the C3-plant *Brachypodium distachyon* (*Brachypodium*) (Figure 1B) was proposed as a good monocot model species since it fits the requirements mentioned above and is part of the *Poaceae* family of grasses (Draper et al. 2001). This family includes among others sugarcane, maize, rice, wheat, barley, sorghum and rye. *Brachypodium* is more closely

related to cereals like barley, rye and wheat than it is to rice and maize (Figure 2). This makes it very suitable to conduct research and transfer the knowledge to these major crops (Draper et al. 2001; Vogel, Gu, et al. 2006; Pacheco-Villalobos and Hardtke 2012; Pacheco-Villalobos et al. 2013; Scholthof et al. 2018; Kapp et al. 2015). The root system of *Brachypodium* is less complex than for example wheat, rice or maize that have many more roots, however root anatomy is similar between the different species (Chochois, Vogel, and Watt 2012; Pacheco-Villalobos and Hardtke 2012). Furthermore, at later stages *Brachypodium* develops several crown roots like rice, maize and wheat.

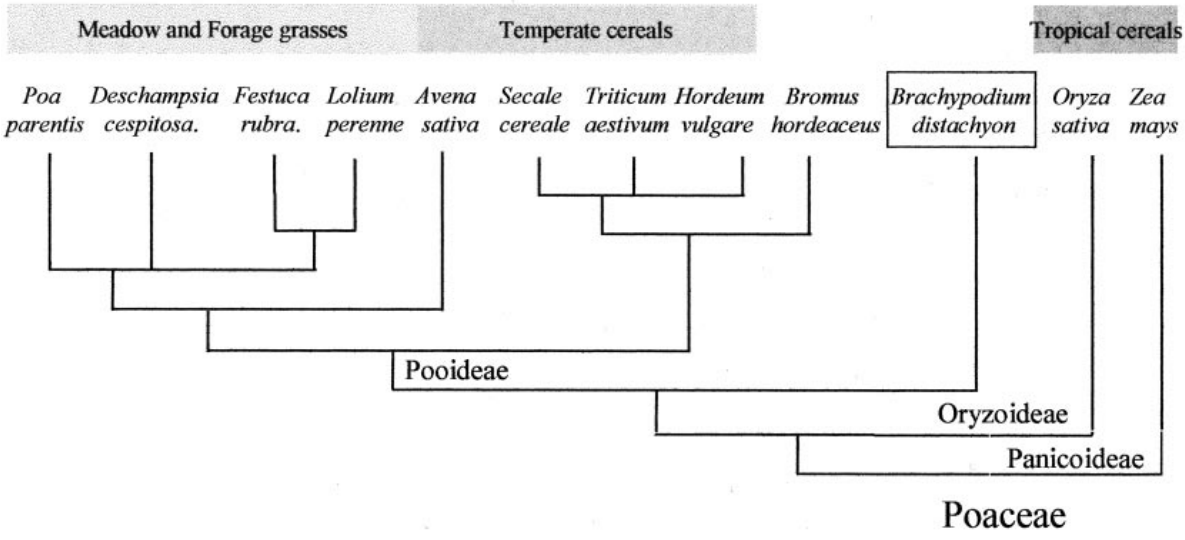

Figure 2: Schematic phylogenetic relationship of Brachypodium distachyon *to other Poaceae, taken from Draper et al. 2001*. Brachypodium *is more closely related to wheat and barley, than it is to rice and maize.*

Twenty different *Brachypodium* taxa are known, of which only three are annual species. They can be auto- or allogamous, diploid, tetraploid or hexaploid with chromosome numbers varying from five to fifteen. There are late and early flowering lineages (Scholthof et al. 2018). *Brachypodium distachyon* is autogamous, diploid with five chromosomes and an annual species. It is found in relatively cool, wet and high places with open habitats and is a not-so-efficient water user. To date, two lines of *B. distachyon* have been fully sequenced; the accession classified as “extremely rapid flowering” Bd21 (or Bd21-0 as we named it in our lab) and the “rapid flowering” Bd21.3 (Sancho et al. 2018; Scholthof et al. 2018). In parallel, some tools have recently been developed, like a diverse collection of *B. distachyon* accessions and several mutant libraries, including T-

DNA insertion lines (Vogel and Hill 2008; Bragg et al. 2012; Scholthof et al. 2018).

1.4 The plant hormone auxin (IAA)

Both monocots and dicots need to modulate many different cellular processes to grow properly and respond to environmental stimuli (Alberts 2002). In order to control these processes, plants make use of signaling molecules, many of which are transported throughout the plant via the vasculature. Some of these molecules are phytohormones, whose existence was discovered in 1927 through a specific hormone called auxin or indole-3-acetic acid (IAA) (Went 1927). Years of additional research have now shown the existence of many more phytohormones that include, amongst others, indole-containing molecules, ethylene and brassinosteroids (Simon and Petrasek 2011; Balzan, Johal, and Carraro 2014). Even though these other indole-containing molecules have similar functions to IAA, the latter is still seen as the most important auxin. It is involved in many aspects of plant development, including cell division, elongation, differentiation and tropisms (Ljung et al. 2005; Simon and Petrasek 2011; Balzan, Johal, and Carraro 2014).

IAA is derived from tryptophan via several possible pathways. However the major pathway involves the enzyme TRYPTOPHAN AMINOTRANSFERASE OF ARABIDOPSIS 1 (TAA1) or TAA1-RELATED (TAR) (Stepanova et al. 2008; Tao et al. 2008). It converts tryptophan into indole-3 pyruvic acid (IPA), which is then converted by YUCCA enzymes into indole-3-acetic acid (Zhao et al. 2001) (Figure 3). This last step is rate limiting in the production of auxin (Zhao et al. 2001; Pacheco-Villalobos et al. 2013). Production of auxin mainly takes place in the aerial parts of the plant, the meristematic region of the root and, although at lower amounts, in other parts of the root (Ljung et al. 2005). IAA is then transported from its site of production throughout the plant via the vasculature (Taiz et al. 2015; Swarup and Peret 2012). In order for auxin to enter cells, the pH of the apoplast between cells is of importance. This pH ranges from 5 to 5.5, which will cause 15-36% of auxin to be in its protonated form (IAAH), allowing it to passively cross the membrane. The charged IAA^- requires a transporter to enter cells.

Since the pH within cells ranges between 7 and 7.5, IAA^- is the major auxin found inside cells and it requires exporters to exit the cell (Taiz et al. 2015; Swarup and Peret 2012). The major auxin-efflux carriers are PIN-FORMED (PIN) and P-GLYCOPROTEIN (PGP), while the AUX1 / LIKE-AUX1 (AUX/LAX) family imports auxin into cells. Especially PIN-proteins are important for the directional movement of auxin due to their asymmetrical localization in cells (Swarup and Peret 2012; Balzan, Johal, and Carraro 2014).

When auxin concentration within cells is low, so-called AUX/IAA proteins repress auxin responses by binding to specific transcription factors (AUXIN RESPONSE FACTORS or ARFs). As auxin levels increase, AUX/IAAs are ubiquitinated and degraded by the proteasome. This releases ARFs to induce the expression of auxin response genes. AUX/IAAs are seen as general corepressors that inhibit auxin-dependent gene regulation (Li et al. 2016; Weijers and Wagner 2016). Furthermore it has been shown several times that the auxin pathway interacts with ethylene. Auxin upregulates AMINOCYCLOPROPANE-1-CARBOXYLATE (ACC) SYNTHASE, an important enzyme for ethylene production (Abel et al. 1995). On the other hand, ethylene can influence the expression of *TAR*- and *YUCCA*-genes (Stepanova et al. 2008; Mashiguchi et al. 2011; Pacheco-Villalobos et al. 2013).

1.5 The auxin importer AUX1

Even though auxin can diffuse into the cell on its own, it was shown that 75% of auxin uptake relies on active transport via importers (Swarup and Peret 2012). In *Arabidopsis* the auxin importer family consists of four members, called AUX1 and LIKE-AUX1 1 to 3 (LAX1-3). In the shoot all AUX/LAX proteins seem important. Higher-order mutants display phenotypes in vascular development and phyllotactic patterning (Bainbridge et al. 2008; Fabregas et al. 2015). In roots, *AUX1* seems to be the most important member of the family, as corresponding mutants have the most severe phenotype. It was shown that AUX1 plays a role in gravitropism, lateral root (LR) initiation and root hair development (Maher and Martindale 1980; Yamamoto and Yamamoto 1998; Marchant and Bennett

1998; Marchant et al. 2002; Swarup et al. 2001; Swarup et al. 2005; Peret et al. 2012). To date a function for LAX1 and LAX2 in roots has not been reported and LAX3 only plays a role in LR emergence (Swarup et al. 2008; Peret et al. 2012).

Arabidopsis AUX1 (AtAUX1) has eleven membrane-spanning helices and is located at the plasma membrane of cells. The N-terminus is located on the cytoplasmic side, while the C-terminus resides in the apoplast (Swarup et al. 2004). Normally AUX1 is localized asymmetrically to the apical side of developing protophloem cells, without polarity in root cap cells and axial in the epidermal cells, although at a lower level (Swarup et al. 2001; Swarup et al. 2004; Dharmasiri et al. 2006). It is also expressed in the columella, in vegetative meristems, in flower primordia and in leaves (Swarup et al. 2001; Bainbridge et al. 2008; Peret et al. 2012; Lampugnani, Kilinc, and Smyth 2013), however *Ataux1* mutants only display phenotypes in the root. Here it plays a dual role in auxin distribution; it transports the phytohormone from the shoot to the root tip (acropetal movement) and then distributes it away from root tip into outer tissues, the lateral root cap (LRC) and epidermis (basipetal movement) (Swarup et al. 2001; Ljung et al. 2005). The role of AUX1 is most prominent in basipetal movement (Swarup et al. 2005; Band et al. 2014). The distribution of auxin into the outer root tissues is important for correct gravity responses and is facilitated by PINs (Swarup et al. 2005; Sato et al. 2015). Gravity responses supposedly initiate by sedimentation of starch-filled amyloplasts in columella cells (Sato et al. 2015). In response PIN3 and PIN7 are relocated to the lateral face of columella cells, transporting auxin from lateral root cap cells to epidermal cells in the elongation zone. The basipetal transport into and through the elongation zone is further mediated by AUX1 and PIN2 (Sato et al. 2015). PIN2 is internalized and degraded on the upper side of gravistimulated roots, which is prevented by auxin in the bottom cells. Auxin then induces cell elongation in the upper root by cell-wall remodeling enzymes, while in the lower root a higher concentration of auxin inhibits cell elongation (Sato et al. 2015). *Ataux1* mutants fail to deliver sufficient amounts of auxin to the root tip and then distribute it asymmetrically into epidermal cells, thus the roots cannot respond properly to gravity

(Swarup et al. 2001; Swarup et al. 2005; Band et al. 2014). A synthetic auxin called 1-NAA is able to rescue gravitropic responses, since it can easily diffuse into cells, whereas importer-dependent auxins like 2,4-D are unable to rescue (Marchant et al. 1999).

1.6 Auxin signaling in monocots and dicots

For many mechanisms that involve auxin it is not yet known exactly what differences there are between monocots and dicots (McSteen 2010). To date, investigated monocot auxin transporters seem to have similar functions as in *Arabidopsis*, however some transporter families are bigger and include members with new functions (Balzan, Johal, and Carraro 2014). An example is Sister-of-PIN1 (SoPIN1) in *Brachypodium,* which is not found in *Arabidopsis*. It determines the sites of organ initiation by producing auxin maxima in the shoot (O'Connor et al. 2014). Also the AUX/LAX family in monocots might have adopted new functions. In addition to the problems in gravitropism observed in *Arabidopsis aux1*, in monocots these mutants sometimes display reduced plant height and increased root lengths (Yu et al. 2015; Zhao et al. 2015; Huang et al. 2017; van der Schuren et al. 2018) (Chapter 3). Moreover, rice, sorghum, *Setaria viridis* and maize contain five different *LAX*-genes instead of four like in *Arabidopsis* (Shen et al. 2010; Huang et al. 2017).

Another example of differences between dicots and monocots in the field of auxin was published in 2013. Pacheco-Villalobos et al. discovered that the auxin-ethylene crosstalk in *Brachypodium* might differ substantially from dicots (Pacheco-Villalobos et al. 2013). The research was performed on a mutant in one of the two *TAA1-RELATED* (*TAR*) homologs in *Brachypodium*. The expression of this *Brachypodium* TAR homolog is severely reduced in the mutant but not totally abolished, therefore it is a hypomorphic mutant (*Bdtar2l*^{hypo}, Pacheco-Villalobos et al. 2013). As TAA/TAR is involved in the auxin biosynthesis pathway, in *Arabidopsis* the down-regulation of TAA1 reduces the amount of auxin and therefore root growth is impaired (Stepanova et al. 2008; Tao et al. 2008) (Figure 3). Surprisingly *Bdtar2l*^{hypo} mutants had an increased root length and displayed

increased auxin levels (Pacheco-Villalobos et al. 2013). Moreover root phenotypes, including auxin levels, could be restored by the addition of the ethylene precursor ACC. This was however not due to a change in *BdTAR2L* or *BdTAR1L* expression. Rather, the ACC-treated roots displayed reduced levels of YUCCA expression, the last enzyme involved in tryptophan-dependent auxin biosynthesis. To explain these paradoxical observations, a model was proposed in which ethylene suppresses instead of induces *YUCCA* expression in *Brachypodium* (Pacheco-Villalobos et al. 2013). It is known that ethylene is linked to the auxin biosynthesis intermediate IPA via VAS1-like enzymes (Zheng et al. 2013; Pacheco-Villalobos et al. 2016), therefore lower levels of IPA in *Bdtar2l*^{hypo} mutants result in lower levels of ethylene. This de-represses the rate-limiting YUCCA step in auxin biosynthesis and results in higher levels of auxin as long as *BdTAR2L* expression does not drop below a certain threshold (Pacheco-Villalobos et al. 2013) (Figure 3).

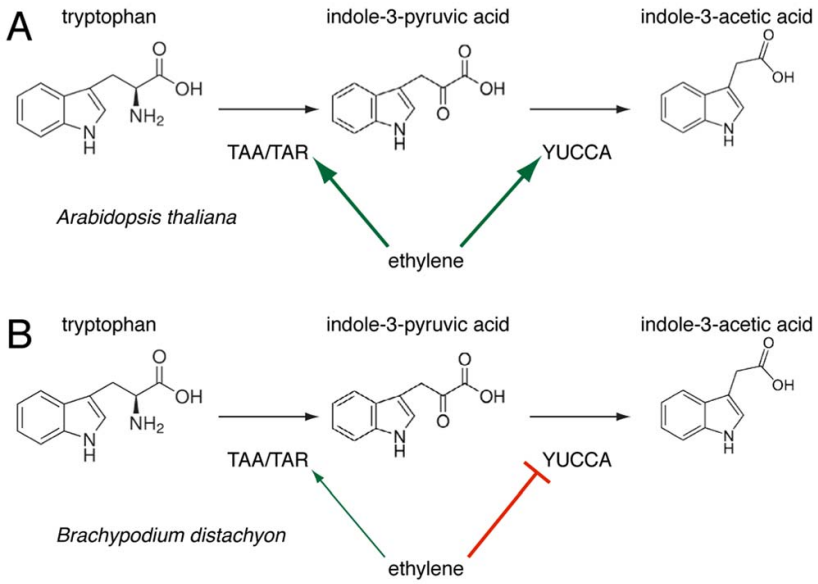

Figure 3 Auxin-ethylene crosstalk model as proposed by Pacheco-Villalobos et al 2013. Ethylene promotes YUCCA expression in Arabidopsis*, while it suppresses YUCCA in* Brachypodium.

Many experiments have shown that correct auxin levels are crucial for normal root development and the addition of external auxin inhibits root growth (Hobbie and Estelle 1995; Marchant et al. 1999; Swarup et al. 2001; Ivanchenko, Muday, and Dubrovsky

2008; Stepanova et al. 2008; Yu et al. 2015). In rice it was concluded that this auxin-induced inhibition of root growth was not caused by ethylene, rather roots need a certain level of ethylene to cope with auxin (Yin et al. 2011). Nonetheless YUCCA in rice is induced by ethylene (Qin et al. 2017). Lee et al. showed that addition of ethylene in a gravity response assay in maize roots makes the root continue to curve where non-treated roots would stop curving. The opposite effect is seen with auxin transport or ethylene inhibitors (Lee, Chang, and Evans 1990). This seems more in line with the model proposed for *Arabidopsis*. Also results by Mulkey et al. in maize seem more in line with the model for *Arabidopsis*; in maize roots that were pre-treated with ethylene inhibitors, low concentrations of auxin strongly promoted growth (Mulkey, Kuzmanoff, and Evans 1982). Neither Yin, nor Lee and Mulkey et al. provide any analysis of amounts of auxin or transport of auxin in roots. Their manipulations were purely pharmacological, whereas the work in *Brachypodium* is based on genetics. This makes it difficult to draw any detailed conclusions on auxin-ethylene cross talk or on differences between monocotyledons and dicotyledons.

1.7 The importance of phloem for the plant

As discussed before, both dicots and monocots have a complex vasculature, consisting of xylem and phloem that connects shoot and root. Xylem transports water and minerals from the root to the other parts of the plant, while phloem transports photosynthetic assimilates and signaling molecules (like auxin) to the developing tissues such as the root (Heo et al. 2014; Dinneny and Yanofsky 2004; Lucas et al. 2013; Pacheco-Villalobos and Hardtke 2012; Rodriguez-Villalon et al. 2014; Marhava et al. 2018; Anne and Hardtke 2018). The development of a vasculature is thought to be one of the major reasons for successful adaptation of plants to the land environment (Lucas et al. 2013; Heo et al. 2014). Fossils and some of the most primitive land plants, like mosses, do not have a vasculature; instead they have water- and food-conducting cells (Lucas et al. 2013). More evolved xylem in higher-order plants like angiosperms consists of dead vessel elements that are all connected to reduce the resistance for water flowing through (Evert 2006;

Lucas et al. 2013). More complex phloem consists of sieve elements with perforated walls at the transversal junctions between two cells, also called sieve plates. The sieve elements form a working sieve tube that permits continuous sap flow within the phloem (Evert 2006; Lucas et al. 2013; Heo et al. 2014; Breda, Hazak, and Hardtke 2017). Unlike xylem, these sieve elements are not completely dead when they mature and they are closely linked to companion cells that provide essential metabolic molecules (Evert 2006; Lucas et al. 2013; Rodriguez-Villalon et al. 2015; Heo et al. 2014).

The exact development from stem cell initial to working sieve element in the root is so far mainly described in *Arabidopsis* (Mahonen et al. 2000; Lucas et al. 2013; Rodriguez-Villalon et al. 2014; Rodriguez-Villalon et al. 2015; Heo et al. 2014). Phloem develops from a precursor cell that undergoes two periclinal divisions; the first division forms a procambial precursor and a sieve element precursor, whereas a second division of the latter cell creates proto- and metaphloem cell files (Bauby et al. 2007; Rodriguez-Villalon et al. 2014; Anne and Hardtke 2018) (Figure 1E). The protophloem in *Arabidopsis* differentiates earlier than other cell types in the root, which is associated with changes in cell wall composition, cell elongation, cytoplasm remodeling and loss of several organelles including the nucleus (Evert 2006; Lucas et al. 2013; Rodriguez-Villalon et al. 2014; Heo et al. 2014; Breda, Hazak, and Hardtke 2017; Ruiz Sola et al. 2017). From here on surrounding companion cells provide essential metabolic functions that sieve tubes cannot produce themselves anymore (Evert 2006; Lucas et al. 2013; Rodriguez-Villalon et al. 2015). These companion cells are derived from the procambium initial and not like the protophloem from the sieve element precursor. Further up in the root the metaphloem develops into functional sieve elements that take over the function of protophloem (Evert 2006; Lucas et al. 2013; Rodriguez-Villalon et al. 2014; Rodriguez-Villalon et al. 2015) (Figure 1C,D). (Mahonen et al. 2000; Rodriguez-Villalon et al. 2014; Ruiz Sola et al. 2017). Solutes are loaded into the phloem at their site of production in the shoot and transported through the metaphloem to the root. Close to the root tip, the protophloem takes over the function of the metaphloem. Since the meristem needs a lot

of energy to sustain organ growth, the phloem unloads its content there (Lucas et al. 2013; Ruiz Sola et al. 2017; Anne and Hardtke 2018).

Phloem-specific root mutants have been studied for several years now and some important factors have been identified in *Arabidopsis.* One of them is *wooden leg (wol)*, which completely lacks phloem cell lineages since it is required for the stem cell divisions that give rise to them (Scheres et al. 1995; Mahonen et al. 2000; Truernit et al. 2012). Another example is the *ALTERED PHLOEM DEVELOPMENT* mutant (*apl*), where phloem initials do develop however phloem differentiation fails (Bonke et al. 2003). Furthermore several regulators have been discovered that are specifically involved in phloem and not xylem development (discussed in more detail below) (Bauby et al. 2007; Mouchel, Briggs, and Hardtke 2004; Truernit et al. 2012; Depuydt et al. 2013; Rodriguez-Villalon et al. 2014; Anne and Hardtke 2018). Mutations in these regulators often result in the "disturbed protophloem syndrome", where roots are smaller than in wild type with an increased amount of lateral roots (Mouchel, Briggs, and Hardtke 2004; Truernit et al. 2012; Depuydt et al. 2013; Rodriguez-Villalon et al. 2015; Breda, Hazak, and Hardtke 2017; Anne and Hardtke 2018). This can be visualized by several cues: the first periclinal division of the sieve element precursor cell is often delayed or even absent and undifferentiated cells that retain a nucleus, lack characteristic cell wall changes and lack an increase of actin filament abundance appear as "gaps" in a protophloem strand (Scacchi et al. 2010; Rodriguez-Villalon et al. 2014; Anne and Hardtke 2018). In more mature roots, non-differentiated phloem cells can also be observed by continued instead of reduced toluene blue staining (Rodriguez-Villalon et al. 2014; Ruiz Sola et al. 2017). Because of the gaps the flow of protophloem sap as well as auxin to the meristem is interrupted, which interferes with normal development of the root (Truernit et al. 2012; Rodriguez-Villalon et al. 2014; Rodriguez-Villalon et al. 2015; Anne and Hardtke 2018; Marhava et al. 2018).

1.8 Regulators involved in the disturbed protophloem syndrome

Originally the disturbed protophloem syndrome was discovered in the *brevis radix* (*brx*) mutant. It was isolated from a screen for regulators in root growth on natural accessions of *Arabidopsis.* The Umkirch-1 (Uk-1) accession stood out because of its short primary root and several adventitious roots due to a mutation in *BRX* (Mouchel, Briggs, and Hardtke 2004). A few years later a similar mutant was discovered and named *octopus (ops*) (Truernit et al. 2012; Rodriguez-Villalon et al. 2014). Both BRX and OPS are important for adopting sieve element fate and are therefore considered positive regulators of protophloem development (Depuydt et al. 2013; Rodriguez-Villalon et al. 2014; Anne and Hardtke 2018). During a screen for genetic suppressors of *brx*, more regulators involved in the control of protophloem differentiation where identified (Depuydt et al. 2013; Rodriguez-Villalon et al. 2014; Rodriguez-Villalon et al. 2015; Kang and Hardtke 2016; Breda, Hazak, and Hardtke 2017; Cattaneo and Hardtke 2017; Anne and Hardtke 2018). A second-site mutation in *BARELY ANY MERISTEM3 (BAM3*) could fully suppress the *brx* phenotype and seemed specifically involved in protophloem development (Depuydt et al. 2013). Second-site mutations in *COTYLEDON VASCULAR PATTERN 2 (CVP2)* and *MEMBRANE-ASSOCIATED KINASE REGULATOR 5 (MAKR5)* could only partially rescue the *brx* phenotype (Rodriguez-Villalon et al. 2015; Kang and Hardtke 2016). Another factor discovered in the screen was *BIG BROTHER (BB)*, whose mutant displayed increased meristematic activity that is not specifically linked to protophloem (Cattaneo and Hardtke 2017). The most important factors in protophloem development will be discussed in more detail below.

Other studies revealed that phytohormones are also involved in the regulation of protophloem development (Kang, Breda, and Hardtke 2017; Marhava et al. 2018). Indeed the induction of brassinosteroid signaling in *ops* or *brx* can partially rescue distinct aspects of their root phenotypes (Mouchel, Osmont, and Hardtke 2006; Anne et al. 2015; Kang, Breda, and Hardtke 2017). In accordance with that, a recent study has shown the implication of the receptor kinase BRASSINOSTEROID INSENSITIVE 1 (BRI1) and its

homologs with protophloem development (Cano-Delgado et al. 2004; Kang, Breda, and Hardtke 2017). This will be discussed in more detail below.

BRX

AtBRX (At1g31880) is expressed at very low levels in the root (Mouchel, Briggs, and Hardtke 2004); it is only expressed in the columella and the developing protophloem (Scacchi et al. 2009; Depuydt et al. 2013). In the protophloem, BRX protein is polarly localized to the rootward end of cells (Mouchel, Osmont, and Hardtke 2006; Bauby et al. 2007; Scacchi et al. 2009; Marhava et al. 2018). Overexpression of *BRX* results in increased hypocotyl length and delayed root gravitropism (Scacchi et al. 2009). *BRX* homologs are found in all higher order plants (Mouchel, Briggs, and Hardtke 2004). They all have four characteristic, highly conserved domains: a 10 and a 25 amino acid stretch at the N-terminus and a tandem of two homologous domains of 55 amino acids with a 100-150 amino acid spacer in between (tandem BRX domain) (Briggs, Mouchel, and Hardtke 2006). In *Arabidopsis* four homologs of *BRX* can be found (*BRXL1-4*), however none seem to act redundantly with *BRX* (Mouchel, Briggs, and Hardtke 2004; Briggs, Mouchel, and Hardtke 2006). Only expression of *BRX* itself, or *BRXL1* expressed constitutively or under the control of *BRX* promoter can rescue the root phenotype of *brx* mutants (Mouchel, Briggs, and Hardtke 2004; Briggs, Mouchel, and Hardtke 2006; Scacchi et al. 2009). *BRXL1* in wild type roots is expressed at much lower levels than *BRX*, which, together with its restriction to mature roots, could explain the lack in redundancy with *BRX* (Briggs, Mouchel, and Hardtke 2006; Scacchi et al. 2009). Apart from the discovery of a lack of redundancy with *BRX*, the remaining homologs of *BRX* in *Arabidopsis* have not yet been analyzed in detail. Interestingly, *brx* mutant could be rescued by ectopic expression of several monocot *BRX* homologs, leading to the conclusion that *BRX* genes might be more diversified in dicots than in monocots (Beuchat et al. 2010).

The detailed function of BRX and the BRX domain remains to be elucidated. It is known

that the N-terminus is important for the localization of BRX to the plasma membrane (Scacchi et al. 2009), and a chimeric fusion of AtBRX-N-terminus with AtBRXL2-C-terminus can rescue *brx* (Beuchat et al. 2010). The N-terminus alone, however, cannot complement *brx*, whereas the C-terminus by itself can partially complement the *brx* mutant. The latter localizes both to the plasma membrane and the nucleus and may even induce overexpression phenotypes (Scacchi et al. 2009). Furthermore BRX can inhibit the export of the plant hormone auxin, whereas high intracellular concentrations of auxin displace BRX protein from the membrane (Scacchi et al. 2009; Marhava et al. 2018). Increased auxin efflux then reduces cellular auxin concentrations, causing BRX to re-associate with the membrane and block auxin efflux again (Marhava et al. 2018). This creates an equilibrium in which BRX is thought to be fine-tuning cellular auxin efflux in developing sieve elements.

OPS

Before the discovery of its mutant phenotype, *OCTOPUS* (At3g09070) was already identified as a good marker for phloem development (Nagawa et al. 2006; Bauby et al. 2007). *OPS* is expressed in phloem vascular initials in embryo, root and leaf that later develop into protophloem and metaphloem, and also in shoot vasculature (Bauby et al. 2007; Truernit et al. 2012; Ruiz Sola et al. 2017). *OPS* seems to be expressed earliest of all the factors involved specifically in protophloem development, namely as early as the sieve element precursor. It is considered a master regulator in protophloem differentiation since an extra copy of *OPS* can rescue several other mutants with the disturbed protophloem syndrome, including *brx* (Scacchi et al. 2009; Rodriguez-Villalon et al. 2014; Breda, Hazak, and Hardtke 2017; Anne and Hardtke 2018). Even though the *ops* root phenotype resembles *brx*, the root phenotype of *brx ops* double mutant is even more severe than either single mutant, suggesting that both genes work in parallel pathways but affect the same downstream targets (Breda, Hazak, and Hardtke 2017). Moreover, unlike *brx, ops* also displays reduced vascular complexity in cotyledons and leaves (Truernit et al. 2012; Ruiz Sola et al. 2017). *OPS* overexpression lines display elongated

hypocotyls, increased vascular pattern complexity, premature protophloem development and wavy roots (Truernit et al. 2012; Anne et al. 2015; Breda, Hazak, and Hardtke 2017). In strong overexpression lines root growth inhibition was reported, possibly because excess levels of *OPS* push cell into premature differentiation (Breda, Hazak, and Hardtke 2017).

The OPS protein contains one domain, the DOMAIN OF UNKNOWN FUNCTION 740 (DUF740), for which, as the name suggests, a function still has to be elucidated. AtOPS remains functional when specific conserved regions are removed since most tested truncated OPS variants could still complement *ops* single mutants and partially complement *brx* or *brx ops* double mutants (Breda, Hazak, and Hardtke 2017). OPS is a membrane-associated protein that in roots is localized to the shootward side of phloem cells, however it is also found in the cytoplasm. Interestingly, polar localization does not seem to be essential for its function in protophloem differentiation, since rootward localization of OPS and constructs with a relatively high cytoplasmic-abundance can still complement the *ops* mutant (Truernit et al. 2012; Breda, Hazak, and Hardtke 2017). However, the charge of specific phosphosites in OPS is crucial for its function. A more positively charged OPS can more efficiently rescue *ops*, *brx* and *brx ops* double mutant phenotypes and additionally induce overexpression phenotypes, contrary to more negatively charged OPS (Breda, Hazak, and Hardtke 2017). In evolution, the appearance of proteins containing the DUF740 domain is thought to correlate with the appearance of sieve elements. It is conserved over all angiosperms sequenced to date, but not found in ferns or gymnosperms (Breda, Hazak, and Hardtke 2017). Interestingly, even an ortholog of the most basal angiosperm *Amborella trichopoda* could rescue the *Arabidopsis ops* mutant, suggesting a strong selective pressure on OPS family members over time (Breda, Hazak, and Hardtke 2017). In *Arabidopsis* five genes that carry DUF740 have been detected. The five genes group into two classes and OPS clusters with two more homologs in the same group (Nagawa et al. 2006). These were named *OPS-LIKE 1* and *2* (*OPL1* and *OPL2*) (Ruiz Sola et al. 2017). *OPL1::GUS* but not *OPL2::GUS* reporter

gene staining was detected in roots (Nagawa et al. 2006), however Sola et al. 2017 report weak *OPL2* expression in developing phloem when using a fluorescent reporter (Ruiz Sola et al. 2017). In addition they report that *OPL1* is mainly expressed in xylem and mature plant tissue and therefore seems an unlikely candidate for redundancy with *OPS* (Ruiz Sola et al. 2017). *OPL2* is expressed everywhere at younger stages and only becomes restricted to vasculature in mature root and leaves (although weaker than *OPS*), whereas OPS is always restricted to provascular cells, even in the embryo (Truernit et al. 2012; Ruiz Sola et al. 2017). Like OPS, OPL2 in the protophloem was restricted to the shootward side of cells at the plasma membrane, which was not always the case in other cell types (Ruiz Sola et al. 2017). *Atopl2* single mutants do not show a root phenotype, however *ops opl2* double mutants display a more severe phenotype than *ops* alone, judged from root length, phloem differentiation defects and shoot vasculature complexity. Furthermore the expression of *OPS::OPL2* could partially rescue the root phenotypes of the *ops* mutant (Ruiz Sola et al. 2017). Interestingly Breda et al. published that *OPL1* could also complement *ops* and even *ops brx* double mutants when expressed under the control of the *OPS* promoter, arguing that the OPS proteins are functionally redundant (Breda, Hazak, and Hardtke 2017).

BAM3 and CLE45

BAM3 (At4g20270) and CLAVATA3/EMBRYO SURROUNDING REGION 45 (CLE45 or At1g69588) form a receptor-ligand pair that is hyperactive in *brx* mutants (Depuydt et al. 2013). Many homologs for both receptor and ligands exist in *Arabidopsis* and ligands may bind to different receptors with different affinities constructing a complicated network of possible interactions (Hazak and Hardtke 2016; Hazak et al. 2017; Anne et al. 2018). In *Arabidopsis* 32 different CLE peptide-encoding genes can be found. The processed, active peptides that are secreted are only 12-13 amino acids in size (Czyzewicz et al. 2015; Hazak and Hardtke 2016; Anne et al. 2018; Yamaguchi et al. 2017). Most of them inhibit root growth when applied to *Arabidopsis* roots in nano- to micromolar concentrations (Kinoshita et al. 2007; Depuydt et al. 2013; Czyzewicz et al. 2015; Anne et

al. 2018). Only *CLE45* and its close homolog *CLE26* have so far been specifically related to protophloem development. Whereas *CLE45* is expressed from early stages on in the protophloem cell lineage, *CLE26* expression is only observed at later stages (Rodriguez-Villalon et al. 2014; Czyzewicz et al. 2015; Anne et al. 2018; Anne and Hardtke 2018). Treating seedlings with CLE45 induces the disturbed protophloem syndrome (Depuydt et al. 2013; Rodriguez-Villalon et al. 2014). Overexpression of fully-functional *CLE45* is lethal, whereas a weaker version can mimic *brx* and *ops* phenotypes (Depuydt et al. 2013). A knock-down and knock-out of CLE45 were published, however no root phenotypes were reported (Endo et al. 2013; Yamaguchi et al. 2017). A mutant with reduced *CLE26* expression resulted in slightly increased root lengths in *Arabidopsis* (Czyzewicz et al. 2015), which was observed as well in over expression lines (Strabala et al. 2006). In monocots, some CLE peptides have been linked to root meristem differentiation, shoot meristem development and cyst nematode infections (Hazak and Hardtke 2016; Kirschner et al. 2017). When AtCLE-peptides were tested on rice roots, they seemed to have similar effects as in *Arabidopsis* (Kinoshita et al. 2007). Interestingly the closest homolog of AtCLE26 in several monocots included a substitution of an amino acid that was crucial for its function in *Arabidopsis* (Czyzewicz et al. 2015). When monocot and dicot CLE peptides were tested, they indeed induced different effects in monocots and *Arabidopsis*. In both species, AtCLE26 reduced primary root length, whereas Bradi1g05010 (the closest homolog of CLE26 in *Brachypodium*) slightly increased primary root length. It was suggested that there might possibly be another, yet unknown, ortholog of AtCLE26 in monocots (Czyzewicz et al. 2015).

The *bam3* mutant is resistant to CLE45 and suppresses the *brx* phenotype as a second site mutations, however as single mutant it lacks a phenotype under normal conditions (Depuydt et al. 2013). *BAM3* is expressed in protophloem and surrounding tissues and is a negative regulator of protophloem differentiation that is under the negative control of BRX (Depuydt et al. 2013; Rodriguez-Villalon et al. 2014; Hazak et al. 2017). In *Arabidopsis* it is part of a three member family, with *BAM1* and *BAM2* being mainly

involved in shoot development and *BAM1* also in cell proliferation in the root (Shimizu et al. 2015; Hazak and Hardtke 2016). Only the expression of *BAM3* is restricted to the vasculature and it is so far the only family member implicated in protophloem development, however since its single mutant is lacking a phenotype it cannot be excluded that other receptor-like kinases may act redundantly (Hazak and Hardtke 2016).

BRI1

BRI1 (At4g39400) is involved in brassinosteroid signaling, a class of phytohormones that, like auxin, affect cell elongation and division (Kang, Breda, and Hardtke 2017). In *Arabidopsis*, BRI1 is the major receptor kinase for brassinosteroid signaling and it can trigger a signaling cascade inside the cell upon perception of brassinosteroids at the plasma-membrane. It contains several leucine-rich-repeats (LRR), a 70 amino acid island domain, a transmembrane domain and a cytoplasmic kinase domain (Cano-Delgado et al. 2004; Kinoshita et al. 2005). Three homologs can be found in *Arabidopsis* that are intron-less like *BRI1* itself, however only *BRI1-LIKE 1* and *3* (*BRL1* and *BRL3*) encode functional brassinosteroid receptors (Cano-Delgado et al. 2004; Kang, Breda, and Hardtke 2017). This is possibly linked to the more divergent island domain in *BRL2* as compared to the other homologs, as the island domain was found to be crucial for binding to brassinosteroids together with its flanking LRR (Cano-Delgado et al. 2004; Kinoshita et al. 2005). Single *bri1* mutants do not display specific protophloem defects, rather they are known for extreme dwarfism in the shoot, male sterility and a reduced root size (Cano-Delgado et al. 2004; Kang, Breda, and Hardtke 2017; Clouse, Langford, and McMorris 1996; Gonzalez-Garcia et al. 2011). *BRI1* expression is observed ubiquitously throughout the plant (Cano-Delgado et al. 2004). By contrast, *BRL1* and *BRL3* expression is restricted to the vasculature and they complement each other's expression pattern; in the root *BRL3* is restricted to protophloem (Cano-Delgado et al. 2004). Neither *brl1* or *brl3* nor the *brl1 brl3* double mutants display root phenotypes in Col-0 wild type background, possibly due to their redundancy with *BRI1*. Concomitantly, a triple *bri1 brl1 brl3* mutant shows a more severe phenotype than any single mutant. It is even smaller than *bri1*,

even less fertile and displays gaps in the protophloem (Cano-Delgado et al. 2004; Kang, Breda, and Hardtke 2017). The amount of gaps in the triple mutant is lower than in *ops* or *brx*. Furthermore the mutant displays aberrant radial divisions in the root, leading to more cell files. Interestingly phloem-specific expression of *BRI1* in triple *bri1 brl1 brl3* mutants could revert all observed root phenotypes back to wild type (Kang, Breda, and Hardtke 2017). Earlier it was already shown that brassinosteroid signaling in *ops* or *brx* can partially rescue distinct aspects of their root phenotypes (Mouchel, Osmont, and Hardtke 2006; Anne et al. 2015; Kang, Breda, and Hardtke 2017). In summary, even though *BRI1* and its homologs may not be directly involved in protophloem development, they may still influence the process and represent interesting candidates for further studies.

1.9 Tools for research in monocotyledon protophloem development

In contrast to *Arabidopsis*, publications on protophloem development in monocot roots are rare. Moreover, mutants for *OPS, CLE45/BAM3* and *BRX* homologs were not available from the T-DNA libraries in *Brachypodium* at the start of my PhD (Vogel, Garvin, et al. 2006; Bragg et al. 2012; Hsia et al. 2017). Therefore in order to perform research on protophloem development in *Brachypodium*, it was important to first establish the homologous mutants. Several possibilities to create mutants have been suggested in the literature: RNA-interference, the Zinc-Finger Nuclease-Technology, the Transcription Activator-Like Effector Nucleases and the Clustered Regulatory Interspersed Short Palindromic Repeat (CRISPR)/CRISPR-associated protein (Cas) genome editing system. Each will be discussed in more detail below. Due to its ease and cost-effective design, the CRISPR-Cas genome editing systems became the system of choice to attempt mutations in *Brachypodium* at the start of my PhD (Chapter 4).

RNA-interference

RNA-interference was first discovered in nematodes, where sequence-specific gene silencing occurred as a response to double-stranded RNA (Fire et al. 1998; Hannon

2002). It makes use of double-stranded RNA that is complementary to a gene of interest and is cleaved into small interfering RNAs (siRNA) by an enzyme called Dicer. The siRNA is then made single-stranded and one of the strands is incorporated in the RNA-induced silencing complex (RISC). The complex is guided to mRNA that is complementary to the incorporated siRNA, and in most cases this mRNA is then cleaved by Argonaute 2. This principle was harnessed to reduce the levels of specific RNAs in many species (Hannon 2002; Miki and Shimamoto 2004; Pacheco-Villalobos et al. 2016). A disadvantage of the system is that the amount of silencing is difficult to control and can vary between different lines with the same construct (Hannon 2002; Miki and Shimamoto 2004; Pacheco-Villalobos et al. 2016), which led researchers to search for alternatives.

ZincFinger Nuclease-technology

An alternative to RNAi was proposed with the discovery of the ZincFinger Nuclease-technology (ZFN) (Jiang 2013, Shiml 2016). This technique makes use of a restriction enzyme from *Flavobacterium okeanokoites* (*FokI*) that cleaves a short distance away from a specific DNA sequence (Wah et al. 1998). *FokI* is brought to selected parts of DNA by a combination of ZF domains that specifically recognize a triplet of DNA each. Once *FokI* opens the DNA, a process called Non-Homologues End Joining (NHEJ) is induced to repair the DNA, which often leads to deletions (Gaj, Gersbach, and Barbas 2013; Gupta et al. 2012). A drawback of this system is that it is time-consuming and costly to design appropriate nucleases and difficult to predict their efficacy (Jiang 2013, Ma 2015, Shiml 2016).

Transcription Activator-Like Effector Nucleases

A second alternative to RNAi is the use of Transcription Activator-Like Effector Nucleases (TALENs) (Jiang 2013, Ma 2015, Shiml 2016). They also make use of the *FokI* enzyme, however instead of ZFs for the recognition of DNA, it requires TALs that are simpler to design. They are nearly identical tandem repeat units that each recognize one nucleotide and were shown to efficiently create mutations in several plant species including

Brachypodium (Shan, Wang, Chen, et al. 2013; Zhang et al. 2013). These repeats also cause a drawback: cloning may be difficult and repeats may lead to vector instability (Jiang 2013, Ma 2015, Shiml 2016).

CRISPR-Cas genome editing system

At almost the same time as the TALENs, another system was discovered: the Clustered Regulatory Interspersed Short Palindromic Repeat (CRISPR)/CRISPR-associated protein (Cas) system for genome editing (Cong et al. 2013; Mali et al. 2013; Jiang et al. 2013; Mao et al. 2013). This system makes use of RNAs and not proteins as DNA recognition units and is therefore much easier to design and clone. It was originally discovered in bacteria as a defense system against viruses and makes use of short pieces of the foreign DNA. This DNA sometimes gets incorporated in the bacterial CRISPR region and in future events it can be transcribed into CRISPR-RNA (crRNA). This crRNA is processed into small pieces (usually 20bp long) with the aid of trans-activating RNA (tracrRNA) and both types of RNA are incorporated in the Cas protein. The match of crRNA with foreign DNA guides the Cas complex to the complementary strand of foreign DNA. Cas has two nuclease domains that can cause Double Strand Breaks (DSBs) in the foreign DNA if it is bound just upstream of a Protospacer Adjacent Motif (PAM). In the case of *Streptococcus pyogenes* Cas9 (SpCas9), this PAM consists only of nucleotides NGG (Cong et al. 2013; Mali et al. 2013; Jiang et al. 2013; Miao et al. 2013; Shan, Wang, Li, et al. 2013). The system can be used to target specific DNA by fusing crucial parts of tracrRNA to any type of crRNA (called single guide RNA or sgRNA), under the control of an RNA polymerase III U3 or U6 promoter. Upon expression, the sgRNA can be loaded onto a Cas protein, which then cuts the targeted DNA. If DNA from an organism itself is targeted, the organism attempts to repair it by NHEJ, hereby often incorporating or deleting one or a few base pairs (Cong et al. 2013; Mali et al. 2013; Jiang et al. 2013; Miao et al. 2013). This can lead to frame shifts and create mutants that can be used for research.

The CRISPR-Cas system has been exploited to create numerous mutants in many different species (Cong et al. 2013; Mali et al. 2013; Jiang et al. 2013; Miao et al. 2013; Shan, Wang, Li, et al. 2013; Johnson et al. 2015; Ma et al. 2015; Schiml and Puchta 2016). Two years after the discovery that CRISPR-Cas can be used for genome editing, a new Cas-protein was discovered, called CRISPR from *Prevotella* and *Francisella* 1 or CpfI (Zetsche et al. 2015). Two CpfI proteins had significant genome-editing activity in human cells, named *Acidaminococcus* CpfI (AsCpfI) and *Lachnospiraceae* CpfI (LbCpfI). Furthermore the new Cas protein has two advantages over SpCas9: it does not need tracrRNA to process crRNA and it introduces staggered double strand breaks and could therefore be interesting for NHEJ-based gene insertion. It requires a T-rich PAM site (Zetsche et al. 2015).

1.10 Research outline

All in all it seems that research in dicots like *Arabidopsis* is not always enough to understand monocot development, since not all findings from *Arabidopsis* can be transferred to monocots one to one. The role of auxin is still poorly understood in monocots, which is peculiar since the *Poaceae* family is economically very important (Vogel and Hill 2008; Kapp et al. 2015). Moreover the exact mechanisms of phloem development, involving factors like BRX, CLE45 and OPS, have to our knowledge not at all been studied in monocots. Experimental data has to be obtained in order to confirm conservation of underlying regulatory pathways. The focus of my PhD has therefore been to characterize more mutants in *Brachypodium* with putative defects in root development, through analogy with *Arabidopsis*.

In order to get familiar with *Brachypodium*, I continued the work of David Pachecco-Villalobos, a former postdoctoral researcher in the laboratory, which resulted in the publication presented in 7.1 The Effects of High Steady State Auxin Levels on Root Cell Elongation in *Brachypodium*. Since *Brachypodium* as a model species has only been proposed recently (Draper et al. 2001; Vogel and Hill 2008; Pacheco-Villalobos and

Hardtke 2012), many protocols were not yet optimized or even tested. Therefore, part of my PhD was spent on optimizing conditions and protocols to work efficiently with this new model species, as will be discussed in Chapter 2. My work with a T-DNA insertion mutant in *AUX1* helped for a deeper understanding of auxin pathways and how to work with *Brachypodium*, which resulted in the publication discussed in Chapter 3. Moreover the T-DNA insertion lines available in *Brachypodium* (Vogel, Garvin, et al. 2006; Bragg et al. 2012; Hsia et al. 2017) did not cover homologs of *OPS*, *CLE45/BAM3*, *BRX* or *BRI1*. The main focus of my PhD was therefore to create and analyze mutants of homologs that were involved in the disturbed protophloem syndrome. This project started with the development of a functional CRISPR-Cas genome editing system in *Brachypodium.* Due to time-consuming transformation protocols and the existence of several homologs per gene of interest, the creation of these mutants took most of my time. Only in the last year, I succeeded in having multiple mutants. Therefore the testing of the CRISPR system and some preliminary results obtained for CRISPR-edited mutants will be discussed in Chapter 4.

2. How to work with *Brachypodium distachyon*

Even though researchers have been working with *Brachypodium* for a few years, many protocols have not yet been optimized and often details are missing, complicating growing *Brachypodium* or performing experiments. Therefore, a lot of time during my PhD was spent on optimizing protocols. This chapter contains all the updated information that I have gathered during my PhD on how to work with *Brachypodium.* It includes growth conditions, crosses, transformation of *Brachypodium* via the isolation of immature embryos, microscopy, embedding of roots, transversal sectioning and *in situ* hybridization on roots. All work was performed on accessions Bd21 and Bd21.3. They are most commonly used in research, due to their fully sequenced genome, diploidy, annual life cycle, self-crossing and status as rapidly flowering accessions (Sancho et al. 2018; Scholthof et al. 2018). The work presented here was done in collaboration with or continued from work of Dr. Pachecco-Villalobos, Dr. Takayuki Tamaki and Dr. Amelia Amiguet Vercher.

2.1 Growth conditions: From seed to next generation seeds

In order to sterilize seeds, they have to be husked. This can be done either by forceps or by hand. For 10-20 seeds per genotype, 12-well plates can be used while higher amounts of seeds can best be collected in petri dishes. The peeled seeds are sterilized for 30s in 70% ethanol with agitation, then remove ethanol with a pipet boy and rinse with sterile deionized water. Add 1.3% sodium hypochlorite solution containing 0.01% triton x-100. Shake at 80rpm for 4 min (for embryo isolation) or 10min (for dried seeds). Rinse four times with sterile deionized water and leave seeds for 3 days at 4°C for the induction of germinatin (shorter time may result in unequal germination). Prepare 1/2MS plates pH=5.7 with 0.3% sucrose and 1% agar to prevent roots from growing into the medium, supplemented with either hygromycin (50 μg/mL) or paromomycin (200 μg/mL) if selection is required. For experiments with low pH, agar should be replaced by 1.2% phytagel. Plate the seeds using sterile forceps with the embryo away from the media,

towards the bottom of the 120mm square plate (Figure 4A) in order to prevent shoots and roots from growing into the media or in the wrong direction. One row of seedlings should be placed at a height of about ¾ of the plate. In case root length will be measured before day 3 or if root length is not important, two rows of seeds can be placed per plate. Close the plates with 3M micropore tape to ensure a proper gas exchange with the air. Put the plates at an angle of about 19° to ensure that roots grow on the medium and not into the air (Figure 4B). Note that roots grow from the embryo, thus on the side of the seed that is not touching the medium. To avoid roots from growing into the medium a sterile mesh can be placed onto the 1/2MS plate and the seeds can be plated on it with a small amount of water to prevent them from falling when the plate is transferred. Leave seeds to grow for 2-4 days at 22°C in continuous light. Check regularly whether roots are indeed growing on the media and not in the air and die, adjust the angle if necessary.

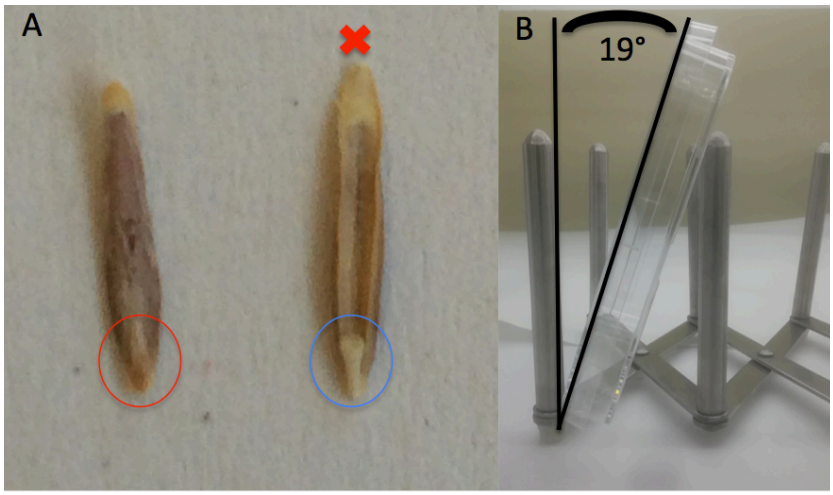

Figure 4: Pictures to show how to best grow Brachypodium *seeds. A) Left: Seeds should be placed with the embryo pointing towards the top of the lid and towards the ground (red circle). Right: Seeds should not be placed with the embryo towards the medium (blue circle). B) Plates should be placed at 19° angle to assure correct root growth.*

After 2 days, seedlings are old enough to be transferred to soil, however wild type can be left up to 1 week on media without roots touching the bottom of the plate. If longer time spans are needed, seedlings can be transferred to square Magenta boxes (Magenta vessel GA-7, #V8505, Sigma) or 100mL glass boiling tubes after 2 days instead. Prepare 1/2MS media with 0.3% sucrose and 0.2% phytagel and fill the box up to ½ or tube up to ¾, then carefully place the seedling inside, making sure the root is pointing to the bottom.

Note that 3 months growth in tubes is not enough to evoke the production of lateral roots, however some crown roots may be formed.

In order to grow seedlings on soil, they can be transferred after a minimum of 2 days on 1/2MS plates (or in petri dishes with sterile filter and sterile mQ, closed with 3M micropore tape). Prepare square pots (8x8x8cm) and fill them with a mixture of soil and vermiculite (4:1), water the pots with 5mg/mL trigard and transfer one or two plants per pot (the latter to optimize space, however plants will give a reduced amount of seeds). Cover the pots with a propagator lid for the first 3 days. Leave the plantlets to grow at 22°C in 20h photoperiod in a growth room or greenhouse, while watering them two or three times a week. Note that 16h photoperiod is also possible, however plants will need 3 months extra to dry and they grow taller, making it impossible to grow them on shelves with similar heights as for example *Arabidopsis*. *Brachypodium* requires more water than *Arabidopsis* and insufficient water will reduce the amount of viable seeds. Plants between 5-8 weeks are extremely sensitive to insufficient water, pests or treatments against pests. Normally after 5-6 weeks, crosses can be performed (see section 2.2 Crosses) and after 7-8 weeks, embryos can be isolated (see section 2.3 Transformation). Note that accession Bd21 reaches these stages on average 1 week earlier than accession Bd21.3, as it is “extremely rapid flowering” versus “rapid flowering” for Bd21.3 (Sancho et al. 2018). Once most seeds have developed, the plants can be transferred to 24h light period in order to dry them faster and prevent them from becoming too tall. They can be moved earlier to develop faster, however if plants are moved too early they will remain small and develop only few spikelets. Keep watering the plants until they have fully dried and no more green parts are visible (on average this takes 4 months), then leave the pots for 3-4 more weeks to also completely dry the soil. Germination problems will arise in the next generation if these guidelines are not followed. Collect seeds by cutting or pulling off the spikelets.

2.2 Crosses

Crosses are well described by Michael Steinwand and John Vogel and the Garvin laboratory (Garvin 2009; Steinwand and Vogel 2010), I have adopted some parts of both protocols. It is crucial to select florets at the correct stage of development, which is normally only during one day for each flower. Good pictures to help deciding the correct stage are shown by Garvin 2009. Check the florets by carefully moving the floret away from the rest of the spikelet. If this is done near a lamp, it is easier to see anthers and stigma. Clip off the other florets and emasculate according to Garvin 2009, sometimes trimming the floret up to ¼ from the top. It works best to emasculate 1 or 2 days before pollinating (as described by Steinwand and Vogel 2010), like that younger florets can be used and it can be made sure that no self-pollination occurs since anthers that are removed are too young to dehisce. Another advantage of this method is that 1 or 2 days after emasculation, it is relatively easy to see whether gynoecia were damaged during the removal of the anthers. Stigma will look dried and not feathery if they were damaged, rather than having developed in every direction. It helps to mark emasculated florets with a wire or sticker to be able to find them back for the pollination step, otherwise it is likely to not re-find all of them. For pollen collection I normally remove entire spikelets and check the florets one by one to see what anthers are in the correct stage. To select the correct stage, Garvin 2009 has very good images to describe which anthers to pick. If anthers are too young, they will never dehisce and just dry out, so it is better to collect many and wait for some to dehisce. Anthers can be collected on microscopy slides. It is best to keep them warm, so they dehisce faster (can take between 5-30min depending on the age of the collected anthers), therefore I normally use a lamp that heats its surroundings and put it close to the slide with anthers. I then cover the slide with a small lid (that does not touch the anthers), to prevent them from drying too fast. Keep the slide and the lamp under a binocular, so it is possible to check often whether anthers are ready. Just before dehiscence, pollen become shiny and bulk out the edge of the anthers. As soon as the pollen are released, the anther including as many pollen as possible

should be moved to the female stigma to pollinate as quickly as possible. Close the floret carefully with a sticker and mark the name of the cross. Wait at least one week before checking whether the cross has indeed successfully given a seed, checking earlier might disrupt seed development.

2.3 Transformation of immature embryos with *Agrobacterium tumefaciens*

A protocol for transformation was already available from Dr. David Paccheco-Villalobos and Dr. Amelia Amiguet Vercher, based on previous publications (Vogel, Garvin, et al. 2006; Alves et al. 2009; Bragg et al. 2012). Transformation of *Brachypodium* most-used accessions (Bd21 and Bd21.3) is based on immature embryos. Protocols for some other accessions are also available for mature embryos (Vogel, Garvin, et al. 2006; Sogutmaz Ozdemir and Budak 2018). Most efficient transformation is obtained when making fresh media for each step in the protocol and closing the plates with 3M micropore tape for proper gas exchange. Most media is prepared with phytagel instead of plant agar, therefore plates will have to be poured the same day media autoclaved to avoid reheating the phytagel. An overview of the used media can be found in section 7.5 Media used during this thesis. For immature embryo isolation, timing is crucial, however less stringent than for crosses. It is best to grow 10-20 plants for 7-8 weeks (as said before Bd21.3 needs more time than Bd21). Bd21 grows and dries faster, while Bd21.3 should be more efficient for transformations (Bragg et al. 2012), however in our hands we did not see a significant difference in transformation efficiency. A single embryo can be ready for isolation during several days, however the younger it is when isolated, the better the chances of it becoming good callus. To select the correct stage of spikelets, a seed that has grown all the way to the top of its floret and looks full, can be removed. Now carefully damage the seed just above the spot where embryos are supposed to develop. If it is easy to damage/remove the green of the seed, this means that the embryo is at a correct stage. Seeds that contain older embryos are difficult to damage and often develop a yellow dot at the bottom of the seed (which is part of the embryo). If plants seem to be at the correct stage, collect the oldest spikelets of each plant (sometimes 2nd or 3rd

generation spikelets are also at the correct stage, however not all may develop into proper calli). Next peel the lemma and sterilize as described in section 2.1 Growth conditions: From seed to next generation seeds. Align the seeds in the lid of a petri dish and use a binocular and sharp forceps to isolate embryos (as described by Vogel, Garvin, et al. 2006). Young embryos are transparent and turn white once they grow older. It is best to isolate the embryos as young as possible, however some young white ones may also develop into calli. Once the embryo is isolated, it can be moved to a plate with basic media, preferably with the scutellum pointing upwards. When embryos are not correctly oriented, it may make the removal of shoots more difficult, but it will not affect calli development. In some cases the embryo may be too small to remove from the embryo sack; then move the full sack with the embryo to basic medium and remove the sack when cutting the shoots. Leave the embryo on basic plates to grow for 3 days at 28°C in the dark before cutting shoots (explained by Vogel, Garvin, et al. 2006). Note that some protocols say 2-3 days, however the younger the embryos are, the longer it will take to develop shoots, so 3 days is preferred. Extremely young embryos will never develop shoots. Cut the shoots as closely as possible to the embryo; normally clipping the shoots with sharp forceps works very well. Transfer the embryos to new basic plates, give them space to expand on the plate (about 30 embryos per plate) and leave them at 28°C in the dark. Check after one week whether some shoots were forgotten or have developed afterwards and cut them if there are any. Three weeks after transformation, calli should be subcultured. Only pick calli that have developed into hard, yellow and crumbly pieces and leave those that look watery, soft and transparent. Subculture with forceps by carefully pushing on the calli until they split in 3-4 pieces (they do not need to be equal size) and then transfer these pieces to new plates. Normally two to three times more plates are needed than before subculturing. Subculture again five weeks after transformation, calli will multiply by three or four. Between 1 and 5 days after subculturing, prepare liquid *Agrobacterium tumefaciens* cultures in Luria-Bertani media (LB); normally we prefer using 2 different colonies per construct in case one of them acquired a mutation after transformation into the bacterium or in case one does not grow

well. Note that most papers prefer the use of strain AGL-1, however in our hands commonly used GV3101 (Hellens, Mullineaux, and Klee 2000; Vogel, Garvin, et al. 2006; Alves et al. 2009; Bragg et al. 2012) is just as efficient and grows faster. Starting the liquid cultures 2 days after subculture is ideal.

Once *Agrobacterium* cultures have grown well overnight, plate out 200uL on MGL-plates (section 7.5 Media used during this thesis) containing the correct antibiotics. Spread the bacteria well and leave at 28°C overnight. Some protocols describe growing the *Agrobacterium* for two nights (Vogel and Hill 2008; Alves et al. 2009; Bragg et al. 2012), however in our hands one night is enough to create a layer that completely covers the plate. Scrape of the bacteria, using a sterile pasteur pipet that is bent in an L-shape near the top (this can easily be done a few days before by heating the bending site by flame and carefully bend it, then autoclave in a box). Collect the bacteria in 50mL falcon tube (both colonies of same construct can be combined) and add between 30-50mL of CIM. Shake well and take 100μL into a cuvette to measure the OD at 600nm, mix it with 900μL of CIM and take 1mL of CIM as blank. Normally the optical density (OD) of this 10x diluted sample will be between 0.25 (for 1 colony) and 0.6 (for 2 colonies). Calculate the amount of bacteria-CIM mixture that is needed to make 20mL of mixture with OD=0.6 per transformation. Normally this is enough for 6-9 plates of subcultured calli. If 10 or more plates are to be combined, use 40mL of bacteria-CIM mixture at OD=0.6. Collect calli in a clean 50mL falcon tube, just like for subculturing squeeze them carefully so they fall into smaller pieces and have more surface for transformation. Right before adding the bacteria-CIM mixture, add 200μL of 10% synperonic acid in water (prepare well in advance, since it is difficult to dissolve) and 20μL of acetosyringone (final concentration 200μM in water) to the 20mL mixture and mix well (section 7.5 Media used during this thesis). Add it to the calli and leave for 5min (timing does not seem to be crucial), while sometimes inverting the tube to mix calli with bacteria. After 5min let the calli sink to the bottom of the tube and pour off the excess of CIM (section 7.5 Media used during this thesis). The last bit can be removed by pipet and all calli can be transferred into a petri

dish with two sterile filter papers, spread them and let them dry for a few minutes. Then transfer them to new petri dishes with filter papers (normally 2-3 dishes is enough for 6-9 subculture plates), close them with 3M micropore tape and leave them overnight at 22°C in the dark. Next day check whether the calli have dried well; when tapping the top of the petri dish, calli should statically attach to the lid and some parts of calli should show a white overlay. If this is not yet the case, leave them to dry longer or transfer them to new petri dishes with sterile filter papers and wait another 2-3 hours. When calli dry for too long, they turn brown and become smaller, which often results in them dying afterwards, therefore we prefer to transfer after 1 day of drying. Other protocols sometimes dry 2 days, since the actual transformation supposedly takes place during this time (Vogel and Hill 2008; Alves et al. 2009; Bragg et al. 2012). For this, calli should be dried on 1-2 petri dishes instead of 2-3 so they remain wet enough. In our hands, no difference in transformation efficiency was found between 1 or 2 days of drying.

Once properly dried, transfer calli to H40 or P400 selection plates (section 7.5 Media used during this thesis), depending on the required selection. Split the calli into smaller pieces, since the sticky CIM mixture often makes them form big aggregates. Note that again the amount of calli will exponentially increase as compared to the 6-9 subculture plates, thus ensure that enough media is available. Also transfer extremely small calli, they often result in good regenerants later on. Place about 30 calli per plate and leave them space to expand. Culture them for another 2 weeks in the dark at 28°C, while checking them every few days for signs of *Agrobacterium* overgrowth. If a circle of bacteria just around and below a callus is observed, immediately transfer the remaining calli to new plates. Be careful not to accidentally touch *Agrobacterium* with the forceps, since this will result in more contamination on the new plate. We suspect *Agrobacterium* contamination to be coupled to how well timentin was solubilized in the culture media, therefore it is important that everything is dissolved by vigorously shaking the media before pouring the plates. After 2-3 weeks, subculture the calli onto new selection plates (H30 or P400, section 7.5 Media used during this thesis). The concentration of

hygromycin is decreased as compared to the first selection media, otherwise even transformed calli will not develop properly. Do not perform this step much later than 2.5 weeks after transformation, since calli will regenerate less well afterwards. Carefully squeeze calli and try to separate black parts from brown or yellow (healthy) calli. Black parts do not need to be transferred, however brown parts may sometimes still recover on H30 media. Often this step leads to about three-four times as many calli than before transfer. Paromomycin selection is weaker and normally yields only brown and yellow calli, therefore transfer to plates with the same amount of paromomycin can be done up to 3 weeks after transformation. After two more weeks of selection, calli can be transferred to regeneration media (H20 or P50, section 7.5 Media used during this thesis). Again, calli should be separated and black pieces of calli can be removed. In this step it is crucial to give calli enough space to expand (20 calli per plate) and poor thick plates, since thin plates may dry out. Close the plates well with 3M micropore tape and leave in 16h photoperiod at 28°C for as long as calli look healthy (light intensity around 60μE m-2 s-1). 6-9 plates of calli for transformation often result in 3 or 4L of regeneration media, therefore it is important to have enough space to keep all calli under proper light conditions at this stage. From this point onwards, transformed pieces of callus should be numbered every time they are transferred to new plates and fall into smaller pieces; all pieces from one callus will have the same insertion site and should therefore have the same number. Check calli regularly to see if they are developing shoots. If plates start to dry or shoots are turning brown, transfer all calli to new regeneration plates. In our hands, changing the plates every 2 weeks for hygromycin selection helps to develop healthier regenerants. For paromomycin selection, drying out is less common, however calli can become large and therefore need to be transferred. Once calli have developed shoots that are about 2.5-3 cm, they can be transferred to rooting media. We normally obtain around 8 shoots per regeneration plate (not all ready at the same time). Also smaller shoots or shoots that are starting to turn brown can be transferred; however they often will not develop proper roots and die afterwards. This is possibly due to them being false positives. Normally after 2-3 months on selection media, no more new shoots will develop

and plates can be thrown away.

About 9 shoots can be kept per magenta box with rooting media. Leave the magenta boxes in the same light conditions (16h photoperiod at 28°C) as regeneration plates. Once some of the regenerants reach the lid of the magenta box and have developed several leaves, they can be transferred to soil. Conditions are the same as discussed in section 2.1 Growth conditions: From seed to next generation seeds. Note that normally all calli will have developed 1 or 2 roots, those that have not, will likely never develop roots and die when they are moved to soil.

2.4 PCR or genotyping

PCR protocols have been optimized for many years, however basic PCRs and genotyping remain challenging in *Brachypodium*. An enzyme that often gives good results is the Q5 high-fidelity polymerase (M0491 NEB) or PrimeSTAR GXL (R051B Takara). Sometimes addition of 1μM betaine or 10% DMSO could help. Also, the annealing temperature of 60°C could be changed by testing a PCR in a gradient PCR program, in some cases higher or lower temperatures may aid the PCR reaction. Furthermore, it is often necessary to split bigger PCRs into smaller pieces of 1-2kb and connect them afterwards with for example a Gibson reaction or overlap-extension PCR. Sometimes it can be beneficial to amplify a piece of DNA that is bigger than the target, since especially the end of UTRs are often GC-rich. Pick a region beyond the GC-rich part for the primer to anneal, and this may make the PCR more successful.

DNA isolation

For genotyping and simple PCRs, it is often not necessary to isolate DNA. In order to save time on DNA extraction and PCR itself, we use the Thermo Scientific Phire Tissue Direct PCR Master Mix (F170 Thermo Scientific). Collect a 2cm piece of shoot in 50μL of dilution buffer in an eppendorf tube. It is not necessary to crush the leaves, however when using the template for a PCR, it may be good to push the leave with the pipet tip. If

PCR remains unsuccessful, DNA can be isolated by hand. This protocol results in DNA that is sufficiently pure for genotyping and most PCRs. Take four to six young leaves (or half of old leaves) per plant in a 2mL-eppendorf tube. Add a wooden ball and freeze in liquid nitrogen. Then use a Tissuelyzer to lyse the tissue for 1min at 30 per second. After lysis check that no tubes have broken, otherwise replace them and add 600μL of Extraction Buffer (50mM Tris (pH=8.0), 10mM EDTA (pH=8.0), 100mM NaCl and 1% SDS). Incubate samples for at least 10min at 65°C. Add 120μL 5M potassium acetate, vortex and incubate on ice for at least 10min (longer is better). Centrifuge at 13000g at 4°C for at least 10min and remove supernatant by decantation. Next rinse the pellet twice with 500μL 70% Ethanol and dry the pellet by vacuum rotation at 30°C. Do not over-dry the pellet. Resuspend the DNA in 50-100μL of water and measure the concentration.

PCR with Phire Tissue Direct PCR Master Mix

This protocol can be used for standard genotyping and simple PCR reactions. Add the following components to a PCR tube: 1μL 10μM forward primer, 1μL 10μM reverse primer, 7.5μL clean mQ, 10μL phire 2x buffer and 0.5μL DNA in dilution buffer. Run the following program: 98°C-5min, 98°C-5sec, (60°C-5sec, 72°C-30sec/kb) repeat 40x, 72°C-10min, 12°C-10min. A disadvantage of this kit is that it often gives false positives, therefore care has to be taken to use new water and primer dilutions.

PCR with GoTaq polymerase

In our hands, GoTaq polymerase (M300, Promega) was mainly used to avoid false positives when genotyping with the Phire Tissue Direct PCR Master Mix. The PCR was assembled as follows: 1μL 10μM forward primer, 1μL 10μM reverse primer, 4μL 5x GoTaq buffer, 0.5μL 10mM dNTP, 1μL DMSO, 0.5μL DNA in dilution buffer or 200ng purified DNA, 0.1μL GoTaq polymerase and mQ up to 20μL. Then run the following program: 95°C-5min, (95°C-30sec, 60°C-30sec, 72°C-1min/kb) repeat 40x, 72°C-10min, 12°C-10min.

PCR with Q5 high fidelity polymerase

Q5 high fidelity polymerase (M0491 NEB) was most often used for cloning. Set up the following reaction: 1μL 10μM forward primer, 1μL 10μM reverse primer, 0.5μL 10mM dNTPs, 100-1000ng purified DNA, 5μL 5x Q5 reaction buffer, 0.25μL Q5 polymerase and mQ to 25μL. Addition of 1μL DMSO or 1μL 25mM $MgCL_2$ could often aid the reaction. The run the following program: 98°C-3min, (98°C-30sec, 55-68°C-30sec, 72°C-30sec/kb) repeat 40x, 72°C-10min, 12°C-10min. The annealing temperature should be optimized with a gradient PCR for each different reaction.

PCR with PrimeSTAR GXL premix

If PCRs or genotyping remain unsuccessful with previously mentioned methods, a more expensive and time-saving solution could be the use of PrimeSTAR GXL premix (R051B, Takara). Assemble the PCR as follows: 1μL 10μM forward primer, 1μL 10μM reverse primer, 12.5μL primeSTAR mix, 1μL DMSO, 0.5μL DNA in phire dilution buffer or 200ng purified DNA, mQ up to 25μL. Takara advises lower concentration of primers, however in our hands these concentrations work better. Run the following program: (98°C-10sec, 60°C-15sec, 68°C-1min/kb) repeat 40x.

2.5 Observation of *Brachypodium* root via microscopy

As said before, 2-4 day old roots, grown on ½ MS plates are good for analysis. Choose roots that have neither grown into the air nor into the medium and cut about 1cm of the root tip. Immediately transfer the root to fixative, since roots start to turn brown as soon as the plate is opened. 24-well plates with 1-2mL of fixative (if roots can be mixed) or 96-well plates with 300μL of fixative (if every root has to be collected separately) are very useful to collect the roots. Since most fixative is toxic, perform these steps in a fumehood. Avoid the transfer of roots straight into an Ethanol-containing solution, this causes the roots to turn black within a few minutes and makes imaging very difficult. Once all roots have been transferred to fixative, they can be vacuum infiltrated to assure proper fixation.

Increase and decrease the vacuum three times and leave for 1-2h, then replace fixative and transfer plates to 4°C overnight. From here on protocols differ for the type of microscopy that needs to be performed, as will be discussed below. Once roots are ready to be checked with the microscope, they can be mounted on slides that have a small spacer. I often use a piece of tape and cut a square in the middle where the roots can be placed, this also prevents the mounting medium to leave the slide.

DIC microscopy

This protocol is obtained from Dr. David Pacheco-Villalobos, with some small adaptations. The procedure is best done in 2mL eppendorf tubes in the fumehood. The fixative (25mL) is prepared by: 1 mL glutaaraldehyde, 2.7 mL formaldehyde, 2.5mL NaPI (10x stock 0.5M pH7.2) and water up to 25mL. The NaPI stock can be made by adding 56mL of 0.5M monobasic sodium phosphate, monohydrate (NaH_2PO_4) and 144mL of 0.5M dibasic sodium phosphate (Na_2HPO_4) together. After overnight fixation at 4°C, rinse the roots 4 times with water. Then add 10% KOH solution until the roots are completely covered and incubate at 95°C in a thermoblock for 30min. After incubating in KOH the roots become very fragile, therefore take care not to damage them. Mount the roots in a few drops of 50% glycerol on top of a slide for microscopy and image the roots with a DIC microscope.

ClearSee protocol

This protocol was adapted from the Geldner laboratory, who based it on Kurihara et al (Kurihara et al. 2015; Ursache et al. 2018). Imaging with this protocol works better than mPS-PI staining, since penetration into the root is higher. The fixative used in this protocol is prepared by weighing 4g of paraformaldehyde and dissolving it in 100ml 1x PBS while heating it on stirrer up to max 60°C (do not boil solution). Raise the pH by adding drops of 1M NaOH until solution clears and then adjust pH to ~ 6.9 with HCl. Cool down the solution before use. After overnight fixation, wash roots twice in 1x PBS and then add ClearSee solution. This solution consists of 10% (w/v) xylitol, 15% (w/v) sodium

deoxycholate (wear mask) and 25% (w/v) urea. Prepare chemicals in water and mix solution well with magnetic stirrer (while warming to max 60°C) until everything is dissolved. Seal the plates and leave for 3-4 weeks at room temperature, replace solution every week and check whether roots are already cleared enough. Samples can be stored like this up to 5 months. 2 days before microscopy, stain the roots with a solution of 0.2% calcofluor in ClearSee. Incubate overnight in the dark and next day wash with agitation for 30min in ClearSee. Then replace the solution and leave in ClearSee overnight before imaging. After staining, roots can be kept in the dark for another week before imaging, however the signal will decrease. If imaging is performed later, redo Calcofluor staining. Mount the samples in 100-200μL of ClearSee solution per slide. Settings for the confocal microscope should be as follows: Calcofluor white: excitation 405 nm and emission 410-509nm, GFP excitation 488nm and emission 493-523nm, NLS3xVenus excitation 488nm and emission 519-572nm, RFP excitation 561nm and emission 600-650nm. There is always background fluorescence in the meristem, therefore it is important to take proper images of controls without fluorophores. *Brachypodium* roots are too thick to be imaged from top to bottom, therefore microscopy is limited to a bit over halfway.

2.6 Transversal sectioning of embedded roots

This protocol was adapted from Dr. Yeon Hee Kang. Cut about 1cm of the root tip and fix as discussed before. Fixative is 1% glutaraldehyde, 4% formaldehyde and 50mM sodium phosphate buffer (pH 7.2). Next, roots are dehydrated by vacuum infiltration for at least 1h in each of following solutions: 15%, 30%, 50%, 70%, 85% and 100% ethanol (EtOH), then 100% EtOH overnight at 4°C. Then infiltrate the roots with 50% infiltration solution (100mL Technovit 7100 and 1g Hardner I; (Kulzer technique 64709003)) and 50% EtOH under vacuum for 3-4 hours. Protect samples from light with aluminium foil. Replace infiltration solution and store at RT for at least overnight. Roots can then be embedded in PCR-tubes to remain relatively straight. Fill the tube with embedding solution (10mL TechnoVit 7100 and 1mL Hardner II) and add the root with the tip pointing to the bottom of the tube. Avoid the root sinking to the bottom before the liquid hardens. Close the lid of

the PCR tubes and avoid air bubbles. Once the solution has hardened, cut the PCR tubes and the upper part of the sample with a scalpel to make it straight. Also cut the thin part that was in the tip of the PCR tube, as close to the root tip as possible. Next attach it to a wooden block with fast-drying glue and wait for at least 1h before going for microtome. At the microtome (Leica RM2255), orient the roots as straight as possible (*Brachypodium* roots are rather easy to see) and trim the first part of the embedding block until the tip of the root, use high speed and 10μm sections (bigger sections may lead to breaking the sample or dis-attachment from the woodblock). Now change to sections of 3μm in size with lower speed (3-5) and carefully collect the sections with forceps, don't squeeze them. Transfer the sections to a preheated slide overlaid with water on a 42°C heating plate. The section should automatically unfold if it was not damaged during transfer. Microtome sectioning may take some time to learn, therefore it is advisable to start with unimportant test samples to get used to working with it. Be very careful with the knife, it should be completely new so that no lines are visible on the section near the sample (lines indicate that the knife is damaged and often pull the section into a different shape or even destroy the sample). If lines do appear, slightly move the knife so that the damaged part is not near the sample on the section. Making sections by manually adjusting the speed may help, as one can speed up or slow down at parts that sometimes break. After drying the sections, stain them by dunking the slides for 30seconds into 0.1% toluidine blue and wash several times in water. Visualize with a Leica DM5000 microscope.

2.7 *In situ* hybridization

This protocol is a combination of protocols obtained from Dr. Zhongjuan Zhang, Dr. Pauline Anne, Cecilia Aligia, the Langdale Laboratory and the Rüdiger laboratory (Roth et al. 2001; Kirschner et al. 2017). For *in situ* hybridization it is very important to work in an RNAse free environment. Glassware and metal can be made RNAse free by baking in a 180°C oven for at least 8 hours. Buffers can be made RNAse free by treatment with DEPC and plastic ware or surfaces should be cleaned with RNAseZAP (Sigma, R2020-

250mL). The sample embedding takes 7 days, after which they will be sectioned (normally also takes 1 day), then the *in situ* itself takes another 3-5 days. The probe can be prepared during the days used for embedding.

Creating the probe

Probe design is crucial for good *in situ* hybridization. Use the cDNA of a gene of interest and BLAST it against the *Brachypodium* genome (Goodstein et al. 2012). Pick a region that has only few matches with other parts of the genome, preferably around 300 base pairs long. The 5'UTR can be included, however most of them have not been experimentally verified and may possibly not exist. 50 base pair overlaps with other parts of the genome may not be a problem, especially if they include some mismatches. The GC content should preferably lie between 40 and 60%. Add a SalI restriction site at the beginning and NotI at the end of the probe and synthesize probe. Note that these restriction sites were chosen since they will not leave a 3'-overhang, which is disadvantageous for probe amplification. Digest pBLUESCRIPT SK- with KpnI and SalI, perform a mungbean treatment to create blunt ends and purify the product. Dephosphorylate at 37°C for 1h and deactivate at 65°C for 5min. Ligate the probe into the KpnI-SalI digested pBLUESCRIPT SK- and obtain a miniprep of a good colony. Note that other vectors are possible as well, as long as they contain two of the following RNA polymerase sites: T7, T3 or SP6. Next linearize the plasmid with probe by digesting with KpnI (for antisense probes) or SalI (for sense probe). If digestion is complete, add 100µl phenol:chloroform:isoamylalcohol (25:24:1), vortex and spin 5min at 13000rpm and transfer upper phase in new EP tube (~100µl). From here on everything should be RNAse free. Precipitate with 0.1 volume of NaOAc (~10µL) and 2.5V EtOH (~250µL) and incubate 30min at -20°C (or overnight). Spin 10min at 4°C at 13000rpm and wash the pellet with 70% EtOH (RNase-free); air-dry and resuspend in H2O (RNase-free) to about 0.5µg/µl (start with 15µl-20µL). Next, prepare the transcription reaction on bench to avoid precipitation of transcription buffer: 1µg of linearized plasmid (also works with down to 0.2µg), 4µl 5x transcription buffer (Promega), 2µl 100mM DTT (Promega), 2µl 10x

Digoxygenin labelling mix (10mM, Roche, Cat.no. 11277073910), 1µl RNase-Inhibitor (Promega, Cat.no. N2111), 2µl appropriate RNA polymerase (Promega, T7-RNA-pol is Cat.no. P2075, T3-RNA-pol is P2083) and RNase-free water to 20µl. Incubate for 2h at 37°C, then perform DNase treatment by adding 1µl DNase (RNase free) and incubate for 15-30min at 37°C. Run 0.5µl on an agarose gel to check whether the transcript has the correct size. The RNA might have bands at multiple sizes due to secondary structures.

If the designed probe is greater than 150bp, the probe could be hydrolyzed to about 150bp pieces, however probes up to 500bp can still enter the cells without problems and have higher specificity. Add 80µl H2O and then 100µl 2x carbonate-buffer (80mM $NaHCO_3$ 120mM Na_2CO_3). Incubate at 60°C for x minutes.

$$X = \frac{\text{Original length of probe (kb)} - \text{desired length (0.15)}}{0.11 * \text{original length} * \text{desired length}}$$

Add 10µl 10% Acetic acid to stop the reaction and precipitate with 0.1 volume 3M NaOAc (21µl) and 2.5 volume EtOH (577µl) at -20°C for 1h to overnight. Spin at 13000rpm, 4°C for 20min and wash with 70% EtOH, then air dry the pellet. Resuspend in 50µl 50% formamide. Check 2µl with nanodrop and dilute probe for first trials; the following amounts of probe should be tested: 2.5, 0.5 and 0.1ng/µl/kb. If probe is 300bp and 100uL of hyb that gives: 75, 15 and 3ng per slide. Therefore make 15ng/µL probe dilution in 50% formamide and use: 10µL, 2µL and 0.4µL resp. Aliquot and store at -80°C for up to 3 months. Note that it may be useful to check the probe labeling by dotting different concentrations of probe on a membrane, this can also be useful to check whether the prepared solutions are indeed working and do not cause unexpected background.

Sample preparations

Cut 1cm of root and fix the samples in fixative (4% paraformaldehyde, 0,1% tween-20, 0,1% triton x-100, 1XPBS). Infiltrate in vacuum on ice, add an release the vacuum

carefully 3 times (5 minutes each), then replace fixative and leave at 4°C overnight. The next day, wash twice in 1xPBS, then 1h in each of the following solutions 30%, 40%, 50%, 60%, 70% and 85% EtOH in DEPC-treated water. Then 1h in 95% EtOH in DEPC-treated water with 0.1% Eosin, move samples to 4°C and leave overnight. If necessary, samples can be transferred to 4°C and left overnight already from 60% EtOH step onwards. The next day, wash the samples in 100% EtOH in DEPC-water twice for 30min and twice for 1h while shaking. Next transfer the samples to falcon tubes and add 25% histoclear and 75% EtOH for 1h (while shaking), then 1h each in 50% histoclear/50% EtOH, 75% histoclear/25% EtOH and 100% histoclear. Next replace histoclear with new 100% histoclear and add a quarter volume of Paraplast Plus (P3683 Sigma) solid pieces and leave overnight at room temperature. Next day, warm sample to 42°C until wax is dissolved, then add a quarter more (solid) wax and keep at 42°C until all wax has melted, then place at 60°C for few hours. In the meantime, dissolve more wax in an RNAse free bottle and after 4-5hours replace the wax-histoclear mixture with pre-melted wax. Since wax solidifies very easily, this is best done with a portable waterbath or preheated DEPC water in an RNAse-free bucket. Keep an RNAse-free falcon tube holder in the water bath or bucket and quickly poor off the wax-histoclear mixture, put it in the 60degrees water and poor new wax. Make sure that the wax in the sample does not solidify in the process. Then leave overnight at 60°C. For the next two days, replace the wax twice a day with pre-melted wax in order to remove all the histoclear from the samples. Now the samples can be sectioned, therefore heat a heat-plate to ~65°C, pre-warm small petri dishes wrapped in aluminium molds on it and pour liquid wax with samples into the petri dishes. Keep the molds warm until samples are oriented correctly, which can be done with RNAse-free forceps that were heated at a fire to prevent the wax from sticking to them. Roots can be placed with the tips in the same direction with ~5mm space or more in between them. Let the wax solidify for at least 30min, then move them to 4°C. Before sectioning, the wax can be cut with a thick razorblade to get close to the sample, however be careful not to break samples in the process. Carefully mark the lines to cut and then slowly apply more preasure. Cut the wax in pieces that have a trapezoid shape, both

sides parallel, leaving ~1mm space to the sample. Attach the samples to the wood blocks by melting wax in 2mL eppendorf tubes. Also quickly heat the bottom of the sample on the heat block, then poor some liquid wax on a wood block and push the sample into it. Samples can be stored like this at 4°C for a few weeks. Next cut 10μm sections as discussed in section “microtome” and collect them on a superfrost slide with DEPC-treated dH_20 that was preheated on 42°C heating plate. Dry the slides and store them in sterilized glass boxes at 4°C.

In situ hybridization

Prepare 250mL (per slide rack of 10 slides) of following solutions:

· _Pronase 0,125mg/ml (250ml for 10slides: 12.5ml 2M Tris pH=7.5, 25ml 0.5M EDTA in DEPC, add 625uL 50mg/mL pronase stock when stated in protocol)

· _Glycine 0.2% in 1x PBS (250mL for 10slides; 5mL 10% Glycine in 245mL 1x PBS)

· _4% PFA in PBS (prepared like for the fixation of the root in the beginning, but without Tween and Triton) (250mL for 10slides, 10g PFA in 225mL DEPC, 25mL 10x PBS add 125uL 1M NaOH, pH = 7)

· _Acetic anhydride in 0.1M triethanolamine pH8 (for 250ml: 3.25mL triethanolamine, 0.875ml HCl, 243.88mL H_2O; measure pH with pH strips)

Add right before/during use: 2ml acetic anhydride; stir well.

· _0.85% NaCl (250 mL for 10slides, 25mL 8.5% NaCl, 225mL DEPC water)

· _95% EtOH (300mL for 10slides, 285mL EtOH, 15mL DEPC water)

· _85% EtOH, 0.85% NaCl (300mL for 10slides, 255mL EtOH, 15mL DEPC water, 30mL 8.5% NaCl)

· _70% EtOH, 0.85% NaCl (300mL for 10slides, 210mL EtOH, 60mL DEPC water, 30mL 8.5% NaCl)

· _50% EtOH, 0.85% NaCl (300mL for 10slides, 150mL EtOH, 120mL DEPC water, 30mL 8.5% NaCl)

· _30% EtOH, 0.85% NaCl (300mL for 10slides, 90mL EtOH, 180mL DEPC water, 30mL 8.5% NaCl)

· _1x PBS (500mL for 10slides, 50mL 10xPBS in 450mL DEPC)

Put the solutions in glass or plastic boxes, labeled as mentioned in table below (5 labeled RNAse free glass boxes in fumehood and 12 labeled RNAse free plastic boxes). Do not add pronase yet to box 12, but move the pronase buffer to 37°C keep box 14 in the fridge until noted in the table and add acetic anhydride to box 16 when noted in table. Add RNAse free stirrer and something to keep slides above the stirrer to boxes 1,2 and 16. Put RNAse free stirring machine ready in hood.

Glass box 1, stir	FUMEHOOD	Histoclear 1	10min
Glass box 2, stir	FUMEHOOD	Histoclear 2	10 min
Add pronase to box12			
Glass box 3	FUMEHOOD	100% EtOH	1min
Plastic box 4, dunk 15x		100% EtOH	30 sek
Plastic box 5, dunk 15x		95% EtOH	30 sek
Plastic box 6, dunk 15x		85% EtOH, 0.85% saline	30 sek
Plastic box 7, dunk 15x		70% EtOH, 0.85% saline	30 sek
Plastic box 8, dunk 15x		50% EtOH, 0.85% saline	30 sek
Plastic box 9, dunk 15x		30% EtOH, 0.85% saline	30 sek
Plastic box 10, just sit		0.85% saline	2 min
Plastic box 11, just sit		PBS1	2 min
Plastic box 12, just sit		Pronase	10 min 37°C (water bath or oven)
Prepare box 14 (Keep PFA cold till use)			
Plastic box 13, just sit		0.2% Glycine	2 min
Plastic box 11, just sit		PBS1	2 min
Glass box 14, just sit	FUMEHOOD	Paraformaldehyde	10 min
Plastic box 11, just sit	FUMEHOOD	PBS1	2 min
Plastic box 15, just sit	FUMEHOOD	PBS2	2 min
Glass box 16, add acetic anhydride while stirring	FUMEHOOD	acetic anhydride in 0.1M triethanolamine	10min
Prepare box 16			
Plastic box 15, just sit	FUMEHOOD	PBS2	2min
Plastic box 10, just sit		0.85% saline	2 min
Dehydrate:		Dehydrate:	
Plastic box 9, dunk 15x		30% EtOH, 0.85% saline	30 sek
Plastic box 8, dunk 15x		50% EtOH, 0.85% saline	30 sek
Plastic box 7, dunk 15x		70% EtOH, 0.85% saline	30 sek
Plastic box 6, dunk 15x		85% EtOH, 0.85% saline	30 sek
Plastic box 5, dunk 15x		95% EtOH	30 sek
Plastic box 4, dunk 15x		100% EtOH	30 sek
Plastic box 17, dunk 15x		100% EtOH	30 sek

Leave the slides on the clean bench to dry. Trash glass box 3 with histoclear waste, PBS1 with PFA waste, PBS2 with acetic anhydride waste. If more slide racks are to be prepared on the same day, replace histoclear, 100% EtOH, pronase solution, PBS1 and 2 and triethanolamine solution in between, other solutions can be reused. A new slide

rack can most easily be started after the acetic anhydride step (during 2min in PBS 2). In the mean time thaw hybridization buffer (84μL per slide) and probes on ice, add 50% Formamide to the probe up to 16μL. As said before, if dilution is 15ng/μL of probe, then for 300bp probes in 100μL hybridization solution per slide, one should use 10μL, 2μL and 0.4μL for the first trials. Place probes for 2min at 80°C and immediately cool them down on ice. Mark slides with Pap pen in a rectangle around the samples. Mix hybridization buffer with probe (16μl probe with 84μL hyb, gives 100μL per slide), this is very difficult, therefore use cut-off pipet tips and warm hybridization buffer before pipetting. Pipette 100μL per slide and carefully place coverslip on top. Prepare a humidity box (2L Tupperware boxes per 10 slides) by soaking paper with 50% formamide. Put the slides in RNAse-free spacers and transfer them to the box without touching the solution. Incubate overnight at 50°C (in oven). Temperature can be somewhere between 45-55°C depending on the probe, however the washing steps should take place at the same temperature. Prepare wash buffer for the next day (2 X SSC, 50% formamide) and keep in oven overnight as well. The amount of SSC can vary between 0.5x and 5x depending on the probe used, also many protocols do not use formamide. Next day, dip slides into trough with pre-warmed 50°C wash buffer to carefully remove coverslips. If they are removed by force this will destroy the samples. Move slides to slide-rack in new box with pre-warmed wash-buffer and incubate at 50°C for 30min, then replace wash buffer and leave for 1.5h at 50°C. If more than one slide rack is to be prepared, keep 7 to 8 minutes in between them to not get into trouble for the timing of the following steps. From here on, buffers do not need to be RNAse free anymore. Prepare 1.5L 1 x NTE per slide rack (150mL 10 X NTE in 1350mL dH2O) and move to 37°C oven or waterbath to preheat. Prepare DIG-buffer 1, 2 and 3 (section 7.5 Media used during this thesis). Wash in 1x NTE at 37°C for 2x5min, during the second washing step pre-incubate 1xNTE containing 20μg/ml RNase in a new glass box for 5min at 37°C. Then move slide-rack into pre-incubated box with RNase A for 30min at 37°C. Wash in NTE three times for 5min at 37°C. These steps in NTE-buffer can be omitted if RNase treatment of non-bound probe

is not needed. Next wash the samples in wash buffer for 1h at 50°C and then in 1X PBS for 5min at RT. If needed, samples can be stored at 4°C in fresh PBS, however the signal will be less intense. Incubate slides (while gently shaking) in the following solutions: for 5min in 1 x DIG-buffer 1, 30min in DIG-buffer 2 and for 30min in DIG-buffer 3. During these washes, cut parafilm in the size of coverslips and carefully loosen one corner without folding the parafilm. Remove the slides from the rack and place them into slide-holders in humid boxes with water (no formamide). Pipette 100μl buffer 4 on top of each slide; cover carefully with parafilm (avoid bubbles) and store them for 2h at RT in the dark on the bench. If needed, slides can then be transferred to the fridge overnight (move them carefully), however it is better to continue to the detection step. Prepare buffer 5 and 6 (keep cold and in the dark) during the waiting. After the antibody step, carefully remove paraflim with forceps without damaging the samples. Then move slides back to racks and wash (while gently shaking): four times 20min in Buffer 3, then 5min in Buffer 1 and 5min in Buffer 5. Place the slides back in humidity box and pipette 200μL buffer 6 on top, cover carefully with coverslip and leave at RT on the bench in the dark. Check staining on the next day, this is best done under a microscope. If longer staining is needed, BCIP-solution has to be changed every day by carefully pipetting more near the edge of the coverslip. Once signal is observed (a purple color), stop the reaction by washing in water or TE-buffer. Now slides can be checked immediately by microscope, samples should be mounted in 50% glycerol (up to 72hours). In case longer storage is required, put the slides back into the racks and wash for 30sec in the following solutions: dH2O, 70% EtOH, 95% EtOH, 100% EtOH, 95% EtOH, 70% EtOH and dH_2O. Incubate slides in 0.1% calcofluor for 5min and wash briefly in dH_20. Air dry slides in fume hood, add 2-3 drops of Entellan mounting medium, cover with cover slip and dry in the fume hood overnight.

3. Broad spectrum developmental role of *Brachypodium* AUX1

Alja van der Schuren, Catalin Voiniciuc, Jennifer Bragg, Karin Ljung, John Vogel, Markus Pauly and Christian S. Hardtke.

New Phytologist, June 2018, **Vol. 28: 1009–1024**

Key Findings

- BdAUX1 is essential for *Brachypodium* development and seems to be involved in many more processes than AUX1 in *Arabidopsis*.
- *Bdaux1* roots display increased cell elongation and counterintuitively have a higher free auxin content.
- *Bdaux1* and *Bdtar2l*^{hypo} mutants have a very similar phenotype.

My contribution

With the exception of Figure 3, I designed and performed all experiments in this paper in discussion with Dr. Christian S. Hardtke. Auxin analysis (Fig 3A) was performed by Dr. Karin Ljung and cell wall analysis (Fig 3B) was performed by Dr. Catalin Voiniciuc. The cloning of *BdAUX1::NLS3xVENUS* and *BdAUX1::BdAUX1* was performed by Dr. Amelia Amiguet Vercher, the latter I used as a template to create the *BdAUX1::GFP-BdAUX1*. I performed phenotype analyses, from seedling to mature plants and flowers. I also introduced the *BdAUX1::NLS3xVENUS* and *BdAUX1::GFP-BdAUX1* constructs *in planta.* After optimization of confocal microscopy analysis, I characterized the expression pattern and protein localization of these constructs. I performed crosses between *Bdaux1* and *Bdtar2l*^{hypo} and analyzed their offspring phenotypes. I optimized microtome sectioning and counted cells for all presented genotypes. I created a CRISPR-Cas vector and used it to create *Bdaux1* CRISPR mutants.

New Phytologist

Research

Rapid report

Broad spectrum developmental role of Brachypodium AUX1

Author for correspondence:
Christian S. Hardtke
Tel: +41 21 692 4251
Email: christian.hardtke@unil.ch

Received: *24 April 2018*
Accepted: *10 June 2018*

Alja van der Schuren[1], Catalin Voiniciuc[2], Jennifer Bragg[3], Karin Ljung[4], John Vogel[3], Markus Pauly[2] and Christian S. Hardtke[1]

[1]Department of Plant Molecular Biology, University of Lausanne, Biophore Building, CH-1015 Lausanne, Switzerland; [2]Institute for Plant Cell Biology and Biotechnology, Heinrich-Heine University, D-40225 Duesseldorf, Germany; [3]DOE Joint Genome Institute, 2800 Mitchell Dr., Walnut Creek, CA 94598, USA; [4]Umeå Plant Science Center, Department of Forest Genetics and Plant Physiology, Swedish University of Agricultural Sciences, SE-901 83 Umeå, Sweden

New Phytologist (2018)
doi: 10.1111/nph.15332

Key words: AUX1, auxin, Brachypodium, monocotyledon, seminal root.

Summary

- Targeted cellular auxin distribution is required for morphogenesis and adaptive responses of plant organs. In *Arabidopsis thaliana* (Arabidopsis), this involves the prototypical auxin influx facilitator AUX1 and its LIKE-AUX1 (LAX) homologs, which act partially redundantly in various developmental processes. Interestingly, *AUX1* and its homologs are not strictly essential for the Arabidopsis life cycle. Indeed, *aux1 lax1 lax2 lax3* quadruple knock-outs are mostly viable and fertile, and strong phenotypes are only observed at low penetrance.
- Here we investigated the *Brachypodium distachyon* (Brachypodium) *AUX1* homolog *BdAUX1* by genetic, cell biological and physiological analyses.
- We report that *BdAUX1* is essential for Brachypodium development. *Bdaux1* loss-of-function mutants are dwarfs with aberrant flower development, and consequently infertile. Moreover, they display a counter-intuitive root phenotype. Although *Bdaux1* roots are agravitropic as expected, in contrast to Arabidopsis *aux1* mutants they are dramatically longer than wild type roots because of exaggerated cell elongation. Interestingly, this correlates with higher free auxin content in *Bdaux1* roots. Consistently, their cell wall characteristics and transcriptome signature largely phenocopy other Brachypodium mutants with increased root auxin content.
- Our results imply fundamentally different wiring of auxin transport in Brachypodium roots and reveal an essential role of *BdAUX1* in a broad spectrum of developmental processes, suggesting a central role for AUX1 in pooideae.

Introduction

Modulation of auxin activity through differential auxin distribution plays a central role in developmental and adaptive growth processes (Benjamins & Scheres, 2008; Zazimalova *et al.*, 2010). It is largely achieved through plasma membrane-integral auxin efflux carriers, the PIN-FORMED (PIN) proteins, whose polar cellular localization can lead to asymmetric auxin secretion. Coordination of PIN polarity across cell files thus can promote targeted, so-called polar auxin transport at the tissue and organ level (Benjamins & Scheres, 2008; Zazimalova *et al.*, 2010). In contrast to the carrier requirement for auxin efflux, cellular auxin influx can occur through diffusion, because in the acidic environment of the apoplast auxin is mostly protonated and thus lipophilic enough to cross the plasma membrane (Zazimalova *et al.*, 2010). Nevertheless, dedicated auxin influx facilitators, AUX1 and the LIKE AUX1 (LAX) proteins that accelerate auxin uptake have been identified (Maher & Martindale, 1980; Bennett *et al.*, 1996; Marchant *et al.*, 2002; Yang *et al.*, 2006; Peret *et al.*, 2012). Their differential expression, as well as often polar localization, can modulate polar auxin transport to reinforce or attenuate local auxin accumulations. *Arabidopsis thaliana* (Arabidopsis) mutants in the prototypical auxin influx facilitator AUX1 have been identified because of their root agravitropism (Maher & Martindale, 1980), which can be rescued by addition of the lipophilic auxin analog 1-naphthylacetic acid (1-NAA) (Swarup *et al.*, 2001). Mutants in the three *AUX1* homologs, *LAX1-3*, display either no, or less conspicuous phenotypes (Ugartechea-Chirino *et al.*, 2010; Vandenbussche *et al.*, 2010; Peret *et al.*, 2012). However, corresponding multiple mutants reveal (partially) redundant roles of AUX1 and LAX1-3, for instance in phyllotaxis (Bainbridge *et al.*, 2008) and embryogenesis (Robert *et al.*,

2015), although mutant phenotypes are not always fully penetrant. Moreover, AUX1 and LAX1-3 proteins are not fully interchangeable in every cellular context (Peret *et al.*, 2012).

Compared to the well characterized roles of AUX1/LAX1-3 in Arabidopsis, little is known about the developmental role of auxin influx facilitators in monocotyledons (Balzan *et al.*, 2014). Yet, AUX1 homologs can be readily identified, since they are highly conserved. For example, in rice (*Oryza sativa*) and the more distantly related panicoid grasses maize (*Zea Mays* L.) and *Setaria viridis* (Setaria), five AUX1 homologs have been identified (Zhao *et al.*, 2012; Huang *et al.*, 2017). In maize, the closest *AtAUX1* homolog has 73% sequence identity (Hochholdinger *et al.*, 2000). Functional studies of mutants in *AUX1* homologs in maize and Setaria demonstrated involvement of those genes in inflorescence development and root gravitropism (Huang *et al.*, 2017). Also, the *OsAUX1* gene has subsequently been implicated in lateral root formation and shoot elongation (Zhao *et al.*, 2015), as well as seminal root elongation and root hair elongation (Yu *et al.*, 2015). Although rice, maize and Setaria can be considered model systems for the grasses, it remains unclear whether findings from these species can be directly transferred to other groups within the poaceae. One such group is the pooideae, which comprise the major cereal crops wheat, rye and barley. The monocotyledon *Brachypodium distachyon* (Brachypodium) is a model species for these temperate cereals (Brkljacic *et al.*, 2011; Girin *et al.*, 2014). AUX1 homologs can be readily identified in the Brachypodium genome. However, unlike rice, maize or Setaria with five homologs, Brachypodium only possesses three AUX1 homologs, which display almost sequence identity with their Arabidopsis counterparts (Supporting Information Fig. S1). Nevertheless, slightly divergent N- and C-termini and the gene sequences allow the assignment of clear one-to-one homologies in sequence similarity analyses (Fig. 1a). Here we investigated the developmental role of the closest AUX1 homolog of Brachypodium, the *Brachypodium distachyon AUX1 (BdAUX1)* gene. We report that *BdAUX1* loss-of-function results in counter-intuitive root phenotypes and reveals its essential role in a broad spectrum of developmental processes, suggesting a more central and diversified role for AUX1 in pooideae.

Materials and Methods

Plant materials, genotyping and growth conditions

The *Bdtar2l*^{hypo} mutant has been described before (Pacheco-Villalobos *et al.*, 2013). The *Bdaux1* mutant line JJ5658 was obtained from a Brachypodium T-DNA insertion library (Bragg *et al.*, 2012). RT-PCR was performed to verify that the T-DNA insertion indeed leads to a truncated *BdAUX1* mRNA. To this end, the following oligonucleotides were used: F1 5′-ATG GTG CCG CGC GAG CAT G-3′, located at the start-codon; R1 5′-GCA TGA TCT CCA CTG TGA CG-3′, at the border of the T-DNA insertion; R2 5′-GGT GAA GCT GAC GAG TAG CG-3′, located 285 bp before the STOP-codon; and R3 5′- GAT CCG GTA GTT GTG GAA GG-3′, located 160 bp before the T-DNA insertion (see Fig. S2A). *Bdaux1*^{CRISPR} mutants were obtained directly as homozygotes from transformations (see below, 'Transformation') and could not be amplified due to their sterility. *Bdtar2l*^{hypo} *Bdaux1* double mutants were obtained by crossing. For tissue culture, seeds were sterilized as described (Bragg *et al.*, 2012) and stratified for 3 d at 4°C before transfer to plates with half-strength Murashige-Skoog (MS) media (2.45 g l^{-1} MS salts with vitamins, 0.3% sucrose, 1% agar, pH 5.7) placed vertically at a slight angle to prevent roots from growing into the media or the air. Unless indicated otherwise, analyses were performed on 2-d-old seedlings raised as previously described (continuous light of 100–120 µE intensity, 22°C, PhilipsF17T8/TL741 fluorescent light bulbs) (Pacheco-Villalobos *et al.*, 2013). Roots that had grown into the media or the air were excluded from analysis. For gravitropism assays, seeds were grown for 1 d on vertically oriented plates, which were then rotated 90° and seedlings were left to grow for another 2 d. Root length was measured using FIJI software (https://imagej.net/Fiji?Downloads). For auxin analysis, cell wall analysis and RNAseq, 1 cm seminal root segments harvested 2–3 mm above the root tip were used (Pacheco-Villalobos *et al.*, 2016). Genotyping of *Bdtar2l*^{hypo} was performed as described (Pacheco-Villalobos *et al.*, 2013). For *Bdaux1* genotyping, the wild type allele was monitored with primers 5′-GTG AAC TTT CCA CAC TGA GC-3′ and 5′-TCA CAA GAG CTG GGC AAT GG-3′, and the T-DNA insertion with 5′-GTG AAC TTT CCA CAC TGA GC-3′ and 5′-CAG GAA TTC ATG CCG ACA GC-3′. Double mutants were genotyped with the same methodology for both T-DNA insertions.

Plasmid construction

To create a vector with kanamycin resistance, the *nptII* sequence was amplified with primers 5′-CCA CTC GAG GAT CTC CAC TCT AGT CGA G-3′ and 5′-TGT CTC GAG TTG AAC GAT CGG GGA TCC-3′. The fragment was digested with *Xho*I and cloned into *Xho*I-digested pCAMBIA1305.1 to replace the hygromycin-resistance gene to give pCAMBIA1305.1-nptII. Next, *BdAUX1::BdAUX1* was amplified in three pieces from genomic DNA with primers 5′-CAT GAT TAC GAA TTC GAG CTC GTC ACT TAA TCT CGT C-3′ and 5′-CGA ATT TCC TCT CTG TCT CC-3′ for piece 1, 5′-GGA GAC AGA GAG GAA ATT CG-3′ and 5′-CAA TGC ACC TCA TCG TTC CA-3′ for piece 2, and 5′-CAA TGC ACC TCA TCG TTC CA-3′ and 5′-GGA AAT TCG AGC TGG TCA CCT AGC AAG CAT TAC TGG GTT-3′ for piece 3. The fragments were combined into *Sac*I–*Sal*I-digested pCAMBIA1305.1-nptII using Gibson ligation. *BdAUX1::NLS3xVENUS* was created by insertion of amplified *NLS3xVENUS* into *Hin*dIII–*Pml*I-digested pCAMBIA1305.1-nptII. The *BdAUX1* promoter was then amplified with primers 5′-CTA GAG CTC TGG ACG TGG TTT TGT CCT AG-3′ and 5′-ACG CGT CGA CAT CTC TTC AAC GCG CTG TC-3′, and inserted in front of *NLS3xVENUS* using *Sac*I and *Sal*I digestion. For BdAUX1 localization, a GFP fusion tag was added to the protein. To this end, *BdAUX1* promoter was amplified with primers 5′-GCG ACT GTG CCA ACA CCC-3′ and 5′-GCC CTT GCT CAC CAT CTC TTC AAC GCG CTG TCC TC-3′, the transcript region was amplified with primers 5′-GTC GAC

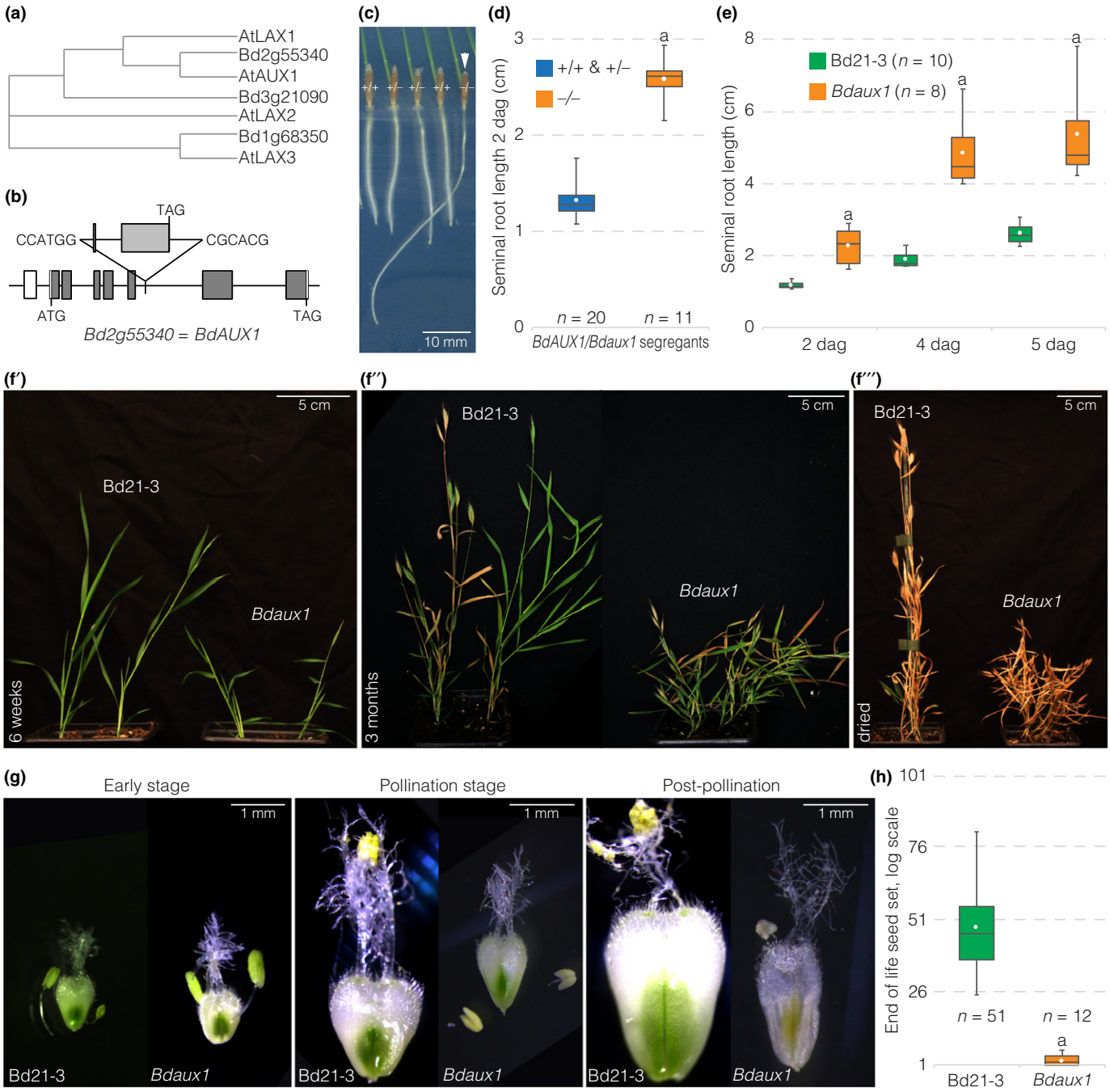

Fig. 1 Root and shoot phenotypes of the *Bdaux1* mutant. (a) Sequence similarity (Clustal alignment, neighbor joining, with distance correction) of Arabidopsis and Brachypodium AUX1 homologs. (b) Schematic presentation of the T-DNA insertion line for *BdAUX1*. (c) Representative seedlings (2-d-old) segregating in the progeny of a heterozygous *BdAUX1/Bdaux1* (±) mother plant, genotypes are indicated. (d, e) Seminal root length of indicated genotypes (dag, days after germination). (f) Shoot development of *Bdaux1* plants in comparison to its Bd21-3 wild type background at different stages of the life cycle. (g) Different stages of flower development in *Bdaux1* plants as compared to Bd21-3. (h) End of life seed set in indicated genotypes. Box plots display second and third quartiles, maximum, minimum and mean (white dot). Statistically significant differences are indicated (Student's *t*-test; a, $P < 0.001$).

TCT AGA GGA TCC ATG GTG CCG CGC GAG CAT-3′ and 5′-TTT TTC CTC GGG TTA GTT AAT TAA TTC-3′, and GFP was amplified from pVec8GFP with primers 5′-ATG GTG AGC AAG GGC GAG G-3′ and 5′-ATC CTC TAG AGT CGA CCT TGT ACA GCT CGT CCA TGC-3′. The three fragments were then combined into *Xma*I–*Pac*I-digested pCAMBIA1305.1-nptII in a Gibson reaction. The *BdAUX1* CRISPR/Cas9 cassette was created by amplifying the *Zea mays UBIQUITIN (UBQ)* promoter (Bragg *et al.*, 2012) using primers 5′-GAG CTC CAG CTT GCA TGC CTG CAG TG-3′ and 5′-GAG CTC TCT AGA GTC GAC CTG CAG AA-3′ and ligation of the fragment into *Sac*I-digested pCAMBIA1305.1. A *Brachypodium*-optimized Cas9 with FLAG-tag and nuclear localization signal (Methods S1), followed by a multiple cloning site, was synthesized and cloned

behind the *UBQ* promoter after *Kpn*I and *Bst*eII digestion, to create vector p5Cas. Next, a 770 bp cassette containing a *Brachypodium U6* promoter, *Bsa*I restriction sites, tracrRNA, a rice *U6* promoter, *Btg*ZI restriction sites and tracrRNA was synthesized (see Methods S1) and cloned into *Bam*HI–*Eco*RI-digested pDONR221. This allowed two sgRNA sequences to be added, using *Bsa*I and *Btg*ZI restriction sites, respectively. The *Bdaux1* knock-out cassette was then assembled by annealing, phosphorylating and ligating the following primer pairs into the *Bsa*I–*Btg*ZI-digested pDONR vector: 5′-TCT CGT CAC CAG CTT CCT CTG GCA-3′ and 5′-AAA CTG CCA GAG GAA GCT GGT GAC-3′ for sgRNA1, and 5′-GTG TGA TCC GGT AGT TGT GGA AGG-3′ and 5′-AAA CCC TTC CAC AAC TAC CGG ATC-3′ for sgRNA2. The sgRNA cassette was then isolated and ligated into p5Cas via *Bam*HI–*Hin*dIII restriction digest. Target specificity of the sgRNA was checked bioinformatically (http://bioinfogp.cnb.csic.es/tools/breakingcas/?gset=8x2_GENOMES_EnsemblGenomes_39).

Transformation

For Brachypodium transformations (Pacheco-Villalobos *et al.*, 2013) the *Agrobacterium tumefaciens* strain GV3101 pMP90 was used. *BdAUX1::NLS-3XVENUS*, *BdAUX1::BdAUX1* and *BdAUX1::GFP-BdAUX1* transformants in Bd21-3 and *Bdaux1* were selected on media with 400 μg ml^{-1} paramomycin and 600 μg ml^{-1} $CuSO_4$. Regeneration media contained 50 μg ml^{-1} paramomycin and 600 μg ml^{-1} $CuSO_4$. Transformants for the CRISPR/Cas9 *BdAUX1* knock out construct were selected on hygromycin as described (Pacheco-Villalobos *et al.*, 2013), with the addition of 600 μg ml^{-1} copper sulfate ($CuSO_4$) to the regeneration media.

Metabolic analyses, qPCR and RNAseq

For auxin measurements, three independent batches of two replicates each, containing 20 pooled 1-cm root segments per genotype were analyzed as described (Pacheco-Villalobos *et al.*, 2013, 2016). For cell wall polysaccharide quantifications, three independent pools of 100 to 120 segments per genotype were collected and freeze-dried overnight. The monosaccharide composition and glycosidic linkages of the wall material was analyzed as described (Pacheco-Villalobos *et al.*, 2016). qPCR on Brachypodium *AUX1* homologs was performed as described normalizing against *UBIQUITIN CONJUGATING ENZYME 18 (BdUBC18)* (Pacheco-Villalobos *et al.*, 2013). The following specific primers were used: 5′-CCA TGT CAT CCA GTG GTT CG-3′ and 5′-GAT GAG CTG GAT GAC GGA GC-3′ for Bradi1g68350; 5′-CGT CAT CCA GTG GTT TGA GG-3′ and 5′-CAG CCG ATG AGC TGG ATC AC-3′ for Bradi3g21090. For RNAseq, two independent pools of segments were collected from 12 roots per genotype. RNAseq was performed as described (Pacheco-Villalobos *et al.*, 2016). The raw data have been deposited in the NCBI Sequence Read Archive (https://www.ncbi.nlm.nih.gov/sra/) under accession SRP137652.

Microscopy

For microscopic imaging, seminal roots of 2-d-old seedlings were fixed 1 wk in 4% (w/v) paraformaldehyde in 1× phosphate-buffered saline (PBS) solution (pH 6.9). Roots were then washed two times in 1× PBS before transfer into ClearSee solution for at least one month, which was necessary to quench the challenging autofluorescence of Brachypodium roots. ClearSee solution was changed weekly. Then, 2–3 d before imaging, roots were stained with 0.2% Calcofluor White (in ClearSee) solution for 1–2 h with gentle shaking, next washed in ClearSee solution until imaging. Root hairs were imaged in differential interference contrast using a Leica DM5000 microscope. For meristem analyses, stained roots were mounted in ClearSee solution and imaged with Zeiss 880 or LSM710 inverted confocal microscopes using ×40 oil objectives. For Calcofluor imaging, roots were excited with a 405 nm laser and emission signal was captured over 410–509 nm. GFP was imaged with sequential scans using the 518 nm Argon laser and a 493–523 nm emission spectrum to reduce background. NLS-3×VENUS was imaged as a sequential scan and excited with a 488 nm laser, emission was recorded at 519–572 nm to reduce background. Cell length measurements were performed with FIJI software.

Microtome sectioning and analysis

Seminal roots of 2-d-old seedlings were fixed overnight at 4°C in 1% glutaraldehyde, 4% formaldehyde and 50 mM sodium phosphate buffer (pH 7.2). Roots were dehydrated for at least 1 h each in 15%, 30%, 50%, 70%, 85% and 100% ethanol (EtOH). Samples were pre-incubated and embedded in TechnoVit 7100 solution as described (Pacheco-Villalobos *et al.*, 2013). 0.3-μm sections were obtained on a Leica RM2255 microtome. Sections were stained with 0.1% toluidine blue before visualization with a Leica DM5000 microscope. Cell numbers were counted in one representative image per root using the cell counter plugin of IMAGEJ software. (https://imagej.nih.gov/ij/plugins/cell-counter.html)

Results and Discussion

To investigate the role of auxin influx facilitators in Brachypodium, we obtained a T-DNA insertion line in Bradi2g55340 (*BdAUX1* hereafter), the closest homolog of Arabidopsis *AUX1* (*AtAUX1*) in Brachypodium. In this *Bdaux1* mutant allele, *BdAUX1* is disrupted by an insertion in the 6th intron, which leads to a truncated mRNA (Figs 1b, S2). Plants that were homozygous for this insertion displayed agravitropic roots (Fig. 1c), similar to *Ataux1* loss-of-function mutants (Maher & Martindale, 1980; Bennett *et al.*, 1996). Thus, the T-DNA insertion apparently results in *BdAUX1* loss of function. However, unlike *Ataux1* mutants, *Bdaux1* mutant roots were considerably longer than those of their wild type siblings or the corresponding Bd21-3 wild type background line (Figs 1c–e, S3A). Quantitative RT-PCR (qPCR) suggested that this phenotype was not due to possible (over)compensatory up-regulation of the two other *AUX1* homologs in Brachypodium (Fig. S2B).

Bdaux1 plants also displayed a dwarf shoot phenotype with aberrant flower development (Fig. 1f,g). *Bdaux1* mutants were thus sterile (Fig. 1h) and could not be maintained as homozygotes in practice. Both the root and shoot phenotypes could be complemented by introduction of transgenes that expressed either BdAUX1 or GFP-BdAUX1 fusion protein under control of the native *BdAUX1* promoter *(BdAUX1::BdAUX1* and *BdAUX1::GFP-BdAUX1)* into the *Bdaux1* background (Fig. S3B,C). Moreover, the mutant phenotypes were also observed in *Bdaux1* homozygous knock out plants that were generated by the CRISPR/Cas9 technique ($Bdaux1^{CRISPR}$). This included the severe shoot phenotype and infertility (Fig. S3C,D), which also precluded recovery of the lines. Therefore, *Bdaux1* loss-of-function was causative for the observed mutant phenotype.

A more detailed characterization of the mutants revealed that their increased root elongation could be attributed to increased mature cell length (Fig. 2a). Moreover, *Bdaux1* roots were markedly thinner than wild type roots (Fig. 2b). Although the number of cell files was significantly reduced in every tissue except xylem and phloem (Fig. 2c), this alone could not entirely account for the overall reduction in root thickness. Rather, cells generally appeared slightly smaller in radial sections (Fig. 2b), and at the same time, root hairs were markedly shorter, reduced in number and appeared later than in wild type (Fig. 2d). Therefore, the *Bdaux1* root elongation phenotype was apparently caused by overall higher cellular anisotropy. Interestingly, it thus resembles the roots of hypomorphic mutants in the Brachypodium *TAR2-LIKE* (*TAR2L*) gene (Pacheco-Villalobos *et al.*, 2013). $Bdtar2l^{hypo}$ mutants are partially impaired in a rate-limiting step of auxin biosynthesis, which results in higher cellular auxin levels in the root because of the particular regulatory wiring in Brachypodium (Pacheco-Villalobos *et al.*, 2013, 2016). To further explore the similarity between *Bdaux1* and $Bdtar2l^{hypo}$ mutant roots, we also determined cellular auxin levels in *Bdaux1* root tips. Indeed, we again observed increased auxin levels (Fig. 3a). This result was surprising, given the Arabidopsis precedent that AUX1 is needed for efficient shoot to root mobilization of auxin, and *Ataux1* mutants therefore have reduced, rather than increased, auxin levels in the root (Marchant *et al.*, 2002). In $Bdtar2l^{hypo}$ plants, the root phenotype was also associated with slight alterations in cell wall composition, notably a reduction in 1,3-galactosyl and 1,2-galactosyl residues, suggesting an altered arabinogalactan structure, and an increase in 1,4-glucosyl residues (Pacheco-Villalobos *et al.*, 2016). Similar changes were observed in *Bdaux1* root tips (Figs 3b, S3E), again confirming similarity with $Bdtar2l^{hypo}$ plants. Finally, a survey of the *Bdaux1* transcriptome in elongating root tip segments revealed a number of differentially expressed genes, mostly in cell wall modifiers (Table S1), which were *c.* 10-fold over-represented ($P = 2.33E\text{-}5$). Again, this observation matches what has been described for $Bdtar2l^{hypo}$root segments (Pacheco-Villalobos *et al.*, 2016), although the scope of transcriptional changes was less dramatic in *Bdaux1*. A notable commonality was the strong upregulation of expansins, which are thought to be primary targets of auxin-induced cell elongation (Cosgrove, 2005). Confirming the qPCR analysis, no differential expression of the two other *AUX1* homologs was observed in the *Bdaux1* transcriptome (Table S2). In summary, in many ways *Bdaux1* roots phenocopy $Bdtar2l^{hypo}$ roots.

Similarities with *Bdtar2l* mutants could also be observed in the shoot. In mutants of the hypomorphic $Bdtar2l^{hypo}$ allele, the root phenotype is accompanied by a slight reduction in leaf blade length and width (Pacheco-Villalobos *et al.*, 2013). However, in mutants of the null allele $Bdtar2l^{null}$, the root phenotype is weaker and transient, while the shoot displays a dwarf phenotype that is accompanied by severely reduced fertility (Pacheco-Villalobos *et al.*, 2013). Thus, the shoot phenotype of $Bdtar2l^{null}$ plants is similar to *Bdaux1* plants. The strongly reduced fertility of *Bdaux1* appeared to be due to delayed development of anthers as compared to gynoecia as well as poor pollen viability (Fig. 1g). Nevertheless, because plants heterozygous for *Bdaux1* were similar to wild type, we could create double mutants with the $Bdtar2l^{hypo}$ allele. Overall, the phenotype of these *Bdaux1* $Bdtar2l^{hypo}$ double mutants appeared to be additive as compared to their segregating single mutants and wild type siblings (with the caveat that background loci might modulate the phenotypes to some degree because the two single mutants had different wild type parents). The dwarfism of *Bdaux1* plants was more exaggerated in *Bdaux1* $Bdtar2l^{hypo}$ double mutants (Fig. S3B,F), and the double mutant roots were thinner than in either single mutant and longer than in $Bdtar2l^{hypo}$ alone (Fig. S3G). This could be attributed to an even higher mature cell length, and an additional reduction in cell files (Fig. S2H). However, unlike the single mutants, the double mutants displayed a reduced root meristem size that was accompanied by slight changes in root meristem organization, such as an apparently smaller quiescent center (Fig. S3I,J). Overall, the data suggest parallel impacts of *BdAUX1* and *BdTAR2L* mutation that reinforce each other. This is also consistent with the absence of significant expression changes in rate-limiting auxin biosynthesis genes in *Bdaux1* (Table S2).

The *BdAUX1::GFP-BdAUX1* plants, as well as *BdAUX1::NLS-3XVENUS* plants, allowed us to assess the expression pattern of *BdAUX1* in the root. *AtAUX1* is expressed specifically in the Arabidopsis root protophloem, epidermis and root cap-columella (Marchant *et al.*, 2002). *BdAUX1* transcriptional and translational reporters displayed similar expression patterns, with the exception of expression in the root cap. Moreover, unlike *AtAUX1*, *BdAUX1* was also expressed throughout the stele and in the outer cortex layers (Fig. 4a–c). Thus, the expression pattern of *BdAUX1* encompasses the combined domains of *AtAUX1*, *AtLAX2* and *AtLAX3* (Peret *et al.*, 2012) with the exception of the root cap, and therefore, possibly, their combined functions in these tissues. Consistent with its homology to AtAUX1, GFP-BdAUX1 protein was localized at the plasma membrane, in a typically polar fashion (Fig. 4d,e). In the stele, the orientation was generally shootward (Fig. 4e), while in the outer cell layers, BdAUX1 polar localization appeared mostly rootward (Fig. 4f). However, in the later epidermis, BdAUX1 was detected on both the apical and basal sides of the cell, as well as facing inside (Fig. 4g). In summary, the localization is consistent with a role of BdAUX1 in promoting auxin transport from the shoot to the root tip, and in evacuating auxin from the tip via the epidermis. Notably, despite the increased auxin level in

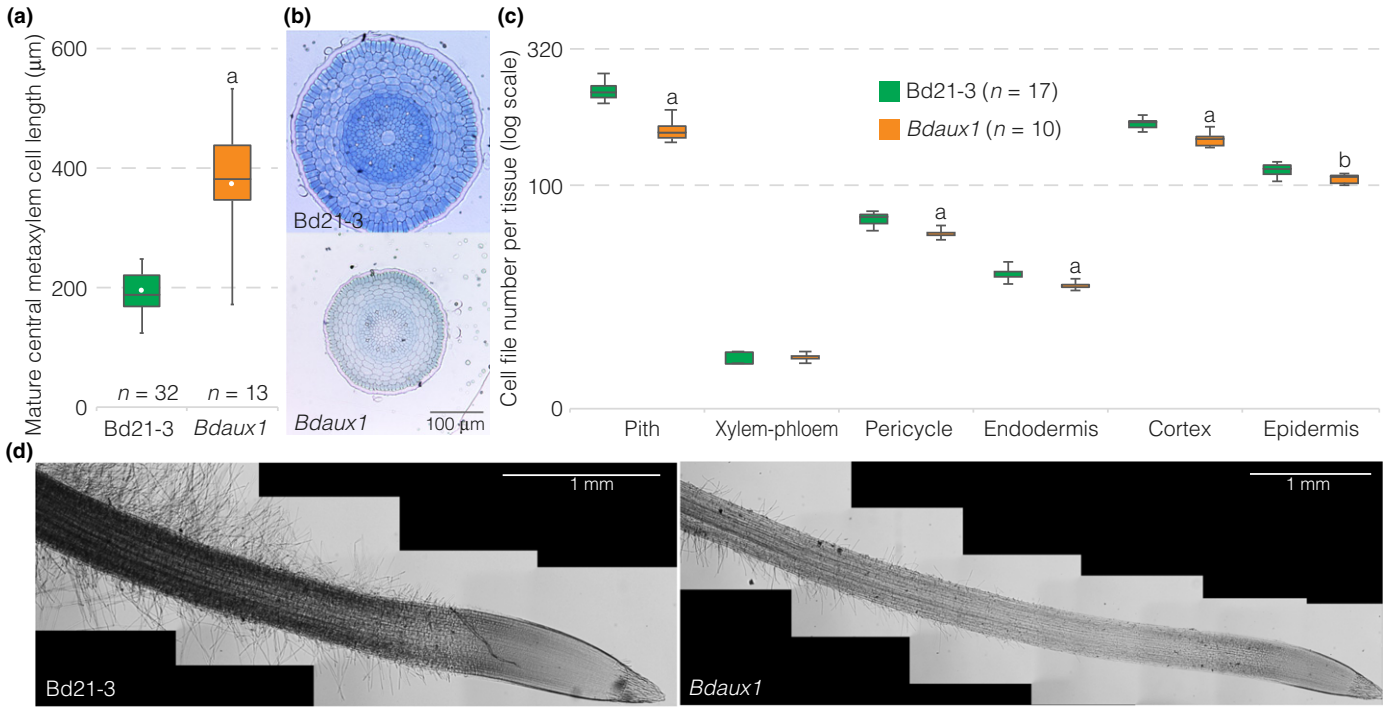

Fig. 2 Cellular root phenotypes of the Brachypodium *Bdaux1* mutant. (a) Mature central metaxylem cell length in indicated genotypes. (b) Histological cross-sections (toluidine blue-stained) through 2-d-old roots of indicated genotypes, taken from the mature part of the root, above the elongation zone. (c) Quantification of cell files in different mature tissue layers of indicated genotypes (2-d-old roots). (d) Illustration of root hair development in indicated genotypes (light microscopy, differential interference contrast; composite images). Box plots display second and third quartiles, maximum, minimum and mean (white dot). Statistically significant differences are indicated (Student's *t*-test: a, $P < 0.001$; b, $P < 0.03$).

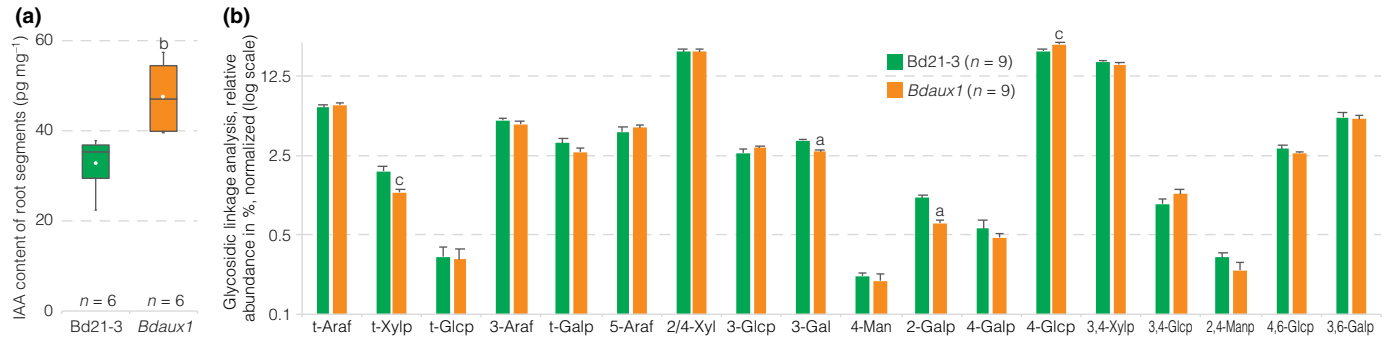

Fig. 3 Metabolic Brachypodium *Bdaux1* phenotypes. (a) Free auxin (indole-3-acetic acid, IAA) content of 1-cm root elongation zone segments (2-d-old roots) of indicated genotypes. (b) Glycosidic linkage analysis of wall material of 1-cm root elongation zone segments (2-d-old roots) of indicated genotypes (error bars, + standard error (SE)). Box plots display second and third quartiles, maximum, minimum and mean (white dot). Statistically significant differences are indicated (Student's *t*-test: a, $P < 0.001$; c, $P < 0.05$).

Bdaux1 root tips (Fig. 3a), the *Bdaux1* root agravitropism could be somewhat rescued by application of 1-NAA (Fig. 5a), similar to *Ataux1* (Swarup *et al.*, 2001). However, 1-NAA levels that rescued agravitropism did not restore normal root elongation (Fig. 5b), which was always higher in *Bdaux1* than in Bd21-3, indicating that the roles of *BdAUX1* in cell elongation and gravitropism are physiologically separable.

In summary, our detailed analyses of *Bdaux1* mutants revealed phenotypes that are counterintuitive with respect to the expectations set by the precedent of corresponding Arabidopsis mutants. However, interestingly, an exaggerated root elongation phenotype has also been described for *Osaux1* mutants (Yu *et al.*, 2015), although it has not been noticed by others working with the same lines (Zhao *et al.*, 2015). Moreover, *Osaux1* mutants also display slightly reduced shoot organ elongation (Zhao *et al.*, 2015). Yet, compared to the *Bdaux1* mutants, these phenotypes appear relatively mild, and no flower development or reproductive phenotypes were reported. Likewise, *AUX1* mutants in maize and Setaria also display apparently milder inflorescence and root phenotypes than *BdAUX1* (Huang *et al.*, 2017). Possibly, this reflects partial genetic redundancy in rice, maize and Setaria, which contain two more *AUX1* homologs than Brachypodium, including close *OsAUX1, ZmAUX1* and *SvAUX1* homologs (Zhao *et al.*, 2012, 2015; Huang *et al.*, 2017). Thus, the auxin uptake facilitator

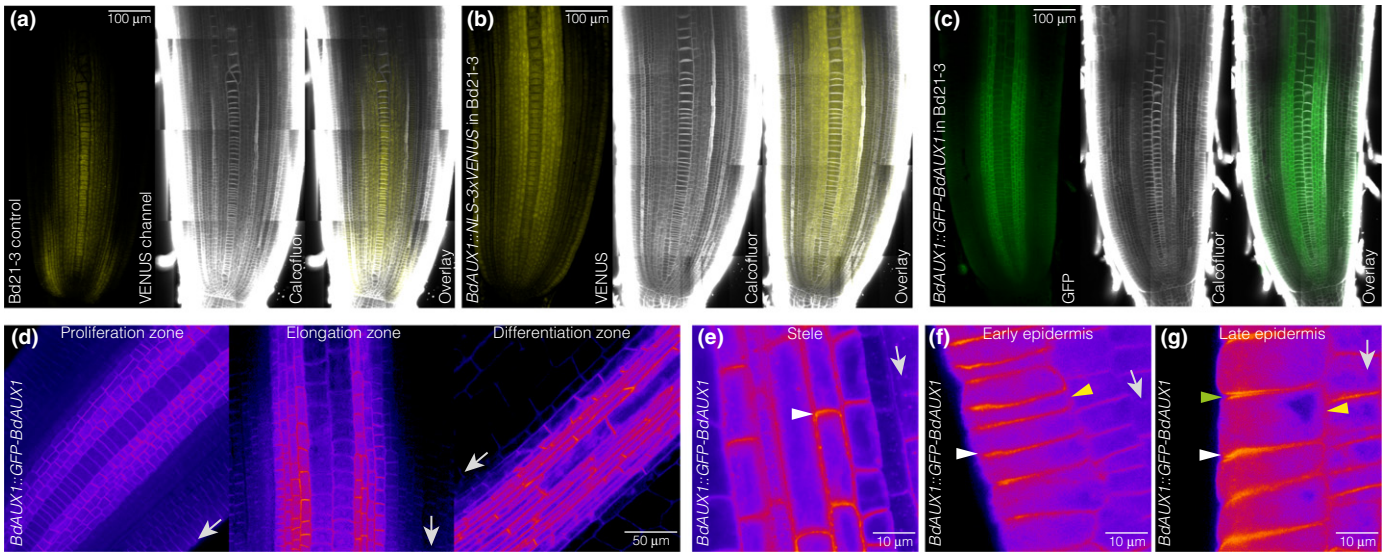

Fig. 4 Brachypodium *BdAUX1* expression. (a) Confocal microscopy of a 2-d-old Bd21-3 root meristem after ClearSee and calcofluor staining (white), illustrating background fluorescence (yellow) in the VENUS channel. Please note that autofluorescence of Brachypodium roots cannot be fully eliminated (see the Materials and Methods section). (b) Expression pattern of a *BdAUX1* transcriptional reporter (nuclear-localized VENUS fluorescence, yellow). (c) Expression pattern of a GFP-BdAUX1 translational reporter fusion protein (plasma membrane-localized green fluorescence). (d) Expression level and cellular localization of GFP-BdAUX1 fusion protein (magenta fluorescence) in different parts of a 2-d-old root meristem (arrows point towards root tip). (e) Cellular localization of GFP-BdAUX1 fusion protein (magenta fluorescence) in the stele, showing shootward polar accumulation of BdAUX1 (arrowhead) (arrow points towards root tip). (f) Cellular localization of GFP-BdAUX1 fusion protein (magenta fluorescence) in the early epidermis, showing rootward polar accumulation of BdAUX1 (white arrowhead) and absence from inward facing side (yellow arrowhead) (arrow points towards root tip). (g) Cellular localization of GFP-BdAUX1 fusion protein (magenta fluorescence) in the late epidermis, showing both rootward (white arrowhead) and shootward polar accumulation (green arrowhead), as well as inward facing localization (yellow arrowhead) of BdAUX1 (arrow points towards root tip). (a–c) are composite images.

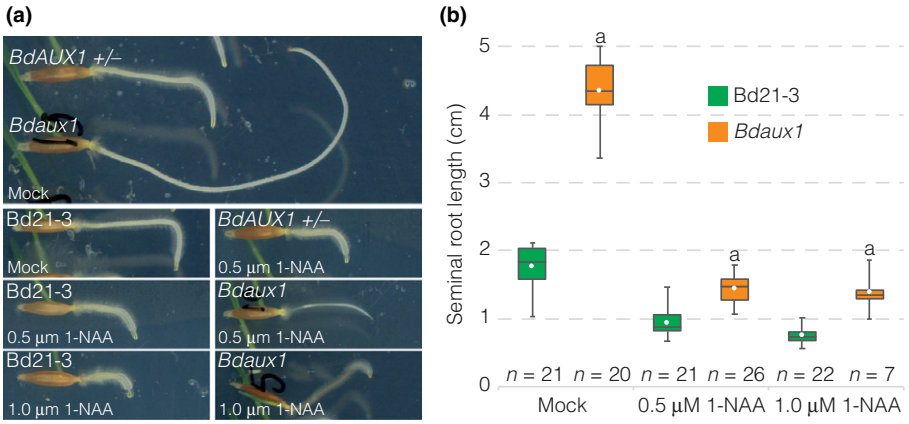

Fig. 5 Rescue of Brachypodium *Bdaux1* agravitropism. (a) Response of indicated genotypes to a 90° change in the gravity vector (3-d-old roots, plates were turned when they were 1-d-old), in the absence or presence of 1-NAA. (b) Root length of indicated genotypes in the absence or presence of 1-NAA. Box plots display second and third quartiles, maximum, minimum and mean (white dot). Statistically significant differences are indicated (Student's *t*-test: a, $P < 0.001$; b, $P < 0.01$; c, $P < 0.05$).

network in Brachypodium might be less complex than in other grasses, confirming once more that the regulatory wiring of auxin biosynthesis or transport can vary between species, and thus can trigger distinct physiological and morphological consequences if tampered with (Pacheco-Villalobos *et al.*, 2013; O'Connor *et al.*, 2014). In summary, our data suggest that in Brachypodium, BdAUX1 primarily assures correct local auxin accumulation and has a broad role in root and shoot development. This role is apparently broader than the role of *AtAUX1* in Arabidopsis, and could potentially encompass activities of *AtLAX* homologs (Marchant *et al.*, 2002). However, a detailed analysis of the other Brachypodium AUX1 homologs will be required to conclusively resolve whether this is indeed the case.

Acknowledgements

The authors would like to thank the Lausanne Genomic Technologies Facility for RNAseq services, and A. Amiguet-Vercher and R. Granbom for excellent technical support. This work was funded by Swiss National Science Foundation grant CR32I3_156724 awarded to C.S.H. and SystemsX funding. Experiments performed by C.V. and M.P. were supported by

CEPLAS (Cluster of Excellence on Plant Sciences – Deutsche Forschungsgemeinschaft EXC1028). K.L. was supported by the Swedish Governmental Agency for Innovation Systems (VINNOVA) and the Swedish Research Council (VR). The work conducted by the US DOE Joint Genome Institute is supported by the Office of Science of the US Department of Energy under Contract no. DE-AC02-05CH11231.

Author contributions

A.v.d.S. and C.S.H. designed the study and wrote the paper. A.v.d.S., C.V., K.L., M.P. and C.S.H. designed experiments. A.v.d.S. and C.V. performed experiments. J.B. and J.V. provided crucial reagents.

References

Bainbridge K, Guyomarc'h S, Bayer E, Swarup R, Bennett M, Mandel T, Kuhlemeier C. 2008. Auxin influx carriers stabilize phyllotactic patterning. *Genes & Development* **22**: 810–823.

Balzan S, Johal GS, Carraro N. 2014. The role of auxin transporters in monocots development. *Frontiers in Plant Science* **5**: 393.

Benjamins R, Scheres B. 2008. Auxin: the looping star in plant development. *Annual Review of Plant Biology* **59**: 443–465.

Bennett MJ, Marchant A, Green HG, May ST, Ward SP, Millner PA, Walker AR, Schulz B, Feldmann KA. 1996. Arabidopsis *AUX1* gene: a permease-like regulator of root gravitropism. *Science* **273**: 948–950.

Bragg JN, Wu J, Gordon SP, Guttman ME, Thilmony R, Lazo GR, Gu YQ, Vogel JP. 2012. Generation and characterization of the Western Regional Research Center Brachypodium T-DNA insertional mutant collection. *PLoS ONE* **7**: e41916.

Brkljacic J, Grotewold E, Scholl R, Mockler T, Garvin DF, Vain P, Brutnell T, Sibout R, Bevan M, Budak H *et al.* 2011. Brachypodium as a model for the grasses: today and the future. *Plant Physiology* **157**: 3–13.

Cosgrove DJ. 2005. Growth of the plant cell wall. *Nature Reviews Molecular Cell Biology* **6**: 850–861.

Girin T, David LC, Chardin C, Sibout R, Krapp A, Ferrario-Mery S, Daniel-Vedele F. 2014. Brachypodium: a promising hub between model species and cereals. *Journal of Experimental Botany* **65**: 5683–5696.

Hochholdinger F, Wulff D, Reuter K, Park WJ, Feix G. 2000. Tissue-specific expression of *AUX1* in maize roots. *Journal of Plant Physiology* **157**: 315–319.

Huang P, Jiang H, Zhu C, Barry K, Jenkins J, Sandor L, Schmutz J, Box MS, Kellogg EA, Brutnell TP. 2017. *Sparse panicle1* is required for inflorescence development in *Setaria viridis* and maize. *Nature Plants* **3**: 17054.

Maher EP, Martindale SJ. 1980. Mutants of *Arabidopsis thaliana* with altered responses to auxins and gravity. *Biochemical Genetics* **18**: 1041–1053.

Marchant A, Bhalerao R, Casimiro I, Eklof J, Casero PJ, Bennett M, Sandberg G. 2002. AUX1 promotes lateral root formation by facilitating indole-3-acetic acid distribution between sink and source tissues in the Arabidopsis seedling. *Plant Cell* **14**: 589–597.

O'Connor DL, Runions A, Sluis A, Bragg J, Vogel JP, Prusinkiewicz P, Hake S. 2014. A division in PIN-mediated auxin patterning during organ initiation in grasses. *PLoS Computational Biology* **10**: e1003447.

Pacheco-Villalobos D, Diaz-Moreno SM, van der Schuren A, Tamaki T, Kang YH, Gujas B, Novak O, Jaspert N, Li Z, Wolf S *et al.* 2016. The effects of high steady state auxin levels on root cell elongation in Brachypodium. *Plant Cell* **28**: 1009–1024.

Pacheco-Villalobos D, Sankar M, Ljung K, Hardtke CS. 2013. Disturbed local auxin homeostasis enhances cellular anisotropy and reveals alternative wiring of auxin-ethylene crosstalk in *Brachypodium distachyon* seminal roots. *PLoS Genetics* **9**: e1003564.

Peret B, Swarup K, Ferguson A, Seth M, Yang Y, Dhondt S, James N, Casimiro I, Perry P, Syed A *et al.* 2012. *AUX/LAX* genes encode a family of auxin influx transporters that perform distinct functions during Arabidopsis development. *Plant Cell* **24**: 2874–2885.

Robert HS, Grunewald W, Sauer M, Cannoot B, Soriano M, Swarup R, Weijers D, Bennett M, Boutilier K, Friml J. 2015. Plant embryogenesis requires AUX/LAX-mediated auxin influx. *Development* **142**: 702–711.

Swarup R, Friml J, Marchant A, Ljung K, Sandberg G, Palme K, Bennett M. 2001. Localization of the auxin permease AUX1 suggests two functionally distinct hormone transport pathways operate in the Arabidopsis root apex. *Genes & Development* **15**: 2648–2653.

Ugartechea-Chirino Y, Swarup R, Swarup K, Peret B, Whitworth M, Bennett M, Bougourd S. 2010. The AUX1 LAX family of auxin influx carriers is required for the establishment of embryonic root cell organization in *Arabidopsis thaliana*. *Annals of Botany* **105**: 277–289.

Vandenbussche F, Petrasek J, Zadnikova P, Hoyerova K, Pesek B, Raz V, Swarup R, Bennett M, Zazimalova E, Benkova E *et al.* 2010. The auxin influx carriers AUX1 and LAX3 are involved in auxin–ethylene interactions during apical hook development in *Arabidopsis thaliana* seedlings. *Development* **137**: 597–606.

Yang Y, Hammes UZ, Taylor CG, Schachtman DP, Nielsen E. 2006. High-affinity auxin transport by the AUX1 influx carrier protein. *Current Biology* **16**: 1123–1127.

Yu C, Sun C, Shen C, Wang S, Liu F, Liu Y, Chen Y, Li C, Qian Q, Aryal B *et al.* 2015. The auxin transporter, OsAUX1, is involved in primary root and root hair elongation and in Cd stress responses in rice (*Oryza sativa* L.). *Plant Journal* **83**: 818–830.

Zazimalova E, Murphy AS, Yang H, Hoyerova K, Hosek P. 2010. Auxin transporters–why so many? *Cold Spring Harbor Perspectives in Biology* **2**: a001552.

Zhao H, Ma T, Wang X, Deng Y, Ma H, Zhang R, Zhao J. 2015. *OsAUX1* controls lateral root initiation in rice (*Oryza sativa* L.). *Plant, Cell & Environment* **38**: 2208–2222.

Zhao H, Ma H, Yu L, Wang X, Zhao J. 2012. Genome-wide survey and expression analysis of amino acid transporter gene family in rice (*Oryza sativa* L.). *PLoS ONE* **7**: e49210.

Supporting Information

Additional Supporting Information may be found online in the Supporting Information section at the end of the article:

Fig. S1 Clustal protein sequence alignment of Arabidopsis and Brachypodium AUX1 homologs.

Fig. S2 Expression analysis of Brachypodium *BdAUX1* and other *AUX1* homologs.

Fig. S3 Various genetic and physiological analyses of Brachypodium *BdAUX1*.

Table S1 List of differentially expressed genes in *Bdaux1* root segments ($P < 0.01$)

Table S2 Comparison of RNAseq analyses of *Bdaux1* and Bd21-3 root segments

Methods S1 DNA sequences of oligonucleotides and the CRISPR/Cas9 cassette used in this study.

Please note: Wiley Blackwell are not responsible for the content or functionality of any Supporting Information supplied by the authors. Any queries (other than missing material) should be directed to the *New Phytologist* Central Office.

3.1 Follow-up experiments

As discussed in the paper, some questions remain to be answered. An important question was where auxin is localized in the roots that have increased cell elongation. The DR5 marker has often been used as a reporter to evaluate auxin response (Ulmasov et al. 1997; Gallavotti et al. 2008; Swarup et al. 2008; Lampugnani, Kilinc, and Smyth 2013; O'Connor et al. 2014; Zhao et al. 2015). This artificial promoter consists of five AuxRE elements that can be bound by ARFs. It can drive the expression of beta-*glucuronidase* (*GUS*) or fluorescent markers like the *Red Fluorescent Protein* (*RFP*), making it possible to evaluate auxin response in a cell (Ulmasov et al. 1997; Gallavotti et al. 2008; O'Connor et al. 2014; Liao et al. 2015). Several attempts were made to cross the *DR5::eRFP* marker obtained from Dr. Devin O'Connor into *Bdaux1*, *Bdtar2l*^{hypo}, *Bdaux1* x *Bdtar2l*^{hypo} and corresponding wild type backgrounds (Bd21.0 and Bd21.3). Unfortunately the only stable line of *DR5::eRFP* available at that time already had a flower phenotype by itself and was therefore impossible to cross into other backgrounds. Therefore, I replaced the basta resistance gene by neomycin phosphotransferase II (nptII), which confers resistance to paromomycin and made new transformants. Preliminary results of these transformations are depicted in Figure 5. Interestingly *DR5::eRFP* seems decreased in *Bdaux1* root tip as compared to its corresponding heterozygote or wild type background (Figure 5A,B). Furthermore auxin response in *Bdtar2l*^{hypo} root tips seems similar to its corresponding wild type (Figure 5C,D), in line with the publication of Pacheco-Villalobos on root tips (Pacheco-Villalobos et al. 2013). Since *Bdaux1* x *Bdtar2l*^{hypo} has a mixed background of two wild type accessions, in T1 not yet enough data was obtained to draw conclusions and analysis of the T2 should give more conclusive results. The expression pattern of *DR5::eRFP* is not changed in any of the mutants as compared to their wild type backgrounds, highest expression is found in and around the quiescent center, the epidermis near the root tip and the xylem poles also in older parts of the root (Figure 5F-I). Weak expression can sometimes be found in protophloem cell files. It is important however to note that variation between transgenic

lines is common and could for instance reflect differences in copy numbers. Therefore, additional lines, and ideally crosses have to be analyzed to draw definite conclusions.

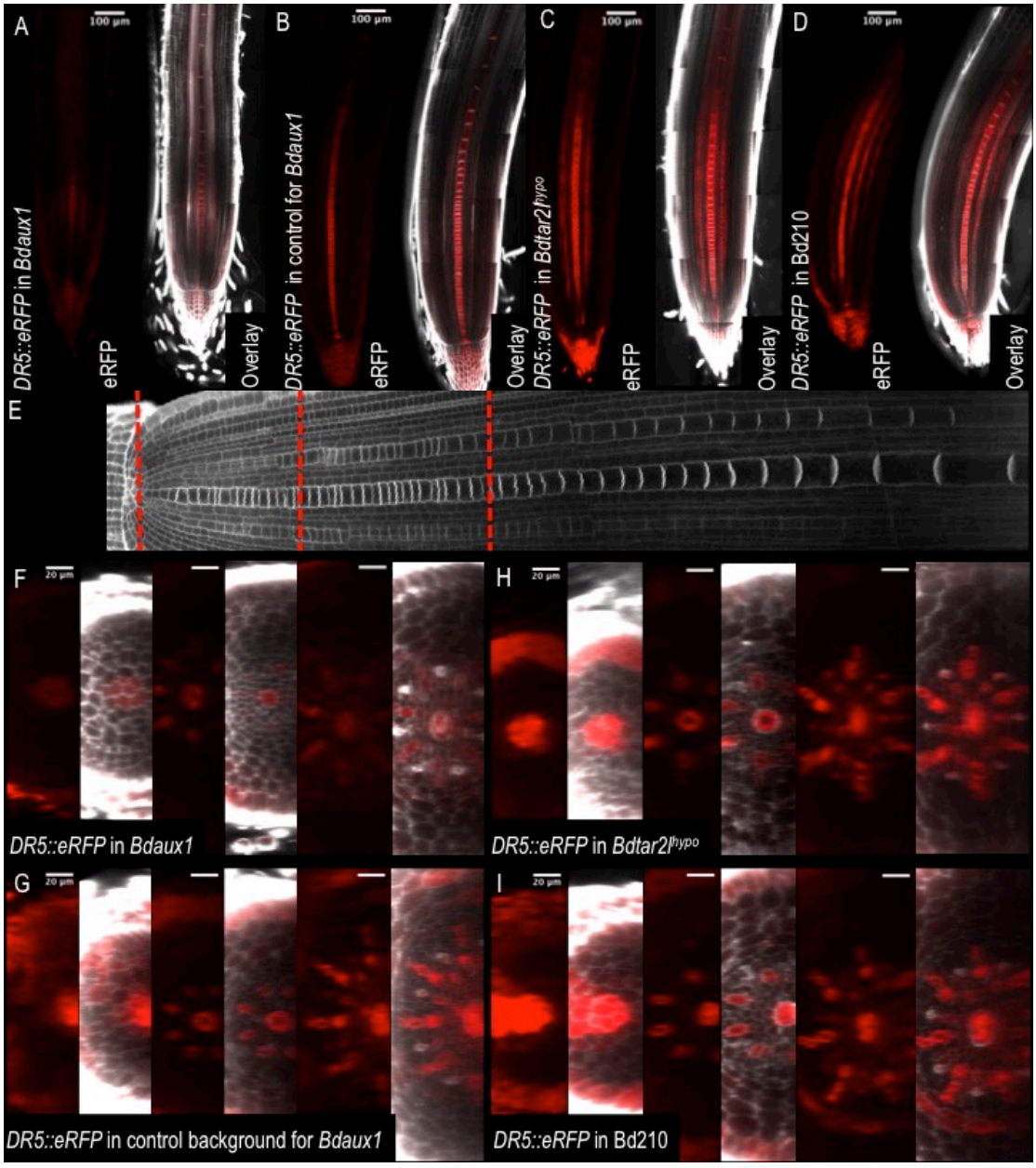

Figure 5: Preliminary results of confocal microscopy on 2-day old roots with DR5-eRFP marker in different Brachypodium *backgrounds. A-D) Longitudinal sections of root meristems with eRFP channel (left) and overlay of eRFP and calcofluor channel (right) in Bdaux1, control background for Bdaux1, Bdtar2l^{hypo} and Bd210 resp. Scalebars are 100um. E) Approximate positions of cross-sections along a root used to create figure F-I. F-I) Cross-sections of root meristems with eRFP channel (left) and overlay of eRFP and calcofluor channel (right) in Bdaux1, control background for Bdaux1, Bdtar2l^{hypo} and Bd210 resp. Scalebars are 20um.*

Another important auxin marker is DII-VENUS, which is a fusion of the auxin-degradable domain II of AUX/IAAs to the fluorescent marker VENUS (Liao et al. 2015). The absence of DII-VENUS signal marks the presence of auxin. However, since some cells already have a lower expression level of *DII-VENUS* by default, the signal should be quantified

relative to specific cell types or the stage of development of a cell. To this end *mDII-TdTomato* was created, which contains a small mutation in the DII-domain and prevents its auxin-dependent degradation. The red fluorescent protein TandemTomato (TdTomato) was used for visualization. Both *DII-VENUS* and *mDII-TdTomato* were combined in the same vector and driven under a constitutive promoter in *Arabidopsis* (Liao et al. 2015). In order to use this vector in *Brachypodium*, I modified it in the following ways: The promoter was changed to *UBIQUITIN* promoter from *Zea mays* (*ZmUBI*) since no clear homologs of *pRPS5A* promoter could be found in *Brachypodium* and ZmUBI had already been tested several times in *Brachypodium* (Vogel and Hill 2008; Bragg et al. 2012). Also no *Brachypodium* transformation protocols were available for methotrexate selection and therefore it was decided to transfer the *DII-VENUS* and *mDII-TdTomato* cassettes into *pCAMBIA1305.1-UBI5'UTR-nptII* (*pCAMBIA1305.1* Genbank accession number AF354045), where selection is based on paromomycin. Unfortunately, regenerants were not ready for analyses at the time of writing this thesis.

In order to look deeper into the AUX/LAX family amongst species, I created a new phylogenetic tree with protein alignments made by Clustal Omega Simple Phylogeny (Sievers and Higgins 2018). It contains all family members for *Arabidopsis, Brachypodium* and monocots closely related to *Brachypodium* for which research has been performed on the family (Figure 6). Therefore *Zea mays, Oryza sativa, Setaria viridis* and *Sorghum bicolor* were included as well (Goodstein et al. 2012; Kersey et al. 2018). When all family members are considered, three different groups become visible. Group 1 contains AtAUX1, AtLAX1, AtLAX2, BdAUX1 and the most closely related AUX1 homologs from other monocots. Interestingly all plants taken along, have two different family members in this group, whereas *Brachypodium* only has one. Group 2 consists of AtLAX3 and two homologs for all monocots tested, divided into two subgroups. Again, *Brachypodium* is an exception, since it only has one homolog in the subgroup that lacks an *Arabidopsis* counterpart. Group 3 seems to be specific for the monocots taken along in this tree and contains one homolog for each monocot. All in all, this cladogram could

point to an evolutionary difference between monocots and dicots and especially the existence and function of the third group in monocots may be interesting to investigate further.

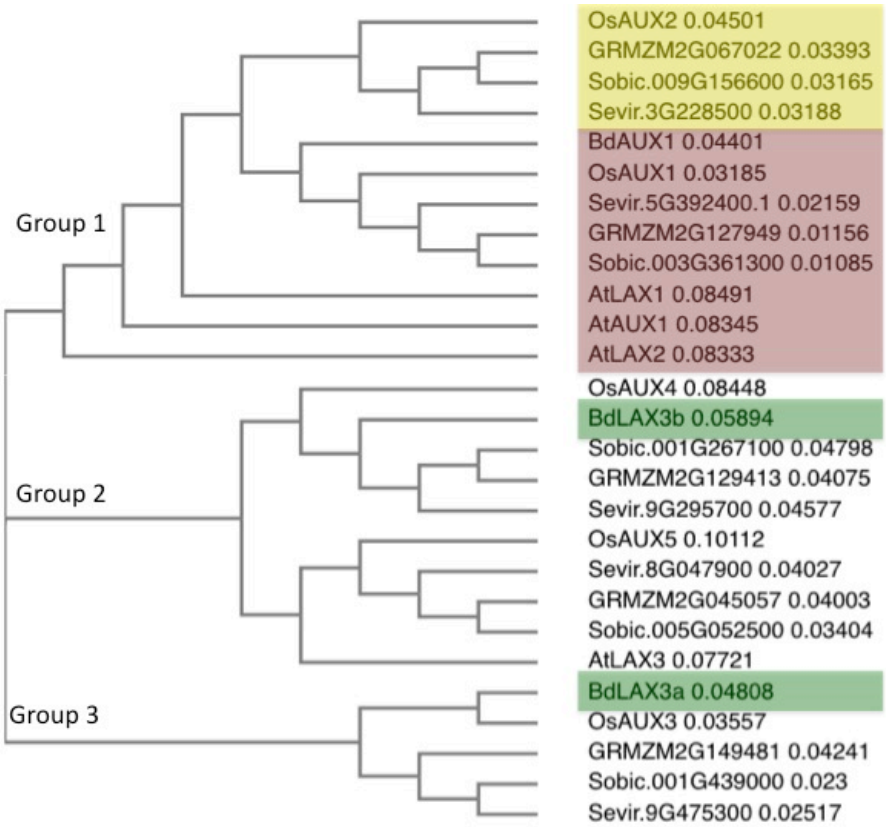

Figure 6: Phylogenetic tree of AUX1-family member proteins from several monocots and Arabidopsis*, based on Clustal Omega Simple Phylogeny protein alignments (Sievers and Higgins 2018). The homologs are divided in three groups, and group 1 is split in a red group (one homolog from each monocot and three from* Arabidopsis*) and a yellow group (second close homolog is all monocots except* Brachypodium*). Other* Brachypodium *AUX1-family members are highlighted in green.*

4. Development of a functional CRISPR-Cas genome editing system for *Brachypodium distachyon*

Since we are interested in phloem development, my goal was to investigate some known gene homologs of *Arabidopsis* for their function in *Brachypodium*. As discussed before, the T-DNA libraries that are currently available for *Brachypodium* (Vogel, Garvin, et al. 2006; Bragg et al. 2012; Hsia et al. 2017) do not include these genes. Therefore we set off to develop a CRISPR-Cas genome editing system in *Brachypodium* and target genes that are known to be involved in protophloem development (*BRX, OPS, CLE45, BAM3, APL* and *BRI1*).

4.1 Optimizing CRISPR-Cas

In order to establish an efficient CRISPR-Cas genome editing system in *Brachypodium*, we designed several vectors (Section 7.2 Materials and methods). We chose a promoter that expresses the Cas9 nuclease ubiquitously in the plant, since this should also be expressed in immature embryos. In *Brachypodium* not yet many of these promoters are known, however the Joint Genome Institute (institute 2019) reports efficiencies for several tested promoters. The use of the *maize UBIQUITIN* with intron (*ZmUBI*) to drive the expression of selection markers led to the highest transformation efficiency in immature embryos. Next we designed a Cas9 that was *Brachypodium* codon-optimized, based on an *Arabidopsis*-optimized Cas9 that was published before (Mao et al. 2013) (Section 7.6 Sequences used during this thesis). To drive expression of sgRNA, normally species-specific *RNAse polymerase III U6* and *U3* promoters are used (Cong et al. 2013; Jiang et al. 2013; Ma et al. 2015; Xie, Minkenberg, and Yang 2015). However, some reports suggest *U3* promoters being less efficient than *U6* promoters (Ma et al. 2015; Mikami, Toki, and Endo 2015). Therefore we chose a *Brachypodium*-specific *U6* promoter (Section 7.6 Sequences used during this thesis). During the course of my PhD also the use of rice *pol III* promoters was reported successful in *Brachypodium* (O'Connor et al. 2017) and we made use of these during later trials to make a working CRISPR-Cas system. The design of sgRNA is the most crucial part of creating a successful genome

editing system (Zhou et al. 2014; Ma et al. 2015; Mikami, Toki, and Endo 2015). sgRNA consists of a 20bp crRNA to target the plant genome and a tracrRNA that is needed for correct folding and maturation of the crRNA so that it can guide the Cas9. Different types of tracrRNA have been tested over the years, however an 85bp-long version has been reported most successful and is most commonly used (Cong et al. 2013; Zhou et al. 2014). All sequences and vector maps can be found in Section 7.6 Sequences used during this thesis.

For the first trial we targeted thirteen different genes: homologs of *BRX*, *BAM3, CLE45, OPS* and *APL* (discussed below in more detail). crRNAs were designed to target the first exon and with the knowledge that PAM-sites should contain the NGG-nucleotide sequence (Suppl. table 1). Unfortunately, none of these resulted in edited genomes. We speculated that there could be a problem with our *Brachypodium* codon-optimized Cas9 (BdCas9) and therefore we sought to test AtCas9 that was used successfully in *Arabidopsis* (Mao et al. 2013; Fauser, Schiml, and Puchta 2014; Johnson et al. 2015). We also sought to test *Brachypodium*-optimized versions of previously mentioned *AsCpfI* and *LbCpfI* (Zetsche et al. 2015) (Section 7.6 Sequences used during this thesis). In order to compare the efficiency of all four Cas9 proteins in vector p5Cas (BdCas9, AtCas9, AsCpfI and LbCpfI), we targeted *BdBRI1* (Bradi2g48279 in *Brachypodium* genome assembly version 3.0 (Kersey et al. 2018)). Mutants for this gene were already published and have a dwarf phenotype that is easily recognizable (Feng et al. 2015). It was therefore a good candidate for comparison of the efficiencies of different Cas9 proteins. Again, crRNAs were designed solely based on the criteria mentioned above: targeting a sequence in the first exon with a PAM-site containing NGG and no mutants were obtained.

Since our cassettes were designed, more research has been published on the use of CRISPR-Cas in plants and the design of sgRNAs was optimized over time (Johnson et al. 2015; Ma et al. 2015; Xie, Minkenberg, and Yang 2015; Schiml and Puchta 2016). By now, several tools are publicly available to aid the design of efficient crRNAs and apart

from using PAM-sites as a criterion they also assign a score to the position of specific nucleotides within the crRNA (Xie et al. 2014; Oliveros et al. 2016; Rauscher et al. 2017). Furthermore these tools check for secondary positions in the genome that resemble the target sequence and they assign likelihood-scores to these so-called off-target sequences in order to reduce the possibility of unwanted mutations. We decided to use the BreakingCas tool for future design of crRNAs, since it includes the newest versions of the *Brachypodium* genome and is user-friendly (Oliveros et al. 2016). In the meantime Dominique Bergmanns laboratory demonstrated the successful use of a rice CRISPR-Cas system in *Brachypodium* (Miao et al. 2013). When combining this vector with a BreakingCas-designed crRNA to target two *Brachypodium* homologs of *BRX* at the same time, we successfully created mutants. Meanwhile, systems containing multiple crRNAs in one vector were published, resulting in the mutation of several genes at once or the deletion of big DNA fragments (Miao et al. 2013; Zhou et al. 2014; Ma et al. 2015; Xie, Minkenberg, and Yang 2015; Zhao et al. 2016). Zhou et al. added BsaI- and BtgZI-sites to introduce crRNA more easily in a vector that already contains a U6 promoter and tracrRNA (Zhou et al. 2014). We therefore optimized our system accordingly, as discussed in more detail in 7.2 Materials and methods. With the use of this new system and the BreakingCas tool for designing sgRNAs (Oliveros et al. 2016), we obtained mutants with our self-designed system. This new strategy worked well for all targets that were tested (Suppl. table 1 and Suppl. table 3) and results will be discussed below.

4.1 BRX

At the start of my PhD, four different protein homologs were annotated as AtBRX homologs that contain the four BRX domains: the 10 and the 25 amino acid stretch at the N-terminus, and the tandem BRX-domains (Briggs, Mouchel, and Hardtke 2006) (based on *Brachypodium distachyon* version 1.0 genome assembly, accession GCA_000005505.1). We named them as follows: BdBRXL1 (Bradi3g52537), BdBRXL2 (Bradi4g31550), BdBRXL3 (Bradi3g37710) and BdBRXL4 (Bradi5g20580). In a phylogenetic tree (Sievers and Higgins 2018), proteins annotated as BdBRXL1 and

BdBRXL4 grouped together and were most closely related to AtBRX and AtBRXL1 (Figure 7A). BdBRXL2 and BdBRXL3 clustered in another group and are more distantly related to AtBRX and more closely to AtBRX2 and AtBRX3. Our original attempts targeted each of these genes individually with crRNA design based on aforementioned simple criteria, however no gene editing was detected. Since *BdBRXL1* and *BdBRXL4* were most likely the closest homologs of *AtBRX*, they were prioritized in later attempts for genome editing. We successfully created double mutants using the CRISPR-Cas system by Miao et al. 2013 with a crRNA that was designed based on BreakingCas (Oliveros et al. 2016) and targeted both genes at the same time. Interestingly this system seems to preferentially delete 1,2 or 5 nucleotides within both genes and therefore many regenerants with similar mutations were obtained. All these mutations led to frameshifts in the beginning of the first exon resulting in preliminary stop-codons. These could therefore all be seen as loss-of-function mutants. One exception was a line with a 24 nucleotide deletion in *BdBRXL1*, leading to a shorter protein. Moreover, the system was very efficient since most lines contained mutations in both genes. In the second generation it was difficult to obtain a single mutant for *BdBRXL1* and not possible for *BdBRXL4* out of the five different T1 lines that were continued to the next generation. Interestingly no macroscopic phenotypes could be observed in any of these mutants; root length was not altered and also shoots seemed similar to wild-type plants. Therefore, we sought to create triple mutants, including *BdBRXL2* or *BdBRXL3* mutations. To this end, we tested our newest CRISPR-Cas system with BreakingCas-designed crRNAs (Oliveros et al. 2016). Indeed we obtained *Bdbrxl1,2,4* and *Bdbrxl1,3,4* triple mutants for ten out of twelve and five out of eight T1 lines tested respectively. Again most mutations were one to five-nucleotide deletions that caused premature stop-codons. Furthermore, no macroscopic phenotypes were observed.

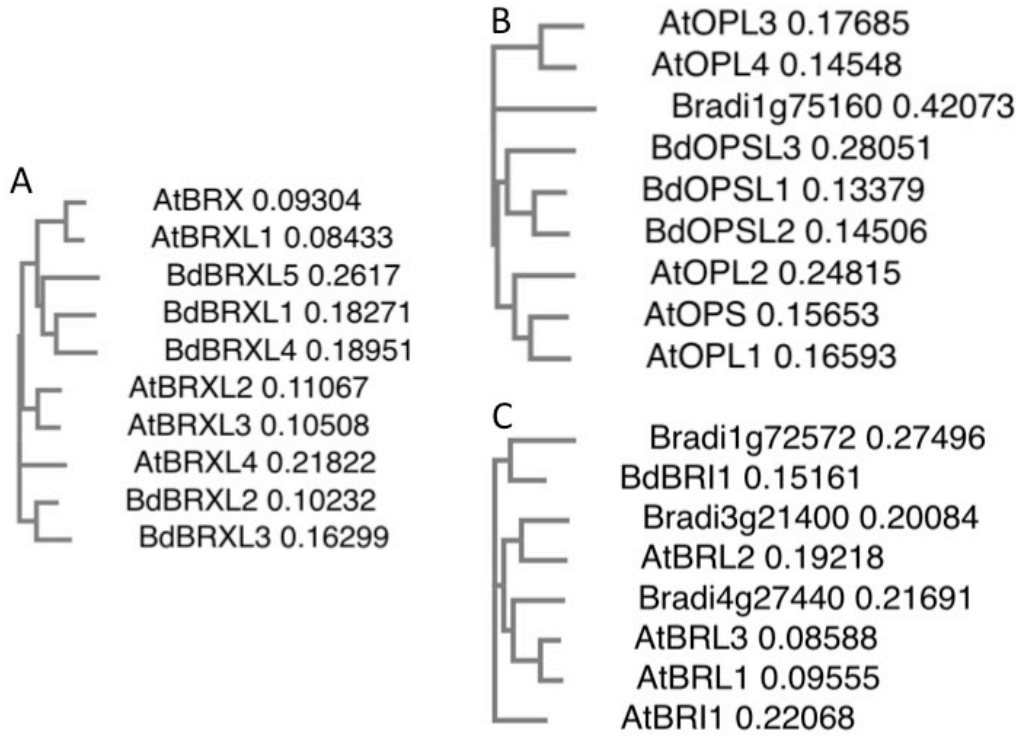

Figure 7: Phylogenetic trees comparing Brachypodium *and* Arabidopsis *BRX-, OPS- and BRI1-gene family members, fig A, B and C resp. Based on Clustal Omega Simple Phylogeny protein alignments (Sievers and Higgins 2018).*

In a more recent release of the *Brachypodium* genome (*Brachypodium distachyon* version 2.0, accession GCA_000005505.2, (International Brachypodium 2010; Kersey et al. 2018)) another protein homolog of BRX was annotated, which we named BdBRXL5 (Bradi1g01210). This homolog groups with BdBRXL1 and BdBRXL4 (Figure 7A) and might therefore act redundantly. This could explain the lack of macroscopic phenotypes observed in *Bdbrxl1 Bdbrxl4* double mutant. Therefore we sought to create *Bdbrxl1 Bdbrxl4 Bdbrxl5* triple mutants and *Bdbrxl1 Bdbrxl2 Bdbrxl4 Bdbrxl5* or *Bdbrxl1 Bdbrxl3 Bdbrxl4 Bdbrxl5* quadruple mutants by targeting *BdBRXL5* with two crRNAs in exon 1. Whether this attempt was successful was not yet known at the time of writing this thesis.

4.2 OPS

In *Brachypodium* three homologs of the OCTOPUS-family can be found, named BdOPSL1 (Bradi2g23700), BdOPSL2 (Bradi2g55160) and BdOPSL3 (Bradi1g74330). There is one more protein that contains a DUF740 domain, however it does not have any

homologs in *Arabidopsis* and is distant from the other *Brachypodium* family members (Figure 7B). BdOPSL1 and BdOPSL2 are closely related to each other and more closely related to AtOPL2 than to AtOPS. Interestingly *BdOPSL2* consists of two exons, whereas all other *OPL* homologs aligned by Breda et al. only consist out of one exon (Breda, Hazak, and Hardtke 2017). Breda et al. proved that *BdOPSL1* could complement *Atops* mutant, thereby making it an interesting target for research in *Brachypodium* (Breda, Hazak, and Hardtke 2017). BdOPSL3 protein in pairwise alignments is most closely related to AtOPL4 and least to AtOPS and was not taken along in alignments performed by Breda et al. 2017. Therefore it was chosen to focus on BdOPSL1 and BdOPSL2.

With the new CRISPR-Cas system and crRNAs whose design was based on BreakingCas software (Oliveros et al. 2016), we obtained several mutants (seven out of twenty-six T1 lines tested for *BdOPSL1* and seven out of twenty-one T1 lines tested for *BdOPSL2*). We attempted to delete several exons from both genes by using two crRNAs that target each gene at two different positions. Unfortunately we could not detect any big deletions and only one to five nucleotide deletions were observed for each crRNA. When the T2 root lengths were tested for several of the mutants, we could not detect clear differences with wild type. It may be necessary to test T2 from fully homozygous lines to see root length phenotypes. Alternatively more homologs may need to be mutated, since in the phylogenetic cladogram (Figure 7B) (Sievers and Higgins 2018) BdOPSL3 protein did not group very far from BdOPSL1 and BdOPSL2 and could function redundantly.

4.3 BRI1

Since it was discovered recently that brassinosteroid receptors are involved in protophloem development (Kang, Breda, and Hardtke 2017), we became interested in studying these receptors in *Brachypodium*. It was already published that *Bdbri1* mutants have a reduced shoot and root size as compared to wild type (Goddard et al. 2014; Feng, Yin, and Fei 2015). However it was not published whether there are problems in protophloem development. At the time of these publications, the closest homolog to

AtBRI1 was Bradi2g48280 (based on *Brachypodium* genome assembly version 1.0 (International Brachypodium 2010; Kersey et al. 2018)), however in assembly version 3.0 of the *Brachypodium* genome, it was re-named Bradi2g48279 (Kersey et al. 2018). It has 63.8% sequence identity with AtBRI1 protein. Three other homologs that belong to the same family as BdBRI1 were found in *Brachypodium*, listed with decreasing sequence identity to AtBRI1: Bradi4g27440 (BdBRL1), Bradi3g21400 (BdBRL2) and Bradi1g72572 (BdBRL3). BdBRL1 was more closely related to AtBRL1 and AtBRL3 than it was to AtBRI1, whereas BdBRL2 was more closely related to AtBRL2 as can be seen in a phylogenetic tree (Figure 7C) (Sievers and Higgins 2018). All homologs contain several leucine-rich-repeats (LRR), a 70 amino acid island domain, a transmembrane domain and a cytoplasmic kinase domain, like BRI1 (Cano-Delgado et al. 2004; Kinoshita et al. 2005). It was shown before that the island domain is crucial for brassinosteroid binding and this is thought to be the reason for the divergent function of AtBRL2 (Kinoshita et al. 2005). Therefore we looked at the existence of this island domain in *Brachypodium*. Surprisingly none of the *Brachypodium* homologs have a very close similarity to AtBRI1 nor to AtBRL1 or AtBRL3 island domains. A possible exception is the AtBRL2 island domain, which overlaps with a higher similarity to BdBRL2. When looking more into the island domains within *Arabidopsis* we saw that also within this family, the domains are very divergent. Only AtBRL1 and AtBRL3 are very similar and therefore the island domain was deemed not valid as a criterion for predicting the most important homologs in *Brachypodium.* Another striking feature in *Arabidopsis* was that all homologs consist out of one exon. This is not the case for *Brachypodium*. In fact, *BdBRI1* itself contains two exons and *BdBRL3* even three; therefore this may also not be used to exclude candidates. Since the triple *bri1 brl1 brl3* mutant in *Arabidopsis* is more interesting in terms of protophloem development than *Atbri1* alone, a new attempt targeted *BdBRI1* (closest homolog to *AtBRI1*) and *BdBRL1* (closest homolog to *AtBRL1* and *AtBRL3*) separately with two different sgRNAs in the same vector. This attempt seemed successful, since indeed small *bri1*-like plants were obtained and genotyping is ongoing at the time of writing this thesis. Since it is possible that BdBRL3 and maybe even

BdBRL2 act redundantly, these may have to be targeted in future attempts.

4.4 APL, CLE45 and BAM3

As discussed before, our original attempt to create mutants with a CRISPR-Cas genome editing systems did not result in any mutations. Thereafter, I focused on *BRX*, *OPS* and brassinosteroid receptors and did not have time to create *Brachypodium* mutants for homologs of *AtAPL*, *AtCLE45* and *AtBAM3.* Nonetheless, creating and investigating these mutants could be of interest in the future. AtAPL had two different annotated protein homologs based on the *Brachypodium* reference genome at the time that I started my PhD (*Brachypodium distachyon* version 1.0, accession GCA_000005505.1, (International Brachypodium 2010; Kersey et al. 2018)), which we named BdAPLL1 (Bradi1g31837) and BdAPLL2 (Bradi3g05500). AtCLE45 had only one homolog based on *Brachypodium* in genome assembly v1.0: Bradi1g05010. In comparisons based on later assemblies of the *Brachypodium* genome (*Brachypodium distachyon* version 3.0, accession GCA_000005505.4) no homologs of AtCLE45 or AtCLE26 can be found and Bradi1g05010 is annotated as a homolog of AtCLE25. Furthermore a second CLE peptide is annotated as a close homolog to Bradi1g05010, namely Bradi1g54656. As mentioned before, Czyzewicz et al. investigated the CLE26 peptide homolog in monocots and revealed that it differs in a crucial amino acid from AtCLE26, resulting in a different effect on root meristem as AtCLE26 (Czyzewicz et al. 2015). When aligning the active peptide sequence of Bradi1g05010, Bradi1g54656, AtCLE26, AtCLE25 and AtCLE45, both *Brachypodium* CLE peptides share the most sequence identity with AtCLE25 (Suppl. table 1). It would therefore be interesting to compare the effects of active peptide AtCLE25 and Bradi1g05010 or Bradi1g54656. Furthermore, due to the lack of closer AtCLE45 or AtCLE26 orthologs, mutants of Bradi1g05010 and Bradi1g54656 may still be of interest regarding protophloem development.

For AtBAM3, four different protein homologs were annotated based on *Brachypodium* genome assembly version 1.0, which we named BdBAM3L1 (Bradi1g07180), BdBAM3L2

(Bradi1g57900), BdBAM3L3 (Bradi1g69097), BdBAM3L4 (Bradi4g21830). In later releases of the *Brachypodium* genome (*Brachypodium distachyon* version 2.0, accession GCA_000005505.2 and *Brachypodium distachyon* version 3.0, accession GCA_000005505.4, (International Brachypodium 2010; Kersey et al. 2018)), a possible new homolog was annotated, which we named BdBAM3L5 (Bradi1g30160). It should be noted that AtBAM3 is part of a family in *Arabidopsis* and therefore some of these homologs in *Brachypodium* may be more closely related to AtBAM1 or AtBAM2 than to AtBAM3. More thorough comparison would be needed to confirm this, for example by making a phylogenetic tree to compare the different homologs between different species.

4.5 Off-target analysis

As stated before, the new CRISPR-Cas system worked efficiently. The efficiency varies between 27 and 83% for transformations where several independent regenerants were obtained (Suppl. table 3). Especially for crRNAs with high efficiency, there is a common concern that there is a possibility of off-target mutations (Xie and Yang 2013; Zhang et al. 2014; Zhou et al. 2014; Oliveros et al. 2016; Schiml and Puchta 2016). BreakingCas predicts the likeliness of off-target mutations and assigns a score (Oliveros et al. 2016). Also Cas-OFFfinder (Bae, Park, and Kim 2014) can be used to predict off-target sites in *Brachypodium*, however when comparing its results with BreakingCas I discovered that Cas-OFFfinder makes use of an out-dated *Brachypodium* genome database and does not assign likelihood scores to each off-site prediction. Nevertheless, predicted targets between both programs were compared and except for targets in the newest genome database, most predicted targets overlapped. For several CRISPR-Cas generated lines, we chose the most likely off-targets to be tested *in planta* and the genomic areas around these sites were sequenced (Suppl. table 4). No off-target mutations were found, however only by full-genome sequencing one can be sure that no off-target mutations have taken place. This confirms that our CRISPR-Cas system with the use of BreakingCas for the design of sgRNA is a good system to create specific mutants and use them for research.

5. Discussion and future perspectives

The goal of my PhD was to find out how similar dicotyledon (dicot) root development, in particular the protophloem tissue, is to that of monocotyledons (monocots), and to find out how applicable insights gained from research in dicots are to monocots. As some researchers already argued before (Draper et al. 2001; McSteen 2010; Pacheco-Villalobos et al. 2013; Hsia et al. 2017), there seem to be some fundamental differences. Several genes that I have looked into during my PhD confirm this hypothesis. For example, the AUX1 auxin importer seems to have a broader function with more severe phenotypes in monocots as compared to dicots (Yu et al. 2015; Zhao et al. 2015; Huang et al. 2017; van der Schuren et al. 2018), especially with regard to stem and flower phenotypes. In *Arabidopsis thaliana* (*Arabidopsis*) the main phenotype observed for *Ataux1* mutants is a problem in the response to changes in gravity, lateral root initiation and root hair development (Maher and Martindale 1980; Yamamoto and Yamamoto 1998; Marchant et al. 1999; Swarup et al. 2001; Marchant et al. 2002; Swarup et al. 2005; Peret et al. 2012). Even though *AtAUX1* is expressed in vegetative meristems, stem and flower, phenotypes can only be observed when other AUX/LAX family members are mutated in addition to *aux1* (Bainbridge et al. 2008; Fabregas et al. 2015). In rice several contradicting papers were published; root length may be increased, shoot size may be reduced, lateral root density may be increased and root hair length is most likely reduced (Yu et al. 2015; Zhao et al. 2015; Giri et al. 2018). Since the same alleles were used in the different publications, possibly different growth conditions could explain the discrepancies in the phenotypes that were observed. Nonetheless, from all these data it is clear that more phenotypes can be observed in rice *aux1* mutants than those reported for *Arabidopsis* single mutant. Also in *Setaria viridis* (*Setaria*) and maize stem phenotypes were more prominent than root phenotypes and included reduced shoot size and reduced tassel (Huang et al. 2017). Interestingly, lateral root density in *Setaria* was unaffected, whereas no data was given for maize (Huang et al. 2017). Lastly *Brachypodium distachyon* (*Brachypodium*) has a more severe phenotype than any other so far

described *aux1* mutant. Roots are agravitropic, root length is increased, root hair length is decreased, stem size is greatly reduced and flowers are sterile (van der Schuren et al. 2018) (Chapter 3). To look more into how these differences may have developed, a phylogenetic tree was constructed based on Clustal Omega Simple Phylogeny protein alignments (Sievers and Higgins 2018) (Figure 6), containing *Arabidopsis, Brachypodium* and several monocots closely related to *Brachypodium.* This resulted in three different groups of homologs and group 1 contains the closest homologs of AtAUX1. In this tree, I used the newest genome assemblies for the different species, which contradicts some results that were published before. Hoyerova et al. published a division where monocot AUX1 homologs fall into a different group than dicot AUX1 homologs (Hoyerova et al. 2008). They used OsAUX4 and GRMZM2G129413 for their alignments, which according to Figure 6 are indeed not the closest homologs of AtAUX1. Also Hochholdinger et al. annotated GRMZM2G129413 as the closest homolog to AtAUX1 and called it ZmAUX1 (Hochholdinger et al. 2000). Later this homolog was renamed ZmLAX2 and indeed its mutant is not associated with root phenotypes, but rather with SAM size (Leiboff et al. 2015). The alignments of Shen et al. 2010 and Yue et al. 2015 were very similar to Figure 6. They lack the monocot-specific group (group 3) however, possibly because they compared fewer monocot species. Furthermore AtLAX2 is part of the second, not the first group in their alignments. The newest tree (Figure 6) could therefore possibly explain why more severe phenotypes in *Arabidopsis* are only observed in higher-order mutants, since it has three different homologs that fall into group 1.

In the particular case of *Brachypodium*, there is a lack of the second homolog in group 1 and group 2 as compared to all other plants included. This could explain why the *aux1* mutant phenotype is even more severe in *Brachypodium* as compared to other monocots. In *Sorghum bicolor* indeed both homologs from group 1 are most highly expressed in roots as compared to the other homologs (Shen et al. 2010). Zhao et al. showed that in rice *OsAUX1* is most highly expressed in roots, but also *OsAUX2* and *OsAUX4* are possibly expressed in the root (Zhao et al. 2012). In maize both homologs from group 1

show a similar expression pattern and are more highly expressed in the roots than other homologs (Yue et al. 2015), To obtain clear evidence for the hypothesis that the second homolog may act redundantly, it is important to check whether double mutants for both group 1 homologs of *Setaria*, *Sorghum*, maize and rice *AUX1* show similar phenotypes to *Bdaux1*. Also different *AUX1* orthologs could be expressed in *Bdaux1* to see if they can complement its phenotype.

Transcriptome analyses of *Osaux1* roots reveals many up- or downregulated genes as compared to wild type background and more than 83% of the genes were annotated in a category named “other” (Zhao et al. 2015). In an RNAseq on *Brachypodium* Bd21.3 versus *Bdaux1* roots, we observed fewer differentially expressed genes, the majority of which was involved with the production or modification of the cell wall (expansins, glucosylases, arabino galactan protein etc). It would be interesting to determine whether *Osaux1* also includes differential expression of cell wall-related genes. Another interesting aspect is the increased level of auxin in *Bdaux1* one centimeter root segments compared to wild type when chromatography was combined with mass spectrometry to determine auxin levels (van der Schuren et al. 2018). In contrast to these results, the preliminary data with *DR5* promoter indicated reduced auxin response in the root tip (Figure 5). Also *Arabidopsis* and rice *aux1* mutants have reduced auxin response as compared to their corresponding wild type backgrounds when *DR5* promoter is examined in the root tip (Swarup et al. 2001; Marchant et al. 2002; Band et al. 2014; Yu et al. 2015; Zhao et al. 2015). This is corroborated by chromatography measurements on full roots in rice and on root tip in *Arabidopsis aux1* (Swarup et al. 2001; Yu et al. 2015; Zhao et al. 2015). Interestingly when *Arabidopsis* root segments further away from the tip (more than ten millimeter) were examined, *aux1* mutants showed increased levels of auxin compared to the same segments in wild type roots (Marchant et al. 2002). Taking all these data together, it seems plausible that AUX1 in all species functions in acropetal transport only close to the root-tip and in *aux1* mutants an auxin “traffic jam” could be caused just above the zone where AUX1 is normally functional. Possibly this zone was overrepresented in

the measurements on *Brachypodium* root segments, which could explain the contradicting results with *DR5* marker in root tips. Cross-sections of auxin markers at specific distances from the root tip in different species should help to elucidate whether this hypothesis is correct.

Also whether OsAUX1, BdAUX1, ZmAUX1 and SvAUX1 are indeed auxin importers, remains to be proven by, for example, auxin transport assays in *Xenopus laevis* oocytes. AUX1 localization in monocots was not researched in high enough detail to draw conclusions about its function in directional auxin transport. The expression pattern of *OsAUX1* is similar to *AtAUX1*, namely in epidermis, root cap and depending on the publication also in the stele (Swarup et al. 2001; Yu et al. 2015; Zhao et al. 2015; Giri et al. 2018). The actual polar localization was only determined in one publication with an *OsAUX1::OsAUX1-GFP* marker line, however it focused on root hairs and lateral roots and they show that expression of *OsAUX1* in root hair cells is different from *AtAUX1* (Yu et al. 2015). In epidermal cells, the signal is localized in a similar fashion as BdAUX1, however no pictures are focused on the primary root phloem and therefore it is difficult to compare the localization pattern to BdAUX1 or AtAUX1 (Yu et al. 2015). This makes the data on primary roots that was published for BdAUX1 unique (van der Schuren et al. 2018) (Chapter 3). BdAUX1 seems to localize in the same way as AtAUX1 (shootward in phloem and axial in epidermis), making it likely that it directs auxin to the root tip and more importantly into the epidermis for gravitropic response. However more thorough experiments would have to be performed in order to confirm this theory. An experiment could be to examine complementation of *Bdaux1* or *Osaux1* with only phloem- or epidermis-specific promoters driving the expression of *AUX1*. Furthermore it should be noted that BdAUX1 signal was not found in columella and this differs from both *Arabidopsis* and some publications from rice (Swarup et al. 2001; Yu et al. 2015). To date there is no explanation for this difference in expression pattern, however even in *Arabidopsis* no proof has yet been obtained for a function of AUX1 in the columella (Swarup et al. 2005).

All in all, much more research is needed in order to compare the functions and localizations of the different AUX1s that have been identified so far. But it has become evident that information obtained in dicots (*Arabidopsis*) cannot directly be applied to monocots. Clearly the phenotypes of *Brachypodium* are more in line with those observed in other monocots. Whether this observation is also applicable for genes involved in protophloem development, was another point of focus during my PhD. Again, looking at the evolution of specific gene families could provide some answers. As said before, the BRX domains were found in all higher order plants (Mouchel, Briggs, and Hardtke 2004). According to Phytozome BRX-domains could also be found in the liverwort *Marchantia polymorpha,* but not *Spagnhum fallax* and *Physcomitrella patens,* all very primitive landplants (embryophytes) (Goodstein et al. 2012). Unfortunately, no other primitive plants are available yet in the database, apart from several algae species. In algae no BRX domain was detected. This may argue for co-evolution of BRX domains with the existence of embryophytes and thus the land colonization of plants. This colonization is thought to have gone hand-in-hand with the occurrence of water- and food-conducting cells, that can be seen as pre-vascular systems (Lucas et al. 2013). It would be very interesting to test this theory by a more thorough bioinformatics search, which could possibly reveal a BRX domain in other mosses or liverworts as well. Complementation studies in *Arabidopsis* with moss-BRX domains or vice versa should reveal whether BRX function is conserved during the course of evolution. Furthermore it was already shown that the *Atbrx* phenotype could be rescued by the introduction of several monocot homologs in the mutant background, whereas within *Arabidopsis* only *AtBRXL1* could complement (Beuchat et al. 2010). This is due to more conserved sequences within monocots than in *Arabidopsis* and may point to a stronger selective pressure for each individual member within the family. This could be a fundamental difference between monocots and dicots. *BdBRXL2* was the only monocot family member tested at the time that could not rescue *Atbrx.* This is peculiar since BdBRXL2 protein and BdBRXL3 group together in Figure 7A, while *BdBRXL3* was able to rescue *Atbrx* (Beuchat et al. 2010). An explanation was found when we aligned AtBRX protein sequences with *Brachypodium* in

Phytozome (Goodstein et al. 2012); BdBRLX3 showed a much higher similarity score with AtBRX than BdBRXL2. Furthermore, the sequence of BdBRXL2 was re-annotated in later genome assemblies of *Brachypodium* and a few nucleotides were added at the end of the BRX N-domain, which could explain why the BdBRXL2 tested by Beuchat et al. was not functional. It also remains to be elucidated whether *BdBRXL5* can complement *Atbrx* phenotypes. Unfortunately within *Brachypodium* for the moment no combination of mutants had an observable phenotype, although we predict that a triple *Bdbrxl1,4,5* mutant may possibly give a notable phenotype. Furthermore, even if gaps are produced in *brx* mutants at the same frequency as in *Arabidopsis*, this may still not result in shorter roots, since *Brachypodium* has many more phloem poles that can compensate for defects in other phloem poles.

OPS evolved later than BRX domains, as it is only found in angiosperms, but not in mosses, ferns or gymnosperms (Goodstein et al. 2012; Breda, Hazak, and Hardtke 2017). This is interesting since OPS is seen as the master regulator of protophloem development (Breda, Hazak, and Hardtke 2017; Anne and Hardtke 2018). The function of OPS is not completely conserved over time, since a second homolog in *Amborella trichopoda* could only partially rescue the *Atops* root phenotype (Breda, Hazak, and Hardtke 2017). Within *Arabidopsis*, *Atops* could only be complemented when homologs were expressed under the *AtOPS* promoter. This shows that their level of redundancy may be determined by different expression patterns and may point to sub-functionalization within the species (Breda, Hazak, and Hardtke 2017; Ruiz Sola et al. 2017). Unfortunately *BdOPSL2* and *BdOPSL3* have not yet been tested in *Arabidopsis* and we cannot draw any conclusions on the function of OPS in *Brachypodium* either. Even though the seemingly most important homologs were knocked out during this PhD, it should be kept in mind that *BdOPSL3* may act redundantly and only triple mutants may show a phenotype.

Several homologs of other genes involved in protophloem development exist in *Brachypodium* as well. Therefore it is possible that multiple mutants have to be created

for all these gene families in order to see a phenotype corresponding to single mutants in *Arabidopsis*. For example, we targeted only two homologs of *AtBRI1* so far, whereas *Brachypodium* has two more putative candidates that may be involved in protophloem development. In order to obtain a similar phenotype to the one observed in *Arabidopsis bri1 brl1 brl3* triple mutants, the other homologs in *Brachypodium* may have to be targeted. As the previous attempts to create *Bdbam3* mutants did not succeed due to the simplified criteria used to design sgRNAs, further attempts with improved criteria for sgRNA design should be performed to understand the role of this gene in *Brachypodium.* Since *BdBAM3* is part of a big family in *Brachypodium,* possibly only higher-order mutants may show a phenotype. Furthermore, it may be possible that *Bdbam3* mutant phenotypes only becomes visible in a background with the disturbed protophloem syndrome, as was seen for *Arabidopsis* (Depuydt et al. 2013; Anne and Hardtke 2018). The only gene of interest with no more than one homolog in older assemblies of the *Brachypodium* genome was *CLE45*. Bradi1g05010 was more closely related to AtCLE26 and AtCLE25, of which the former was shown to be expressed in the protophloem as well (Rodriguez-Villalon et al. 2015; Anne et al. 2018; Anne and Hardtke 2018). In alignments based on later *Brachypodium* genome assemblies no more protein homologs of AtCLE45 or AtCLE26 were annotated, however Bradi1g05010 remained a homolog of AtCLE25. Since external application of AtCLE25 and AtCLE26 has different effects in *Arabidopsis* and Czyzewicz et al. already showed that AtCLE26 and Bradi1g05010 seem to function differently, it would be interesting to compare the effects of active peptide AtCLE25 and Bradi1g05010 or Bradi1g54656 (Czyzewicz et al. 2015). As Czyzewicz et al. suggested, possibly a yet unknown ortholog of AtCLE45 and AtCLE26 remains to be found in monocots (Czyzewicz et al. 2015) and Bradi1g05010 may just be the equivalent of AtCLE25. This unknown ortholog may not have been found due to a problem in aligning, as the active CLE domain is only a small percentage of the full peptide sequence and the remaining sequence is not well conserved (Strabala et al. 2006; Kinoshita et al. 2007). Possibly alignments of only the active domains could solve the problem and give more reliable alignments between *Brachypodium* and *Arabidopsis*. Another possibility could be

that the function of common CLE peptide “precursors” has been split into more different CLE-peptides over time, like the closely related CLE25, 26 and 45 (Strabala et al. 2006; Yamaguchi et al. 2017), and they may have evolved differently between dicots and monocots. Even within *Arabidopsis* the effect of mutating CLE peptides has not yet been characterized in great detail or led to conflicting results like the increased root lengths when *AtCLE26* expression was increased but also when it was reduced (Strabala et al. 2006; Yamaguchi et al. 2017). Therefore more research will be needed to answer these questions. Mutating Bradi1g05010, Bradi1g54656 and possible other homologs in *Brachypodium* could be a good start for a thorough comparison of CLE peptides between dicots and monocots.

Apart from gathering evidence for possible differences between dicots and monocots, several other aspects have become evident over the course of my PhD. Working with *Brachypodium* is very time consuming and slow as compared to *Arabidopsis*. Nonetheless, it is doable and transformations have been optimized so they are normally successful. Many more protocols have been optimized for *Brachypodium* during this PhD that should help future research. Furthermore, a working CRISPR-Cas system was created. When our first attempts did not produce any mutations, we thought that there might be a problem with the expression of Cas9. Therefore we tested CpfI and *Arabidopsis* codon-optimized Cas9 (AtCas9) as well and discovered that none led to mutations. Therefore we cannot draw conclusions about efficiency differences between Cas9 or CpfI. Other researchers have proven that CpfI indeed results in good mutation frequencies in rice (Begemann et al. 2017; Hu et al. 2017; Wang et al. 2017; Yin et al. 2017). It is even suggested that CpfI may have a higher efficiency than other Cas9 nucleases (Begemann et al. 2017; Yin et al. 2017), however mutation frequency is very dependent on the genes targeted and the choice of guideRNA, whose design criteria are different for CpfI and Cas9. According to several publications, expression of Cas9 is generally not the limiting factor in the genome editing system (Zhou et al. 2014; Ma et al. 2015; Mikami, Toki, and Endo 2015) and this was also proven during my PhD. Indeed we

realized that the correct design of crRNAs is crucial and that having an appropriate PAM-site is not the only criterium to be considered for choosing a crRNA. Efficiency scores can be attributed to the positions of specific nucleotides within the crRNA and therefore the use of online tools is crucial in their design. With our CRISPR-Cas system and the BreakingCas-tool (Oliveros et al. 2016) we obtained mutation efficiencies between 27 and 83% of all T1 regenerants tested (Suppl. table 3). This seems in line with other reports, where values vary from 20 to 100% efficiency for different plant species (Miao et al. 2013; Zhang et al. 2014; Zhou et al. 2014; Zhao et al. 2016; Zhu et al. 2016). This variability could depend on accessibility of target gene and chromosome structure (Zhu et al. 2016). Furthermore, a common concern of CRISPR-Cas editing systems is the possibility of mutations in positions that were not intentionally targeted with the CRISPR-Cas system. Off-target sites in the genome have been computed and tested before (Xie and Yang 2013; Zhang et al. 2014; Zhou et al. 2014; Oliveros et al. 2016; Schiml and Puchta 2016). For the tests that were performed in plants, no off-target mutations were reported and in the rare case that there was an off-target, it was mutated in a much lower frequency than the actual target (Xie and Yang 2013; Feng et al. 2014; Zhang et al. 2014; Zhou et al. 2014; Baysal et al. 2016). It was proposed that the nucleotide position of mismatches within the guideRNA can be used to predict the likeliness of off-target mutations (Xie and Yang 2013; Upadhyay et al. 2013). Also in our hands, CRISPR-Cas did not lead to unwanted mutations when we tested predicted off-targets in lines with CRISPR-edited genomes (Suppl. table 4). This is likely due to the program that is used to design target crRNA, since BreakingCas assigns scores to each prediction and takes off-targets and the position of mismatches into account (Oliveros et al. 2016). It should be kept in mind that one would have to sequence the full genome in order to be completely sure that no unwanted mutations have taken place anywhere else in the genome.

In summary, there is much work left in the field of root development, especially when it comes to monocots. Several tools to aid this work have been developed by now, most importantly the use of model systems with the CRISPR-Cas system and *in situ*

hybridization to analyze the expression pattern of specific genes can save a lot of time. Phylogenetic trees and complementation studies may sometimes help to determine primary important candidates based on research in dicots and could guide research in monocots. However, ultimately it is necessary to perform experiments in monocot model systems and maybe even crops themselves in order to determine the exact function of the chosen gene in a specific species.

6. References

Abel, S., M. D. Nguyen, W. Chow, and A. Theologis. 1995. 'ACS4, a primary indoleacetic acid-responsive gene encoding 1-aminocyclopropane-1-carboxylate synthase in Arabidopsis thaliana. Structural characterization, expression in Escherichia coli, and expression characteristics in response to auxin [corrected]', *J Biol Chem*, 270: 19093-9.

Aiken, R. M., and A. J. Smucker. 1996. 'Root system regulation of whole plant growth', *Annu Rev Phytopathol*, 34: 325-46.

Alberts, Bruce. 2002. *Molecular biology of the cell* (Garland Science: New York).

Alves, S. C., B. Worland, V. Thole, J. W. Snape, M. W. Bevan, and P. Vain. 2009. 'A protocol for Agrobacterium-mediated transformation of Brachypodium distachyon community standard line Bd21', *Nat Protoc*, 4: 638-49.

Anne, P., A. Amiguet-Vercher, B. Brandt, L. Kalmbach, N. Geldner, M. Hothorn, and C. S. Hardtke. 2018. 'CLERK is a novel receptor kinase required for sensing of root-active CLE peptides in Arabidopsis', *Development*, 145.

Anne, P., M. Azzopardi, L. Gissot, S. Beaubiat, K. Hematy, and J. C. Palauqui. 2015. 'OCTOPUS Negatively Regulates BIN2 to Control Phloem Differentiation in Arabidopsis thaliana', *Curr Biol*, 25: 2584-90.

Anne, P., and C. S. Hardtke. 2018. 'Phloem function and development-biophysics meets genetics', *Curr Opin Plant Biol*, 43: 22-28.

Bae, S., J. Park, and J. S. Kim. 2014. 'Cas-OFFinder: a fast and versatile algorithm that searches for potential off-target sites of Cas9 RNA-guided endonucleases', *Bioinformatics*, 30: 1473-5.

Bainbridge, K., S. Guyomarc'h, E. Bayer, R. Swarup, M. Bennett, T. Mandel, and C. Kuhlemeier. 2008. 'Auxin influx carriers stabilize phyllotactic patterning', *Genes Dev*, 22: 810-23.

Balzan, S., G. S. Johal, and N. Carraro. 2014. 'The role of auxin transporters in monocots development', *Front Plant Sci*, 5: 393.

Band, L. R., D. M. Wells, J. A. Fozard, T. Ghetiu, A. P. French, M. P. Pound, M. H. Wilson, L. Yu, W. Li, H. I. Hijazi, J. Oh, S. P. Pearce, M. A. Perez-Amador, J. Yun, E. Kramer, J. M. Alonso, C. Godin, T. Vernoux, T. C. Hodgman, T. P. Pridmore, R. Swarup, J. R. King, and M. J. Bennett. 2014. 'Systems analysis of auxin transport in the Arabidopsis root apex', *Plant Cell*, 26: 862-75.

Bauby, H., F. Divol, E. Truernit, O. Grandjean, and J. C. Palauqui. 2007. 'Protophloem differentiation in early Arabidopsis thaliana development', *Plant Cell Physiol*, 48: 97-109.

Baysal, Can, Luisa Bortesi, Changfu Zhu, Gemma Farré, Stefan Schillberg, and Paul Christou. 2016. 'CRISPR/Cas9 activity in the rice OsBEIIb gene does not induce off-target effects in the closely related paralog OsBEIIa', *Molecular Breeding*, 36: 108.

Begemann, M. B., B. N. Gray, E. January, G. C. Gordon, Y. He, H. Liu, X. Wu, T. P. Brutnell, T. C. Mockler, and M. Oufattole. 2017. 'Precise insertion and guided editing of higher plant genomes using Cpf1 CRISPR nucleases', *Sci Rep*, 7: 11606.

Beuchat, J., S. Li, L. Ragni, C. Shindo, M. H. Kohn, and C. S. Hardtke. 2010. 'A hyperactive quantitative trait locus allele of Arabidopsis BRX contributes to natural variation in root growth vigor', *Proc Natl Acad Sci U S A*, 107: 8475-80.

Bonke, M., S. Thitamadee, A. P. Mahonen, M. T. Hauser, and Y. Helariutta. 2003. 'APL regulates vascular tissue identity in Arabidopsis', *Nature*, 426: 181-6.

Bragg, J. N., J. Wu, S. P. Gordon, M. E. Guttman, R. Thilmony, G. R. Lazo, Y. Q. Gu, and J. P. Vogel. 2012. 'Generation and characterization of the Western Regional Research Center Brachypodium T-DNA insertional mutant

collection', *PLoS One*, 7: e41916.
Breda, A. S., O. Hazak, and C. S. Hardtke. 2017. 'Phosphosite charge rather than shootward localization determines OCTOPUS activity in root protophloem', *Proc Natl Acad Sci U S A*, 114: E5721-E30.
Briggs, G. C., C. F. Mouchel, and C. S. Hardtke. 2006. 'Characterization of the plant-specific BREVIS RADIX gene family reveals limited genetic redundancy despite high sequence conservation', *Plant Physiol*, 140: 1306-16.
Cano-Delgado, A., Y. Yin, C. Yu, D. Vafeados, S. Mora-Garcia, J. C. Cheng, K. H. Nam, J. Li, and J. Chory. 2004. 'BRL1 and BRL3 are novel brassinosteroid receptors that function in vascular differentiation in Arabidopsis', *Development*, 131: 5341-51.
Cattaneo, P., and C. S. Hardtke. 2017. 'BIG BROTHER Uncouples Cell Proliferation from Elongation in the Arabidopsis Primary Root', *Plant Cell Physiol*, 58: 1519-27.
Chochois, V., J. P. Vogel, and M. Watt. 2012. 'Application of Brachypodium to the genetic improvement of wheat roots', *J Exp Bot*, 63: 3467-74.
Clouse, S. D., M. Langford, and T. C. McMorris. 1996. 'A brassinosteroid-insensitive mutant in Arabidopsis thaliana exhibits multiple defects in growth and development', *Plant Physiol*, 111: 671-8.
Cong, L., F. A. Ran, D. Cox, S. Lin, R. Barretto, N. Habib, P. D. Hsu, X. Wu, W. Jiang, L. A. Marraffini, and F. Zhang. 2013. 'Multiplex genome engineering using CRISPR/Cas systems', *Science*, 339: 819-23.
Coudert, Y., C. Perin, B. Courtois, N. G. Khong, and P. Gantet. 2010. 'Genetic control of root development in rice, the model cereal', *Trends Plant Sci*, 15: 219-26.
Czyzewicz, N., C. L. Shi, L. D. Vu, B. Van De Cotte, C. Hodgman, M. A. Butenko, and I. De Smet. 2015. 'Modulation of Arabidopsis and monocot root architecture by CLAVATA3/EMBRYO SURROUNDING REGION 26 peptide', *J Exp Bot*, 66: 5229-43.
Depuydt, S., A. Rodriguez-Villalon, L. Santuari, C. Wyser-Rmili, L. Ragni, and C. S. Hardtke. 2013. 'Suppression of Arabidopsis protophloem differentiation and root meristem growth by CLE45 requires the receptor-like kinase BAM3', *Proc Natl Acad Sci U S A*, 110: 7074-9.
Dharmasiri, S., R. Swarup, K. Mockaitis, N. Dharmasiri, S. K. Singh, M. Kowalchyk, A. Marchant, S. Mills, G. Sandberg, M. J. Bennett, and M. Estelle. 2006. 'AXR4 is required for localization of the auxin influx facilitator AUX1', *Science*, 312: 1218-20.
Dinneny, J. R., and M. F. Yanofsky. 2004. 'Vascular patterning: xylem or phloem?', *Curr Biol*, 14: R112-4.
Draper, J., L. A. Mur, G. Jenkins, G. C. Ghosh-Biswas, P. Bablak, R. Hasterok, and A. P. Routledge. 2001. 'Brachypodium distachyon. A new model system for functional genomics in grasses', *Plant Physiol*, 127: 1539-55.
Endo, S., H. Shinohara, Y. Matsubayashi, and H. Fukuda. 2013. 'A novel pollen-pistil interaction conferring high-temperature tolerance during reproduction via CLE45 signaling', *Curr Biol*, 23: 1670-6.
Evert, Ray F. 2006. *Esau's Plant Anatomy: Meristems, Cells, and Tissues of the Plant Body: Their Structure, Function, and Development, Third Edition* (John Wiley & Sons, Inc.).
Fabregas, N., P. Formosa-Jordan, A. Confraria, R. Siligato, J. M. Alonso, R. Swarup, M. J. Bennett, A. P. Mahonen, A. I. Cano-Delgado, and M. Ibanes. 2015. 'Auxin influx carriers control vascular patterning and xylem differentiation in Arabidopsis thaliana', *PLoS Genet*, 11: e1005183.
Fauser, F., S. Schiml, and H. Puchta. 2014. 'Both CRISPR/Cas-based nucleases and nickases can be used efficiently for genome engineering in Arabidopsis thaliana', *Plant J*, 79: 348-59.
Feng, Y., Y. Yin, and S. Fei. 2015. 'Down-regulation of BdBRI1, a putative

brassinosteroid receptor gene produces a dwarf phenotype with enhanced drought tolerance in Brachypodium distachyon', *Plant Sci*, 234: 163-73.
Feng, Z., Y. Mao, N. Xu, B. Zhang, P. Wei, D. L. Yang, Z. Wang, Z. Zhang, R. Zheng, L. Yang, L. Zeng, X. Liu, and J. K. Zhu. 2014. 'Multigeneration analysis reveals the inheritance, specificity, and patterns of CRISPR/Cas-induced gene modifications in Arabidopsis', *Proc Natl Acad Sci U S A*, 111: 4632-7.
Fire, A., S. Xu, M. K. Montgomery, S. A. Kostas, S. E. Driver, and C. C. Mello. 1998. 'Potent and specific genetic interference by double-stranded RNA in Caenorhabditis elegans', *Nature*, 391: 806-11.
Food Agriculture Organization of the United Nations. 2018. 'World food situation'. http://www.fao.org/worldfoodsituation/csdb/en/.
Gaj, T., C. A. Gersbach, and C. F. Barbas, 3rd. 2013. 'ZFN, TALEN, and CRISPR/Cas-based methods for genome engineering', *Trends Biotechnol*, 31: 397-405.
Gallavotti, A., Y. Yang, R. J. Schmidt, and D. Jackson. 2008. 'The Relationship between auxin transport and maize branching', *Plant Physiol*, 147: 1913-23.
Garvin, D. 2009. 'Illustrated Guide to Crossing Brachypodium'.
Giri, J., R. Bhosale, G. Huang, B. K. Pandey, H. Parker, S. Zappala, J. Yang, A. Dievart, C. Bureau, K. Ljung, A. Price, T. Rose, A. Larrieu, S. Mairhofer, C. J. Sturrock, P. White, L. Dupuy, M. Hawkesford, C. Perin, W. Liang, B. Peret, C. T. Hodgman, J. Lynch, M. Wissuwa, D. Zhang, T. Pridmore, S. J. Mooney, E. Guiderdoni, R. Swarup, and M. J. Bennett. 2018. 'Rice auxin influx carrier OsAUX1 facilitates root hair elongation in response to low external phosphate', *Nat Commun*, 9: 1408.
Goddard, R., A. Peraldi, C. Ridout, and P. Nicholson. 2014. 'Enhanced disease resistance caused by BRI1 mutation is conserved between Brachypodium distachyon and barley (Hordeum vulgare)', *Mol Plant Microbe Interact*, 27: 1095-106.
Gonzalez-Garcia, M. P., J. Vilarrasa-Blasi, M. Zhiponova, F. Divol, S. Mora-Garcia, E. Russinova, and A. I. Cano-Delgado. 2011. 'Brassinosteroids control meristem size by promoting cell cycle progression in Arabidopsis roots', *Development*, 138: 849-59.
Goodstein, D. M., S. Shu, R. Howson, R. Neupane, R. D. Hayes, J. Fazo, T. Mitros, W. Dirks, U. Hellsten, N. Putnam, and D. S. Rokhsar. 2012. 'Phytozome: a comparative platform for green plant genomics', *Nucleic Acids Res*, 40: D1178-86.
Gupta, A., R. G. Christensen, A. L. Rayla, A. Lakshmanan, G. D. Stormo, and S. A. Wolfe. 2012. 'An optimized two-finger archive for ZFN-mediated gene targeting', *Nat Methods*, 9: 588-90.
Hannon, G. J. 2002. 'RNA interference', *Nature*, 418: 244-51.
Hazak, O., B. Brandt, P. Cattaneo, J. Santiago, A. Rodriguez-Villalon, M. Hothorn, and C. S. Hardtke. 2017. 'Perception of root-active CLE peptides requires CORYNE function in the phloem vasculature', *EMBO Rep*, 18: 1367-81.
Hazak, O., and C. S. Hardtke. 2016. 'CLAVATA 1-type receptors in plant development', *J Exp Bot*, 67: 4827-33.
Hellens, R., P. Mullineaux, and H. Klee. 2000. 'Technical Focus:a guide to Agrobacterium binary Ti vectors', *Trends Plant Sci*, 5: 446-51.
Heo, J. O., P. Roszak, K. M. Furuta, and Y. Helariutta. 2014. 'Phloem development: current knowledge and future perspectives', *Am J Bot*, 101: 1393-402.
Hobbie, L., and M. Estelle. 1995. 'The axr4 auxin-resistant mutants of Arabidopsis thaliana define a gene important for root gravitropism and lateral root initiation', *Plant J*, 7: 211-20.
Hochholdinger, F., W. J. Park, M. Sauer, and K. Woll. 2004. 'From weeds to crops: genetic analysis of root development in cereals', *Trends Plant Sci*, 9: 42-8.
Hochholdinger, F., D. Wulff, K. Reuter, W.J. Park, and Feix G. 2000. 'Tissue-specific

expression of AUX1 in maize roots', *Journal of Plant Physiology*, 157: 5.
Hoyerova, K., L. Perry, P. Hand, M. Lankova, T. Kocabek, S. May, J. Kottova, J. Paces, R. Napier, and E. Zazimalova. 2008. 'Functional characterization of PaLAX1, a putative auxin permease, in heterologous plant systems', *Plant Physiol*, 146: 1128-41.
Hsia, M. M., R. O'Malley, A. Cartwright, R. Nieu, S. P. Gordon, S. Kelly, T. G. Williams, D. F. Wood, Y. Zhao, J. Bragg, M. Jordan, M. Pauly, J. R. Ecker, Y. Gu, and J. P. Vogel. 2017. 'Sequencing and functional validation of the JGI Brachypodium distachyon T-DNA collection', *Plant J*, 91: 361-70.
Hu, X., C. Wang, Q. Liu, Y. Fu, and K. Wang. 2017. 'Targeted mutagenesis in rice using CRISPR-Cpf1 system', *J Genet Genomics*, 44: 71-73.
Huang, P., H. Jiang, C. Zhu, K. Barry, J. Jenkins, L. Sandor, J. Schmutz, M. S. Box, E. A. Kellogg, and T. P. Brutnell. 2017. 'Sparse panicle1 is required for inflorescence development in Setaria viridis and maize', *Nat Plants*, 3: 17054.
institute, JGI Joint genome. 2019. "*Brachypodium* T-DNA collection." In.
International Brachypodium, Initiative. 2010. 'Genome sequencing and analysis of the model grass Brachypodium distachyon', *Nature*, 463: 763-8.
Ivanchenko, M. G., G. K. Muday, and J. G. Dubrovsky. 2008. 'Ethylene-auxin interactions regulate lateral root initiation and emergence in Arabidopsis thaliana', *Plant J*, 55: 335-47.
Ivanov, V. B., and J. G. Dubrovsky. 2013. 'Longitudinal zonation pattern in plant roots: conflicts and solutions', *Trends Plant Sci*, 18: 237-43.
Jiang, W., H. Zhou, H. Bi, M. Fromm, B. Yang, and D. P. Weeks. 2013. 'Demonstration of CRISPR/Cas9/sgRNA-mediated targeted gene modification in Arabidopsis, tobacco, sorghum and rice', *Nucleic Acids Res*, 41: e188.
Johnson, R. A., V. Gurevich, S. Filler, A. Samach, and A. A. Levy. 2015. 'Comparative assessments of CRISPR-Cas nucleases' cleavage efficiency in planta', *Plant Mol Biol*, 87: 143-56.
Kang, Y. H., A. Breda, and C. S. Hardtke. 2017. 'Brassinosteroid signaling directs formative cell divisions and protophloem differentiation in Arabidopsis root meristems', *Development*, 144: 272-80.
Kang, Y. H., and C. S. Hardtke. 2016. 'Arabidopsis MAKR5 is a positive effector of BAM3-dependent CLE45 signaling', *EMBO Rep*, 17: 1145-54.
Kapp, N., W. J. Barnes, T. L. Richard, and C. T. Anderson. 2015. 'Imaging with the fluorogenic dye Basic Fuchsin reveals subcellular patterning and ecotype variation of lignification in Brachypodium distachyon', *J Exp Bot*, 66: 4295-304.
Keller, B., and C. Feuillet. 2000. 'Colinearity and gene density in grass genomes', *Trends Plant Sci*, 5: 246-51.
Kersey, P. J., J. E. Allen, A. Allot, M. Barba, S. Boddu, B. J. Bolt, D. Carvalho-Silva, M. Christensen, P. Davis, C. Grabmueller, N. Kumar, Z. Liu, T. Maurel, B. Moore, M. D. McDowall, U. Maheswari, G. Naamati, V. Newman, C. K. Ong, M. Paulini, H. Pedro, E. Perry, M. Russell, H. Sparrow, E. Tapanari, K. Taylor, A. Vullo, G. Williams, A. Zadissia, A. Olson, J. Stein, S. Wei, M. Tello-Ruiz, D. Ware, A. Luciani, S. Potter, R. D. Finn, M. Urban, K. E. Hammond-Kosack, D. M. Bolser, N. De Silva, K. L. Howe, N. Langridge, G. Maslen, D. M. Staines, and A. Yates. 2018. 'Ensembl Genomes 2018: an integrated omics infrastructure for non-vertebrate species', *Nucleic Acids Res*, 46: D802-D08.
Kinoshita, A., Y. Nakamura, E. Sasaki, J. Kyozuka, H. Fukuda, and S. Sawa. 2007. 'Gain-of-function phenotypes of chemically synthetic CLAVATA3/ESR-related (CLE) peptides in Arabidopsis thaliana and Oryza sativa', *Plant Cell Physiol*, 48: 1821-5.
Kinoshita, T., A. Cano-Delgado, H. Seto, S. Hiranuma, S. Fujioka, S. Yoshida, and J. Chory. 2005. 'Binding of brassinosteroids to the extracellular domain of plant receptor kinase BRI1', *Nature*, 433: 167-71.
Kirschner, G. K., Y. Stahl, M. Von Korff, and R. Simon. 2017. 'Unique and Conserved

Features of the Barley Root Meristem', *Front Plant Sci*, 8: 1240.
Kurihara, D., Y. Mizuta, Y. Sato, and T. Higashiyama. 2015. 'ClearSee: a rapid optical clearing reagent for whole-plant fluorescence imaging', *Development*, 142: 4168-79.
Lampugnani, E. R., A. Kilinc, and D. R. Smyth. 2013. 'Auxin controls petal initiation in Arabidopsis', *Development*, 140: 185-94.
Lee, J. S., W. K. Chang, and M. L. Evans. 1990. 'Effects of ethylene on the kinetics of curvature and auxin redistribution in gravistimulated roots of Zea mays', *Plant Physiol*, 94: 1770-5.
Legland, D., I. Arganda-Carreras, and P. Andrey. 2016. 'MorphoLibJ: integrated library and plugins for mathematical morphology with ImageJ', *Bioinformatics*, 32: 3532-34.
Leiboff, S., X. Li, H. C. Hu, N. Todt, J. Yang, X. Li, X. Yu, G. J. Muehlbauer, M. C. Timmermans, J. Yu, P. S. Schnable, and M. J. Scanlon. 2015. 'Genetic control of morphometric diversity in the maize shoot apical meristem', *Nat Commun*, 6: 8974.
Li, S. B., Z. Z. Xie, C. G. Hu, and J. Z. Zhang. 2016. 'A Review of Auxin Response Factors (ARFs) in Plants', *Front Plant Sci*, 7: 47.
Liao, C. Y., W. Smet, G. Brunoud, S. Yoshida, T. Vernoux, and D. Weijers. 2015. 'Reporters for sensitive and quantitative measurement of auxin response', *Nat Methods*, 12: 207-10, 2 p following 10.
Ljung, K., A. K. Hull, J. Celenza, M. Yamada, M. Estelle, J. Normanly, and G. Sandberg. 2005. 'Sites and regulation of auxin biosynthesis in Arabidopsis roots', *Plant Cell*, 17: 1090-104.
Lucas, W. J., A. Groover, R. Lichtenberger, K. Furuta, S. R. Yadav, Y. Helariutta, X. Q. He, H. Fukuda, J. Kang, S. M. Brady, J. W. Patrick, J. Sperry, A. Yoshida, A. F. Lopez-Millan, M. A. Grusak, and P. Kachroo. 2013. 'The plant vascular system: evolution, development and functions', *J Integr Plant Biol*, 55: 294-388.
Ma, X., Q. Zhang, Q. Zhu, W. Liu, Y. Chen, R. Qiu, B. Wang, Z. Yang, H. Li, Y. Lin, Y. Xie, R. Shen, S. Chen, Z. Wang, Y. Chen, J. Guo, L. Chen, X. Zhao, Z. Dong, and Y. G. Liu. 2015. 'A Robust CRISPR/Cas9 System for Convenient, High-Efficiency Multiplex Genome Editing in Monocot and Dicot Plants', *Mol Plant*, 8: 1274-84.
Maher, E. P., and S. J. Martindale. 1980. 'Mutants of Arabidopsis thaliana with altered responses to auxins and gravity', *Biochem Genet*, 18: 1041-53.
Mahonen, A. P., M. Bonke, L. Kauppinen, M. Riikonen, P. N. Benfey, and Y. Helariutta. 2000. 'A novel two-component hybrid molecule regulates vascular morphogenesis of the Arabidopsis root', *Genes Dev*, 14: 2938-43.
Mali, P., L. Yang, K. M. Esvelt, J. Aach, M. Guell, J. E. DiCarlo, J. E. Norville, and G. M. Church. 2013. 'RNA-guided human genome engineering via Cas9', *Science*, 339: 823-6.
Mao, Y., H. Zhang, N. Xu, B. Zhang, F. Gou, and J. K. Zhu. 2013. 'Application of the CRISPR-Cas system for efficient genome engineering in plants', *Mol Plant*, 6: 2008-11.
Marchant, A., and M. J. Bennett. 1998. 'The Arabidopsis AUX1 gene: a model system to study mRNA processing in plants', *Plant Mol Biol*, 36: 463-71.
Marchant, A., R. Bhalerao, I. Casimiro, J. Eklof, P. J. Casero, M. Bennett, and G. Sandberg. 2002. 'AUX1 promotes lateral root formation by facilitating indole-3-acetic acid distribution between sink and source tissues in the Arabidopsis seedling', *Plant Cell*, 14: 589-97.
Marchant, A., J. Kargul, S. T. May, P. Muller, A. Delbarre, C. Perrot-Rechenmann, and M. J. Bennett. 1999. 'AUX1 regulates root gravitropism in Arabidopsis by facilitating auxin uptake within root apical tissues', *EMBO J*, 18: 2066-73.
Marhava, P., A. E. L. Bassukas, M. Zourelidou, M. Kolb, B. Moret, A. Fastner, W. X. Schulze, P. Cattaneo, U. Z. Hammes, C. Schwechheimer, and C. S. Hardtke.

2018. 'A molecular rheostat adjusts auxin flux to promote root protophloem differentiation', *Nature*, 558: 297-300.
Mashiguchi, K., K. Tanaka, T. Sakai, S. Sugawara, H. Kawaide, M. Natsume, A. Hanada, T. Yaeno, K. Shirasu, H. Yao, P. McSteen, Y. Zhao, K. Hayashi, Y. Kamiya, and H. Kasahara. 2011. 'The main auxin biosynthesis pathway in Arabidopsis', *Proc Natl Acad Sci U S A*, 108: 18512-7.
McSteen, P. 2010. 'Auxin and monocot development', *Cold Spring Harb Perspect Biol*, 2: a001479.
Miao, J., D. Guo, J. Zhang, Q. Huang, G. Qin, X. Zhang, J. Wan, H. Gu, and L. J. Qu. 2013. 'Targeted mutagenesis in rice using CRISPR-Cas system', *Cell Res*, 23: 1233-6.
Mikami, M., S. Toki, and M. Endo. 2015. 'Comparison of CRISPR/Cas9 expression constructs for efficient targeted mutagenesis in rice', *Plant Mol Biol*, 88: 561-72.
Miki, D., and K. Shimamoto. 2004. 'Simple RNAi vectors for stable and transient suppression of gene function in rice', *Plant Cell Physiol*, 45: 490-5.
Mouchel, C. F., G. C. Briggs, and C. S. Hardtke. 2004. 'Natural genetic variation in Arabidopsis identifies BREVIS RADIX, a novel regulator of cell proliferation and elongation in the root', *Genes Dev*, 18: 700-14.
Mouchel, C. F., K. S. Osmont, and C. S. Hardtke. 2006. 'BRX mediates feedback between brassinosteroid levels and auxin signalling in root growth', *Nature*, 443: 458-61.
Mulkey, T. J., K. M. Kuzmanoff, and M. L. Evans. 1982. 'Promotion of growth and hydrogen ion efflux by auxin in roots of maize pretreated with ethylene biosynthesis inhibitors', *Plant Physiol*, 70: 186-8.
Nagawa, S., S. Sawa, S. Sato, T. Kato, S. Tabata, and H. Fukuda. 2006. 'Gene trapping in Arabidopsis reveals genes involved in vascular development', *Plant Cell Physiol*, 47: 1394-405.
O'Connor, D. L., S. Elton, F. Ticchiarelli, M. M. Hsia, J. P. Vogel, and O. Leyser. 2017. 'Cross-species functional diversity within the PIN auxin efflux protein family', *Elife*, 6.
O'Connor, D. L., A. Runions, A. Sluis, J. Bragg, J. P. Vogel, P. Prusinkiewicz, and S. Hake. 2014. 'A division in PIN-mediated auxin patterning during organ initiation in grasses', *PLoS Comput Biol*, 10: e1003447.
Oliveros, J. C., M. Franch, D. Tabas-Madrid, D. San-Leon, L. Montoliu, P. Cubas, and F. Pazos. 2016. 'Breaking-Cas-interactive design of guide RNAs for CRISPR-Cas experiments for ENSEMBL genomes', *Nucleic Acids Res*, 44: W267-71.
Osmont, K. S., R. Sibout, and C. S. Hardtke. 2007. 'Hidden branches: developments in root system architecture', *Annu Rev Plant Biol*, 58: 93-113.
Pacheco-Villalobos, D., S. M. Diaz-Moreno, A. van der Schuren, T. Tamaki, Y. H. Kang, B. Gujas, O. Novak, N. Jaspert, Z. Li, S. Wolf, C. Oecking, K. Ljung, V. Bulone, and C. S. Hardtke. 2016. 'The Effects of High Steady State Auxin Levels on Root Cell Elongation in Brachypodium', *Plant Cell*, 28: 1009-24.
Pacheco-Villalobos, D., and C. S. Hardtke. 2012. 'Natural genetic variation of root system architecture from Arabidopsis to Brachypodium: towards adaptive value', *Philos Trans R Soc Lond B Biol Sci*, 367: 1552-8.
Pacheco-Villalobos, D., M. Sankar, K. Ljung, and C. S. Hardtke. 2013. 'Disturbed local auxin homeostasis enhances cellular anisotropy and reveals alternative wiring of auxin-ethylene crosstalk in Brachypodium distachyon seminal roots', *PLoS Genet*, 9: e1003564.
Peret, B., B. De Rybel, I. Casimiro, E. Benkova, R. Swarup, L. Laplaze, T. Beeckman, and M. J. Bennett. 2009. 'Arabidopsis lateral root development: an emerging story', *Trends Plant Sci*, 14: 399-408.
Peret, B., K. Swarup, A. Ferguson, M. Seth, Y. Yang, S. Dhondt, N. James, I. Casimiro, P. Perry, A. Syed, H. Yang, J. Reemmer, E. Venison, C. Howells,

M. A. Perez-Amador, J. Yun, J. Alonso, G. T. Beemster, L. Laplaze, A. Murphy, M. J. Bennett, E. Nielsen, and R. Swarup. 2012. 'AUX/LAX genes encode a family of auxin influx transporters that perform distinct functions during Arabidopsis development', *Plant Cell*, 24: 2874-85.

Qin, H., Z. Zhang, J. Wang, X. Chen, P. Wei, and R. Huang. 2017. 'The activation of OsEIL1 on YUC8 transcription and auxin biosynthesis is required for ethylene-inhibited root elongation in rice early seedling development', *PLoS Genet*, 13: e1006955.

Rauscher, B., F. Heigwer, M. Breinig, J. Winter, and M. Boutros. 2017. 'GenomeCRISPR - a database for high-throughput CRISPR/Cas9 screens', *Nucleic Acids Res*, 45: D679-D86.

Rodriguez-Villalon, A., B. Gujas, Y. H. Kang, A. S. Breda, P. Cattaneo, S. Depuydt, and C. S. Hardtke. 2014. 'Molecular genetic framework for protophloem formation', *Proc Natl Acad Sci U S A*, 111: 11551-6.

Rodriguez-Villalon, A., B. Gujas, R. van Wijk, T. Munnik, and C. S. Hardtke. 2015. 'Primary root protophloem differentiation requires balanced phosphatidylinositol-4,5-biphosphate levels and systemically affects root branching', *Development*, 142: 1437-46.

Roth, R., R. J. Sawers, H. L. Munn, and J. A. Langdale. 2001. 'Plastids undifferentiated, a nuclear mutation that disrupts plastid differentiation in Zea mays L', *Planta*, 213: 647-58.

Ruiz Sola, M. A., M. Coiro, S. Crivelli, S. C. Zeeman, S. Schmidt Kjolner Hansen, and E. Truernit. 2017. 'OCTOPUS-LIKE 2, a novel player in Arabidopsis root and vascular development, reveals a key role for OCTOPUS family genes in root metaphloem sieve tube differentiation', *New Phytol*, 216: 1191-204.

Sancho, R., C. P. Cantalapiedra, D. Lopez-Alvarez, S. P. Gordon, J. P. Vogel, P. Catalan, and B. Contreras-Moreira. 2018. 'Comparative plastome genomics and phylogenomics of Brachypodium: flowering time signatures, introgression and recombination in recently diverged ecotypes', *New Phytol*, 218: 1631-44.

Sato, E. M., H. Hijazi, M. J. Bennett, K. Vissenberg, and R. Swarup. 2015. 'New insights into root gravitropic signalling', *J Exp Bot*, 66: 2155-65.

Scacchi, E., K. S. Osmont, J. Beuchat, P. Salinas, M. Navarrete-Gomez, M. Trigueros, C. Ferrandiz, and C. S. Hardtke. 2009. 'Dynamic, auxin-responsive plasma membrane-to-nucleus movement of Arabidopsis BRX', *Development*, 136: 2059-67.

Scacchi, E., P. Salinas, B. Gujas, L. Santuari, N. Krogan, L. Ragni, T. Berleth, and C. S. Hardtke. 2010. 'Spatio-temporal sequence of cross-regulatory events in root meristem growth', *Proc Natl Acad Sci U S A*, 107: 22734-9.

Scarpella, E., and A. H. Meijer. 2004. 'Pattern formation in the vascular system of monocot and dicot plant species', *New Phytologist*, 164: 209-42.

Scheres, B., L. Di Laurenzio, V. Willemsen, M. T. Hauser, K. Janmaat, P. Weisbeek, and P. N. Benfey. 1995. 'Mutations affecting the radial organisation of the Arabidopsis root display specific defects throughout the embryonic axis', *Development*, 121: 53-62.

Schiml, S., and H. Puchta. 2016. 'Revolutionizing plant biology: multiple ways of genome engineering by CRISPR/Cas', *Plant Methods*, 12: 8.

Schindelin, J., I. Arganda-Carreras, E. Frise, V. Kaynig, M. Longair, T. Pietzsch, S. Preibisch, C. Rueden, S. Saalfeld, B. Schmid, J. Y. Tinevez, D. J. White, V. Hartenstein, K. Eliceiri, P. Tomancak, and A. Cardona. 2012. 'Fiji: an open-source platform for biological-image analysis', *Nat Methods*, 9: 676-82.

Scholthof, K. G., S. Irigoyen, P. Catalan, and K. K. Mandadi. 2018. 'Brachypodium: A Monocot Grass Model Genus for Plant Biology', *Plant Cell*, 30: 1673-94.

Shan, Q. W., Y. P. Wang, K. L. Chen, Z. Liang, J. Li, Y. Zhang, K. Zhang, J. X. Liu, D. F. Voytas, X. L. Zheng, Y. Zhang, and C. X. Gao. 2013. 'Rapid and Efficient Gene Modification in Rice and Brachypodium Using TALENs', *Molecular Plant*, 6: 1365-68.

Shan, Q., Y. Wang, J. Li, Y. Zhang, K. Chen, Z. Liang, K. Zhang, J. Liu, J. J. Xi, J. L. Qiu, and C. Gao. 2013. 'Targeted genome modification of crop plants using a CRISPR-Cas system', *Nat Biotechnol*, 31: 686-8.

Shen, C., Y. Bai, S. Wang, S. Zhang, Y. Wu, M. Chen, D. Jiang, and Y. Qi. 2010. 'Expression profile of PIN, AUX/LAX and PGP auxin transporter gene families in Sorghum bicolor under phytohormone and abiotic stress', *FEBS J*, 277: 2954-69.

Shimizu, N., T. Ishida, M. Yamada, S. Shigenobu, R. Tabata, A. Kinoshita, K. Yamaguchi, M. Hasebe, K. Mitsumasu, and S. Sawa. 2015. 'BAM 1 and RECEPTOR-LIKE PROTEIN KINASE 2 constitute a signaling pathway and modulate CLE peptide-triggered growth inhibition in Arabidopsis root', *New Phytol*, 208: 1104-13.

Sievers, F., and D. G. Higgins. 2018. 'Clustal Omega for making accurate alignments of many protein sequences', *Protein Sci*, 27: 135-45.

Simon, S., and J. Petrasek. 2011. 'Why plants need more than one type of auxin', *Plant Sci*, 180: 454-60.

Sogutmaz Ozdemir, B., and H. Budak. 2018. 'Application of Tissue Culture and Transformation Techniques in Model Species Brachypodium distachyon', *Methods Mol Biol*, 1667: 289-310.

Steinwand, M., and J. Vogel. 2010. "Crossing Brachypodium." In.

Stepanova, A. N., J. Robertson-Hoyt, J. Yun, L. M. Benavente, D. Y. Xie, K. Dolezal, A. Schlereth, G. Jurgens, and J. M. Alonso. 2008. 'TAA1-mediated auxin biosynthesis is essential for hormone crosstalk and plant development', *Cell*, 133: 177-91.

Strabala, T. J., J. O'Donnell P, A. M. Smit, C. Ampomah-Dwamena, E. J. Martin, N. Netzler, N. J. Nieuwenhuizen, B. D. Quinn, H. C. Foote, and K. R. Hudson. 2006. 'Gain-of-function phenotypes of many CLAVATA3/ESR genes, including four new family members, correlate with tandem variations in the conserved CLAVATA3/ESR domain', *Plant Physiol*, 140: 1331-44.

Swarup, K., E. Benkova, R. Swarup, I. Casimiro, B. Peret, Y. Yang, G. Parry, E. Nielsen, I. De Smet, S. Vanneste, M. P. Levesque, D. Carrier, N. James, V. Calvo, K. Ljung, E. Kramer, R. Roberts, N. Graham, S. Marillonnet, K. Patel, J. D. Jones, C. G. Taylor, D. P. Schachtman, S. May, G. Sandberg, P. Benfey, J. Friml, I. Kerr, T. Beeckman, L. Laplaze, and M. J. Bennett. 2008. 'The auxin influx carrier LAX3 promotes lateral root emergence', *Nat Cell Biol*, 10: 946-54.

Swarup, R., J. Friml, A. Marchant, K. Ljung, G. Sandberg, K. Palme, and M. Bennett. 2001. 'Localization of the auxin permease AUX1 suggests two functionally distinct hormone transport pathways operate in the Arabidopsis root apex', *Genes Dev*, 15: 2648-53.

Swarup, R., J. Kargul, A. Marchant, D. Zadik, A. Rahman, R. Mills, A. Yemm, S. May, L. Williams, P. Millner, S. Tsurumi, I. Moore, R. Napier, I. D. Kerr, and M. J. Bennett. 2004. 'Structure-function analysis of the presumptive Arabidopsis auxin permease AUX1', *Plant Cell*, 16: 3069-83.

Swarup, R., E. M. Kramer, P. Perry, K. Knox, H. M. Leyser, J. Haseloff, G. T. Beemster, R. Bhalerao, and M. J. Bennett. 2005. 'Root gravitropism requires lateral root cap and epidermal cells for transport and response to a mobile auxin signal', *Nat Cell Biol*, 7: 1057-65.

Swarup, R., and B. Peret. 2012. 'AUX/LAX family of auxin influx carriers-an overview', *Front Plant Sci*, 3: 225.

Taiz, Lincoln, Eduardo Zeiger, I. M. Møller, and Angus S. Murphy. 2015. *Plant physiology and development*.

Tao, Y., J. L. Ferrer, K. Ljung, F. Pojer, F. Hong, J. A. Long, L. Li, J. E. Moreno, M. E. Bowman, L. J. Ivans, Y. Cheng, J. Lim, Y. Zhao, C. L. Ballare, G. Sandberg, J. P. Noel, and J. Chory. 2008. 'Rapid synthesis of auxin via a new tryptophan-dependent pathway is required for shade avoidance in plants',

Cell, 133: 164-76.
Tao, Y., S. W. Nadege, C. Huang, P. Zhang, S. Song, L. Sun, and Y. Wu. 2016. 'Brachypodium distachyon is a suitable host plant for study of Barley yellow dwarf virus', *Virus Genes*, 52: 299-302.
Truernit, E., H. Bauby, K. Belcram, J. Barthelemy, and J. C. Palauqui. 2012. 'OCTOPUS, a polarly localised membrane-associated protein, regulates phloem differentiation entry in Arabidopsis thaliana', *Development*, 139: 1306-15.
Ulmasov, T., J. Murfett, G. Hagen, and T. J. Guilfoyle. 1997. 'Aux/IAA proteins repress expression of reporter genes containing natural and highly active synthetic auxin response elements', *Plant Cell*, 9: 1963-71.
Upadhyay, S. K., J. Kumar, A. Alok, and R. Tuli. 2013. 'RNA-guided genome editing for target gene mutations in wheat', *G3 (Bethesda)*, 3: 2233-8.
Ursache, R., T. G. Andersen, P. Marhavy, and N. Geldner. 2018. 'A protocol for combining fluorescent proteins with histological stains for diverse cell wall components', *Plant J*, 93: 399-412.
van der Schuren, A., C. Voiniciuc, J. Bragg, K. Ljung, J. Vogel, M. Pauly, and C. S. Hardtke. 2018. 'Broad spectrum developmental role of Brachypodium AUX1', *New Phytol*, 219: 1216-23.
Vogel, J., and T. Hill. 2008. 'High-efficiency Agrobacterium-mediated transformation of Brachypodium distachyon inbred line Bd21-3', *Plant Cell Rep*, 27: 471-8.
Vogel, J. P., Y. Q. Gu, P. Twigg, G. R. Lazo, D. Laudencia-Chingcuanco, D. M. Hayden, T. J. Donze, L. A. Vivian, B. Stamova, and D. Coleman-Derr. 2006. 'EST sequencing and phylogenetic analysis of the model grass Brachypodium distachyon', *Theor Appl Genet*, 113: 186-95.
Vogel, John P., David F. Garvin, Oymon M. Leong, and Daniel M. Hayden. 2006. 'Agrobacterium-mediated transformation and inbred line development in the model grass Brachypodium distachyon', *Plant Cell, Tissue and Organ Culture*, 84: 199-211.
Wah, D. A., J. Bitinaite, I. Schildkraut, and A. K. Aggarwal. 1998. 'Structure of FokI has implications for DNA cleavage', *Proc Natl Acad Sci U S A*, 95: 10564-9.
Wang, M., Y. Mao, Y. Lu, X. Tao, and J. K. Zhu. 2017. 'Multiplex Gene Editing in Rice Using the CRISPR-Cpf1 System', *Mol Plant*, 10: 1011-13.
Weijers, D., and D. Wagner. 2016. 'Transcriptional Responses to the Auxin Hormone', *Annu Rev Plant Biol*, 67: 539-74.
Went, F. W. 1927. 'On growth-accelerating substances in the coleoptile of Avena sativa', *Proceedings of the Koninklijke Akademie Van Wetenschappen Te Amsterdam*, 30: 10-19.
Xie, K., B. Minkenberg, and Y. Yang. 2015. 'Boosting CRISPR/Cas9 multiplex editing capability with the endogenous tRNA-processing system', *Proc Natl Acad Sci U S A*, 112: 3570-5.
Xie, K., and Y. Yang. 2013. 'RNA-guided genome editing in plants using a CRISPR-Cas system', *Mol Plant*, 6: 1975-83.
Xie, S., B. Shen, C. Zhang, X. Huang, and Y. Zhang. 2014. 'sgRNAcas9: a software package for designing CRISPR sgRNA and evaluating potential off-target cleavage sites', *PLoS One*, 9: e100448.
Yamaguchi, Y. L., T. Ishida, M. Yoshimura, Y. Imamura, C. Shimaoka, and S. Sawa. 2017. 'A Collection of Mutants for CLE-Peptide-Encoding Genes in Arabidopsis Generated by CRISPR/Cas9-Mediated Gene Targeting', *Plant Cell Physiol*, 58: 1848-56.
Yamamoto, M., and K. T. Yamamoto. 1998. 'Differential effects of 1-naphthaleneacetic acid, indole-3-acetic acid and 2,4-dichlorophenoxyacetic acid on the gravitropic response of roots in an auxin-resistant mutant of arabidopsis, aux1', *Plant Cell Physiol*, 39: 660-4.
Yin, Changxi, Quanrong Wu, Hanlai Zeng, Kai Xia, Jiuwei Xu, and Rongwei Li. 2011. 'Endogenous Auxin is Required but Supraoptimal for Rapid Growth of Rice

(Oryza sativa L.) Seminal Roots, and Auxin Inhibition of Rice Seminal Root Growth is Not Caused by Ethylene', *Journal of Plant Growth Regulation*, 30: 20-29.

Yin, X., A. K. Biswal, J. Dionora, K. M. Perdigon, C. P. Balahadia, S. Mazumdar, C. Chater, H. C. Lin, R. A. Coe, T. Kretzschmar, J. E. Gray, P. W. Quick, and A. Bandyopadhyay. 2017. 'CRISPR-Cas9 and CRISPR-Cpf1 mediated targeting of a stomatal developmental gene EPFL9 in rice', *Plant Cell Rep*, 36: 745-57.

Yu, C., C. Sun, C. Shen, S. Wang, F. Liu, Y. Liu, Y. Chen, C. Li, Q. Qian, B. Aryal, M. Geisler, A. Jiang de, and Y. Qi. 2015. 'The auxin transporter, OsAUX1, is involved in primary root and root hair elongation and in Cd stress responses in rice (Oryza sativa L.)', *Plant J*, 83: 818-30.

Yue, R., S. Tie, T. Sun, L. Zhang, Y. Yang, J. Qi, S. Yan, X. Han, H. Wang, and C. Shen. 2015. 'Genome-wide identification and expression profiling analysis of ZmPIN, ZmPILS, ZmLAX and ZmABCB auxin transporter gene families in maize (Zea mays L.) under various abiotic stresses', *PLoS One*, 10: e0118751.

Zetsche, B., J. S. Gootenberg, O. O. Abudayyeh, I. M. Slaymaker, K. S. Makarova, P. Essletzbichler, S. E. Volz, J. Joung, J. van der Oost, A. Regev, E. V. Koonin, and F. Zhang. 2015. 'Cpf1 is a single RNA-guided endonuclease of a class 2 CRISPR-Cas system', *Cell*, 163: 759-71.

Zhang, H., J. Zhang, P. Wei, B. Zhang, F. Gou, Z. Feng, Y. Mao, L. Yang, H. Zhang, N. Xu, and J. K. Zhu. 2014. 'The CRISPR/Cas9 system produces specific and homozygous targeted gene editing in rice in one generation', *Plant Biotechnol J*, 12: 797-807.

Zhang, Y., F. Zhang, X. Li, J. A. Baller, Y. Qi, C. G. Starker, A. J. Bogdanove, and D. F. Voytas. 2013. 'Transcription activator-like effector nucleases enable efficient plant genome engineering', *Plant Physiol*, 161: 20-7.

Zhao, H., H. Ma, L. Yu, X. Wang, and J. Zhao. 2012. 'Genome-wide survey and expression analysis of amino acid transporter gene family in rice (Oryza sativa L.)', *PLoS One*, 7: e49210.

Zhao, H., T. Ma, X. Wang, Y. Deng, H. Ma, R. Zhang, and J. Zhao. 2015. 'OsAUX1 controls lateral root initiation in rice (Oryza sativa L.)', *Plant Cell Environ*, 38: 2208-22.

Zhao, Y., S. K. Christensen, C. Fankhauser, J. R. Cashman, J. D. Cohen, D. Weigel, and J. Chory. 2001. 'A role for flavin monooxygenase-like enzymes in auxin biosynthesis', *Science*, 291: 306-9.

Zhao, Y., C. Zhang, W. Liu, W. Gao, C. Liu, G. Song, W. X. Li, L. Mao, B. Chen, Y. Xu, X. Li, and C. Xie. 2016. 'An alternative strategy for targeted gene replacement in plants using a dual-sgRNA/Cas9 design', *Sci Rep*, 6: 23890.

Zheng, Z., Y. Guo, O. Novak, X. Dai, Y. Zhao, K. Ljung, J. P. Noel, and J. Chory. 2013. 'Coordination of auxin and ethylene biosynthesis by the aminotransferase VAS1', *Nat Chem Biol*, 9: 244-6.

Zhou, H., B. Liu, D. P. Weeks, M. H. Spalding, and B. Yang. 2014. 'Large chromosomal deletions and heritable small genetic changes induced by CRISPR/Cas9 in rice', *Nucleic Acids Res*, 42: 10903-14.

Zhu, J., N. Song, S. Sun, W. Yang, H. Zhao, W. Song, and J. Lai. 2016. 'Efficiency and Inheritance of Targeted Mutagenesis in Maize Using CRISPR-Cas9', *J Genet Genomics*, 43: 25-36.

7. Supplementary data

7.1 The Effects of High Steady State Auxin Levels on Root Cell Elongation in *Brachypodium*

David Pacheco-Villalobos, Sara M. Díaz-Moreno, Alja van der Schuren, Takayuki Tamaki, Yeon Hee Kang, Bojan Gujas, Ondrej Novak, Nina Jaspert, Zhenni Li, Sebastian Wolf, Claudia Oecking, Karin Ljung, Vincent Bulone, and Christian S. Hardtke.

The Plant Cell, May 2016, **Vol. 28: 1009–1024**

Key Findings

- Elevated auxin levels in elongating roots upregulate cell wall remodeling factors.
- These changes are caused by reduced cell wall arabinogalactan complexity.
- Root zones with higher auxin levels seem to have reduced proton secretion.

My contribution

In order to learn how to work with *Brachypodium*, I first corroborated some experiments that were already performed by previous researchers in our Laboratory. Next, to test the effect of differences in pH, I grew *Brachypodium* seedlings on MS media with different pH. Since normal agar could not resist low pH, I had to test several other gelating agents, choosing phytagel as the best reagent. I measured root length with and without transfer to different media and used DIC-microscopy to measure differences in cortex cell length at different conditions. Furthermore I measured the micro-pH-environment near root-tips with a micro pH meter, which confirmed the hypothesis that elevated auxin levels in roots do not result in increased, but rather possibly decreased excreted proton levels. Furthermore I performed the analyses on VAS1 RNAi lines.

The Plant Cell, Vol. 28: 1009–1024, May 2016, www.plantcell.org

The Effects of High Steady State Auxin Levels on Root Cell Elongation in Brachypodium[OPEN]

David Pacheco-Villalobos,[a] Sara M. Díaz-Moreno,[b] Alja van der Schuren,[a] Takayuki Tamaki,[a] Yeon Hee Kang,[a] Bojan Gujas,[a] Ondrej Novak,[c,d] Nina Jaspert,[e] Zhenni Li,[f] Sebastian Wolf,[f] Claudia Oecking,[e] Karin Ljung,[c] Vincent Bulone,[b] and Christian S. Hardtke[a,1]

[a] Department of Plant Molecular Biology, University of Lausanne, CH-1015 Lausanne, Switzerland
[b] Division of Glycoscience, School of Biotechnology, Royal Institute of Technology (KTH), AlbaNova University Centre, 106 91 Stockholm, Sweden
[c] Umeå Plant Science Centre, Department of Forest Genetics and Plant Physiology, Swedish University of Agricultural Sciences, SE-901 83 Umeå, Sweden
[d] Laboratory of Growth Regulators, Centre of the Region Haná for Biotechnological and Agricultural Research, Institute of Experimental Botany AS CR and Faculty of Science of Palacký University, CZ-78371 Olomouc, Czech Republic
[e] Center for Plant Molecular Biology, Plant Physiology, University of Tübingen, 72074 Tübingen, Germany
[f] Centre for Organismal Studies, University of Heidelberg, 69120 Heidelberg, Germany

ORCID IDs: 0000-0002-3369-2440 (S.M.D.-M.); 0000-0003-3064-6016 (A.v.d.S.); 0000-0002-3924-0146 (Y.H.K.); 0000-0003-3452-0154 (O.N.); 0000-0003-1475-2265 (Z.L.); 0000-0003-0832-6315 (S.W.); 0000-0003-2901-189X (K.L.)

The long-standing Acid Growth Theory of plant cell elongation posits that auxin promotes cell elongation by stimulating cell wall acidification and thus expansin action. To date, the paucity of pertinent genetic materials has precluded thorough analysis of the importance of this concept in roots. The recent isolation of mutants of the model grass species *Brachypodium distachyon* with dramatically enhanced root cell elongation due to increased cellular auxin levels has allowed us to address this question. We found that the primary transcriptomic effect associated with elevated steady state auxin concentration in elongating root cells is upregulation of cell wall remodeling factors, notably expansins, while plant hormone signaling pathways maintain remarkable homeostasis. These changes are specifically accompanied by reduced cell wall arabinogalactan complexity but not by increased proton excretion. On the contrary, we observed a tendency for decreased rather than increased proton extrusion from root elongation zones with higher cellular auxin levels. Moreover, similar to Brachypodium, root cell elongation is, in general, robustly buffered against external pH fluctuation in *Arabidopsis thaliana*. However, forced acidification through artificial proton pump activation inhibits root cell elongation. Thus, the interplay between auxin, proton pump activation, and expansin action may be more flexible in roots than in shoots.

Coordinated cell division and expansion is crucial for plant organogenesis because cell walls restrict the movement of cells relative to each other (Cosgrove, 1999; Wolf et al., 2012). The cell wall is a complex structure of intertwined and sometimes cross-linked polymers, comprising cellulose, xyloglucans, pectins, and arabinogalactans, which resists the internal turgor pressure. Therefore, cell wall elasticity has to be regulated to permit cellular growth (Cosgrove et al., 1984; Cosgrove, 1993, 2005; Wolf et al., 2012). This is achieved through selective loosening of cell wall polymer interactions, which allows cellulose microfibrils and associated matrix polysaccharides to displace relative to each other. As cellulose microfibrils are typically arranged in a nonrandom, parallel orientation, most cells expand along one principal axis. This process is easily observed in organs with one principal growth vector, for instance, in hypocotyls or root tips. In both organs, hormones strongly influence cell elongation. Among these, auxin is most prominent because it not only orchestrates developmental programs, but also conveys environmental inputs to trigger adaptive responses such as tropisms (Sánchez-Rodríguez et al., 2010; Depuydt and Hardtke, 2011). It is generally assumed that auxin promotes cell elongation by inducing the expression of cell wall remodeling factors (Sánchez-Rodríguez et al., 2010; Wolf et al., 2012). These include expansins, which are considered facilitators of cell wall loosening by physically opening up the fiber network, thereby facilitating the access of other enzymes to their substrates (Cosgrove, 2005). Moreover, in parallel, auxin supposedly stimulates cell elongation via a nongenomic pathway, since it enhances cell elongation within minutes in classical assay systems, such as hypocotyls or coleoptiles. In these model organs, auxin treatment correlates with increased acidification of the apoplast, which presumably promotes cell elongation because central cell wall loosening factors and enzymes, e.g., expansins, polygalacturonases, endoglucanases, and pectin methylesterases, work optimally under acidic conditions. Cell wall acidification, in turn, is thought to arise from auxin-induced activation of plasma membrane-localized proton pumps (PM-H^+-ATPases). This long-standing concept, named the Acid Growth Theory, was formulated in the 1970s (Rayle and Cleland, 1970, 1977, 1992; Hager et al., 1971).

[1] Address correspondence to christian.hardtke@unil.ch.
The author responsible for distribution of materials integral to the findings presented in this article in accordance with the policy described in the Instructions for Authors (www.plantcell.org) is: Christian S. Hardtke (christian.hardtke@unil.ch).
[OPEN]Articles can be viewed without a subscription.
www.plantcell.org/cgi/doi/10.1105/tpc.15.01057

Whether the Acid Growth Theory is universally applicable to plant cell expansion remains controversial. For instance, even for the classic assay systems (coleoptiles or hypocotyls), some authors have concluded that cell wall acidification indeed stimulates growth, but that this is not an auxin-dependent effect (Kutschera and Schopfer, 1985b, 1985a; Schopfer, 1989, 1993). Validation of the Acid Growth Theory is most difficult in roots, where analyses are complicated by the fact that as opposed to hypocotyls or coleoptiles, cell proliferation and cell expansion are deeply intertwined. Because both processes require variable threshold auxin activities, they are difficult to uncouple, which might account for the observation that auxin application generally inhibits or at best only slightly promotes root growth (Moloney et al., 1981; Evans et al., 1994). Likewise, *Arabidopsis thaliana* roots are shorter upon both a genetically imposed strong decrease as well as a strong increase in auxin production (Chen et al., 2014). Moreover, reduced mature cell length is typically accompanied by reduced meristem size and vice versa (Moubayidin et al., 2010; Scacchi et al., 2010; Rodriguez-Villalon et al., 2015), which makes it difficult to distinguish whether observed phenotypes are primarily caused by altered cell elongation or cell proliferation and/or differentiation. Thus, a paucity of clear-cut conditions and pertinent genetic material has prevented conclusive analyses of the Acid Growth Theory in Arabidopsis roots.

In this study, we took advantage of recently isolated mutants of the model grass species *Brachypodium distachyon* in the *TAA1-RELATED2-LIKE* (*TAR2L*) and *ETHYLENE INSENSITIVE2-LIKE1* (*EIN2L1*) genes. *TAR2L* encodes an enzyme of the TRYPTOPHAN AMINOTRANSFERASE OF ARABIDOPSIS1 (TAA1) and TAA1-RELATED (TAR) family of proteins, which catalyze conversion of tryptophan to indole-3-pyruvic acid (IPA) in the two-step auxin biosynthesis pathway (Stepanova et al., 2011; Won et al., 2011). IPA is subsequently converted to indole-3-acetic acid (IAA), the major active auxin, by the YUCCA cytochrome P450 enzymes. Two TAR homologs exist in Brachypodium, with *TAR2L* dominating in the seminal root elongation zone, where cell differentiation and elongation occur (Pacheco-Villalobos et al., 2013). Bd-*EIN2L1* is a homolog of Arabidopsis *EIN2*, an essential positive regulator of ethylene signaling (Alonso et al., 1999; Qiao et al., 2012). Both hypomorphic Brachypodium *tar2l*^{hypo} and *ein2l1*^{hypo} mutants display different degrees of elevated IAA levels in the seminal root elongation zone as well as dramatically enhanced cell elongation. This initially counterintuitive phenotype could be explained by the observation that the regulatory logic of the two-step auxin biosynthetic pathway is different in Brachypodium compared with Arabidopsis: Whereas ethylene positively regulates both steps in Arabidopsis, it negatively regulates the second, rate-limiting step in Brachypodium (Pacheco-Villalobos et al., 2013). The pathway intermediate IPA is metabolically linked to ethylene biosynthesis through the VAS1 enzyme, which catalyzes the formation of tryptophan from IPA using hydrophobic amino acids, mostly L-methionine, as amino group donor (Zheng et al., 2013). Because the size of the L-methionine pool limits the biosynthesis of the rate-limiting ethylene precursor 1-aminocyclopropane-1-carboxylate, not only IPA, but also ethylene biosynthesis are increased in Arabidopsis *vas1* mutants. By analogy, the Brachypodium *tar2l*^{hypo} mutation apparently creates a situation where reduced TAR activity leads to reduced IPA production and thereby also reduced ethylene production, while ethylene signaling is directly dampened in *ein2l1*^{hypo} mutants. Thus, in both hypomorphic mutants, *YUCCA* genes become derepressed to different degrees and eventually more IPA is converted to IAA than in the wild type (Pacheco-Villalobos et al., 2013). Because a unique feature of both Brachypodium *tar2l*^{hypo} and *ein2l1*^{hypo} mutants is that their root meristem size and activity are not affected, their longer seminal roots are entirely explained by the increased mature cell length (Pacheco-Villalobos et al., 2013). Thus, cell proliferation and cell expansion are uncoupled in seminal roots of Brachypodium *tar2l*^{hypo} and *ein2l1*^{hypo} mutants, which both display elevated auxin levels in conjunction with greatly exaggerated cell elongation. Therefore, they offer an unprecedented opportunity to monitor the consequences of high steady state auxin levels in a monocotyledon root type.

RESULTS

Metabolic Analysis Confirms Higher Auxin Levels in *tar2l*^{hypo} Root Segments Despite Reduced Tryptophan Aminotransferase Activity

The strongly enhanced mature root cell length in Brachypodium *tar2l*^{hypo} mutants (Figure 1A) (Pacheco-Villalobos et al., 2013) is apparently cell autonomous because in regenerating excised *tar2l*^{hypo} root tips (Supplemental Figure 1A), newly formed cells are still longer than in its wild-type background, Bd21-0 (Figure 1B). The same is true for *ein2l1*^{hypo} compared with its wild-type background Bd21-3 (Supplemental Figure 1B). In our subsequent analyses, we primarily concentrated on the *tar2l*^{hypo} mutant because of the relatively strong phenotype of *tar2l*^{hypo} seminal roots. For a more complete analysis of auxin metabolism in *tar2l*^{hypo}, we measured the tryptophan aminotransferase background activity (Figure 1C) as well as total (Figure 1D) activity, in Bd21-0 and *tar2l*^{hypo} seminal roots, which revealed an approximately 30% reduction in specific activity in the mutant (Figure 1D). Full-scale analysis of auxin biosynthesis intermediates in 1-cm segments from the root elongation zone of 4-d-old seedlings (Supplemental Figure 1C) with comparable fresh weight in Bd21-0 and *tar2l*^{hypo} (Supplemental Figure 1D) produced a matching metabolic profile; that is, tryptophan levels were slightly increased while IPA levels were substantially decreased in the *tar2l*^{hypo} mutant (Figure 1E). Concurrently, the abundance of a few (inactive) auxin conjugates was shifted, while as previously observed (Pacheco-Villalobos et al., 2013), the level of free auxin (IAA) was significantly increased. Also consistent with previous findings (Zheng et al., 2013), downregulation of a Brachypodium *VAS1-LIKE* gene (*VAS1L*) by RNA interference suppressed the *tar2l*^{hypo} phenotype genetically (Supplemental Figures 1E and F). In summary, these observations confirm our previous finding that downregulation of *TAR2L* results in increased rather than decreased cellular auxin levels and causes strongly enhanced root cell elongation (Pacheco-Villalobos et al., 2013).

High Auxin Steady State Is Associated with Remarkable Transcriptional Homeostasis of the Auxin Signaling Network

The *tar2l*^{hypo} mutant offers a unique opportunity to survey a steady state high auxin concentration transcriptome that is associated with enhanced cell elongation. To this end, we performed mRNA

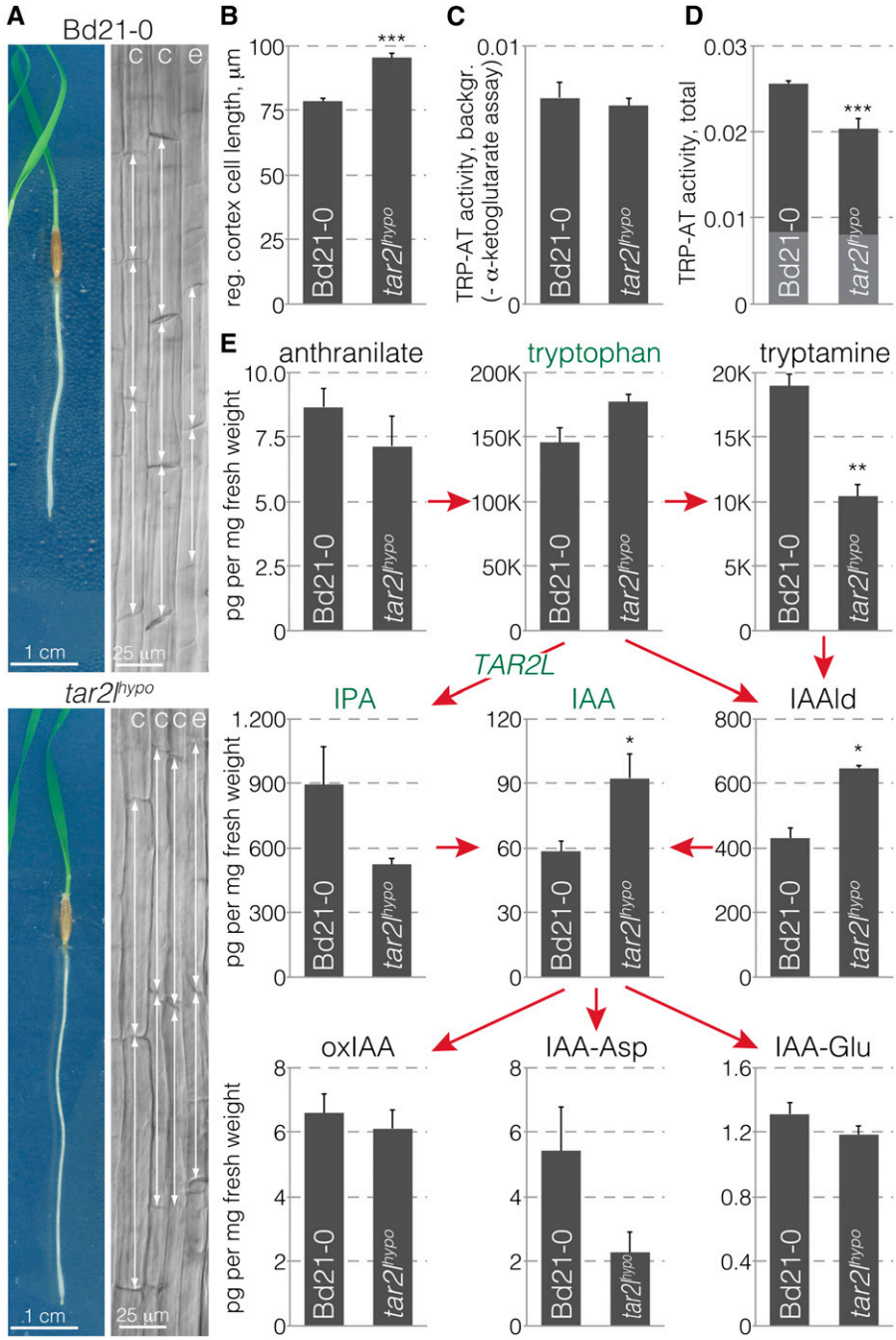

Figure 1. Reduced Tryptophan Aminotransferase Activity in Seminal Roots of Hypomorphic *tar2l* Mutants Results in Higher Cellular Auxin Levels and Strongly Enhanced Cell Elongation.

(A) Four-day-old tissue culture-grown Brachypodium wild type (Bd21-0) and hypomorphic *tar2l* mutant (*tar2l*^{hypo}) seedlings (left) and light microscopy images of their mature cortex (c) and epidermal (e) cell layers (right). Double-sided arrows point out the longitudinal dimensions of individual cells.
(B) Mature cortex cell length in roots 4 d after regeneration from isolated Bd21-0 and *tar2l*^{hypo} root tips (40 cells per root, 10 roots).
(C) Tryptophan aminotransferase background activity in Bd21-0 and *tar2l*^{hypo} roots.
(D) Total tryptophan aminotransferase activity in Bd21-0 and *tar2l*^{hypo} roots, background portion indicated in gray.
(E) Quantification of auxin and auxin metabolites in 1-cm segments from the root elongation zone of 4-d-old Bd21-0 or *tar2l*^{hypo} seedlings. Error bars indicate SE of the mean (three to four biological replicates). Differences were not statistically significant (Student's *t* test) unless indicated as follows: *$P < 0.05$, **$P < 0.01$, and ***$P < 0.001$.

sequencing (RNAseq) of 1-cm root elongation zone segments, grown and harvested in parallel with those used for the metabolic analysis. Complementary to this experiment, we also performed RNAseq on equivalent segments from wild-type plants that had been transferred onto medium containing L-kynurenine for 2 d. Mild concentrations of this tryptophan aminotransferase inhibitor induce higher auxin levels and enhanced cell elongation in wild-type roots, thus mimicking the *tar2l*^{hypo} phenotype (Pacheco-Villalobos et al., 2013). The reads from the Bd21-0, *tar2l*^{hypo}, and L-kynurenine-treated Bd21-0 samples mapped onto more than 27,000 mRNA transcripts out of the 31,679 nuclear genes annotated in the Brachypodium reference genome sequence (version 2.1) (Supplemental Data Set 1), with a pairwise overlap between samples of more than 97%. Compared with the wild type, 957 and 2657 genes were differentially expressed in *tar2l*^{hypo} and L-kynurenine-treated roots, respectively (q value < 0.01, fold change > 2×) (Figure 2A) (Supplemental Data Sets 2 and 3). The higher number of differentially expressed genes in the L-kynurenine-treated samples is consistent with an organ-wide systemic effect of the treatment that includes transcriptome remodeling toward a new steady state. The overlap between the two sets was 344 genes, which represents ~4-fold enrichment over neutral expectation ($P < 0.0001$, χ^2 test). A similar RNAseq experiment was performed with root segments from Bd21-3 and *ein2l1*^{hypo} seedlings. Again, over 27,000 transcripts were detected and 356 genes were differentially expressed (Supplemental Data Sets 1 and 4). Overlap with the *tar2l*^{hypo} and L-kynurenine-treated sets was 140 and 112, respectively, which again represented high enrichment (~12- and ~3.5-fold, respectively) over neutral expectation ($P < 0.0001$, χ^2 test). In summary, the RNAseq profiles indicated high overlap between the mutants and the L-kynurenine condition, with the extent of differentially expressed genes correlating with phenotype strength. Despite the similarities between their transcriptome profiles, the samples were clearly grouped apart. Both mutants were more similar to their wild-type backgrounds than to each other, and the L-kynurenine-treated samples were most distant to all others (Figure 2B). A principal component analysis confirmed that parental background was the dominant factor in the grouping of samples (Figure 2C).

Analysis of the annotations of the differentially expressed genes revealed a rather low occurrence of genes involved in auxin or other hormone signaling pathways (Figure 3A). Significant differential expression was observed for six out of 26 annotated auxin response factors, seven out of 32 annotated *AUX/IAA* genes, and one out of five annotated auxin receptor genes (Figure 3B; Supplemental Data Set 5). However, the expression changes were moderate throughout. Likewise, mostly small effects were observed for the few differentially expressed genes involved in polar auxin transport, which included two auxin influx facilitators and three auxin efflux carriers. Overall, the data indicate that the transcriptional steady state of the auxin-signaling network is well buffered with respect to variation in auxin levels. Interestingly, however, some primary auxin target genes of the *SMALL AUXIN UP-REGULATED* (*SAUR*) category were differentially expressed (five out of 42 annotated genes) and mostly upregulated (four out of the five) (Figure 3C). *SAUR* genes are classic auxin signaling output genes, and it has been suggested that SAUR proteins antagonize posttranslational inhibition of PM-H$^+$-ATPases (Spartz et al., 2014). Finally, with the exception of two genes that were substantially downregulated (Figure 3D), Brachypodium genes that encode PM-H$^+$-ATPases displayed no differential expression.

High Auxin Steady State Is Associated with Transcriptional Changes in Cell Wall Remodeling Factors

The majority of significantly enriched terms that stood out in a word cloud made from annotation of differentially expressed genes was related to the cell wall and associated processes (Figure 3A). Yet, only a small proportion of genes encoding cell wall remodeling proteins displayed differential expression, and these were restricted to a few groups. For example, while 6 out of 15 annotated xyloglucan endotrans-glycosylases/hydrolases were up- or downregulated at roughly equal measure (Figure 3E), no differential expression was observed among cellulose synthase genes. The most prominent differentially expressed cell wall modulators were expansins (23 out of 54 annotated expansin genes), which were significantly enriched ($P = 0.0078$ for the overlap between all samples, χ^2 test) and are also considered classic auxin target genes. The majority (18 out of 23) displayed comparatively strong upregulation (Figure 3F). Finally, three genes encoding arabinogalactan peptides or proteins stood out because of their consistent upregulation (Figure 3G). Verification of differential expression by qPCR was performed for a selected set of genes of interest in independent RNA samples from *tar2l*^{hypo} and L-kynurenine-treated root segments, confirming the RNAseq results (Figure 3H). In summary, the transcriptomic data indicate that in the presence of higher cellular auxin levels, the auxin signaling network maintains remarkable homeostasis at the transcriptional level, while the bulk of expression changes are observed in cell wall remodeling genes, notably expansins.

High Auxin Steady State Is Associated with a Specific Change in Glycosidic Cell Wall Linkages

The robust changes in the arabinogalactan protein/peptide genes were of particular interest in light of our results from chemical cell wall analyses. To monitor the structural effect of altered expression in cell wall remodeling genes, we performed cell wall polysaccharide analysis of root segments from parallel samples that were grown and harvested concomitantly with the segments analyzed by RNAseq. The analysis of the glycosidic linkages occurring in the cell wall polymers detected only few significant differences between Bd21-0 and *tar2l*^{hypo}, or Bd21-3 and *ein2l1*^{hypo}. However, both profiles were consistent, with a specific significant decrease in 1,3-galactosyl residues in the mutants relative to their wild-type backgrounds (Figures 4A and 4B). 1,3-Linked galactose is found specifically in the glycosidic moiety of the arabinogalactan proteins (AGPs) (Seifert and Roberts, 2007; Ellis et al., 2010; Kitazawa et al., 2013; Knoch et al., 2014). 1,3-Linked galactosyl residues represented ~10% of all linked sugar residues detected in both wild-type backgrounds and were reduced by about 2- to 3-fold in *ein2l1*^{hypo} and *tar2l*^{hypo}, respectively. Moreover, the analysis of the cell wall neutral sugars indicated similar relative abundance of the different monosaccharides in the mutants and wild types, with one notable exception, fucose, a minor cell wall sugar (Figures 4C and 4D). Relative fucose

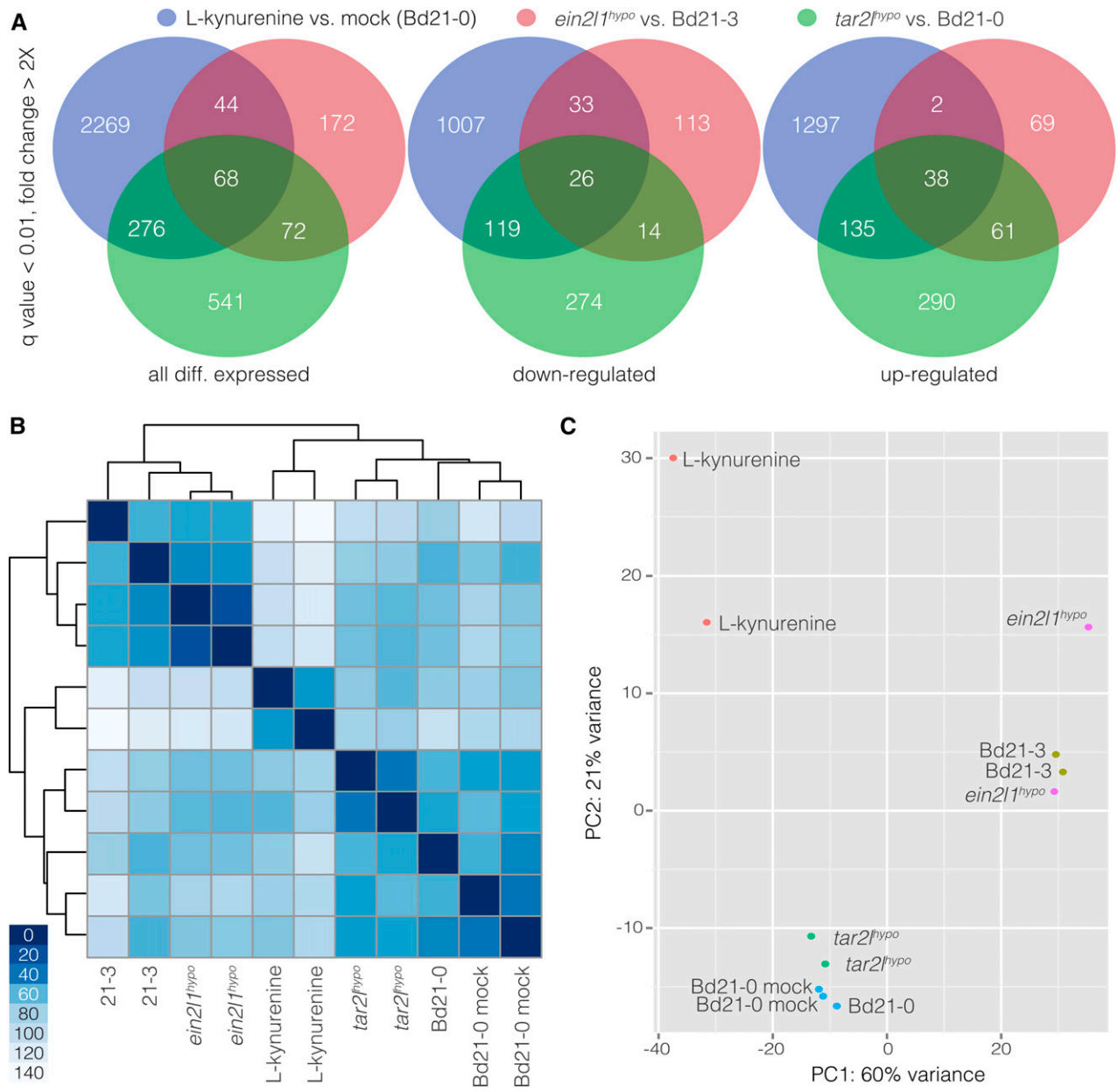

Figure 2. Differential Gene Expression in Root Segments as Determined by RNA Sequencing.

(A) Venn diagrams illustrating overlaps between the gene sets that were differentially expressed in root segments of Bd21-0 versus *tar2l*^{hypo}, Bd21-3 versus *ein2l1*^{hypo}, and mock-treated versus L-kynurenine-treated Bd21-0.
(B) and **(C)** Cluster analysis **(B)** and principal component (PC) **(C)** analysis of the different RNA sequencing samples.

abundance was more than halved in *tar2l*^{hypo} and reduced by about one-third in *ein2l1*^{hypo}. Interestingly, just like β-1,3-linked galactose, fucose is found in AGPs (van Hengel and Roberts, 2002). Thus, the analyses point to a very specific effect of elevated cellular auxin levels on arabinogalactan complexity or abundance in Brachypodium. To confirm this observation with an alternative technique, we performed in situ Yariv staining on Bd21-0 and *tar2l*^{hypo} roots. The Yariv reagent is known to specifically detect β-1,3-galactan (Yariv et al., 1967; Kitazawa et al., 2013). Staining was considerably reduced in the root elongation zone of *tar2l*^{hypo}, thereby corroborating the chemical cell wall analyses (Figure 4E). Moreover, we probed transverse sections in the root elongation zone with antibodies directed against demethylesterified pectin (2F4 antibody; Figure 4F), methylesterified pectin (JIM7 antibody; Figure 4G), and arabinogalactan side chains (LM2 antibody; Figure 4H). None of these stainings showed a marked difference in epitope abundance or distribution, except that in general, the mean fluorescence signal of the LM2 antibody was reduced. This

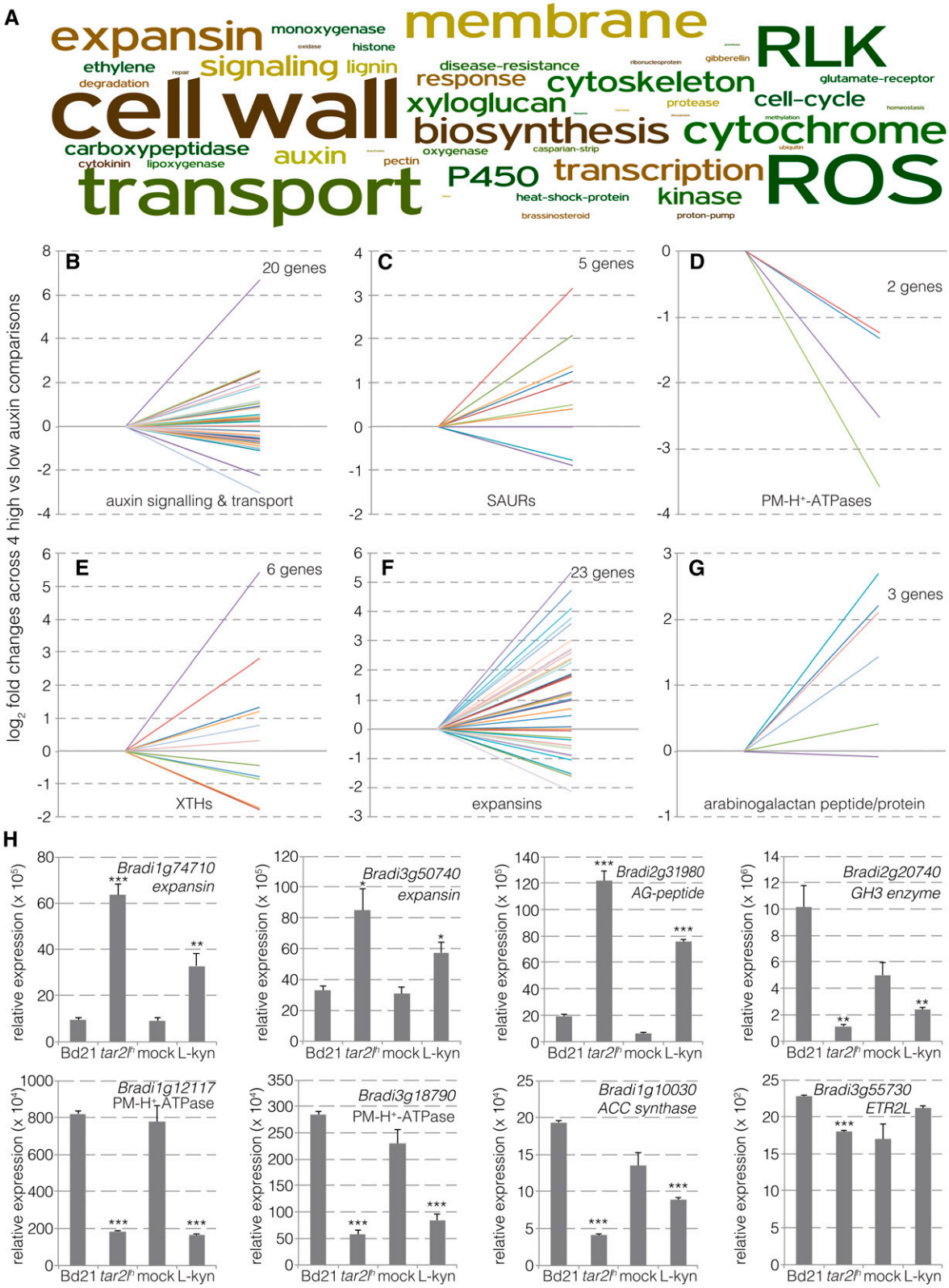

Figure 3. Differential Expression of Auxin- and Cell Wall-Related Genes in Root Segments.

(A) Word cloud from annotations of genes differentially expressed between Bd21-0 versus *tar2l*^{hypo}, or mock-treated versus L-kynurenine-treated Bd21-0.

might hint to lower AGP abundance; however, it is unclear to what degree the antibody stainings are quantitative. Importantly, unlike the Yariv reagent, the LM2 antibody does not recognize the β-1,3-galactan linkages in the arabinogalactan backbone, but rather an epitope that comprises β-linked glucuronic acid, which is found at the side chain termini (Smallwood et al., 1996; Knoch et al., 2014). Therefore, collectively, the results point to reduced AGP complexity.

High Auxin Steady State Is Not Associated with Markedly Increased Proton Excretion

Our transcriptomic and cell wall analyses indicate that elevated cellular auxin levels in Brachypodium roots are indeed associated with differential expression of cell wall remodeling genes and matching changes in cell wall composition. To determine whether this also applies to the hallmark of the Acid Growth Theory, apoplastic acidification, we next investigated the capacity of Bd21-0 and *tar2l*^{hypo} roots to acidify the medium. To this end, we first visualized rhizosphere acidification by transferring seedlings onto medium supplemented with pH indicator. Acidification was readily detected within 4 h but was not apparently stronger for *tar2l*^{hypo} roots compared with Bd21-0 roots (Figures 5A and 5B). Likewise, in a quantitative assay with liquid medium, acidification could be readily followed over time; however, no difference in proton pumping activity of root tips could be detected between Bd21-0 and *tar2l*^{hypo} (Figure 5C). Finally, we measured apoplast acidification more directly at the root surface using fiber optic pH microfiber sensors. To this end, five roughly equidistant measuring points from the root tip through the elongation zone were monitored along individual roots. As could be expected, these measurements revealed a gradient of increasingly acidic pH from the root tip to the differentiated cells. However, this gradient was less rather than more pronounced in *tar2l*^{hypo} compared with Bd21-0 (Figure 5D). Likewise, in general, reduced rather than increased acidification was observed in *ein2l1*^{hypo} roots compared with their Bd21-3 wild type background (Supplemental Figure 2A). Finally, we monitored the phosphorylation state of PM-H$^+$-ATPases in root segments. Phosphorylation of the penultimate amino acid within the autoinhibitory C-terminal domain of PM-H$^+$-ATPase and subsequent binding of 14-3-3 proteins is the major mechanism of enzyme activation (Palmgren et al., 1991; Portillo et al., 1991; Speth et al., 2010). We therefore monitored both the capability of 14-3-3 proteins to associate with PM-H$^+$-ATPase in microsomal membranes of root segments (14-3-3 overlay), reflecting its phosphorylation level, and the amount of PM-H$^+$-ATPase (Ottmann et al., 2007; Speth et al., 2010). Interestingly, phosphorylation-dependent binding of 14-3-3 proteins to the PM-H$^+$-ATPase was reduced, rather than increased, in microsomal preparations from *tar2l*^{hypo} root segments compared with Bd21-0 (Figure 5E). This is in striking contrast to the effect of auxin on PM-H$^+$-ATPase phosphorylation in hypocotyl elongation in Arabidopsis (Takahashi et al., 2012). Collectively, these experiments suggest that higher cellular auxin levels in Brachypodium roots are not associated with proton pump activation or markedly elevated proton excretion at the mesoscopic level.

Forced Apoplastic Acidification Inhibits Root Cell Elongation

Next, to conversely determine whether acidity affects Brachypodium root cell elongation, we monitored the response of the root to externally imposed pH changes. In Arabidopsis, strong acidity eventually impairs overall root growth by inhibiting meristematic activity (Gujas et al., 2012), and the same applies to Brachypodium (see below). Reduced meristematic activity could alter mature cell length because it shifts the balance between proliferation and differentiation (Moubayidin et al., 2010; Scacchi et al., 2010). Therefore, we chose to examine mature cortex cell length after transfer of seedlings from standard medium (pH 5.7) to mildly more acidic conditions (pH 5.2), which nevertheless represent an approximately 3-fold increase in H$^+$ concentration. Only cells formed after the transfer were scored. In these experiments, no significant length difference was observed between cells formed on either pH (Figure 6A) and overall root growth was not affected (Supplemental Figure 2B). At the same time, fiber optic pH sensor measurements along the root surface performed in parallel revealed converging pH gradients under the two conditions (Figure 6B), to approximately pH 4.9 in the root elongation zone. Medium acidification by Brachypodium root tips to pH 4.8 to 4.9 was observed repeatedly and appears to represent a lower limit in tissue culture. Therefore, we challenged roots with pH 3.7, a respective approximately 10-fold increase in acidity. Surprisingly, while overall root growth was substantially reduced at this acidic pH (Figure 6C), this was entirely attributable to reduced meristematic activity. Mature cell length was again not affected (Figure 6D). Likewise, even shortly after transfer of root tips into acidic medium, at best a small and transient significant positive effect on cell elongation could be observed (Supplemental Figure 2C). The same applies to similar experiments where root tips were transferred into medium that contained fusicoccin, a proton pump stimulant (Supplemental Figure 2D). In summary, these results suggest that cell elongation in Brachypodium roots is robustly buffered against external pH fluctuations.

To further explore the relation between apoplastic acidification and cell elongation, we turned to a model system that allows more direct manipulations, Arabidopsis. Similar to Brachypodium,

Figure 3. (continued).

(B) to **(G)** Expression changes (fold changes) for individual members of the indicated gene classes in Bd21-0 versus *tar2l*^{hypo} and mock-treated versus L-kynurenine-treated Bd21-0 (Bd21-0/mock set to 1 on the left, *tar2l*^{hypo}/L-kynurenine-treated Bd21-0 values on the right). Only genes that showed differential expression and a q value < 0.01 in at least one comparison are plotted. See Supplemental Data Set 5 for gene identifiers and expression values.
(H) qPCR verification of differential gene expression in independent RNA samples prepared from independent root segments (three biological replicates). Error bars indicate SE of the mean. Differences were not statistically significant (Student's *t* test) unless indicated as follows: *P < 0.05, **P < 0.01, and ***P < 0.001.

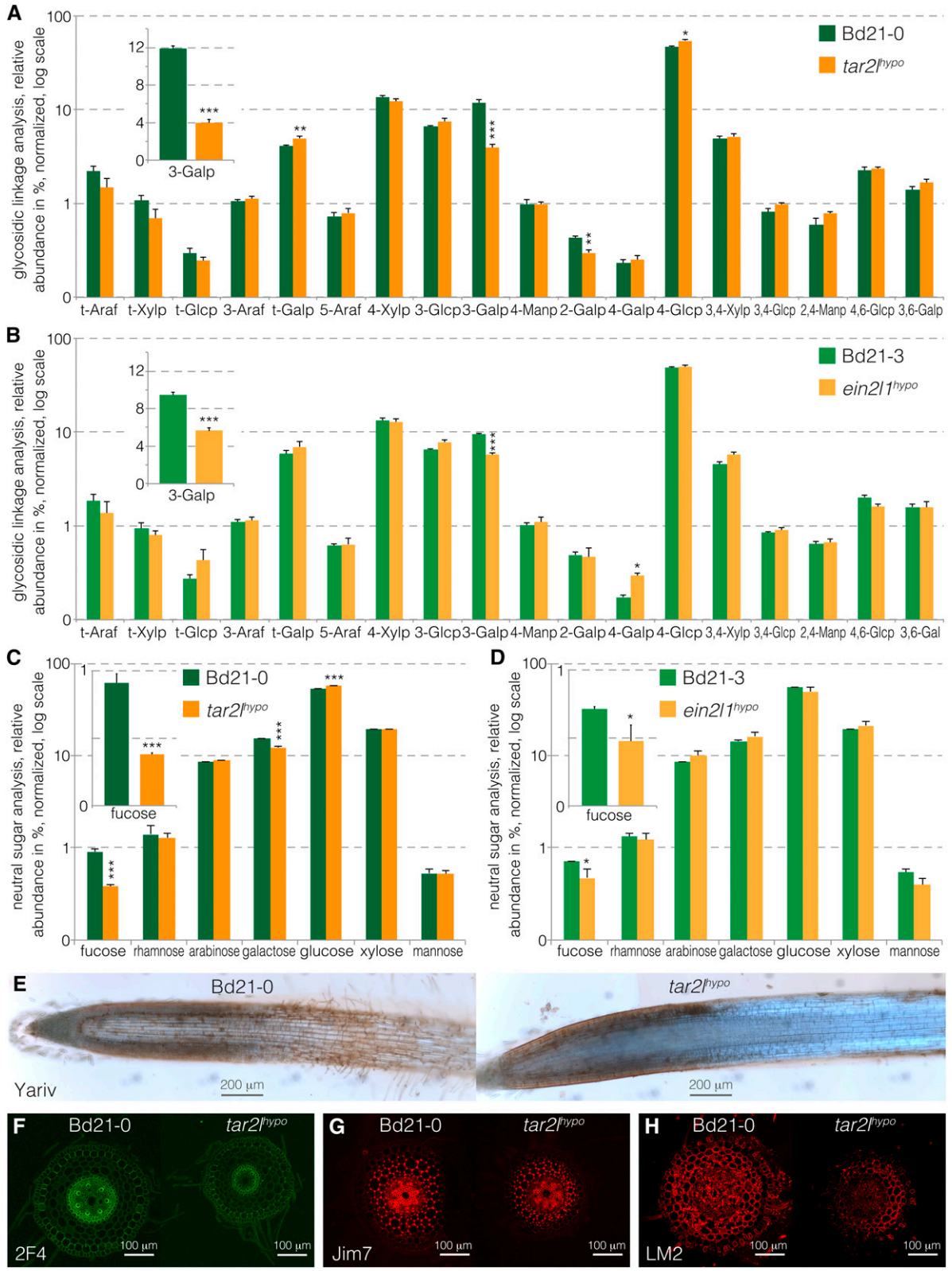

Figure 4. Cell Wall Analyses of *tar2l*^{hypo} and *ein2l1*^{hypo} Root Segments Compared with Their Wild-Type Backgrounds.

(A) Glycosidic linkage analysis of Bd21-0 and *tar2l*^{hypo} root segments.

mature cortex cell length was scarcely sensitive to pH variations in the medium (Figure 6E), meaning that again reduced overall root growth on acidic medium (Supplemental Figure 2E) can be largely attributed to decreased meristematic activity, as previously observed (Gujas et al., 2012). Thus, apparently root cell elongation is also robustly buffered against external pH changes in Arabidopsis roots. To override this buffering effect, we sought to uncouple proton pump activity from homeostatic inputs and stimulate it at will. To this end, we again applied fusicoccin, which at low concentration again resulted at most in a small significant stimulation of cell elongation, while higher concentration clearly reduced cell elongation (Figure 6F). In a more direct, genetic approach, we investigated wild-type seedlings that carried an inducible transgene for conditional expression of the Arabidopsis PM-H^+-ATPase AHA2 devoid of its C terminus ($AHA2^{\delta 95}$). This 95-amino acid deletion removes the autoinhibitory domain of the protein, which is therefore turned into a hyperactive proton pump that is uncoupled from regulatory inputs (Regenberg et al., 1995; Axelsen et al., 1999). Similar to high fusicoccin concentrations, strong induction of the $AHA2^{\delta 95}$ construct resulted in the cessation of meristem activity, massive root cell swelling, and eventual rupture of the root tissues. By contrast, at lower induction levels, which maintained root growth, cell elongation was strongly reduced (Figure 6G). In these conditions, some cellular swelling was observed, consistent with an increased vacuole size (Figure 6H), yet this vacuolar size increase by itself was apparently not sufficient to drive significant cell elongation. Finally, in all conditions, both fusicoccin exposure and $AHA2^{\delta 95}$ induction resulted in reduced meristematic activity and thus reduced meristem size (Supplemental Figures 2F and 2G). Yet even when strong vacuolar swelling was induced, we did not observe longer cells.

DISCUSSION

The importance of auxin in plant development cannot be overstated. Auxin impinges on a large variety of physiological and morphological processes, for which both absolute and relative auxin levels can be determinants. For instance, this is illustrated in root development, where auxin biosynthesis, polar transport, and signaling are required for proper morphogenesis, growth, and integration of environmental signals (Hardtke and Berleth, 1998; Sabatini et al., 1999; Zhao, 2014; Adamowski and Friml, 2015). A wealth of genetic and physiological data underpins the role of auxin in root development, yet root responses to systemically applied external auxin have been difficult to interpret. While picomolar levels of auxin sometimes stimulate root growth, physiological, nanomolar concentrations in general suppress root growth (Sutcliffe and Sexton, 1969; Evans et al., 1994; Overvoorde et al., 2010). Likewise, genetically increased excess cellular auxin production through ectopic overexpression of YUCCA enzymes inhibits rather than enhances root growth (Chen et al., 2014). These results indicate that in the absence of correct tissue context, increased auxin levels fail to reveal the central role of auxin in root growth, possibly because crucial auxin gradients are overridden (Benjamins and Scheres, 2008). In summary, pertinent auxin biosynthesis, transport, or signaling mutants and transgenic lines, mostly in Arabidopsis, do not display substantially enhanced root growth. Therefore, the Brachypodium *tar2l*^{hypo} and *ein2l1*^{hypo} mutants represent a so far very unusual situation because here locally increased auxin levels are associated with a specific and strong stimulatory effect on root cell elongation while meristematic activity and meristem size are not affected (Pacheco-Villalobos et al., 2013). This observation also contradicts the sometimes voiced argument that root cell elongation is typically maximal and therefore cannot be stimulated further by hormone action.

A Transcriptome Associated with High Auxin Steady State

The remarkable phenotypic specificity of both Brachypodium mutants with respect to root cell elongation offered us the unique opportunity to survey a transcriptome that is associated with a high auxin steady state. Auxin-regulated genes have so far been mainly identified through their response to external auxin application. This approach has been tremendously successful in identifying the principal auxin target genes and the autoregulatory feedback in the auxin signaling networks. Most prominently, they include *AUX/IAA* genes, which encode repressors of auxin signaling and respond rapidly and strongly to auxin application. Compared with these classic auxin-responsive transcriptomes, components of the auxin signaling network are rare among the differentially expressed genes in our RNAseq analyses. Even when significant, their expression fold changes are very moderate throughout, typically smaller than 1.5. Overall, the differentially expressed auxin signaling genes are downregulated in our samples, which could indicate a compensatory mechanism in response to higher cellular auxin levels. Thus, at the transcriptional level, the auxin signaling network maintains a remarkably buffered homeostasis. By contrast, a number of classic auxin target genes that are considered physiologically relevant immediate outputs

Figure 4. (continued).

(B) Glycosidic linkage analysis of Bd21-3 and *ein2l1*^{hypo} root segments.
(C) Neutral sugar analysis of Bd21-0 and *tar2l*^{hypo} root segments.
(D) Neutral sugar analysis of Bd21-3 and *ein2l1*^{hypo} root segments.
(E) Yariv staining (brownish) against β-1,3-galactan linkages in AGPs on longitudinal sections of Bd21-0 and *tar2l*^{hypo} root tips.
(F) 2F4 antibody staining against demethylesterified pectin (green) on transverse sections from the elongation zone of Bd21-0 and *tar2l*^{hypo} root tips.
(G) JIM7 antibody staining against methylesterified pectin (red) on transverse sections from the elongation zone of Bd21-0 and *tar2l*^{hypo} root tips.
(H) LM2 antibody staining against AGP side chains (red) on transverse sections from the elongation zone of Bd21-0 and *tar2l*^{hypo} root tips. Error bars indicate SE of the mean (two technical replicates per each of three biological replicates). Differences were not statistically significant (Student's *t* test) unless indicated as follows: *$P < 0.05$, **$P < 0.01$, and ***$P < 0.001$.

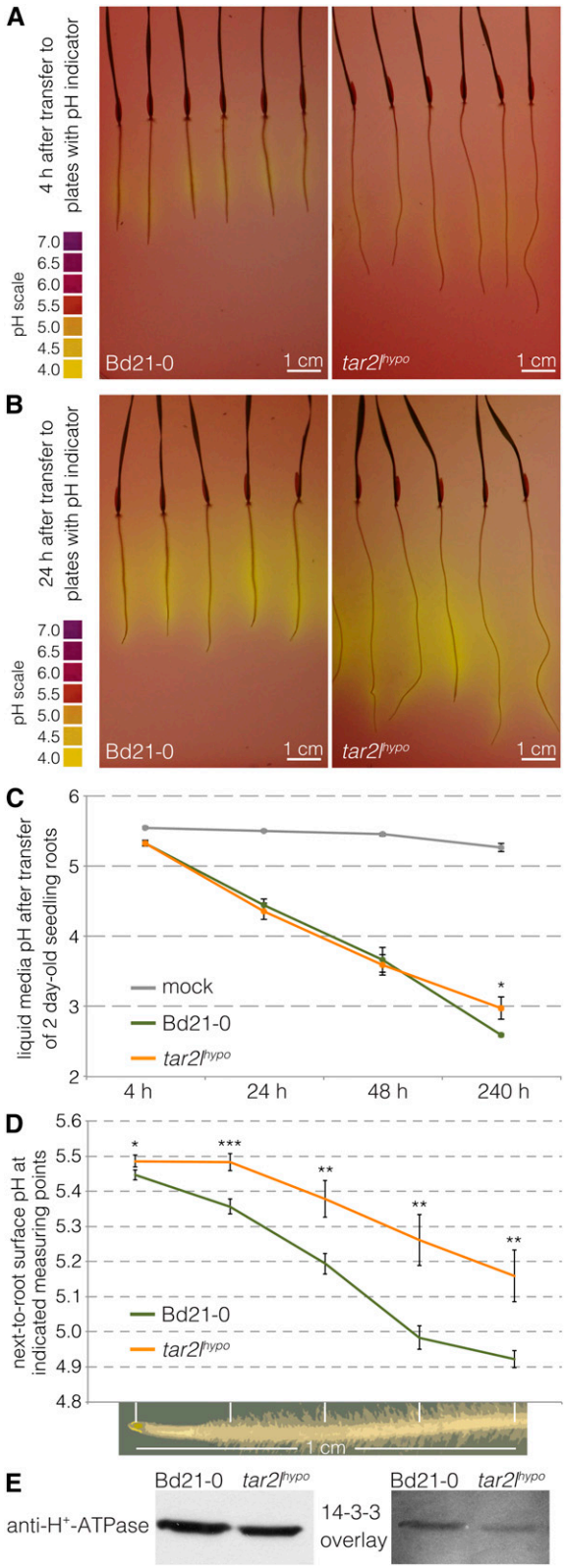

Figure 5. Medium Acidification by Bd21-0 and *tar2l*^{hypo} Root Tips.

(A) Medium acidification through proton excretion from seminal roots of 3-d-old seedlings, 4 h after transfer onto fresh medium with pH indicator.
(B) Same as **(A)**, 24 h after transfer.
(C) Progressive acidification of liquid medium through proton excretion from seminal root tips starting with 2-d-old seedlings (six biological replicates).
(D) pH traces along the surface of root tips, measured with a fiber-optic pH microsensor at five equidistant points as indicated (10 to 12 biological replicates).
(E) Protein gel blot antibody detection of H^+-ATPases in protein samples isolated from microsomes of root segments and overlay with 14-3-3 protein binding. Error bars indicate SE of the mean. Differences were not statistically significant (Student's *t* test) unless indicated as follows: *$P < 0.05$, **$P < 0.01$, and ***$P < 0.001$.

of auxin action are differentially expressed at higher levels in the mutants and are upregulated overall. Most notably, these include genes related to cell wall remodeling, among which substantial differential expression of genes encoding expansins is most robust. In summary, these observations suggest that our mutant transcriptomes could be indicative of physiologically relevant auxin targets.

Between the five types of transcriptomes, we not only observed increasing differential expression as a function of phenotypic strength, or, in the case of roots grown on L-kynurenine, systemic action, but also in relation to parental background. However, although all samples were harvested in parallel, the *ein2l1*^{hypo} and Bd21-3 root segments were processed at a different time from the other samples, and their RNAseq was performed in a separate instrument run. Thus, it is possible that the *ein2l1*^{hypo} versus *tar2l*^{hypo} transcriptome comparison is to some degree not only constrained by parental background, but also by batch effect. Although this limits the validity of any derived analyses, it is noteworthy that across all possible cross-comparisons, the by far most robust differential expression was observed for a gene that encodes an arabinogalactan peptide.

A Specific Effect of High Steady State Auxin Levels on Arabinogalactan Complexity

AGPs are a group of highly diverse cell surface glycoproteins (Seifert and Roberts, 2007; Ellis et al., 2010). Their protein backbone is characterized by dipeptide motifs that comprise hydroxyproline residues, which serve as attachment points for β-1,3-linked galactose oligosaccharides. These galactans can themselves serve as secondary branch points for additional side chains, which can contain a variety of other sugars, such as arabinose or fucose. The exact roles of AGPs in plant development remain somewhat unclear, in part because of their structural variety and the resultant fuzziness of analyses, but they have been implicated in various growth-related processes (Seifert and Roberts, 2007; Ellis et al., 2010). The most clear-cut evidence for a role in root development so far comes from genetic analyses of Arabidopsis plants with altered expression of enzymes that have an experimentally proven role in the biosynthesis or degradation of arabinogalactan side chains (Knoch et al., 2014). An interesting finding from this small set of studies is that while arabinogalactans appear to be generally required for cell elongation, in mutants or

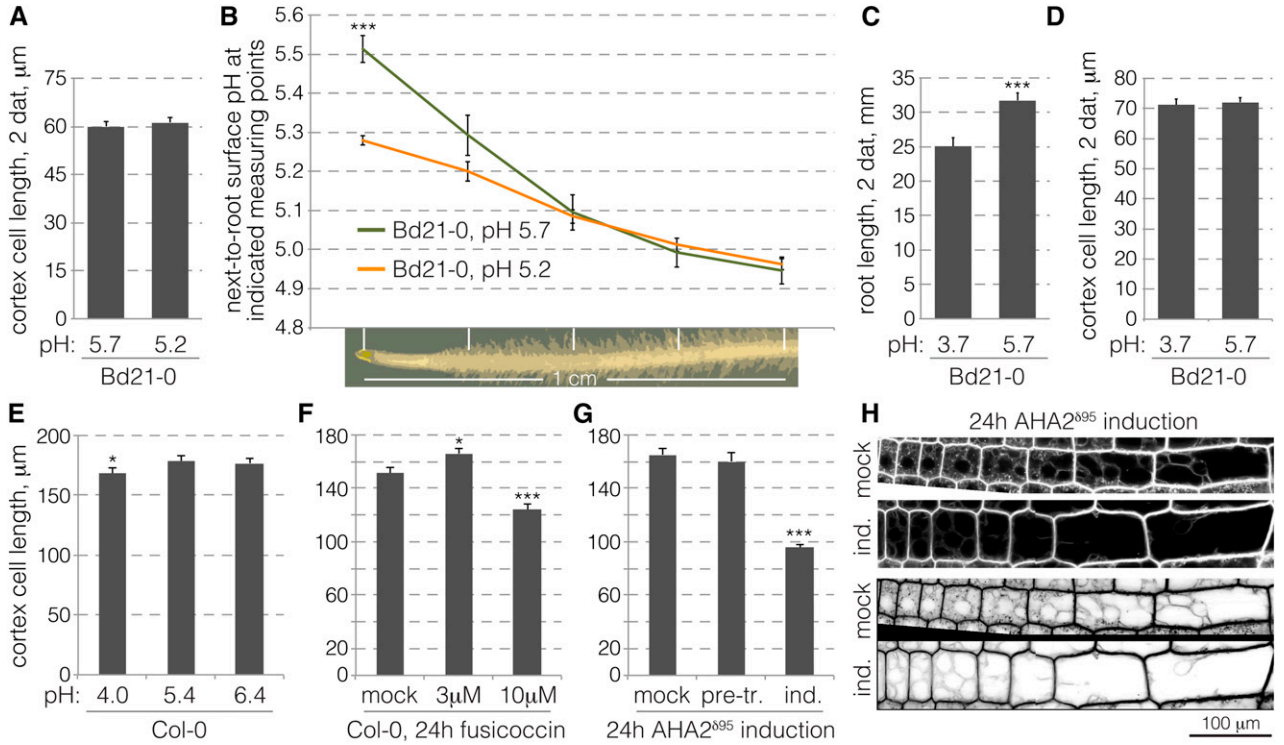

Figure 6. Root Cell Elongation in Response to External pH Variation or Forced Apoplastic Acidification.

(A) Mature cortex cell length in Bd21-0 wild-type roots 2 d after transfer of 2-d-old seedlings from standard pH (5.7) to standard pH or more acidic pH (5.2) (103 to 122 cells from six to eight roots). Only cells formed after transfer were scored.

(B) Root tip surface pH traces obtained with a fiber optic pH microsensor at five equidistant points as indicated (eight biological replicates).

(C) Root length of Bd21-0 wild-type seedlings 2 d after transfer of 2-d-old seedlings from standard pH (5.7) to standard pH or very acidic pH (3.7) (8 to 10 roots). Note that on pH 3.7, root growth is severely inhibited and meristematic activity gradually ceases.

(D) Mature cortex cell length of roots in **(C)** (75 to 97 cells). Only cells formed after transfer were scored.

(E) Mature cortex cell length in roots of 5-d-old Arabidopsis Col-0 wild-type seedlings grown on media with different pH (145 to 157 cells from 19 to 20 roots).

(F) Mature cortex cell length in roots of 4-d-old Arabidopsis Col-0 wild-type seedlings, 24 h after transfer from standard medium onto mock- or fusicoccin-supplemented medium. Only cells formed after transfer were scored (28 to 53 cells from six roots).

(G) Mature cortex cell length in roots of 4-d-old transgenic Arabidopsis AHA2$^{\delta 95}$ seedlings, 24 h after transfer on medium supplemented with 1 µM dexamethasone to induce expression of the hyperactive proton pump (25 to 74 cells from five roots). Cells were scored in mock-treated roots, as well as before (pretreatment) and after induction in the same roots.

(H) Confocal microscopy of epidermal root cells in mock-treated or dexamethasone-induced AHA2$^{\delta 95}$ seedlings, 4 h after induction, with FM4-64 staining. Vacuoles can be easily distinguished in the inverted gray-scale images. Error bars indicate SE of the mean. Differences were not statistically significant (Student's *t* test) unless indicated as follows: *P < 0.05, **P < 0.01, and ***P < 0.001.

transgenic lines with mildly reduced arabinogalactan complexity, root elongation is substantially stimulated (van Hengel and Roberts, 2002; Eudes et al., 2008; Knoch et al., 2013). However, whether this is mainly due to enhanced cell elongation has not been reported.

The published genetic data on the role of arabinogalactans in Arabidopsis root development match our observations for Brachypodium. In our root segments, we did not observe any changes in the expression of Brachypodium homologs of proven arabinogalactan metabolism enzymes. Yet, we observed a clear reduction in β-1,3-galactan levels in biochemical and in situ analyses of our mutants. Overall, the data suggest reduced complexity and possibly also abundance of arabinogalactans. It is conceivable that these observations could be linked to changes in AGP expression in response to higher steady state auxin levels. AGP protein backbones, which are typically approximately 100 amino acids long, are secreted and attached to the plasma membrane via a glycosylphosphatidylinositol membrane anchor that is added during their processing. The same applies to the much shorter arabinogalactan peptides, which are only 10 to 12 amino acids long (Schultz et al., 2004). Of the three differentially expressed arabinogalactan backbone genes in our data set, the one encoding an 11-amino acid arabinogalactan peptide is most dynamically and robustly overexpressed (4 to 7×) in the high cellular auxin situation across all comparisons. Perhaps this shift in arabinogalactan protein backbone length distribution to a higher proportion of short backbones could lead to a looser, less complex AGP network. Future approaches, for instance, transgenic overexpression, could be used to address this notion directly.

Root Cell Elongation Is Robustly Buffered against External pH Fluctuation

The Acid Growth Theory of plant cell elongation has been formulated with respect to the elongation of shoot organs, with an experimental focus on coleoptiles and hypocotyls. To what degree it is pertinent for root cell elongation has been controversial from the beginning because of early observations that auxin application to intact roots generally inhibits growth or has no effect (Sutcliffe and Sexton, 1969). At best, growth stimulation could be observed with very low auxin concentrations or in treatments of auxin-depleted roots (Edwards and Scott, 1977; Pilet et al., 1979; Evans et al., 1994). However, in all cases, the size of the effect was small, and it was not reported whether the effect was due to altered root meristem activity or cell elongation. In accordance with these results, the impact of auxin on proton excretion also did not match observations in shoot organs and was generally variable. For example, proton efflux upon treatment of maize (*Zea mays*) roots was reported for nanomolar concentrations of auxin, while proton uptake was observed with micromolar concentrations, with the caveat that these roots had been pretreated with ethylene biosynthesis inhibitors (Mulkey et al., 1982). Others suggested that growing parts of barley (*Hordeum vulgare*) roots take up protons, while nongrowing parts secrete them (Weisenseel et al., 1979). Finally, a recent study that monitored apoplastic pH using a fluorescent molecular marker in planta found that auxin treatment has little effect on pH in the meristem tip but leads to alkalization rather than acidification in the root cell elongation zone (Gjetting et al., 2012), corroborating similar earlier claims (Evans et al., 1980; Moloney et al., 1981; Luthen and Bottger, 1993). Eventually, for maize roots, it was concluded that the pH growth curve exhibits a broad optimum ranging from pH 4.5 to 9, that any acid-induced growth is of very short duration, that the low sensitivity of root growth to external pH is independent of both pump activity and buffering capacity of the bathing solution, and that neither incubation in acidic buffer nor stimulation of the proton pump reverts auxin-induced root growth inhibition (Luthen and Bottger, 1993).

Our observations largely second these conclusions for Brachypodium as well as Arabidopsis. Although it is evident from our assays that the root tips acidify the rhizosphere as could be expected, we did not detect enhanced proton excretion at the surface of mutant roots. Thus, although a few *SAUR* genes are upregulated under the high auxin conditions in our transcriptomes and could possibly stimulate proton pumps indirectly, similar to Arabidopsis *SAUR19* (Spartz et al., 2014), this apparently does not translate into a detectable increase in proton excretion at the mesoscopic level. Likewise, the two proton pump genes that are downregulated under high auxin conditions should have little impact on overall proton pump abundance because they are only weakly expressed. The by far preponderant proton pump gene that we detected (Bradi5g24690) was expressed very robustly across all conditions tested at levels over 10 times higher than the other nine proton pump genes combined. Indeed, our protein gel blot analysis confirmed that PM-H$^+$-ATPase abundance in *tar2l*^{hypo} was comparable to the wild type or at best mildly reduced. Moreover, given that proton pump activity is mostly regulated through posttranslational modifications, one would not expect that their mild transcriptional regulation would play a major role.

Based on our data, we cannot exclude the possibility that elevated proton pumping is induced by higher cellular auxin content, but it does not propagate beyond the immediate vicinity of the cell surface because of the concomitantly increasing membrane potential. Such proton pumping could therefore not be detected by our methods. Although our observation that PM-H$^+$-ATPase phosphorylation is decreased rather than increased in *tar2l*^{hypo} argues against this scenario, it is important to note that the interpretation of our findings is constrained by the lack of single cell resolution of our observations and morphological features, such as the shorter root hairs in *tar2l*^{hypo} mutants (Pacheco-Villalobos et al., 2013). Perhaps very local and transient acidification is sufficient to trigger cell elongation, which would make the observation that cell elongation in both Brachypodium and Arabidopsis roots is robustly buffered against external pH fluctuation, including imposed acidity, even more remarkable. Consistently, throughout our experiments, excess acidity eventually suppressed root growth by impairing meristematic activity rather than cell expansion. This finding suggests that compensatory mechanisms act to keep apoplastic root cell pH optimal for cell elongation. Our finding that forced apoplastic acidification, for instance, through induction of a constitutively active proton pump, strongly impairs root cell elongation underlines this notion.

In summary, our data suggest that elevated steady state auxin levels in Brachypodium seminal roots are associated with specific transcriptomic and cell wall changes. While some of those changes match expectations, e.g., enhanced expression of expansin genes, others come as a surprise, notably the specific effect on arabinogalactans. Whether all of the observed changes are direct effects of auxin or emerge indirectly, for example, from hormonal crosstalk, notably with ethylene, remains to be determined. At this point, our data provide a phenotypic reference framework for future investigations that might also clarify to what degree our observations are specific for Brachypodium. Robust buffering of root cell elongation against pH fluctuation would surely make sense in the universal biological context of root growth. Unlike the shoot system, the root system is in close contact with a solid phase environment, the soil, which imposes its pH. Roots can modify the rhizosphere pH by proton pumping to increase the solubility of essential nutrients and promote their uptake, which has an optimum in the range of pH 5.0 to 6.5. Given the variability of soil pH values and their seasonal fluctuation, it appears advantageous for the plant if root growth capacity is not dictated by the soil environment pH. From this perspective, it would make sense that the interplay between auxin, proton pump activation, and expansin action at the heart of the Auxin Growth Theory is possibly more flexible in the root than in the shoot.

METHODS

Plant Materials and Growth Conditions

The *Brachypodium distachyon* mutants *tar2l*^{hypo} and *ein2l1*^{hypo} and their respective wild-type backgrounds Bd21-0 and Bd21-3 have been described before (Pacheco-Villalobos et al., 2013). Unless indicated otherwise, analyses were performed on tissue culture-grown 4-d-old

seedlings raised under previously described conditions (continuous light, 100 to 120 μE intensity, 22°C, Philips F17T8/TL741 fluorescent light bulbs) (Pacheco-Villalobos et al., 2013). Solid media were prepared using Phytagel (Sigma-Aldrich) and Murashige and Skoog (MS) salts (Sigma-Aldrich). Care was taken to place the 10-cm square Petri dishes at a slight angle from the vertical to assure seminal root growth along the agar surfaces. Roots that had grown into the plate were excluded from analysis. For metabolic profiling, chemical cell wall analysis, and RNAseq, parallel grown ~1-cm seminal root pieces harvested from 2 to 3 mm above the root tip were sampled (Supplemental Figure 1D). To generate *VAS1L* RNAi knockdown lines, a DNA fragment of 422 bp containing the *VAS1L 3′-UTR* was amplified using the oligonucleotides attB1-BdVAS1L-F 5′-GGGGACAAGTTTGTACAAAAAAGCAGGCTTGGTACAGTAACAGCCCATC-3′ and attB2-BdVAS1L-R 5′-GGGGACCACTTTGTACAAGAAAGCTGGGTGGAAGTGGCAGTTCTGTCAG-3′ and cloned into pDONR207 (Life Technologies). This 3′-UTR-specific DNA fragment was then cloned into the pANDA RNAi vector (Miki and Shimamoto, 2004). Transformation of the pANDA-BdVAS1Li plasmid into *tar2l*^{hypo} embryo-derived callus was performed as described (Pacheco-Villalobos et al., 2013). Arabidopsis experiments were performed with the standard Col-0 accession under the growth conditions described above. For dexamethasone-inducible expression of AHA2 (AT4G30190) devoid of its autoinhibitory C-terminal domain (AHA2$^{\delta 95}$) the corresponding cDNA was amplified by PCR and cloned into pTA7002 (Aoyama and Chua, 1997) via *Xho*I and *Spe*I restriction enzyme sites. Transgenic lines were obtained after transformation of Col-0 plants using standard procedures (Clough and Bent, 1998).

Tryptophan Aminotransferase Activity Assays

Seminal roots were ground in liquid nitrogen with a TissueLyser II (Qiagen). Root tissue was homogenized in a precooled mortar on ice with one volume of extraction buffer [100 mM 4-(2-hydroxyethyl)-1-piperazineethanesulfonic acid buffer, pH 7.2, 250 mM sorbitol, 5 mM β-mercaptoethanol, 0.5% (v/v) Triton X-100, and 0.1% (w/v) phenylmethylsulfonyl fluoride). The protein extract was centrifuged at 16,000*g* for 30 min at 4°C. The supernatant was used for determination of tryptophan aminotransferase activity with the Salkowski reagent as described (Szkop et al., 2012). Briefly, the reactions were performed in 100 mM phosphate buffer, pH 8.0, 10 mM L-tryptophan, 10 μM pyridoxal phosphate, and 50 μg of soluble proteins. The mixture was preincubated for 3 min at 35°C. The transamination reactions were initiated by the addition of 3 mM 2-oxoglutarate and incubated for 15 min at 35°C. To estimate the basal tryptophan aminotransferase activity of the crude extracts, control samples without 2-oxoglutarate were also assayed. To terminate the reactions, 1 mL of Salkowski reagent (10 mM $FeCl_3$ and 35% [v/v] H_2SO_4) was added and the samples were incubated in the dark for 10 min at room temperature. The absorbance at 530 nm of four replicates was measured.

Detection of Proton Pump Phosphorylation Status

To determine the abundance of activated PM-H$^+$-ATPase, microsomes were prepared from root segments and analyzed with the overlay assay as described (Ottmann et al., 2007), except that RGS-$(His)_6$-tagged 14-3-3 was applied. Bound 14-3-3 was visualized by means of an antibody raised against the RGS-His_6 epitope (20 μg/mL; Qiagen; catalog no./ID 34610).

Auxin Metabolite Profiling

For full-scale profile of auxin metabolites, four independent replicate samples of pooled 1-cm root segments were analyzed. Upon harvest, samples were immediately frozen in liquid nitrogen and stored at −80°C until they were analyzed as described (Novák et al., 2012).

RT-PCR

To monitor the expression of *VAS1L* full-length transcript by RT-PCR, the full-length transcript was amplified using oligonucleotides 5′-ATGAGCAGCTTTGCCAAGCT-3′ and 5′-GGAAGTGGCAGTTCTGTCAG-3′. *UBIQUITIN CONJUGATING ENZYME18* (see below) was used as a control.

RNA Sequencing and Data Analysis

For RNAseq, total RNA was extracted from 8 to 12 pooled root segments using RNA extraction kits (Qiagen). cDNA libraries for sequencing were then prepared with the TruSeq Stranded mRNA Library Prep Kit (Illumina) using 1 μg of RNA starting material. Sequencing was performed on HiSeq 2500 instruments (Illumina) to yield 100-bp reads. The Bd21-0, *tar2l*^{hypo}, mock-treated Bd21-0, and L-kynurenine-treated Bd21-0 samples were prepared and run in parallel, multiplexed in the same sequencing lane. The Bd21-3 and *ein2l1*^{hypo} samples, although grown and harvested in parallel, were processed in a separate run in the same manner. The 100-bp single reads were then mapped onto the Brachypodium primary transcripts (version 2.1, http://phytozome.jgi.doe.gov/pz/portal.html) using kallisto software (version 0.42.1, http://pachterlab.github.io/kallisto/) (Bray et al., 2016) with default settings (100 bootstrap samples). Subsequent differential expression analysis was performed using sleuth software (version 0.27.3, http://pachterlab.github.io/sleuth/), again with default settings. The word cloud was produced using the wordle online tool (www.wordle.net).

qPCR

qPCR was performed on three biological replicates with a Stratagene MxPro 3005P real-time PCR system (Stratagene), using SYBR Green to monitor DNA synthesis. Relative gene expression levels were calculated as described in Pacheco-Villalobos et al. (2013). The following oligonucleotides were used: reference gene *UBIQUITIN CONJUGATING ENZYME18* (*Bradi4g00660*), 5′-GGAGGCACCTCAGGTCATTT-3′ and 5′-ATAGCGGTCATTGTCTTGCG-3′; *EXPANSIN* (*Bradi1g74710*), 5′-GTCCTCTACCAACAGGTGAAG-3′and 5′-AGTTCCTGGACATCTGGATC-3′; *EXPANSIN* (*Bradi3g50740*), 5′-CGCGTGCTATCAGGTTAAATGC-3′ and 5′-TCTTGTACTGGATTCTGAGGAC-3′; *AG-peptide* (*Bradi2g31980*), 5′-AGTACCCCCTTCGGTTTCGT-3′ and 5′-TGGTCGATGGACGATGCGTC-3′; *GH3 enzyme* (*Bradi2g20740*), 5′-ACCACTTACTCCGGGCTGTA-3′ and 5′-CGTGTACTCCACTAAAGACG-3′; *PM-H*$^+$*-ATPase* (*Bradi1g12117*), 5′-AGATGGGAGGAAAGAGAGTC-3′ and 5′-AATGGCTAGCTGATCACCTG-3′; *PM-H*$^+$*-ATPase* (*Bradi3g18790*), 5′-CCAGAGGATGAAGAACTACACG-3′ and 5′-GATCGTCATGATTGTGCCATCG-3′; *ACC synthase* (*Bradi1g10030*), 5′-CCACTGGCATCATCCAGATG-3′ and 5′-TGAACCTCGCCAATGCATTC-3′; and *ETRL2* (*Bradi3g55730*), 5′-GCAGAAAGCTTGTGCAGATGATG-3′ and 5′-GCATGACGGCGATGTATATTGC-3′.

Yariv Staining

For arabinogalactan staining with Yariv reagent, roots isolated from Bd21-0 and *tar2l*^{hypo} seedlings were embedded in 6% agarose and longitudinally sectioned with a Leica-VT 1000S vibratome. Root sections were then incubated in a Yariv reagent (Biosupplies) solution (freshly prepared according to the manufacturer's instructions) for 5 min and directly examined under a Leica DM5500B compound microscope.

Rhizosphere Acidification Assays

Media acidification assays were performed as described (Gujas et al., 2012). To visualize rhizosphere acidification, 3-d-old Brachypodium seedlings were transferred to half-strength MS-agar plates supplemented with 0.15 mM bromocresol purple (Sigma-Aldrich) (sensitivity range pH 5.2 to 6.8). The plates were incubated in the same culture chamber and

scanned after 4 and 24 h. For liquid medium pH assays, 2-d-old Brachypodium seedlings were transferred on a sterile mesh attached to a tube containing 10 mL of nonbuffered half-strength liquid MS medium and 0.15 mM bromocresol green (Sigma-Aldrich) (sensitivity range pH 3.8 to 5.4). Measurement of pH was performed in a time series at 4, 24, 48, and 240 h. Three replicates consisting of eight plants per tube were measured. Negative controls (mock) without plants were measured in parallel.

Root Tip Regeneration Assays

For root tip regeneration experiments, ~1-cm root segments from above the root tip were excised with a razor blade. The isolated root tips were then incubated on the same plates under the same conditions. De novo root tissue formation from the tips was monitored by scanning the plates after 1, 2, 3, and 4 d. Length quantification of newly formed cortex cell was performed by microscopy at 4 d after excision.

Antibody Staining of Brachypodium Root Sections

Bd21-0 and *tar2l*^{hypo} plants were grown on half strength MS plates containing 1% sucrose and 0.9% agarose under long-day conditions (16 h light/8 h dark) at 22°C. Four-day-old roots were then sectioned with a vibratome (Leica VT1000 S). For immunolabeling of demethylesterified pectin, freshly cut 100-μm cross sections were first rinsed with 2F4 buffer (20 mM Tris-HCl, pH 8.2, 0.5 mM $CaCl_2$, and 150 mM NaCl) for 10 min. The samples were then incubated with 2F4 monoclonal antibody (Plantprobes) diluted 1:250 in 2F4 buffer with 5% skim milk powder (w/v) under gentle stirring for 1 h. After washing three times with 2F4 buffer, the samples were incubated with secondary antibody (goat anti-mouse IgG (H+L), Alexa Fluor 488 conjugate, ThermoFischer A-11001) diluted 1:1000 in 2F4 buffer with 5% skim milk powder (w/v) for 3 h in the dark and then washed three times in 2F4 buffer. For immunolabeling of methylesterified homogalacturonan and arabinogalactan, the sections were incubated in 1× PBS buffer with 1% BSA and 0.05% Tween, respectively, for 1 h at room temperature, washed with 1× PBS and then incubated with JIM7 or LM2 (PLANTPROBES) diluted 1:25 in 1× PBS buffer with 1% BSA and 0.05% Tween for 1 h at room temperature. The samples were washed three times with 1× PBS and incubated with secondary antibody (donkey anti-rat Cy3; Jackson ImmunoResearch) diluted 1:500 in 1× PBS for 1 to 3 h in the dark. The samples were washed three times with 1× PBS buffer after incubation. Z-stacks were acquired using a Zeiss LSM 510 Meta confocal microscope.

Analysis of Cell Wall Polysaccharides

Biological replicates consisted of two pools of root segments harvested from 300 to 400 seedlings per genotype. The biological material was freeze-dried overnight and ground to a fine powder using a Mixer Mill MM 400 (Retsch). Cell wall preparation was performed by incubating the samples three consecutive times in 95% ethanol at 65°C for 30 min, followed by a treatment in chloroform:methanol (2:1, v/v) at room temperature for 1 h under gentle agitation. The insoluble material was then successively washed in 70% (two times 1.5 h), 80% (1 h), and 95% (2 h) ethanol and dried under vacuum (SpeedVac Plus; Savant) after a final wash in acetone. The resulting alcohol-insoluble residue was resuspended in 500 μL of an α-amylase solution (5 units/mL; Sigma-Aldrich) in 0.01 M phosphate buffer, pH 7.0, and incubated for 24 h at 37°C under continuous stirring (Mélida et al., 2009). The resulting destarched cell wall residue was washed three times with 70% ethanol, followed by three times with acetone, and stored at room temperature for further analysis. Neutral sugar composition was determined after sulfuric acid hydrolysis (Saeman et al., 1954). For this purpose, the cell wall samples were resuspended in 72% sulfuric acid and kept in this solution for 3 h at room temperature before being heated at 100°C for 3 h. *Myo*-inositol was used as an internal standard. The samples were then passed through 0.2-μm nylon filters and diluted 5× with deionized water. The hydrolysates were then subjected to high-performance anion-exchange chromatography using a Dionex Carbopac PA1 column and a Dionex HPLC fitted with a pulsed amperometric detector (Dionex ICS 3000 system). The samples were eluted over 20 min with deionized water and the neutral monosaccharides were detected following postcolumn addition of 300 mM sodium hydroxide at a flow rate of 0.5 mL/min. Glycosidic linkage analyses were performed using 0.8 mg of cell wall samples. The latter were swollen in 400 μL dry dimethyl sulfoxide for 3 h with stirring at room temperature prior to sugar derivatization to permethylated alditol acetates and gas chromatography-mass spectrometry analysis, as described earlier (Mélida et al., 2013). Neutral sugar and linkage analyses were performed in triplicate.

Fusicoccin Treatment and AHA2$^{\delta 95}$ Induction

Col-0 or AHA2$^{\delta 95}$ seeds were stratified for 4 d in water at 4°C and then germinated and grown for 4 d in half-strength MS medium adjusted to pH 5.7. For fusicoccin treatment, Col-0 seedlings were transferred to solid medium supplemented with DMSO (mock), or either 3 or 10 μM fusicoccin (Sigma-Aldrich) and grown for an additional 24 h. For analysis of forced apoplastic acidification, AHA2$^{\delta 95}$ seedlings were transferred to solid medium supplemented with DMSO (mock) or 1 μM dexamethasone (Sigma-Aldrich) and grown for an additional 24 h. Propidium iodide-stained roots were then analyzed under a Zeiss LSM780 confocal microscope.

pH Microelectrode Measurements

For root surface pH measurements, we used a pH*Optica* micro fiber optic pH system (World Precision Instruments) with pH1-micro-AOT-06-059 fiber optic microsensors (PreSens) (pH range 4.0 to 9.0). Five equidistant points along the root tip surface were measured in 4-d-old seedlings grown in tissue culture. Media pH was verified in a distant location from the seedlings.

Accession Numbers

Sequence data from this article can be found in the GenBank/EMBL libraries under accession numbers *Bradi2g04290* (*TAR2L*), *Bradi4g08380* (*EIN2L1*), *Bradi2g04860* (*VAS1L*), and *AT4G30190* (*AHA2*). The RNAseq raw data are available at the National Center for Biotechnology Information Sequence Read Archive under accession number SRP072551.

Supplemental Data

Supplemental Figure 1. Supplemental illustrations of Brachypodium phenotypes.

Supplemental Figure 2. Supplemental illustrations of pH experiments.

Supplemental Data Set 1. RNAseq quantification and read counts for all samples.

Supplemental Data Set 2. Gene expression level comparison of *tar2l*^{hypo} versus Bd21-0.

Supplemental Data Set 3. Gene expression level comparison of L-kynurenine-treated versus mock-treated Bd21-0.

Supplemental Data Set 4. Gene expression level comparison of *ein2l1*^{hypo} versus Bd21-3.

Supplemental Data Set 5. Gene expression level data for selected genes of interest plotted in Figures 3B to 3G.

ACKNOWLEDGMENTS

This work was funded by Swiss National Science Foundation Grant CR32I3_156724 awarded to C.S.H. K.L. acknowledges the Swedish

Governmental Agency for Innovation Systems (VINNOVA) and the Swedish Research Council (VR). O.N. acknowledges the Czech Science Foundation (GA14-34792S) and the Ministry of Education, Youth, and Sports of the Czech Republic-NPU I program with project LO1204.

AUTHOR CONTRIBUTIONS

D.P.-V., S.W., C.O., K.L., V.B., and C.S.H. designed the research. D.P.-V., S.M.D.-M., A.v.d.S., T.T., Y.H.K., B.G., O.N., N.J., and Z.L. performed the research. All authors analyzed data. D.P.-V. and C.S.H. wrote the paper with input from the other authors.

Received January 5, 2016; revised April 21, 2016; accepted May 2, 2016; published May 5, 2016.

REFERENCES

Adamowski, M., and Friml, J. (2015). PIN-dependent auxin transport: action, regulation, and evolution. Plant Cell **27:** 20–32.

Alonso, J.M., Hirayama, T., Roman, G., Nourizadeh, S., and Ecker, J.R. (1999). EIN2, a bifunctional transducer of ethylene and stress responses in Arabidopsis. Science **284:** 2148–2152.

Aoyama, T., and Chua, N.H. (1997). A glucocorticoid-mediated transcriptional induction system in transgenic plants. Plant J. **11:** 605–612.

Axelsen, K.B., Venema, K., Jahn, T., Baunsgaard, L., and Palmgren, M.G. (1999). Molecular dissection of the C-terminal regulatory domain of the plant plasma membrane H+-ATPase AHA2: mapping of residues that when altered give rise to an activated enzyme. Biochemistry **38:** 7227–7234.

Benjamins, R., and Scheres, B. (2008). Auxin: the looping star in plant development. Annu. Rev. Plant Biol. **59:** 443–465.

Bray, N.L., Pimentel, H., Melsted, P., and Pachter, L. (2016). Near-optimal probabilistic RNA-seq quantification. Nat. Biotechnol. **34:** 525–527.

Chen, Q., Dai, X., De-Paoli, H., Cheng, Y., Takebayashi, Y., Kasahara, H., Kamiya, Y., and Zhao, Y. (2014). Auxin overproduction in shoots cannot rescue auxin deficiencies in Arabidopsis roots. Plant Cell Physiol. **55:** 1072–1079.

Clough, S.J., and Bent, A.F. (1998). Floral dip: a simplified method for Agrobacterium-mediated transformation of Arabidopsis thaliana. Plant J. **16:** 735–743.

Cosgrove, D.J. (1993). Wall extensibility: its nature, measurement and relationship to plant cell growth. New Phytol. **124:** 1–23.

Cosgrove, D.J. (1999). Enzymes and other agents that enhance cell wall extensibility. Annu. Rev. Plant Physiol. Plant Mol. Biol. **50:** 391–417.

Cosgrove, D.J. (2005). Growth of the plant cell wall. Nat. Rev. Mol. Cell Biol. **6:** 850–861.

Cosgrove, D.J., Van Volkenburgh, E., and Cleland, R.E. (1984). Stress relaxation of cell walls and the yield threshold for growth: demonstration and measurement by micro-pressure probe and psychrometer techniques. Planta **162:** 46–54.

Depuydt, S., and Hardtke, C.S. (2011). Hormone signalling crosstalk in plant growth regulation. Curr. Biol. **21:** R365–R373.

Edwards, K.L., and Scott, T.K. (1977). Rapid-growth responses of corn root segments: Effect of auxin on elongation. Planta **135:** 1–5.

Ellis, M., Egelund, J., Schultz, C.J., and Bacic, A. (2010). Arabinogalactan-proteins: key regulators at the cell surface? Plant Physiol. **153:** 403–419.

Eudes, A., Mouille, G., Thévenin, J., Goyallon, A., Minic, Z., and Jouanin, L. (2008). Purification, cloning and functional characterization of an endogenous beta-glucuronidase in *Arabidopsis thaliana*. Plant Cell Physiol. **49:** 1331–1341.

Evans, M.L., Mulkey, T.J., and Vesper, M.J. (1980). Auxin action on proton influx in corn roots and its correlation with growth. Planta **148:** 510–512.

Evans, M.L., Ishikawa, H., and Estelle, M.A. (1994). Responses of Arabidopsis roots to auxin studied with high temporal resolution - Comparison of wild-type and auxin-response mutants. Planta **194:** 215–222.

Gjetting, K.S., Ytting, C.K., Schulz, A., and Fuglsang, A.T. (2012). Live imaging of intra- and extracellular pH in plants using pHusion, a novel genetically encoded biosensor. J. Exp. Bot. **63:** 3207–3218.

Gujas, B., Alonso-Blanco, C., and Hardtke, C.S. (2012). Natural Arabidopsis brx loss-of-function alleles confer root adaptation to acidic soil. Curr. Biol. **22:** 1962–1968.

Hager, A., Menzel, H., and Krauss, A. (1971). [Experiments and hypothesis concerning the primary action of auxin in elongation growth]. Planta **100:** 47–75.

Hardtke, C.S., and Berleth, T. (1998). The Arabidopsis gene MONOPTEROS encodes a transcription factor mediating embryo axis formation and vascular development. EMBO J. **17:** 1405–1411.

Kitazawa, K., Tryfona, T., Yoshimi, Y., Hayashi, Y., Kawauchi, S., Antonov, L., Tanaka, H., Takahashi, T., Kaneko, S., Dupree, P., Tsumuraya, Y., and Kotake, T. (2013). β-Galactosyl Yariv reagent binds to the β-1,3-galactan of arabinogalactan proteins. Plant Physiol. **161:** 1117–1126.

Knoch, E., Dilokpimol, A., and Geshi, N. (2014). Arabinogalactan proteins: focus on carbohydrate active enzymes. Front. Plant Sci. **5:** 198.

Knoch, E., et al. (2013). A β-glucuronosyltransferase from *Arabidopsis thaliana* involved in biosynthesis of type II arabinogalactan has a role in cell elongation during seedling growth. Plant J. **76:** 1016–1029.

Kutschera, U., and Schopfer, P. (1985a). Evidence against the acid-growth theory of auxin action. Planta **163:** 483–493.

Kutschera, U., and Schopfer, P. (1985b). Evidence for the acid-growth theory of fusicoccin action. Planta **163:** 494–499.

Luthen, H., and Bottger, M. (1993). The role of protons in the auxin-induced root-growth inhibition: a critical reexamination. Bot. Acta **106:** 58–63.

Mélida, H., Sandoval-Sierra, J.V., Diéguez-Uribeondo, J., and Bulone, V. (2013). Analyses of extracellular carbohydrates in oomycetes unveil the existence of three different cell wall types. Eukaryot. Cell **12:** 194–203.

Mélida, H., García-Angulo, P., Alonso-Simón, A., Encina, A., Alvarez, J., and Acebes, J.L. (2009). Novel type II cell wall architecture in dichlobenil-habituated maize calluses. Planta **229:** 617–631.

Miki, D., and Shimamoto, K. (2004). Simple RNAi vectors for stable and transient suppression of gene function in rice. Plant Cell Physiol. **45:** 490–495.

Moloney, M.M., Elliott, M.C., and Cleland, R.E. (1981). Acid growth effects in maize roots: Evidence for a link between auxin-economy and proton extrusion in the control of root growth. Planta **152:** 285–291.

Moubayidin, L., Perilli, S., Dello Ioio, R., Di Mambro, R., Costantino, P., and Sabatini, S. (2010). The rate of cell differentiation controls the Arabidopsis root meristem growth phase. Curr. Biol. **20:** 1138–1143.

Mulkey, T.J., Kuzmanoff, K.M., and Evans, M.L. (1982). Promotion of growth and hydrogen ion efflux by auxin in roots of maize pretreated with ethylene biosynthesis inhibitors. Plant Physiol. **70:** 186–188.

Novák, O., Hényková, E., Sairanen, I., Kowalczyk, M., Pospíšil, T., and Ljung, K. (2012). Tissue-specific profiling of the *Arabidopsis thaliana* auxin metabolome. Plant J. **72:** 523–536.

Ottmann, C., Marco, S., Jaspert, N., Marcon, C., Schauer, N., Weyand, M., Vandermeeren, C., Duby, G., Boutry, M., Wittinghofer, A., Rigaud, J.L., and Oecking, C. (2007). Structure of a 14-3-3 coordinated hexamer of the plant plasma membrane H+-ATPase by combining X-ray crystallography and electron cryomicroscopy. Mol. Cell **25:** 427–440.

Overvoorde, P., Fukaki, H., and Beeckman, T. (2010). Auxin control of root development. Cold Spring Harb. Perspect. Biol. **2:** a001537.

Pacheco-Villalobos, D., Sankar, M., Ljung, K., and Hardtke, C.S. (2013). Disturbed local auxin homeostasis enhances cellular anisotropy and reveals alternative wiring of auxin-ethylene crosstalk in *Brachypodium distachyon* seminal roots. PLoS Genet. **9:** e1003564.

Palmgren, M.G., Sommarin, M., Serrano, R., and Larsson, C. (1991). Identification of an autoinhibitory domain in the C-terminal region of the plant plasma membrane H(+)-ATPase. J. Biol. Chem. **266:** 20470–20475.

Pilet, P.E., Elliott, M.C., and Moloney, M.M. (1979). Endogenous and exogenous auxin in the control of root growth. Planta **146:** 405–408.

Portillo, F., Eraso, P., and Serrano, R. (1991). Analysis of the regulatory domain of yeast plasma membrane H+-ATPase by directed mutagenesis and intragenic suppression. FEBS Lett. **287:** 71–74.

Qiao, H., Shen, Z., Huang, S.S., Schmitz, R.J., Urich, M.A., Briggs, S.P., and Ecker, J.R. (2012). Processing and subcellular trafficking of ER-tethered EIN2 control response to ethylene gas. Science **338:** 390–393.

Rayle, D.L., and Cleland, R. (1970). Enhancement of wall loosening and elongation by acid solutions. Plant Physiol. **46:** 250–253.

Rayle, D.L., and Cleland, R. (1977). Control of plant cell enlargement by hydrogen ions. Curr. Top. Dev. Biol. **11:** 187–214.

Rayle, D.L., and Cleland, R.E. (1992). The Acid Growth Theory of auxin-induced cell elongation is alive and well. Plant Physiol. **99:** 1271–1274.

Regenberg, B., Villalba, J.M., Lanfermeijer, F.C., and Palmgren, M.G. (1995). C-terminal deletion analysis of plant plasma membrane H(+)-ATPase: yeast as a model system for solute transport across the plant plasma membrane. Plant Cell **7:** 1655–1666.

Rodriguez-Villalon, A., Gujas, B., van Wijk, R., Munnik, T., and Hardtke, C.S. (2015). Primary root protophloem differentiation requires balanced phosphatidylinositol-4,5-biphosphate levels and systemically affects root branching. Development **142:** 1437–1446.

Sabatini, S., Beis, D., Wolkenfelt, H., Murfett, J., Guilfoyle, T., Malamy, J., Benfey, P., Leyser, O., Bechtold, N., Weisbeek, P., and Scheres, B. (1999). An auxin-dependent distal organizer of pattern and polarity in the Arabidopsis root. Cell **99:** 463–472.

Saeman, J.F., Moore, W.E., Mitchell, R.L., and Millett, M.A. (1954). Techniques for the determination of pulp constituents by quantitative paper chromatography. TAPPI Journal **37:** 336–343.

Sánchez-Rodríguez, C., Rubio-Somoza, I., Sibout, R., and Persson, S. (2010). Phytohormones and the cell wall in Arabidopsis during seedling growth. Trends Plant Sci. **15:** 291–301.

Scacchi, E., Salinas, P., Gujas, B., Santuari, L., Krogan, N., Ragni, L., Berleth, T., and Hardtke, C.S. (2010). Spatio-temporal sequence of cross-regulatory events in root meristem growth. Proc. Natl. Acad. Sci. USA **107:** 22734–22739.

Schopfer, P. (1989). pH-dependence of extension growth in Avena coleoptiles and its implications for the mechanism of auxin action. Plant Physiol. **90:** 202–207.

Schopfer, P. (1993). Determination of auxin-dependent pH changes in coleoptile cell walls by a null-point method. Plant Physiol. **103:** 351–357.

Schultz, C.J., Ferguson, K.L., Lahnstein, J., and Bacic, A. (2004). Post-translational modifications of arabinogalactan-peptides of *Arabidopsis thaliana*. Endoplasmic reticulum and glycosylphosphatidylinositol-anchor signal cleavage sites and hydroxylation of proline. J. Biol. Chem. **279:** 45503–45511.

Seifert, G.J., and Roberts, K. (2007). The biology of arabinogalactan proteins. Annu. Rev. Plant Biol. **58:** 137–161.

Smallwood, M., Yates, E.A., Willats, W.G.T., Martin, H., and Knox, J.P. (1996). Immunochemical comparison of membrane-associated and secreted arabinogalactan-proteins in rice and carrot. Planta **198:** 452–459.

Spartz, A.K., Ren, H., Park, M.Y., Grandt, K.N., Lee, S.H., Murphy, A.S., Sussman, M.R., Overvoorde, P.J., and Gray, W.M. (2014). SAUR inhibition of PP2C-D phosphatases activates plasma membrane H+-ATPases to promote cell expansion in Arabidopsis. Plant Cell **26:** 2129–2142.

Speth, C., Jaspert, N., Marcon, C., and Oecking, C. (2010). Regulation of the plant plasma membrane H+-ATPase by its C-terminal domain: what do we know for sure? Eur. J. Cell Biol. **89:** 145–151.

Stepanova, A.N., Yun, J., Robles, L.M., Novak, O., He, W., Guo, H., Ljung, K., and Alonso, J.M. (2011). The Arabidopsis YUCCA1 flavin monooxygenase functions in the indole-3-pyruvic acid branch of auxin biosynthesis. Plant Cell **23:** 3961–3973.

Sutcliffe, J.F., and Sexton, R. (1969). Cell differentiation in the root in relation to physiological function. In Root Growth: Proceedings of the 15th Easter School in Agricultural Sciences, University of Nottingham, W.J. Whittington, ed (London: Butterworths), pp. 80–102.

Szkop, M., Sikora, P., and Orzechowski, S. (2012). A novel, simple, and sensitive colorimetric method to determine aromatic amino acid aminotransferase activity using the Salkowski reagent. Folia Microbiol. (Praha) **57:** 1–4.

Takahashi, K., Hayashi, K., and Kinoshita, T. (2012). Auxin activates the plasma membrane H+-ATPase by phosphorylation during hypocotyl elongation in Arabidopsis. Plant Physiol. **159:** 632–641.

van Hengel, A.J., and Roberts, K. (2002). Fucosylated arabinogalactan-proteins are required for full root cell elongation in arabidopsis. Plant J. **32:** 105–113.

Weisenseel, M.H., Dorn, A., and Jaffe, L.F. (1979). Natural H currents traverse growing roots and root hairs of barley (*Hordeum vulgare* L.). Plant Physiol. **64:** 512–518.

Wolf, S., Hématy, K., and Höfte, H. (2012). Growth control and cell wall signaling in plants. Annu. Rev. Plant Biol. **63:** 381–407.

Won, C., Shen, X., Mashiguchi, K., Zheng, Z., Dai, X., Cheng, Y., Kasahara, H., Kamiya, Y., Chory, J., and Zhao, Y. (2011). Conversion of tryptophan to indole-3-acetic acid by TRYPTOPHAN AMINOTRANSFERASES OF ARABIDOPSIS and YUCCAs in Arabidopsis. Proc. Natl. Acad. Sci. USA **108:** 18518–18523.

Yariv, J., Lis, H., and Katchalski, E. (1967). Precipitation of arabic acid and some seed polysaccharides by glycosylphenylazo dyes. Biochem. J. **105:** 1C–2C.

Zhao, Y. (2014). Auxin biosynthesis. Arabidopsis Book **12:** e0173.

Zheng, Z., Guo, Y., Novák, O., Dai, X., Zhao, Y., Ljung, K., Noel, J.P., and Chory, J. (2013). Coordination of auxin and ethylene biosynthesis by the aminotransferase VAS1. Nat. Chem. Biol. **9:** 244–246.

7.2 Materials and methods

Creation of schematic images from Figure 1

For the longitudinal section, a good confocal image of a Bd21.3 root was used where cell walls were stained with Calcofluor white. Next the picture was opened in Fiji version 2.0.0-rc-69/1.52i (Schindelin et al. 2012) and the plugin Morphological segmentation was used to create a watershed image from a border image, with a tolerance of 15 (Legland, Arganda-Carreras, and Andrey 2016). Each cell was then filled in with a color using Photoshop. A similar method was used for the image of a cross-section, however for this a picture taken from a Bd21.3 microtome section was used. The morphological segmentation was performed from an object image with a tolerance of 8.

Creating the CRISPR-Cas vectors

As already discussed in Chapter 4, we designed four different vectors to test different Cas9 nucleases. We ordered an Arabidopsis-optimized Cas9 (AtCas9) as published before (Mao et al. 2013) and designed *Brachypodium* codon-optimized versions of AtCas9, AsCpfI and LbCpfI (Zetsche et al. 2015), named BdCas9, BdAsCpfI and BdLbCpfI resp. (Section 7.6 Sequences used during this thesis). I created the four different vectors by cloning BdCas9, AtCas9, AsCpfI or LbCpfI into a pCAMBIA1305.1-UBI5'UTR vector (pCAMBIA1305.1 Genbank accession number AF354045) using KpnI and BstEII (Suppl. figure 1). The vectors are called p5BdCas9, p5AtCas9, p5BdAsCpfI and p5BdLbCpfI resp. For our original CRSIPR-Cas system, we ordered several cassettes with a RNA polymerase III U6 promoter from *Brachypodium* (BdU6prom), a 20bp sgRNA target sequence for a gene of interest and a tracrRNA (Mao et al. 2013; Cong et al. 2013; Jiang et al. 2013). These cassettes could be transferred into the aforementioned vectors with the use of BamHI and HindIII restriction sites. In order to include several guideRNAs in one vector, another cassette was designed (pDON2, Suppl. figure 1), based on a publication by Zhou et al. 2014. sgRNAs were first transferred into the shuttle vector and could then be transferred into the p5Cas-vectors

with BamHI and HindIII. An advantage of the shuttle vector is that it can be used to add crRNA in the form of primers, instead of ordering a full cassette with promoter and tracrRNA. Primers have to be annealed and phosphorylated before ligating into the vector, as discussed herafter. The cassette contains BsaI and BtgZI restriction sites, wherein crRNAs can be ligated with the correct overlap with the vector (Miao et al. 2013; Zhou et al. 2014).

Cloning crRNA into p5Cas (a specific *Brachypodium* CRISPR-Cas vector)

Once a crRNA is chosen, primers can be ordered with a 4 nucleotide overhang to anneal to pDON2. For our CRISPR-Cas system, the forward primer for crRNA1 (in BsaI restriction site) requires tctc as overhang → tctc crRNA1. The reverse primer for crRNA1 (in BsaI restriction site) is reverse complement of crRNA1 with aaac as overhang → aaac crRNA1reversecompl. Forward primer for crRNA2 (in BtgZI restriction site) requires gtgt as overhang → gtgt crRNA2 and reverse primer for crRNA2 (in BtgZI restriction site): is the reverse complement of crRNA2 with aaac overhang → aaac crRNA2reversecompl. Digest a big batch of vector pDON2 in Cutsmart buffer 10x with BsaI at 37°C. Stop reaction for 20min at 65°C. Add BtgZI and Cutsmart 10x and digest at 60°C. Stop reaction for 5min at 80°C. Run digested vector on gel and cut out the bands of 4001bp (backbone) and of 397bp (middle piece). Purify pieces and store digested vector in -20°C. Optimal final concentrations are around 100ng/μL for the vector and 30ng/μL for the middle piece. Anneal primers (final concentration will be around 0.74ng/μL). Use 1uL of each 10uM primer stock, add 18uL of mQ and anneal with T7E1 touch-down program (95°C – 5min; 95→85°C - -2°C/sec; 85-25°C - -0.1°C/sec). Phosphorylate primers using 0.2μLT4 kinase, 1μL 10mM ATP, 2μL 10x PNK buffer, 2μL annealed primers and 14.8μL mQ. Phosphorylate at 37°C for 30min, then stop at 65°C for 20min. Ligate primers into vector pDON by combining 100ng vector backbone pDON2-Bsa/BtgZI, 30ng middle piece of pDON2-Bsa/BtgZI(30ng), 3μL of annealed primer-BtgZI (note that this is 3 times higher than required, but it works better), 1μL T4 ligase buffer 10x, 1μL T4 ligase and mQ up to

10μL. Leave overnight at RT, then add: 1μL primer-BsaI, 0.5μL T4 ligase buffer 10x, 0.5μL T4 ligase and 3μL of mQ. Leave the reaction at RT for at least 1h and transform into *E.Coli*. Select a good colony and digest a miniprep with BamHI and HindIII, then cut out 760bp fragment from gel. Transfer into BamHI/HindIII digested and dephosphorylated p5Cas, 15ng of insert with 100ng of vector. For adding additional crRNAs, have 2 constructs ready in p5Cas and then digest recipient vector with SbfI (blunt) & HindIII, while donor vector with BamHI (blunt) & HindIII.

7.3 Supplementary figures

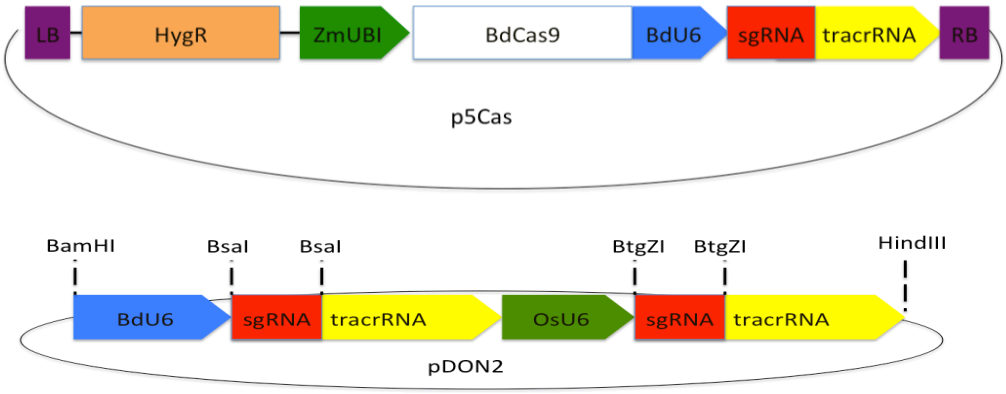

Suppl. figure 1: Schematic representation of the CRISPR-Cas system that was designed during this thesis. p5Cas contains the Cas9 protein under the control of a UBIQUITIN promoter. sgRNA can be subcloned in pDON2, flanked by a BdU6 or OsU6 promoter and tracrRNA. From the shuttle vector the complete sgRNA cassette can be transferred into p5Cas with BamHI and HindIII.

7.4 Supplementary tables

Suppl. table 1: Alignment of the active site of several CLE-peptides from Brachypodium and Arabidopsis. Red amino acids indicate differences with the consensus.

Bradi1g05010	RRVPNGPDPIHN
Bradi1g54656	RRVPNGPDPVHN
AtCLE45	RRVRRGSDPIHN
AtCLE26	RKVPRGPDPIHN
AtCLE25	RKVPNGPDPIHN

Suppl. table 2: Summary of different crRNAs tested during this thesis. Yellow crRNAs were designed with simplified criteria and tested with the old system.

Target name	Sequence crRNA
BdAPLL1	GTGCGTCGTTCAGGGCCAGC
BdAPLL2	GCTCGGCGGCCCAGACAGTA
BdBAM3-1L	GGGGTTGGCGCGGCAGCCGA
BdBAM3-2L	GGCCGCCCTCGACGACCCCA
BdBAM3-3L	GCGGCGCTCGCCGATCCATC
BdBAM3-4L	GCTGGCCTTGCTCTCCCTCA
BdBRXL1	GCTTGTTCGACCAAGGACGG
BdBRXL2	GTCGTCGCGCGTCCGTGAGA
BdBRXL3	GCGTGCTCCAAGCAACTCGA
BdBRXL4	GCGTGCACCTCAAAGGAAGG
BdCLEL45	GATTCTGATGTCCTTGGTCG
BdOPSL1	GCGGAGGTGGACTTGCGGCC
BdOPSL2	GCCGCCGCGGCCTCCGCGCC
BdAux1a	GTCACCAGCTTCCTCTGGCA
BdAux1b	GATCCGGTAGTTGTGGAAGG
BdBRXL1,4*	GACATGGTGCTCAAGTTCTC
BdBRXL2,3,4*	GCCGGGAGATGTTTAACAAG
BdBRXL2a	CTTGATGGCCAGCCGCGTGC
BdBRXL2b	GCGCGCACCGACTTCCCCAC
BdBRXL2c	GGATGGTAATATATACACCG
BdBRXL3c	GAGCATCAGTCTAAACACCT
BdBRXL3e	GATAGCCTCCCTCGTGCTGG
BdBRXL2,5*	TGGGTGGCGCAGGTGGAGCC
BdBRXL5b	GACATGGTGCTGAAGCTGTC
BdOPSL1,2a*	GCCGCCGCGGCCGCACGAGA
BdOPSL1,2b*	GCGCAAGCAGAAGCTCAAGA
BdBRIL1a	CCGAACCAGGCGTCGCTCTC
BdBRIL2a	CGCTTCCTCGGCGCTGGCAA

**In case a crRNA has multiple numbers, it means that it can target multiple homologs of the same family (BdBRXL1,4 can target both BdBRXL1 and BdBRXL4).*

Suppl. table 3: Efficiency analysis of our CRISPR-Cas system.

crRNA	# tested	# unknown	# mutants	# non-mutant	% mutated
BdBRXL1 and 4**	7	0	5	2	71.4
BdBRXL2c	15	3	10	2	83.3
BdBRXL3b	19	0	13	6	68.4
AUX1a and b*	38	5	9	24	27.3
OPSL1a and b*	26	0	7	19	26.9
OPSL2a and b*	25	4	7	14	33.3

**In the case that multiple crRNAs were used to target the same gene (a and b), either both targets were mutated or none, therefore no separate row was created.*
***In the case that the same crRNA was used to target two different genes, either both targets were mutated or none, therefore no separate row was created*

Suppl. table 4: Off-target analysis for AUX1b crRNA CRISPR-Cas lines

	crRNA tested	BreakingCas score	# tested	# mutant	% mutated
BdLAX3b	AUX1b	3.4	35	0	0
BRADI3g50990	AUX1b	1.3	35	0	0

7.5 Media used during this thesis

Media for Brachypodium transformation protocol

Media for Brachypodium calli culture (1L)

	Basic media	Selection media (H40, H30, P400)	Regeneration media (H20, P50)
MS powder (M0221 Duchefa)	4.3g	4.3g	4.3g
Sucrose grade I (Sigma S5390)	30g	30g	30g
FeNaEDTA (4mg/mL)	825µL	825µL	825µL
$CuSO_4.5H_20$ (1mg/mL)	600µL	600µL	600µL
2.4-D (5mg/mL)	0.5mL	0.5mL	x
*Phytagel / Plant Agar	2.1g x	2.1g/ 7g	2.1g/ 7g
Fill to 990mL with water and adjust pH with few drops of 1M KOH to 5.8 . Autoclave and cool down before adding the following:			
M5 vitamins (100x stock)	10mL	10mL	10mL
Timentin (320mg/mL)	x	700uL	700uL
*Hygromycin / Paromomycin	x	H40: 800µL/ H30: 600µL**/ P400: 2mL	H20: 400µL/ P50: 250µL
Kinetin (0.1mg/mL stock)	x	x	2mL

* For selection on hygromycin, phytagel is required. For paromomycin selection, plant agar is required instead.

** Hygromycin selection takes place on two different media, the first contains higher amounts of hygromycin (H40), whereas the second selection step requires lower amount of hygromycin in the media (H30). Paromomycin selection takes place at the same concentration for both selection steps (P400).

M5 vitamins 100x stock (1L)

Nicotinic acid	0.04g
Thiamine-HCl	0.05g
Cysteine	4g
Glycine	0.2g
Pyridoxine-HCl	0.04g

Filter-sterilize, aliquot in 50mL tubes, wrap in aluminium foil and keep at -20°C.

1mg/mL CuSO4 stock solution

Dissolve 50mg of $CuSO_4.5H_20$ in 50mL of distilled water. Wrap tube with aluminum foil and store at 4°C in the dark. Keep solution max. 3 months.

4mg/mL FeNaEDTA stock solution

Dissolve 4g of $C_{10}H_{12}FeN_2NaO_8$ in 1L of water and wrap with aluminium foil. Store at 4°C for max. 6months.

5mg/mL 2,4-D

Dissolve 500mg of 2,4-Dicholorophenoxyacetic acid in 1.5-2mL of 1M KOH in a fumehood. Heat the solution while gently shaking until dissolved, then immediately add water up to 100mL. Aliquot in 2mL eppendorf tubes and keep in -20°C.

320mg/mL timentin stock

Dissolve 3.2g of timentin (ticarcillin disodium mixture Duchefa T0190.0025) in 10mL of sterile deionized water and filter-sterilize. Aliquot in 2mL eppendorf tubes and store in -20°C away from the dark.

0.1mg/mL kinetin stock solution

Dissolve 5mg of kinetin in 5mL of acetic acid under a fume hood. Add 45mL of sterile deionized water, wrap in aluminium foil and store at 4°C. Replace solution every month.

200mg/mL paromomycin stock solution

Dissolve 10g paromomycin sulfate in 50mL sterile deionized water, filter-sterilize and aliquot in 2mL eppendorf tubes. Keep at -20°C.

MGL media for *Agrobacterium*

Tryptone	5g
Yeast extract	2.5g
Sodium Chloride	5.2g
Mannitol	10g
L-glutamic acid sodium salt	2.32g
Monopotassium phosphate (KH_2PO_4)	0.5g
Magnesium sulfate heptahydrate ($MgSO_4.7H_20$)	0.2g
Adjust pH to 7.2 wih 10M KOH	
Bacteria agar	10g
Autoclave	
After sterilization, let the medium cool down and add:	
Biotin (1mg/mL)	2mL
*Rifampicin (10-25mg/mL)	1mL

*More antibiotics may need to be added, depending on what resistance the vector contains

Store wrapped in aluminium foil for max 1 month at 4°C.

1mg/mL biotin stock solution

Dissolve 10mg of biotin in 200-300µL 1M KOH and add up to 10mL deionized water. Filer-sterilize, wrap in aluminium foil and store at 4°C for max. 1month.

CIM media (1L)

MS powder (Duchefa M0221)	2.15g
FeNaEDTA (4mg/mL)	825µL
Sucrose grade I (Sigma S5390)	10g
Mannitol	10g

30mg/mL acetosyringone stock solution

Dissolve 600mg of 3',5'-dimethoxyl-4'-hydroxyacetophenone in 20mL DMSO. Aliquot in 1.5mL eppendorf tubes, wrap with aluminium foil and keep in -20°C.

Rooting media (1L)

MS powder incl. buffer and vitamins (Duchefa M0255)	2.45g
sucrose	10g
FeNaEDTA (4mg/mL)	825µL
Adjust pH to 5.8 by adding a few drops of 1M KOH	
Plant agar	6g
Phytagel	2g
Charcoal	7g

Autoclave, cool down and add 350µL timentin (320mg/mL). Poor into Magenta boxes.

Buffers for in situ hybridization

Buffers to be made in advance

2x Carbonate-buffer (200mM, pH=10.2 = 80mM $NaHCO_3$ & 120mM Na_2CO_3) (100mL)
0.672g $NaHCO_3$
1.277g Na_2CO_3
Treat with 100µL DEPC → autoclave

3M NaOAc (100mL)
Dissolve 24.6g of sodium acetate in 70 mL of dH2O.
Adjust the pH to 5.2 with glacial acetic acid.
Adjust the volume to 100 mL with H2O.
Treat with 100µL DEPC → Autoclave

5M LiCl (100mL) → cleaner than other precipitation methods, but not good for small RNA (smaller than 300bp)
Dissolve 21.2g of Lithium Chloride in 100mL d H20.
Treat with 100µL DEPC → Autoclave

1M Tris-HCl pH 9.5 (1L)
121.1g Tris (RNA)
800ml H2O
pH9.5 with HCl (ca.9ml)
up to 1L with H2O → autoclave

2M Tris-HCl pH 7.5 (1L)
242.2g Tris (RNA)
800ml H2O
pH7.5 with HCl (ca.194ml)
up to 1L with H2O → autoclave

1M Tris-HCl pH 6.8(100mL)
12.11g Tris
80mL H2O
pH6.8 with HCl
Up to 100mL with H2O → autoclave

DEPC treated water (1L) x 10
1mL DEPC in 1L dH2O in fumehood → shake overnight → autoclave

10x PBS (1L) (1.5M NaCl, 0.07M Na_2HPO_4, 0.03M NaH_2PO_4, pH7)
85 g NaCl (is only 76g in other protocols)
9.94 g Na_2HPO_4
4.14 g $NaH_2PO_4.H_20$
pH to 7.0 (with HCl)
treat with 1mL DEPC overnight → autoclave.

0.5M EDTA pH8.0 (1L)
186g EDTA ($Na_2EDTA.2H_20$ or disodium-ethylenediaminetetraacetate)
800ml DEPC Water
NaOH-Chips (ca. 20g)
pH8.0
up to 1000 ml with H_20, treat with DEPC → Autoclave

8.5% NaCl (1L) x2
85g NaCl to 1L → treat with DEPC → autoclave

5M NaCl (1L)
292g NaCl to 1L → autoclave

1x Pronase buffer (100mM Tris-HCl pH 7.5, 50mM EDTA, 250mL in DEPC)
12.5 mL 2M Tris-HCl pH=7.5
25 mL 0.5M EDTA pH8.0
212.5 mL water
NB: in some protocols Tris-HCl is only 50mM!
Autoclave

Pronase stock (50mg/mL)
Dissolve 1g Pronase (Sigma, 10165921001) in 20 mL dH20
Predigest by incubating 4h at 37°C
Store at -20°C (1 year!)

Glycine 10% (100mL)
10g Glycine in 100ml dH2O → treat with DEPC → autoclave → store aliquots at -20°C or 4°C, not in direct sunlight

10x Salts pH6.8 (3M NaCl, 0.1M Tris-HCl pH 6.8, 0.1M $NaPO_4$ buffer, 50mM EDTA) (50mL)
8.77g NaCl
345mg $NaH_2PO_4*H_2O$
355mg $Na_2HPO_4.2H_20$
Up to 40ml with dH2O → DEPC treat → autoclave
Add 5ml 0.5M EDTA pH8
5ml 1M Tris pH6.8

tRNA (100mg/mL)
Dissolve 100mg of tRNA (Sigma, 10109495001) in 1 mL DEPC-treated water

Hybridization buffer (840µL = 10slides) → can be stored in aliquots at -20°C

10x Salts	100µL
Deinonized formamide	420µL
tRNA (100mg/mL)	10µL
50x Denhardts	20µL
H20	90µL
50% Dextran sulfate	200µL (warm to 55 before pipetting)

NB: Rudiger protocol has 2µL and less formamide and 2µL less H2O per slide, results in different amount of probe per hyb mix!

20 X SSC (3M NaCl, 0.3M Na_3-citrate) (1L)
175.3g NaCl
88.2g $Na_3Citrate.2H_2O$
pH = 7.0 with HCl → DEPC

10X NTE buffer (5M NaCl, 100mM Tris.HCl pH7.5, 10mM EDTA) (1L non-DEPC)
292.2g NaCl
50ml 2M Tris-HCl pH7.5
20ml 0.5M EDTA pH 8.0
(Autoclave optional)

RNase A (Sigma)
10mg/ml in autoclaved dH2O, stored at -20°C

10 x DIG-buffer1 (1M Tris, 1.5M NaCl) (1L non-DEPC)
500ml 2M Tris pH7.5
300mL 5M NaCl (87.7g NaCl)
check final pH is 7.5
(Autoclave optional)

Levimasole store at -20°C in aliquots
24mg Levimasole (Sigma, L9756-5G) in 1ml dH2O

Buffers to be freshly prepared

Fixative (200ml):
heat 180ml DEPC-treated water in the microwave until boiling
add 8g of PFA powder (fumehood), stir (with stirrer that has been washed with ethanol and DEPC-treated water)
add 100µl 1M NaOH, wait until PFA is dissolved
add 200µl triton x-100 and 200µl tween-20
add 20ml 10X PBS
check pH = 7, otherwise lower pH with HCl.

4% PFA in PBS (250mL)
heat 225ml DEPC-treated water in the microwave until boiling
add 10g of PFA powder (fumehood), stir (with stirrer that has been washed with ethanol and DEPC-treated water)
add 125µl 1M NaOH, wait until PFA is dissolved
add 25ml 10X PBS
check pH = 7, otherwise lower pH with HCl.

Acetic anhydride in 0.1M triethanolamine pH8 (250mL for 10slides) → in fume hood!
prepare freshly immediately before use, stir well
3.25 mL Triethanolamine
875uL HCl for pH to 8.0, measure with pH strips!
243.88ml H_2O
(Add 2ml Acetic anhydride while dunking your slides)

Pronase (0.125mg/mL, 50mL)
Add 625µL Pronase stock (50mg/mL) in 250mL pre-heated 1x Pronase buffer

Wash buffer (2x SSC, 50% formamide) (1L per 10 slides)
100mL 20x SSC
500mL deionized formamide
400mL DEPC water

1x NTE buffer (1.5L per 10 slides)
150mL 10x NTE in 1350mL of DEPC-treated water

DIG-buffer2 (make fresh every day, or store in the fridge oN) (250mL per 10 slides)
0.5% (w/v) blocking reagent (Sigma, 11096176001) in DIG-buffer 1
1.25g blocking reagent in 250mL DIG-buffer 1

DIG-buffer 3 (make fresh every day, or store in the fridge oN) (1L per 10 slides)

1% BSA	10g BSA(Sigma, A3912-50G)
0.3% Triton-x-100	3mL Triton-x-100
DIG-buffer 1	to 1L

DIG-buffer 4 (make fresh every day)
1:1250 dilution of anti-digoxigenin-AP FAB fragments (Sigma, 11093274910)
For 10 slides: 0.8µL per 1mL DIG-buffer 3

DIG-buffer 5 (100mM Tris pH9.5, 100mM NaCl, 50mM $MgCl_2$) (make fresh every day) (250mL for 10slides)
25ml 1M Tris-HCl pH9.5
5ml 5M NaCl
1.19g $MgCl_2$
220ml H_2O

DIG-buffer 6 (2mL per 10slides)
20µl Levamisole
40µl BCIP/NBT
to 2mL in DIG-buffer 5

7.6 Sequences used during this thesis

Maize Ubiquitin promoter incl intron (ZmUBI):

CTGCAGCCCCTCCAGCTTGCATGCCTGCAGTGCAGCGTGACCCGGTCGTGCCCCTCTCTAGAGATAATGAGC
ATTGCATGTCTAAGTTATAAAAAATTACCACATATTTTTTTTGTCACACTTGTTTGAAGTGCAGTTTATCTA
TCTTTATACATATATTTAAACTTTACTCTACGAATAATATAATCTATAGTACTACAATAATATCAGTGTTTT
AGAGAATCATATAAATGAACAGTTAGACATGGTCTAAAGGACAATTGAGTATTTTGACAACAGGACTCTACA
GTTTTATCTTTTTAGTGTGCATGTGTTCTCCTTTTTTTTTTGCAAATAGCTTCACCTATATAATACTTCATCC
ATTTTATTAGTACATCCATTTAGGGTTTAGGGTTAATGGTTTTTATAGACTAATTTTTTTTAGTACATCTATT
TTATTCTATTTTAGCCTCTAAATTAAGAAAACTAAAACTCTATTTTAGTTTTTTTATTTAATAATTTAGATA
TAAAATAGAATAAAATAAAGTGACTAAAAATTAAACAAATACCCTTTAAGAAATTAAAAAAACTAAGGAAAC
ATTTTTCTTGTTTCGAGTAGATAATGCCAGCCTGTTAAACGCCGTCGACGAGTCTAACGGACACCAACCAGC
GAACCAGCAGCGTCGCGTCGGGCCAAGCGAAGCAGACGGCACGGCATCTCTGTCGCTGCCTCTGGACCCCTC
TCGAGAGTTCCGCTCCACCGTTGGACTTGCTCCGCTGTCGGCATCCAGAAATTGCGTGGCGGAGCGGCAGAC
GTGAGCCGGCACGGCAGGCGGCCTCCTCCTCCTCTCACGGCACCGGCAGCTACGGGGGATTCCTTTCCCACC
GCTCCTTCGCTTTCCCTTCCTCGCCCGCCGTAATAAATAGACACCCCCTCCACACCCTCTTTCCCCAACCTC
GTGTTGTTCGGAGCGCACACACACACAACCAGATCTCCCCCAAATCCACCCGTCGGCACCTCCGCTTCAAGG
TACTACCTTCTCTAGATCGGCGTTCCGGTCCATGGTTAGGGCCCGGTAGTTCTACTTCTGTTCATGTTTGTG
TTAGATCCGTGTTTGTGTTAGATCCGTGCTGCTAGCGTTCGTACACGGATGCGACCTGTACGTCAGACACGT
TCTGATTGCTAACTTGCCAGTGTTTCTCTTTGGGGAATCCTGGGATGGCTCTAGCCGTTCCGCAGACGGGAT
CGATTTCATGATTTTTTTTGTTTCGTTGCATAGGGTTTGGTTTGCCCTTTTCCTTTATTTCAATATATGCCG
TGCACTTGTTTGTCGGGTCATCTTTTCATGCTTTTTTTTGTCTTGGTTGTGATGATGTGGTCTGGTTGGGCG
GTCGTTCTAGATCGGAGTAGAATTAATTCTGTTTCAAACTACCTGGTGGATTTATTAATTTTGGATCTGTAT
GTGTGTGCCATACATATTCATAGTTACGAATTGAAGATGATGGATGGAAATATCGATCTAGGATAGGTATAC
ATGTTGATGCGGGTTTTACTGATGCATATACAGGATGCTTTTTGTTCGCTTGGTTGTGATGATGTGGTGTGG
TTGGGCGGTCGTTCATTCGTTCTAGATCGGAGTAGAATACTGTTTCAAACTACCTGGTGTATTTATTAATTT
TGGAACTGTATGTGTGTGTCATACATCTTCATAGTTACGAGTTTAAGATGGATGGAAATATCGATCTAGGAT
AGGTATACATGTTGATGTGGGTTTTACTGATGCATATACATGATGGCATATGCAGCATCTATTCATATGCTC
TAACCTTGAGTACCTATCTATTATAATAAACAAGTATGTTTTATAATTATTTTGATCTTGATATACTTGGAT
GATGGCATATGCAGCAGCTATATGTGGATTTTTTTAGCCCTGCCTTCATACGCTATTTATTTGCTTGGTACT
GTTTCTTTTGTCGATGCTCACCCTGTTGTTTGGTGTTACTTCTGCAGGTCGACTCTAGA

Brachypodium-optimized Cas9

KpnI restriction site, Multiple cloning site

GGTACCATGATGATCGACTACAAGGACGACGACGACAAGATGGCCCCGAAGAAGAAGCGCAAGGTGGGCATG
GACAAGAAGTACTCCATCGGCCTCGACATCGGCACGAACTCCGTGGGCTGGGCCGTGATCACGGACGAGTAC
AAGGTGCCGTCCAAGAAGTTCAAGGTGCTCGGCAACACGGACCGCCACTCCATCAAGAAGAACCTCATCGGC
GCCCTCCTCTTCGACTCCGGCGAGACGGCCGAGGCCACGCGCCTCAAGCGCACGGCCCGCCGCCGCTACACG
CGCCGCAAGAACCGCATCTGCTACCTCCAGGAGATCTTCTCCAACGAGATGGCCAAGGTGGACGACTCCTTC

TTCCACCGCCTCGAGGAGTCCTTCCTCGTGGAGGAGGACAAGAAGCACGAGCGCCACCCGATCTTCGGC
AACATCGTGGACGAGGTGGCCTACCACGAGAAGTACCCGACGATCTACCACCTCCGCAAGAAGCTCGTGGAC
TCCACGGACAAGGCCGACCTCCGCCTCATCTACCTCGCCCTCGCCCACATGATCAAGTTCCGCGGCCACTTC
CTCATCGAGGGCGACCTCAACCCGGACAACTCCGACGTGGACAAGCTCTTCATCCAGCTCGTGCAGACGTAC
AACCAGCTCTTCGAGGAGAACCCGATCAACGCCTCCGGCGTGGACGCCAAGGCCATCCTCTCCGCCCGCCTC
TCCAAGTCCCGCCGCCTCGAGAACCTCATCGCCCAGCTCCCGGGCGAGAAGAAGAACGGCCTCTTCGGCAAC
CTCATCGCCCTCTCCCTCGGCCTCACGCCGAACTTCAAGTCCAACTTCGACCTCGCCGAGGACGCCAAGCTC
CAGCTCTCCAAGGACACGTACGACGACGACCTCGACAACCTCCTCGCCCAGATCGGCGACCAGTACGCCGAC
CTCTTCCTCGCCGCCAAGAACCTCTCCGACGCCATCCTCCTCTCCGACATCCTCCGCGTGAACACGGAGATC
ACGAAGGCCCCGCTCTCCGCCTCCATGATCAAGCGCTACGACGAGCACCACCAGGACCTCACGCTCCTCAAG
GCCCTCGTGCGCCAGCAGCTCCCGGAGAAGTACAAGGAGATCTTCTTCGACCAGTCCAAGAACGGCTACGCC
GGCTACATCGACGGCGGCGCCTCCCAGGAGGAGTTCTACAAGTTCATCAAGCCGATCCTCGAGAAGATGGAC
GGCACGGAGGAGCTCCTCGTGAAGCTCAACCGCGAGGACCTCCTCCGCAAGCAGCGCACGTTCGACAACGGC
TCCATCCCGCACCAGATCCACCTCGGCGAGCTCCACGCCATCCTCCGCCGCCAGGAGGACTTCTACCCGTTC
CTCAAGGACAACCGCGAGAAGATCGAGAAGATCCTCACGTTCCGCATCCCGTACTACGTGGGCCCGCTCGCC
CGCGGCAACTCCCGCTTCGCCTGGATGACGCGCAAGTCCGAGGAGACGATCACGCCGTGGAACTTCGAGGAG
GTGGTGGACAAGGGCGCCTCCGCCCAGTCCTTCATCGAGCGCATGACGAACTTCGACAAGAACCTCCCGAAC
GAGAAGGTGCTCCCGAAGCACTCCCTCCTCTACGAGTACTTCACGGTGTACAACGAGCTCACGAAGGTGAAG
TACGTGACGGAGGGCATGCGCAAGCCGGCCTTCCTCTCCGGCGAGCAGAAGAAGGCCATCGTGGACCTCCTC
TTCAAGACGAACCGCAAGGTGACGGTGAAGCAGCTCAAGGAGGACTACTTCAAGAAGATCGAGTGCTTCGAC
TCCGTGGAGATCTCCGGCGTGGAGGACCGCTTCAACGCCTCCCTCGGCACGTACCACGACCTCCTCAAGATC
ATCAAGGACAAGGACTTCCTCGACAACGAGGAGAACGAGGACATCCTCGAGGACATCGTGCTCACGCTCACG
CTCTTCGAGGACCGCGAGATGATCGAGGAGCGCCTCAAGACGTACGCCCACCTCTTCGACGACAAGGTGATG
AAGCAGCTCAAGCGCCGCCGCTACACGGGCTGGGGCCGCCTCTCCCGCAAGCTCATCAACGGCATCCGCGAC
AAGCAGTCCGGCAAGACGATCCTCGACTTCCTCAAGTCCGACGGCTTCGCCAACCGCAACTTCATGCAGCTC
ATCCACGACGACTCCCTCACGTTCAAGGAGGACATCCAGAAGGCCCAGGTGTCCGGCCAGGGCGACTCCCTC
CACGAGCACATCGCCAACCTCGCCGGCTCCCCGGCCATCAAGAAGGGCATCCTCCAGACGGTGAAGGTGGTG
GACGAGCTCGTGAAGGTGATGGGCCGCCACAAGCCGGAGAACATCGTGATCGAGATGGCCCGCGAGAACCAG
ACGACGCAGAAGGGCCAGAAGAACTCCCGCGAGCGCATGAAGCGCATCGAGGAGGGCATCAAGGAGCTCGGC
TCCCAGATCCTCAAGGAGCACCCGGTGGAGAACACGCAGCTCCAGAACGAGAAGCTCTACCTCTACTACCTC
CAGAACGGCCGCGACATGTACGTGGACCAGGAGCTCGACATCAACCGCCTCTCCGACTACGACGTGGACCAC
ATCGTGCCGCAGTCCTTCCTCAAGGACGACTCCATCGACAACAAGGTGCTCACGCGCTCCGACAAGAACCGC
GGCAAGTCCGACAACGTGCCGTCCGAGGAGGTGGTGAAGAAGATGAAGAACTACTGGCGCCAGCTCCTCAAC
GCCAAGCTCATCACGCAGCGCAAGTTCGACAACCTCACGAAGGCCGAGCGCGGCGGCCTCTCCGAGCTCGAC
AAGGCCGGCTTCATCAAGCGCCAGCTCGTGGAGACGCGCCAGATCACGAAGCACGTGGCCCAGATCCTCGAC
TCCCGCATGAACACGAAGTACGACGAGAACGACAAGCTCATCCGCGAGGTGAAGGTGATCACGCTCAAGTCC
AAGCTCGTGTCCGACTTCCGCAAGGACTTCCAGTTCTACAAGGTGCGCGAGATCAACAACTACCACCACGCC
CACGACGCCTACCTCAACGCCGTGGTGGGCACGGCCCTCATCAAGAAGTACCCGAAGCTCGAGTCCGAGTTC
GTGTACGGCGACTACAAGGTGTACGACGTGCGCAAGATGATCGCCAAGTCCGAGCAGGAGATCGGCAAGGCC
ACGGCCAAGTACTTCTTCTACTCCAACATCATGAACTTCTTCAAGACGGAGATCACGCTCGCCAACGGCGAG
ATCCGCAAGCGCCCGCTCATCGAGACGAACGGCGAGACGGGCGAGATCGTGTGGGACAAGGGCCGCGACTTC
GCCACGGTGCGCAAGGTGCTCTCCATGCCGCAGGTGAACATCGTGAAGAAGACGGAGGTGCAGACGGGCGGC
TTCTCCAAGGAGTCCATCCTCCCGAAGCGCAACTCCGACAAGCTCATCGCCCGCAAGAAGGACTGGGACCCG
AAGAAGTACGGCGGCTTCGACTCCCCGACGGTGGCCTACTCCGTGCTCGTGGTGGCCAAGGTGGAGAAGGGC
AAGTCCAAGAAGCTCAAGTCCGTGAAGGAGCTCCTCGGCATCACGATCATGGAGCGCTCCTCCTTCGAGAAG
AACCCGATCGACTTCCTCGAGGCCAAGGGCTACAAGGAGGTGAAGAAGGACCTCATCATCAAGCTCCCGAAG
TACTCCCTCTTCGAGCTCGAGAACGGCCGCAAGCGCATGCTCGCCTCCGCCGGCGAGCTCCAGAAGGGCAAC
GAGCTCGCCCTCCCGTCCAAGTACGTGAACTTCCTCTACCTCGCCTCCCACTACGAGAAGCTCAAGGGCTCC
CCGGAGGACAACGAGCAGAAGCAGCTCTTCGTGGAGCAGCACAAGCACTACCTCGACGAGATCATCGAGCAG
ATCTCCGAGTTCTCCAAGCGCGTGATCCTCGCCGACGCCAACCTCGACAAGGTGCTCTCCGCCTACAACAAG
CACCGCGACAAGCCGATCCGCGAGCAGGCCGAGAACATCATCCACCTCTTCACGCTCACGAACCTCGGCGCC
CCGGCCGCCTTCAAGTACTTCGACACGACGATCGACCGCAAGCGCTACACGTCCACGAAGGAGGTGCTCGAC
GCCACGCTCATCCACCAGTCCATCACGGGCCTCTACGAGACGCGCATCGACCTCTCCCAGCTCGGCGGCGAC
TAGCTGCTTTAATGAGATATGCGAGACGCCTATGATCGCATGATATTTGCTTTCAATTCTGTTGTGCACGTT
GTAAAAACCTGAGCATGTGTAGCTCAGATCCTTACCGCCGGTTTCGGTTCATTCTAATGAATATATCACCCG
TTACTATCGTATTTTTATGAATAATATTCTCCGTTCAATTTACTGATTGTACCCTACTACTTATATGTACAA
TATTAAAATGAAAACAATATATTGTGCTGAATAGGTTTATAGCGACATCTATGATAGAGCGCCACAATAACA
AACAATTGCGTTTTATTATTACAAATCCAATTTTCGGGGATCCTCTAGAGTCGACCTGCAGGCATGCAAGCT
TGGCACGGTGACC

Brachypodium-optimized AsCpfI

GGTACCATGACCCAGTTCGAGGGCTTCACCAACCTCTACCAGGTGTCCAAGACCCTCAGGTTCGAG
CTGATCCCACAGGGCAAGACCCTGAAGCACATTCAGGAGCAGGGCTTCATCGAGGAGGACAAGGCT
AGGAACGACCACTACAAGGAGCTGAAGCCGATCATCGACAGGATCTACAAGACCTACGCCGACCAG
TGCCTCCAGCTCGTTCAGCTCGATTGGGAGAACCTCTCCGCCGCCATTGACTCCTACCGCAAGGAG
AAGACCGAGGAGACGAGGAACGCCCTGATTGAGGAGCAGGCTACCTACCGGAACGCCATCCACGAC
TACTTCATCGGCAGGACCGACAACCTCACCGACGCCATCAACAAGAGGCACGCCGAGATCTACAAG
GGCCTCTTCAAGGCCGAGCTGTTCAACGGCAAGGTGCTCAAGCAGCTCGGCACCGTGACCACCACC
GAGCATGAGAACGCCCTTCTCCGCTCCTTCGACAAGTTCACCACCTACTTCTCCGGCTTCTACGAG
AACCGCAAGAACGTGTTCTCCGCCGAGGATATCTCCACCGCCATCCCACATAGGATCGTGCAGGAC
AACTTCCCGAAGTTCAAGGAGAACTGCCACATCTTCACCAGGCTCATCACCGCCGTTCCATCCCTC
CGCGAGCATTTCGAGAACGTGAAGAAGGCCATCGGCATCTTCGTGTCCACCTCTATTGAGGAGGTG
TTCTCCTTCCCGTTCTACAACCAGCTCCTCACCCAGACCCAGATCGACCTGTACAACCAGCTTCTC
GGCGGCATTTCCCGCGAGGCCGGCACCGAGAAGATTAAGGGCCTTAACGAGGTCCTCAACCTCGCC
ATCCAGAAGAACGACGAGACCGCCCACATCATTGCCTCACTCCCACACCGCTTCATCCCGCTGTTC
AAGCAGATCCTCTCCGACCGCAACACCCTCAGCTTCATTCTCGAGGAGTTCAAGTCCGACGAGGAG
GTGATCCAGTCCTTCTGCAAGTACAAGACGCTCCTGAGGAACGAGAACGTGCTCGAGACCGCTGAG
GCCCTCTTCAACGAGCTTAACTCCATCGACCTCACCCATATCTTCATCTCCCACAAGAAGCTCGAG
ACGATCTCCTCCGCCCTCTGCGACCATTGGGACACCCTCCGCAACGCCCTCTACGAGAGGCGCATC
TCCGAGCTTACCGGCAAGATTACCAAGAGCGCGAAGGAGAAGGTCCAGCGCTCTCTCAAGCACGAG
GACATCAACCTCCAGGAGATCATCTCCGCTGCCGGCAAGGAGCTTTCCGAGGCCTTCAAGCAGAAG
ACCTCCGAGATCCTCTCTCACGCCCATGCCGCTCTCGATCAGCCACTTCCAACCACCCTCAAGAAG
CAGGAGGAGAAGGAGATCCTCAAGTCCCAGCTCGATAGCCTCCTCGGCCTCTACCATCTCCTCGAT
TGGTTCGCCGTGGACGAGTCCAACGAGGTGGACCCAGAGTTCTCTGCTAGGCTCACCGGCATCAAG
CTCGAGATGGAGCCAAGCCTCAGCTTCTACAACAAGGCCCGCAACTACGCCACCAAGAAGCCGTAC
TCCGTCGAGAAGTTCAAGCTCAACTTCCAGATGCCGACCCTCGCCTCTGGCTGGGATGTGAACAAG
GAGAAGAACAACGGCGCCATCCTCTTCGTCAAGAACGGCCTGTACTACCTCGGCATCATGCCAAAG
CAGAAGGGCAGGTACAAGGCCCTGTCCTTCGAGCCAACCGAGAAGACCTCTGAGGGCTTCGACAAG
ATGTACTACGATTACTTCCCGGACGCCGCCAAGATGATCCCGAAGTGCTCTACCCAGCTCAAGGCC
GTGACCGCCCATTTCCAGACCCATACCACCCCAATCCTGCTCTCCAACAACTTCATTGAGCCGCTC
GAGATCACCAAGGAGATCTACGACCTCAACAACCCCGAGAAGGAGCCGAAGAAGTTCCAGACCGCC
TACGCCAAGAAGACCGGCGATCAGAAGGGCTACCGCGAGGCTCTCTGCAAGTGGATCGATTTCACC
AGGGACTTCCTCAGCAAGTACACCAAGACGACCAGCATCGATCTCTCCAGCCTCAGGCCATCCTCC
CAGTACAAGGACCTCGGCGAGTACTACGCTGAGCTGAACCCTCTCCTCTACCACATCTCCTTCCAG
CGCATTGCCGAGAAGGAGATTATGGACGCCGTCGAGACCGGCAAGCTCTACCTCTTCCAGATCTAC
AACAAGGACTTCGCCAAGGGCCACCACGGCAAGCCAAACCTCCATACCCTCTACTGGACCGGCCTG
TTCTCCCCAGAGAACCTCGCTAAGACCTCCATCAAGCTGAACGGCCAGGCGGAGCTTTTCTACAGG
CCGAAGTCCCGCATGAAGCGCATGGCTCACAGGCTCGGCGAGAAGATGCTCAACAAGAAGCTGAAG
GACCAGAAGACCCCGATCCCGGACACCCTGTACCAGGAGCTTTACGACTACGTCAACCACAGGCTC
TCCCACGACCTCTCAGATGAGGCTAGGGCTCTCCTCCCGAACGTCATCACGAAGGAGGTGTCCCAC
GAGATCATTAAGGACAGGCGCTTCACCTCCGATAAGTTCTTCTTCCACGTGCCGATCACCCTCAAC
TACCAGGCCGCCAACTCCCCGTCCAAGTTCAACCAGAGGGTGAACGCCTACCTGAAGGAGCACCCA
GAGACCCCCATCATCGGCATTGACAGGGGCGAGAGGAACCTCATCTACATCACCGTGATCGACTCC
ACGGGCAAGATCCTTGAGCAGCGCAGCCTCAACACCATCCAGCAGTTCGACTACCAGAAGAAGCTG
GATAACCGCGAGAAGGAGCGCGTTGCCGCCAGGCAGGCCTGGTCCGTGGTGGGCACCATTAAGGAT
CTCAAGCAGGGCTACCTCTCCCAGGTCATCCATGAGATCGTGGACCTCATGATCCATTACCAGGCG
GTCGTGGTCCTTGAGAACCTCAACTTCGGCTTCAAGTCCAAGCGCACCGGGATCGCTGAGAAGGCC
GTTTACCAGCAGTTCGAGAAGATGCTGATCGACAAGCTCAACTGCCTCGTCCTCAAGGACTACCCG
GCTGAGAAGGTGGGCGGCGTTCTGAACCCATACCAGCTGACCGATCAGTTCACCAGCTTCGCTAAG
ATGGGGACCCAGTCCGGCTTCCTGTTCTACGTGCCAGCTCCGTACACCTCCAAGATCGACCCACTC
ACCGGCTTCGTGGACCCGTTCGTGTGGAAGACCATCAAGAACCACGAGTCCCGCAAGCACTTCCTC
GAGGGGTTCGACTTCCTCCACTACGACGTTAAGACGGGCGACTTCATCCTCCACTTCAAGATGAAC
CGCAACCTGAGCTTCCAGAGGGGCCTCCCAGGCTTCATGCCAGCTTGGGATATCGTTTTCGAGAAG
AACGAGACGCAGTTCGACGCCAAGGGCACCCCATTCATTGCGGGCAAGAGGATCGTCCCGGTGATC
GAGAACCATAGGTTCACCGGCCGCTACAGGGACCTGTACCCAGCCAACGAGCTGATTGCTCTGCTC
GAGGAGAAGGGGATCGTTTTCAGGGACGGCTCCAACATCCTCCCCAAGCTGCTCGAGAACGATGAC
TCCCATGCCATCGACACCATGGTCGCCCTCATTCGCTCTGTGCTCCAGATGAGGAACTCCAACGCC

GCTACCGGCGAGGACTACATCAACTCCCCAGTGAGGGATCTCAACGGCGTGTGCTTCGACTCC
AGGTTCCAGAACCCAGAGTGGCCGATGGACGCTGATGCTAACGGCGCCTACCATATCGCTCTCAAG
GGCCAGCTCCTGCTCAACCATCTCAAGGAGTCCAAGGACCTTAAGCTCCAGAACGGCATCTCCAAC
CAGGACTGGCTCGCCTACATCCAGGAGCTGAGGAACAAGCGCCCAGCCGCTACCAAGAAGGCTGGC
CAGGCTAAGAAGAAGAAGGGCTCCTACCCGTACGACGTGCCGGATTACGCCTACCCATACGATGTC
CCCGACTACGCGTACCCCTACGACGTTCCAGACTACGCTTGACTGCTTTAATGAGATATGCGAGAC
GCCTATGATCGCATGATATTTGCTTTCAATTCTGTTGTGCACGTTGTAAAAACCTGAGCATGTGTA
GCTCAGATCCTTACCGCCGGTTTCGGTTCATTCTAATGAATATATCACCCGTTACTATCGTATTTT
TATGAATAATATTCTCCGTTCAATTTACTGATTGTACCCTACTACTTATATGTACAATATTAAAAT
GAAAACAATATATTGTGCTGAATAGGTTTATAGCGACATCTATGATAGAGCGCCACAATAACAAAC
AATTGCGTTTTATTATTACAAATCCAATTTTCGGGGATCCTCTAGAGTCGACCTGCAGGCATGCAA
GCTTGGCACGGTTACC

Brachypodium-optimized LbCpfI

GGTACCATGTCCAAGCTCGAGAAGTTCACCAACTGCTACTCCCTCAGCAAGACCCTCAGGTTCAAG
GCCATCCCAGTGGGCAAGACCCAGGAGAACATCGACAACAAGAGGCTCCTCGTCGAGGACGAGAAG
AGGGCCGAGGATTACAAGGGCGTGAAGAAGCTCCTCGACAGGTACTACCTCTCCTTCATCAACGAC
GTGCTCCACTCCATCAAGCTCAAGAACCTCAACAACTACATCAGCCTCTTCCGCAAGAAGACCAGG
ACCGAGAAGGAGAACAAGGAGCTTGAGAACCTCGAGATCAACCTCCGCAAGGAGATCGCCAAGGCC
TTCAAGGGCAACGAGGGCTACAAGAGCCTCTTCAAGAAGGACATCATCGAGACCATCCTCCCCGAG
TTCCTCGATGACAAGGACGAGATCGCCCTCGTGAACTCCTTCAACGGCTTCACCACCGCGTTCACC
GGCTTCTTCGATAACCGCGAGAACATGTTCAGCGAGGAGGCCAAGTCCACCTCGATTGCCTTCCGC
TGCATCAACGAGAACCTCACCCGCTACATCTCCAACATGGATATCTTCGAGAAGGTGGACGCCATC
TTCGACAAGCACGAGGTGCAGGAGATTAAGGAGAAGATCCTCAACTCCGACTACGACGTCGAGGAT
TTCTTCGAGGGCGAGTTCTTCAACTTCGTGCTCACCCAGGAGGGGATCGACGTCTACAACGCCATC
ATTGGCGGCTTCGTTACCGAGTCCGGCGAGAAGATTAAGGGCCTCAACGAGTACATCAACCTGTAC
AACCAGAAGACCAAGCAGAAGCTCCCGAAGTTCAAGCCGCTCTACAAGCAGGTTCTCTCCGACCGC
GAGTCCCTCTCATTCTACGGCGAGGGGTACACCTCCGATGAGGAGGTGCTCGAGGTTTTCCGCAAC
ACCCTCAACAAGAACTCCGAGATCTTCAGCAGCATCAAGAAGCTCGAGAAGCTGTTCAAGAACTTC
GACGAGTACTCCTCCGCCGGCATCTTCGTGAAGAACGGCCCAGCCATCTCCACCATCAGCAAGGAC
ATTTTCGGCGAGTGGAACGTGATCAGGGACAAGTGGAACGCCGAGTACGACGACATCCACCTCAAG
AAGAAGGCCGTCGTCACCGAGAAGTACGAGGACGATAGGCGCAAGTCGTTCAAGAAGATCGGCTCC
TTCAGCCTCGAGCAGCTGCAGGAGTACGCTGACGCTGATCTCTCCGTGGTTGAGAAGCTCAAGGAG
ATTATCATCCAGAAGGTCGACGAGATCTACAAGGTGTACGGCTCCTCGGAGAAGCTGTTCGACGCC
GATTTCGTGCTCGAGAAGTCCCTGAAGAAGAACGACGCCGTCGTCGCGATCATGAAGGACCTGCTC
GATTCCGTGAAGTCCTTCGAGAACTACATTAAGGCTTTCTTCGGGGAGGGCAAGGAGACCAACAGG
GACGAGTCTTTCTACGGGGACTTCGTCCTCGCCTACGACATCCTGCTCAAGGTGGACCATATCTAC
GACGCGATCCGCAACTACGTGACCCAGAAGCCGTACTCCAAGGACAAGTTCAAGCTCTACTTCCAG
AACCCGCAGTTCATGGGCGGCTGGGACAAGGATAAGGAGACCGATTACAGGGCCACCATCCTCAGG
TACGGCAGCAAGTACTACCTGGCCATCATGGACAAGAAGTACGCCAAGTGCCTGCAGAAGATCGAT
AAGGACGACGTGAACGGCAACTACGAGAAGATCAACTACAAGCTCCTCCCAGGCCCGAACAAGATG
CTCCCCAAGGTGTTCTTCTCAAAGAAGTGGATGGCCTACTACAACCCGTCCGAGGATATCCAGAAG
ATCTACAAGAACGGCACCTTCAAGAAGGGCGACATGTTCAACCTCAACGACTGCCACAAGCTCATC
GATTTCTTCAAGGACTCCATCTCCCGCTACCCGAAGTGGTCCAACGCGTACGATTTCAACTTCAGC
GAGACCGAGAAGTACAAGGATATCGCCGGCTTCTACCGCGAGGTTGAGGAGCAGGGGTACAAGGTG
AGCTTCGAGTCCGCCTCCAAGAAGGAGGTCGACAAGCTGGTTGAGGAGGGCAAGCTCTACATGTTC
CAGATCTACAACAAGGACTTCTCCGACAAGTCCCACGGCACCCCAAACCTCCACACCATGTACTTC
AAGCTGCTTTTCGACGAGAACAACCACGGCCAGATTAGGCTTTCTGGCGGCGCTGAGCTTTTCATG
AGGCGCGCGAGCCTTAAGAAGGAGGAGCTGGTTGTTCACCCGGCCAACTCCCCAATCGCGAACAAG
AACCCGGACAACCCGAAGAAGACGACCACCCTCTCCTACGACGTGTACAAGGACAAGCGCTTCTCG
GAGGACCAGTACGAGCTGCACATCCCGATCGCCATCAACAAGTGCCCGAAGAACATCTTCAAGATC
AACACCGAGGTGAGGGTGCTGCTCAAGCACGACGACAACCCATACGTGATCGGCATCGATAGGGGC
GAGAGGAACCTCCTCTACATCGTGGTGGTTGACGGGAAGGGCAACATCGTCGAGCAGTACTCCCTG
AACGAGATCATCAACAACTTCAACGGGATCAGGATCAAGACCGACTACCACTCCCTGCTCGACAAG
AAGGAGAAGGAGCGCTTCGAGGCCAGGCAGAACTGGACCTCCATCGAGAACATCAAGGAGCTGAAG
GCCGGCTACATTTCCCAGGTGGTGCACAAGATCTGCGAGCTTGTTGAGAAGTACGACGCGGTGATC
GCGCTCGAGGATCTGAACTCCGGCTTCAAGAACAGCAGGGTGAAGGTCGAGAAGCAGGTCTACCAG

AAGTTCGAGAAGATGCTCATCGACAAGCTCAACTACATGGTGGATAAGAAGTCCAACCCCTGC
GCTACCGGCGGCGCCCTCAAGGGCTACCAGATTACCAACAAGTTCGAGTCCTTCAAGTCCATGTCC
ACCCAGAACGGCTTCATCTTCTACATCCCGGCCTGGCTCACCTCCAAGATCGACCCATCTACCGGC
TTCGTGAACCTTCTCAAGACGAAGTACACCTCTATCGCCGACAGCAAGAAGTTCATCTCCAGCTTC
GACAGGATCATGTACGTGCCCGAGGAGGACCTCTTCGAGTTCGCCCTTGACTACAAGAACTTCTCC
AGGACCGACGCCGACTACATCAAGAAGTGGAAGCTCTACTCCTACGGCAACCGCATCAGGATCTTC
CGGAACCCCAAGAAGAACAACGTTTTCGATTGGGAGGAGGTGTGCCTCACCTCCGCCTACAAGGAG
CTGTTCAACAAGTACGGCATCAACTACCAGCAGGGCGATATCAGGGCTCTCCTGTGCGAGCAGTCC
GACAAGGCGTTCTACAGCAGCTTCATGGCCCTCATGAGCCTCATGCTCCAGATGAGGAACTCCATC
ACCGGCAGGACCGATGTCGACTTCCTCATCAGCCCGGTGAAGAACAGCGACGGGATCTTCTACGAC
AGCCGGAACTACGAGGCTCAGGAGAACGCCATCCTGCCGAAGAACGCTGATGCCAACGGCGCCTAC
AACATTGCCCGCAAGGTGCTCTGGGCCATCGGCCAGTTCAAGAAGGCTGAGGACGAGAAGCTCGAC
AAGGTGAAGATCGCCATCTCGAACAAGGAGTGGCTCGAGTACGCCCAGACCTCCGTGAAGCACAAG
AGGCCAGCTGCTACCAAGAAGGCGGGCCAGGCTAAGAAGAAGAAGGGCTCCTACCCGTACGACGTG
CCGGATTACGCCTACCCATACGATGTCCCCGACTACGCGTACCCCTACGACGTTCCAGACTACGCT
TGACTGCTTTAATGAGATATGCGAGACGCCTATGATCGCATGATATTTGCTTTCAATTCTGTTGTG
CACGTTGTAAAAACCTGAGCATGTGTAGCTCAGATCCTTACCGCCGGTTTCGGTTCATTCTAATGA
ATATATCACCCGTTACTATCGTATTTTTATGAATAATATTCTCCGTTCAATTTACTGATTGTACCC
TACTACTTATATGTACAATATTAAAATGAAAACAAAATATTGTGCTGAATAGGTTTATAGCGACAT
CTATGATAGAGCGCCACAATAACAAACAATTGCGTTTTATTATTACAAATCCAATTTTCGGGGATC
CTCTAGAGTCGACCTGCAGGCATGCAAGCTTGGCACGGTTACC

Cassette with BdU6 promoter, OsU6 promoter, 2 tracrRNA and space for 2 sgRNAs

BdU6 promoter
tracrRNA
OsU6 promoter
BsaI restriction site
BtgZI restriction site

TACTTGGGCTGTTGCTCTCTACTGGGTTGGGCCGCATGGACTGACACAGGCCCACGCGCGGTCCTTCACGAG
CCTGGGGCTGGCCTGATCCGATGGTTGCTGATCAAGGCAACAGGCTAGAAAGTTTAGTCCCACCTCGCGAGA
TGAAGGATAGTTTGACTAGATTATAAACATTCTGCTACCACCCTTCTCagagaccgagctcggtctcaGTTT
TAGAGCTAGAAATAGCAAGTTAAAATAAGGCTAGTCCGTTATCAACTTGAAAAAGTGGCACCGAGTCGGTGC
TTTTTTTTGAGATTTCCAACCAGGTCCCTGGAGCCCATAGTCTAGTAACGGCCGCCAGTGTGCTGGAATTGC
CCTTGGATCATGAACCAACGGCCTGGCTGTATTTGGTGGTTGTGTAGGGAGATGGGGAGAAGAAAAGCCCGA
TTCTCTTCGCTGTGATGGGCTGGATGCATGCGGGGGAGCGGGAGGCCCAAGTACGTGCACGGTGAGCGGCCC
ACAGGGCGAGTGTGAGCGCGAGAGGCGGGAGGAACAGTTTAGTACCACATTGCCCAGCTAACTCGAACGCGA
CCAACTTATAAACCCGCGCGCTGTCGCTTGTGTGGCTAGGATCCATCGCAGTCAGCGATGAGTACAGCAAGT
TTTAGAGCTAGAAATAGCAAGTTAAAATAAGGCTAGTCCGTTATCAACTTGAAAAAGTGGCACCGAGTCGGT
GCTTTTTTT

Sequences for Clustal Omega alignments for AUX1

> AtAUX1
MSEGVEAIVANDNGTDQVNGNRTGKDNEEHDGSTGSNLSNFLWHGGSVWDAWFSCASNQVAQVLLT
LPYSFSQLGMLSGIVLQIFYGLLGSWTAYLISVLYVEYRARKEKEGKSFKNHVIQWFEVLDGLLGS
YWKALGLAFNCTFLLFGSVIQLIACASNIYYINDHLDKRTWTYIFGACCATTVFIPSFHNYRIWSF
LGLGMTTYTAWYLAIASIIHGQAEGVKHSGPTKLVLYFTGATNILYTFGGHAVTVEIMHAMWKPQK
FKYIYLMATLYVFTLTIPSAAAVYWAFGDALLDHSNAFSLMPKNAWRDAAVILMLIHQFITFGFAC
TPLYFVWEKVIGMHDTKSICLRALARLPVVIPIWFLAIIFPFFGPINSAVGALLVSFTVYIIPSLA
HMLTYRSASARQNAAEKPPFFMPSWTAMYVLNAFVVVWVLIVGFGFGGWASVTNFVRQVDTFGLFA
KCYQCKPAAAAAHAPVSALHHRL*

> AtLAX1
MSGEKQAEESIVVSGEDEVAGRKVEDSAAEEDIDGNGGNGFSMKSFLWHGGSAWDAWFSCASNQVA
QVLLTLPYSFSQLGMLSGILLQIFYGLMGSWTAYLISVLYVEYRARMEKQEAKSFKNHVIQWFEVL
DGLLGPYWKAAGLAFNCTFLLFGSVIQLIACASNIYYINDRLDKRTWTYIFGACCATTVFIPSFHN
YRIWSFLGLGMTTYTAWYLTIASFLHGQAEGVTHSGPTKLVLYFTGATNILYTFGGHAVTVEIMHA
MWKPRKFKSIYLMATLYVFTLTLPSASAVYWAFGDQLLNHSNAFSLLPKTRFRDTAVILMLIHQFI
TFGFACTPLYFVWEKAIGMHHTKSLCLRALVRLPVVVPIWFLAIIFPFFGPINSAVGALLVTFTVY
IIPALAHMLTYRTASARRNAAEKPPFFIPSWAGVYVINAFIVVWVLVLGFGFGGWASMTNFIRQID
TFGLFAKCYQCKPPPAPIAAGAHHRR*

> AtLAX2
MENGEKAAETVVVGNYVEMEKDGKALDIKSKLSDMFWHGGSAYDAWFSCASNQVAQVLLTLPYSFS
QLGMLSGILFQLFYGILGSWTAYLISILYVEYRTRKEREKVNFRNHVIQWFEVLDGLLGKHWRNVG
LAFNCTFLLFGSVIQLIACASNIYYINDNLDKRTWTYIFGACCATTVFIPSFHNYRIWSFLGLLMT
TYTAWYLTIASILHGQVEGVKHSGPSKLVLYFTGATNILYTFGGHAVTVEIMHAMWKPQKFKSIYL
FATLYVLTLTLPSASAVYWAFGDLLLNHSNAFALLPKNLYRDFAVVLMLIHQFITFGFACTPLYFV
WEKLIGMHECRSMCKRAAARLPVVIPIWFLAIIFPFFGPINSTVGSLLVSFTVYIIPALAHIFTFR
SSAARENAVEQPPRFLGRWTGAFTINAFIVVWVFIVGFGFGGWASMINFVHQIDTFGLFTKCYQCP
PPVMVSPPPISHPHFNHTHGL*

> AtLAX3
MAAEKIETVVAGNYLEMEREEENISGNKKSSTKTKLSNFFWHGGSVYDAWFSCASNQVAQVLLTLP
YSFSQLGMMSGILFQLFYGLMGSWTAYLISVLYVEYRTRKEREKFDFRNHVIQWFEVLDGLLGKHW
RNLGLIFNCTFLLFGSVIQLIACASNIYYINDKLDKRTWTYIFGACCATTVFIPSFHNYRIWSFLG
LAMTTYTSWYLTIASLLHGQAEDVKHSGPTTMVLYFTGATNILYTFGGHAVTVEIMHAMWKPQKFK
AIYLLATIYVLTLTLPSASAVYWAFGDKLLTHSNALSLLPKTGFRDTAVILMLIHQFITFGFASTP
LYFVWEKLIGVHETKSMFKRAMARLPVVVPIWFLAIIFPFFGPINSAVGSLLVSFTVYIIPALAHM
LTFAPAPSRENAVERPPRVVGGWMGTYCINIFVVVWVFVVGFGFGGWASMVNFVRQIDTFGLFTKC
YQCPPHKP*

> BdAUX1
MVPREHGDEAIVADGNGKEEEVGVMGVGAADGDEEQHGAGGKFSVTSFLWHGGSVWDAWFSCASNQ
VAQVLLTLPYSFSQLGMLSGVLLQLFYGFLGSWTAYLISVLYVEYRSRKEKEGVSFKNHVIQWFEV
LDGLLGPYWKAAGLAFNCTFLLFGTVIQLIACASNIYYINDRLDKRTWTYIFGACCATTVFIPSFH
NYRIWSFLGLGMTTYTAWYLAIAALINGQVEGVTHTGPNKLVLYFTGATNILYTFGGHAVTVEIMH
AMWKPAKFKYIYLLATLYVFTLTLPSASAMYWAYGDELLSHANAFSLLPKTAWRDAAVVLMLIHQF
ITFGFACTPLYFVWEKVIGMHDCKSICLRALARLPIVVPIWFLAIIFPFFGPINSAVGALLVSFTV
YIIPALAHILTYRTASARANAAEKPPFFLPSWTGMFVLNAFIVVWVFVVGFGLGGWASMVNFIRQI
DTFGLFAKCYQCPKPPVMAAAPSSSHH*

> BdLAX3a
MAAAANGSLADEKAPETIGVGRYVEMEQDGNSGSTAKSRLSGLLWHGGSAYDAWFSCASNQVAQVL
LTLPYSFSQLGMLSGILFQLFYGLMGSWTAYLISILYVEYRTRKEREKADFRNHVIQWFEVLDGLL
GRHWRNVGLAFNCTFLLFGSVIQLIACASNIYYINDRLDKRTWTYIFGACCATTVFIPSFHNYRIW
SFLGLVMTTYTAWYLAIASILHGQVDGVKHSGPTKMVLYFTGATNILYTFGGHAVTVEVMHAMWRP
QKFKAIYLMATLYVLTLTLPSAASVYWAFGDDLLTHSNALSLLPRTAFRDAAVVLMLVHQFITFGF
ACTPLYFVWEKLIGLHDCRSLCKRAAARLPVVVPIWFLAIVFPFFGPINSAVGSLLVSFTVYIIPA
LAHMITYRSAPARENAVEPPPRFVGRWTGTYMINAFVVAWVLVVGFGFGGWASMTNFIRQIDTFGL
FTKCYQCPTTAQPGLAPPLPSAAPDASWPFPGVLSNFTMPAPAPSPAHFFRHPRHHSHGPALK*

> BdLAX3b
MASETAAGSALADEKAEAMEQQEAGGKSRLSGLLWHGGSAYDAWFSCASNQVAQVLLTLPYSFAQL
GMLSGILFQLFYGLLGSWTAYLISILYLEYRTRKEKDKVDFRNHVIQWFEVLDGLLGRHWRNVGLA
FNCTFLLFGSVIQLIGCASNIYYVNDHLDKRTWTYIFGACCATTVFIPSFHNYRVWSFLGLLMTTY
TAWYIAVASLVHGQVEGVRHSGPTTIMLYFTGATNILYTFGGHAVTVEIMHAMWRPQKFKAIYLLA
TLYVLTLTLPSASAAYWAFGDQLLTHSNALSLLPRDAWRDAAVVLMLIHQFITFGFACTPLYFVWE
KLIGLHDCKSLCKRAAARLPVVVPIWFLAIIFPFFGPINSAVGSLLVSFTVYIIPAMAHMVTFRSP
QSRENAVERPPRFAGGWTGAYVINSFVVAWVLVVGFGFGGWASITNFVQQVSTFGLFAKCYQCPPR
PAASPFLSPPVAFSPSMPPTPFSFNFTGIFAPMSSTPSPAPAPMPFGLGHHHHRHHRHGL*

> OsAUX1
MVPREQAEEAIVADSNGKEEEVGVMGVSAGEHGADDHHGGGGKFSMKNLLWHGGSVWDAWFSCASN
QVAQVLLTLPYSFSQLGMLSGVLLQLFYGFMGSWTAYLISVLYVEYRSRKEKEGVSFKNHVIQWFE
VLDGLLGPYWKAAGLAFNCTFLLFGSVIQLIACASNIYYINDRLDKRTWTYIFGACCATTVFIPSF
HNYRIWSFLGLGMTTYTAWYLAIAALLNGQAEGITHTGPTKLVLYFTGATNILYTFGGHAVTVEIM
HAMWKPAKFKYIYLLATLYVFTLTLPSASAMYWAFGDELLTHSNAFSLLPKTGWRDAAVILMLIHQ
FITFGFACTPLYFVWEKVIGMHDTKSICLRALARLPIVVPIWFLAIIFPFFGPINSAVGALLVSFT
VYIIPALAHILTYRTASARMNAAEKPPFFLPSWTGMFVLNMFIVVWVLVVGFGLGGWASMVNFIRQ
IDTFGLFAKCYQCPKPAPALAQSPVPLPHH*

> OsAUX2
MVPAGDQAEEAIVADAGKEEAEVRAAMGVEQDGKFSMTSLLWHGGSVWDAWFSCASNQVRPTTNDL
VMPLAHISFGILQVAQVLLTLPYSFSQLGMLSGLLLQVFYGLMGSWTAYLISVLYVEYRARKEKEG
VSFKNHVIQWFEVLDGLLGPYWKAAGLAFNCTFLLFGSVIQLIACASNIYYINDRLDKRTWTYIFG
ACCSTTVFIPSFHNYRIWSFLGLGMTTYTAWYLAIAAAVHGQVDGVTHSGPSKMVLYFTGATNILY
TFGGHAVTVEIMHAMWKPQKFKYIYLVATLYVFTLTLPSASAMYWAFGDALLTHSNAFSLLPRSGW
RDAAVILMLIHQFITFGFACTPLYFVWEKAIGMHGTRSVLTRALARLPIVVPIWFLAIIFPFFGPI
NSAVGALLVSFTVYIIPSLSHILTYRSASARLNAAEKPPPFLPSWSGMFVVNVFVVAWVLVVGFGL
GGWASVTNFIKQIDTFGLFAKCYQCPPRAHAGAPLPAPPRH*

> OsAUX3
MGSAADGSLANEKAPAETVGVGRYVEMEQDGGGPSTAKSRLSGLLWHGGSAYDAWFSCASNQVAQV
LLTLPYSFSQLGMLSGILFQLFYGLLGSWTAYLISILYVEYRTRKEREKVDFRNHVIQWFEVLDGL
LGRHWRNVGLAFNCTFLLFGSVIQLIACASNIYYINDKLDKRTWTYIFGACCATTVFIPSFHNYRI
WSFLGLVMTTYTAWYLAVASLIHGQVDGVKHSGPTKMVLYFTGATNILYTFGGHAVTVEIMHAMWR
PQKFKAIYLMATLYVLTLTLPSAASVYWAFGDELLTHSNALALLPRTAFRDAAVVLMLIHQFITFG
FACTPLYFVWEKLIGLHDCRSLFKRAAARLPVVVPIWFLAIIFPFFGPINSAVGSLLVSFTVYIIP
ALAHMITFRSAHARENAVEPPPRFVGRWTGTFIINAFVVAWVLVVGFGFGGWASMTNFVRQIDTFG
LFTKCYQCPPPPLPPAGAAPNATWPPFPATPFNATTAGLAPAPAPSPAHFFGRHHRHHSHGL*

> OsAUX4
MASGSSGGGYADEKGPGAATMQALGLQQQHGGGGEVEEESSEMGEKTAARTRLSGLLWHGGSAYDA
WFSCASNQVAQVLLTLPYSFAQLGMASGLLFQLFYGLLGSWTAYLISILYLEYRTRKERDKVDFRN
HVIQWFEVLDGLLGRHWRNVGLAFNCTFLLFGSVIQLIGCASNIYYINDHLDKRTWTYIFGACCAT
TVFIPSFHNYRIWSFLGLLMTTYTAWYIAVASLIHGQVEGVAHSGPTSIVLYFTGATNILYTFGGH
AVTVEIMHAMWRPQKFKAIYLLATVYVLTLTLPSASAAYWAFGDALLTHSNALALLPRTPWRDAAV
VLMLIHQFITFGFACTPLYFVWEKLVGLHGCPSLCKRAAARLPVVLPIWFLAIIFPFFGPINSAVG
SLLVSFTVYIIPSLAYMVTFRSPQSRQNAVERPPRFAGGWTGAYVINSFVVAWVLVVGFGFGGWAS
ITNFVHQVDTFGLFAKCYQCPPHPAAAALSPPGAIAPAPASMLPPFNSTAAGIFAAPVPSPAPAPA
PMHFVLGHHHHHRHHRHGL*

> OsAUX5
MASEKVETIVAGNYVEMEREGAATAGEGVGGAAAASGRRRGKLAVSSLFWHGGSVYDAWFSCASNQ
VAQVLLTLPYSFSQLGMASGVAFQVFYGLMGSWTAYLISVLYVEYRTRRERDKVDFRNHVIQWFEV
LDGLLGRHWRNAGLLFNCTFLLFGSVIQLIACASNIYYINDRLDKRTWTYIFGACCATTVFVPSFH
NYRVWSFLGLLMTSYTAWYLTVAAVVHGKVDGAAPRAGPSKTMVLYFTGATNILYTFGGHAVTVEI
MHAMWRPRRFKMIYLAATAYVLTLTLPSAAAMYWAFGDALLDHSNAFALLPRTPWRDAAVVLMLIH
QFITFGFACTPLYFVWEKAIGVHGGAGVLRRAAARLPVVLPIWFLAVIFPFFGPINSTVGSFLVSF
TVYIIPAMAHMATFAPAAARENAVEPPPRALGGWPGTFAANCFVVAWVLVVGFGFGGWASTVNFVR
QVDTFGLFTKCYQCPPRH*

> GRMZM2G149481
MSSEASSVVVADENGAAETVGVGRYVEMEKDQESSAAKSRLSGLLWHGGSAYDAWFSCASNQVAQV
LLTLPYSFSQLGMLSGILFQLLYGLMGSWTAYLISVLYVEYRARKEREKADFRNHVIQWFEVLDGL
LGRHWRNVGLAFNCTFLLFGSVIQLIACASNIYYINDKLDKRTWTYIFGACCATTVFIPSFHNYRI
WSFLGLVMTTYTAWYLAVASLIHGQVDGVKHSGPTKMVLYFTGATNILYTFGGHAVTVEIMHAMWR
PQKFKAIYLMATLYVLTLTLPSAASVYWAFGDQLLTRSNALALLPRTAFRDAAVVLMLAHQFITFG
FACTPLYFVWEKLVGLHDCRSLCRRAAARLPVVVPIWFLAIIFPFFGPINSAVGSLLVSFTVYIIP
ALAHMITFRSATARENAMEPPPRLLGRWTGAYMINAFVVAWVLVVGFGFGGWASMTNFVRQIDTFG

LFTKCYQCPPPPPLPFPGGGLGNITMPFNGDGLPPTPAPSPAHYFFRHHRHHSHHRGL*

> GRMZM2G127949
MAREQLEESIVADGNGKEEEVGVMGIGAADGADDQHGGGKLSMKSLLWHGGSVWDAWFSCASNQVA
QVLLTLPYSFSQLGMLSGVLLQIFYGFLGSWTAYLISVLYVEYRSRKEKEGVSFKNHVIQWFEVLD
GLLGPYWKAAGLAFNCTFLLFGSVIQLIACASNIYYINDRLDKRTWTYIFGACCATTVFIPSFHNY
RIWSFLGLGMTTYTAWYLAIAALLNGQAEGVAHSGPTKLVLYFTGATNILYTFGGHAVTVEIMHAM
WKPAKFKYIYLLATLYVFTLTLPSSAAMYWAFGDELLTHSNAFSLLPKTRWRDAAVILMLIHQFIT
FGFACTPLYFVWEKVIGMHDAKSIFKRALARLPIVVPIWFLAIIFPFFGPINSAVGALLVSFTVYI
IPALAHVLTYRTASARMNAAEKPPFFLPSWTGMFVLNMFIVVWVLVVGFGLGGWASMVNFVRQIDT
FGLFAKCYQCPKPPVPAAAQSPAPLPHH*

> GRMZM2G129413
MHTTPVSKHRQHAQAGKALDHRSEGLMAAGGGGGGIADEKAPAAEAFGGHLEAAEMTEAEEEHSGV
KSRLSGLLWHGGSAYDAWFSCASNQVAQVLLTLPYSFAQLGMLSGVLFQLFYGLLGSWTAYLISIL
YLEYRTRREREKAADFRNHVIQWFEVLDGLLGRHWRNAGLAFNCTFLLFGSVIQLIGCASNIYYVN
DRLDKRTWTYVFGACCATTVFIPSFHNYRVWSFLGLVMTTYTAWYMAVASLVHGQVEGVQHSGPTR
IVLYFTGATNILYTFGGHAVTVEIMHAMWRPQKFKAIYLLATLYVLTLTLPSAAASYWAFGDELLT
HSNALALLPRTPFRDAAVVLMLIHQFITFGFACTPLYFVWEKLIGLHDCRSLCKRAAARLPVVVPI
WFLAIIFPFFGPINSAVGSLLVSFTVYIIPALAHMVTFRSPQSRENAVERPPRFAGGWTGAYVINS
FVVAWVLVVGFGFGGWASITNFVQQVNTFGLFAKCYQCPPHLTAAPPAAFMPPPPPMAAAPSMPPA
ATAFNATGLFFPPLPAPAPAPSPMINFFLRHHHRGHHGRHGL*

> GRMZM2G045057
MASEKVETIVAGNYMEMEHEPGGGGDHDQQPSGGAASSTSSSSRGGGKKKALSSLFWHGGSVYDAW
FSCASNQVAQVLLTLPYSFSQLGMASGVVFQLFYGLMGSWTAYLISILYVEYRTRKEREKVDFRNH
VIQWFEVLDGLLGKHWRNVGLFFNCTFLLFGSVIQLIACASNIYYINDKYDKRTWTYIFGACCATT
VFIPSFHNYRIWSFLGLLMTTYTAWYLTIAAIAHGQVEGVTHSGPSKMVLYFTGATNILYTFGGHA
VTVEIMHAMWKPHKFKLIYLVATLYVLTLTLPSASAVYWAFGDMLLDHSNAFALLPRSGFRDAAVI
FMLIHQFITFGFACTPLYFVWEKLIGVHETGSVALRAAARLPIVAPIWFLAVVFPFFGPINSTVGS
LLVSFTVYIIPALAHMATFLPPAARENAVERPPRGLGGWAGMYAANFFVVAWVLVVGFGFGGWAST
VNFVRQVNTFGLFTRCYQCPPRH*

> GRMZM2G067022
MNRAGGHRRRVSILHRYKKKVSCASLSHLNSLRHDSGRGRSGRAVRLPAEILQTARRSYSGLCASS
AVPALLFFPAPPACLPARKRRGRAVFSPPPRFSISSSQQRSKFRRRVGQQQQQLAANVPLPRPLLL
PQLRDKLGARRPCAPLQQNELPALRVQLRLARMATGEQAEDAIVADVVGNGKGEEVRAMGDDAEQQ
RDGGKVSMKSLLWHGGSVWDAWFSCASNQVAQVLLTLPYSFSQLGMLSGVLLQVWYGLMGSWTAYL
ISVLYVEYRTRKEKEGVSFRNHVIQWFEVLDGLLGPYWKAAGLAFNCTFLLFGTVIQLIACASNIY
YINDRLDKRTWTYIFGACCATTVFIPSYHNYRVWSFLGLGMTTYTAWYLTIAAAVHGQVPGVTHSG
PSKLVPYFTGATNILYTFGGHAITVEIMHAMWKPRKFKYIYLLATLYVFTLTLPSAAAMYWAFGDQ
LLTHSNAFSLLPRTPWRDAAVVLMLVHQFITFGFACTPLYFVWEKAVGMHVTRSVFLRALVRLPIV
VPVWFLAIIFPFFGPINSAVGALLVSFTVYVIPALAHMLTYRSASARLNAAEKPPSFLPSWSGMFV
LNAFVVAWMLVVGFGLGGWASVTNFIKQIDTFGLFAKCYQCPTKPHPGSPLPAPPHH*

> Sobic.003G361300
MAREQLEESIVADGNGKEEEVGVMGIGAADGADDQHGRGGGGKLSMTSLLWHGGSVWDAWFSCASN
QVAQVLLTLPYSFSQLGMLSGILLQIFYGFLGSWTAYLISVLYVEYRSRKEKEGVSFKNHVIQWFE
VLDGLLGPYWKAAGLAFNCTFLLFGSVIQLIACASNIYYINDRLDKRTWTYIFGACCATTVFIPSF
HNYRIWSFLGLGMTTYTAWYLAIAALINGQVEGVEHTGPTKLVLYFTGATNILYTFGGHAVTVEIM
HAMWKPAKFKYIYLLATLYVFTLTLPSAAAMYWAFGDELLTHSNAFSLLPKTGWRDAAVILMLIHQ
FITFGFACTPLYFVWEKVIGMHDTKSIFKRALARLPIVVPIWFLAIIFPFFGPINSAVGALLVSFT
VYIIPALAHILTYRTASARMNAAEKPPFFLPSWTGMFVLNMFIVVWVLVVGFGLGGWASMVNFIRQ
IDTFGLFAKCYQCPKPPVPAAAQSPAPLPHH*

> Sobic.009G156600
MVPGEQAEDAIVAADVGNGKDAGEVRAAMGVVGGDDAEQLQQQHGGGGKFSMKSLLWHGGSVWDAW
FSCASNQVAQVLLTLPYSFSQLGMVSGVLLQVFYGLMGSWTAYLISVLYVEYRARKEKEGVSFKNH
VIQWFEVLDGLLGPYWKAAGLAFNCTFLLFGTVIQLIACASNIYYINDRLDKRTWTYIFGACCATT
VFIPSFHNYRVWSFLGLGMTTYTAWYLTIAAAVHGQVDGVTHSGPNKLVPYFTGATNILYTFGGHA
ITVEIMHAMWKPRRFKYIYLLATVYVFTLTLPSAAAMYWAFGDQLLTHSNAFSLLPRTPWRDAAVV
LMLIHQFITFGFACTPLFFVWEKAVGMHETPSVFLRALVRLPIVVPVWFLAIIFPFFGPINSAVGA
LLVSFTVYIIPALAHMLTYRSASARLNAAEKPPSFLPSWSGMFVLNAFVVAWVLVVGFGLGGWASV
TNFVKQIDTFGLFAKCYQCPTKTHAGSPLPAPPHH*

> Sobic.001G439000
MASEANGGVVANEKGAETVGVGRYVEMEQDQESNTVKSRLSGLLWHGGSAYDAWFSCASNQVAQVL
LTLPYSFSQLGMLSGILFQLFYGLMGSWTAYLISILYVEYRTRKEREKADFRNHVIQWFEVLDGLL
GRHWRNVGLAFNCTFLLFGSVIQLIACASNIYYINDKLDKRTWTYIFGACCATTVFIPSFHNYRIW
SFLGLVMTTYTAWYLAVASLIHGQVDGVKHSGPTKMVLYFTGATNILYTFGGHAVTVEIMHAMWRP
QKFKAIYLMATLYVLTLTLPSAASVYWAFGDQLLTHSNALALLPRTPFRDAAVVLMLVHQFITFGF
ACTPLYFVWEKLIGLHDCRSLCKRAAARLPVVVPIWFLAIIFPFFGPINSAVGSLLVSFTVYIIPA
LAHMITFRSATARENAVEPPPRLVGRWTGTYMINAFVVAWVLVVGFGFGGWASMTNFVRQIDTFGL
FTKCYQCPPPPLPPGAALLPFPGGLANITMPFNGTAELPPAPAPSPAHFFRHHHRHHSHRL*

> Sobic.001G267100
MAAGGGIADEKQQAPADSAEMMTMEPEEEEEYNSSNNTTTKGGGGGVKSRLSGLLWHGGSAYDAWF
SCASNQVAQVLLTLPYSFAQLGMVSGILFQLFYGILGSWTAYLISILYLEYRTRRERDKVDFRNHV
IQWFEVLDGLLGRHWRNAGLAFNCTFLLFGSVIQLIGCASNIYYVNDRLDKRTWTYVFGACCATTV
FIPSFHNYRVWSFLGLVMTTYTAWYIAVASLVHGQVQGVQHSGPTRIVLYFTGATNILYTFGGHAV
TVEIMHAMWRPQKFKAIYLLATLYVLTLTLPSAAAAYWAFGDELLTHSNALALLPRTRFRDAAVVL
MLIHQFITFGFACTPLYFVWEKLIGLHDCRSLCKRAAARLPVVVPIWFLAIIFPFFGPINSAVGSL
LVSFTVYIIPALAHMVTFRSPQSRENAVERPPRFAGGWTGAYVINSFVVAWVLVVGFGFGGWASIT
NFVQQVNTFGLFAKCYQCPPHLTAPPAAPAFTPPPPMATAPSAMTPATAFNATAGGLLFPPVPAPA
PAPSPMINFFLRHHHRRHHGGRHGL*

> Sobic.005G052500
MASEKVETIVAGNYMEMERDVVVGGGHGDDQPGGGDAASSGARAAGGKKKLGLSSRLFWHGGSVYD
AWFSCASNQVAQVLLTLPYSFSQLGMASGVVFQLFYGLMGSWTAYLISVLYVEYRTRKERDKVDFR
NHVIQWFEVLDGLLGKHWRNVGLFFNCTFLLFGSVIQLIACASNIYYINDKYDKRTWTYIFGACCA
TTVFIPSFHNYRIWSFLGLLMTTYTAWYLTIAAIAHGQVEGVTHSGPSKMVLYFTGATNILYTFGG
HAVTVEIMHAMWKPQKFKLIYLVATLYVLTLTLPSASAVYWAFGDMLLDHSNAFSLLPRSGFRDAA
VILMLIHQFITFGFACTPLYFVWEKLIGVHETGSVALRAAARLPVVVPIWFLAIIFPFFGPINSTV
GSLLVSFTVYIIPALAHMATFAPPAARENAVERPPRGVGGWAGMYAANCFVVAWVLVVGFGFGGWA
STVNFVRQVDTFGLFTRCYQCPPKH*

> Sevir.5G392400.1
MAREQLEESIVADGNGKEEEVGVMGIGTAGDGDEHHGGGGFNMKRFLWHGGSVWDAWFSCASNQVA
QVLLTLPYSFSQLGMLSGVLLQIFYGFLGSWTAYLISVLYVEYRSRKEKEGVSFKNHVIQWFEVLD
GLLGPYWKAAGLAFNCTFLLFGSVIQLIACASNIYYINDRLDKRTWTYIFGACCATTVFIPSFHNY
RIWSFLGLGMTTYTAWYLAIAALLNGQVEGVAHTGPTKLVLYFTGATNILYTFGGHAVTVEIMHAM
WKPAKFKYIYLLATLYVFTLTLPSAAAMYWAFGDELLNHSNAFSLLPKTAWRDAAVILMLIHQFIT
FGFACTPLYFVWEKVIGMHDTKSIFKRALARLPIVVPIWFLAIIFPFFGPINSAVGALLVSFTVYI
IPSLAHILTYRTASARMNAAEKPPFFLPSWTGMFVLNMFIVVWVLVVGFGLGGWASMVNFIRQIDT
FGLFAKCYQCPKPPVPAAAQSPAPLPHH*

> Sevir.3G228500
MVPGELAEDAIVADAGNSKDGEVRAMGIGDDAEQQQQRDGGFGLKSLLWHGGSVWDAWFSCASNQV
AQVLLTLPYSFSQLGMVSGVLLQVFYGLMGSWTAYLISVLYVEYRARKEKEGVSFKNHVIQWFEVL
DGLLGPYWKAAGLAFNCTFLLFGSVIQLIACASNIYYINDRLDKRTWTYIFGACCATSVFIPSFHN
YRVWSFLGLGMTTYTAWYLTIAAAIDGVTHSGPNKLVLYFTGATNILYTFGGHAVTVEIMHAMWKP
RKFKYIYLLATLYVFTLTLPCAAAMYWAFGDQLLTHSNAFSLLPRTGWRDAAVILMLIHQFITFGF
ACTPLYFVWEKVVGMHETRSVCLRALVRLPIVVPIWFLAIIFPFFGPINSAVGALLVSFTVYVIPA
LAHMLTYRSASARLNAAEKPPSFLPSWSGMFVVNAFVVAWVLVVGFGLGGWASVTNFVKQIDTFGL

FARCYQCPPKPHAGSPLPAPPHH*

> Sevir.9G295700
MAAGGGVGGVADKKAPEAFGLSRHVAEAEMEEEHGGSGESSVKSKLSGFLWHGGSAYDAWFSCASN
QVAQVLLTLPYSFAQLGMLSGILFQLFYGLLGSWTAYLISILYLEYRTRRERDKVDFRNHVIQWFE
VLDGLLGRHWRNAGLAFNCTFLLFGSVIQLIGCASNIYYVNDRLDKRTWTYIFGACCATTVFIPSF
HNYRVWSFLGLVMTTYTAWYIAVASLVNGQVEGVTHSGPTRIVLYFTGATNILYTFGGHAVTVEIM
HAMWRPQKFKSIYLLATVYVLTLTLPSAAAAYWAFGDALLTHSNALALLPRTAFRDAAVVLMLIHQ
FITFGFACTPLYFVWEKLIGLHDCRSLCKRAAARLPVVVPIWFLAIIFPFFGPINSAVGSLLVSFT
VYIIPALAHMVTFRSPQSRENAVERPPRFAGGWTGAYVINSFVVAWVLVVGFGFGGWASITNFVQQ
VNTFGLFAKCYQCPPHLTAPPAAPFAPPPMAPAPAMLPATVFNATGFFPPVPSPAPAPSPMMNFFL
RHHHHRHHGRHGL*

> Sevir.9G475300
MDSEANGSLANEKAPETVGVGRYVEMEQDGDSNTVKSRLSGLLWHGGSAYDAWFSCASNQVAQVLL
TLPYSFSQLGMLSGILFQLFYGLMGSWTAYLISILYVEYRTRKEREKKADFRNHVIQWFEVLDGLL
GRHWRNVGLAFNCTFLLFGSVIQLIACASNIYYINDKLDKRTWTYIFGACCATTVFIPSFHNYRIW
SFLGLVMTTYTAWYLAIASIIHGQVDGVKHSGPTMMVLYFTGATNILYTFGGHAVTVEIMHAMWRP
QKFKAIYLLATLYVLTLTLPSAASVYWAFGDQLLTHSNAFALLPRTAFRDAAVVLMLVHQFITFGF
ACTPLYFVWEKLIGLHDCRSLCKRAAARLPVVVPIWFLAIVFPFFGPINSAVGSLLVSFTVYIIPA
LAHMITFRSASARENAVEPPPRLVGRWTGTYMINAFVVAWVLVVGFGFGGWASMTNFVHQIDTFGL
FTKCYQCPPPPLPPAAPLPFPGGLGNITMPFAGGLPPAAAPSPAHFLHHHRHHSHGL*

> Sevir.8G047900
MASEKVETIVAGNYMEMERAGGVVGGDAGGGGEEAASAATSRRGGNKALSSLFWHGGSVYDAWFSC
ASNQVAQVLLTLPYSFSQLGMASGIVFQLFYGLMGSWTAYLISVLYVEYRTRKEREKVDFRNHVIQ
WFEVLDGLLGKHWRNMGLFFNCTFLLFGSVIQLIACASNIYYINDKYDKRTWTYIFGACCATTVFI
PSFHNYRIWSFLGLLMTTYTAWYLTIAAITHGQVEGVTHSGPTKMVLYFTGATNILYTFGGHAVTV
EIMHAMWKPQKFKLIYLAATLYVLTLTIPSASAVYWAFGDTLLDHSNAISLLPRSGFRDAAVVLML
VHQFITFGFACTPLYFVWEKLVGVHESRSLALRAAARLPIVLPIWFLAIIFPFFGPINSTVGSLLV
SFTVYIIPALAHMAVFAPAAARENAVERPPRGVGGWAGMYAANCFVVAWVLVVGFGFGGWASTVNF
VRQIDTFGLFTKCYQCPPKH*

Sequences for Clustal Omega alignments for BRX

> AtBRX
MFSCIACTKADGGEEVEHGARGGTTPNTKEAVKSLTIQIKDMALKFSGAYKQCKPCTGSSSSPLKK
GHRSFPDYDNASEGVPYPFMGGSAGSTPAWDFTNSSHHPAGRLESKFTSIYGNDRESISAQSCDVV
LDDDGPKEWMAQVEPGVHITFASLPTGGNDLKRIRFSREMFDKWQAQRWWGENYDKIVELYNVQRF
NRQALQTPARSDDQSQRDSTYSKMDSARESKDWTPRHNFRPPGSVPHHFYGGSSNYGPGSYHGGPP
MDAARTTTSSRDDPPSMSNASEMQAEWIEEDEPGVYITIRQLSDGTRELRRVRFSRERFGEVHAKT
WWEQNRERIQTQYL*

> AtBRXL1
MFTCINCTKMADRGEEDEEDEARGSTTPNTKEAVKSLTTQIKDMASKFSGSHKQSKPTPGSSSSNL
RKFPDFDTASESVPYPYPGGSTSSTPAWDLPRSSYHQSGRPDSRFTSMYGGERESISAQSCDVVLE
DDEPKEWMAQVEPGVHITFVSLPSGGNDLKRIRFSREVFDKWQAQRWWGENYDRIVELYNVQRFNR
QALQTPGRSEDQSQRDSTYTRIDSARESRDWTQRDNNFRPPGGSVPHHFYGPPMDAARITTSSRDE
PPSMSNASEMQGEWVEEDEPGVYITIRQLPDGTRELRRVRFSRERFGEVHAKTWWEQNRDRIQTQY
L*

> AtBRXL2
MLTCIACTKQLNTNNGGSKKQEEDEEEEDRVIETPRSKQIKSLTSQIKDMAVKASGAYKSCKPCSG
SSNQNKNRSYADSDVASNSGRFRYAYKRAGSGSSTPKILGKEMESRLKGFLSGEGTPESMSGRTES
TVFMEEEDELKEWVAQVEPGVLITFVSLPEGGNDMKRIRFSREMFDKWQAQKWWAENFDKVMELYN
VQQFNQQSVPLPTPPRSEDGSSRIQSTKNGPATPPLNKECSRGKGYASSGSLAHQPTTQTQSRHHD
SSGLATTPKLSSISGTKTETSSVDESARSSFSREEEEADHSGEELSVSNASDIETEWVEQDEAGVY
ITIRALPDGTRELRRVRFSREKFGETNARLWWEQNRARIQQQYL*

> AtBRXL3
MLTCIACTKQLNTNNGGSTREEDEEHGVIGTPRTKQAIKSLTSQLKDMAVKASGAYKNCKPCSGTT
NRNQNRNYADSDAASDSGRFHYSYQRAGTATSTPKIWGNEMESRLKGISSEEGTPTSMSGRTESIV
FMEDDEVKEWVAQVEPGVLITFVSLPQGGNDLKRIRFRSTRFPYYRDQLLLWCRQGWVFWPQNCRE
MFNKWQAQKWWVENFEKVMELYNVQFNQQSVPLQTPPVSEDGGSQIQSVKDSPVTPPLERERPHRN
IPGSSGFASTPKLSSISGTKTETSSIDGSARSSSVDRSEEVSVSNASDMESEWVEQDEPGIYITIR
ALPDGNRELRRVRFSRDKFGETHARLWWEQNRARIQQQYL*

> AtBRXL4
MLTCIARSKRAGDESSGQPDDPDSKNAKSLTSQLKDMALKASGAYRHCTPCTAAQGQGQGQGPIKN
NPSSSSVKSDFESDQRFKMLYGRSNSSITATAAVAATQQQQPRVWGKEMEARLKGISSGEATPKSA
SGRNRVDPIVFVEEKEPKEWVAQVEPGVLITFVSLPGGGNDLKRIRFSRDMFNKLQAQRWWADNYD
KVMELYNVQKLSRQAFPLPTPPRSEDENAKVEYHPEDTPATPPLNKERLPRTIHRPPGLAAYSSSD
SLDHNSMQSQQFYDSGLLNSTPKVSSISVAKTETSSIDASIRSSSSRDADRSEEMSVSNASDVDNE
WVEQDEPGVYITIKVLPGGKRELRRVRFSRERFGEMHARLWWEENRARIHEQYL*

> BdBRXL1
MLACIACSTKDGGEDGGTRAVATPNGRDAGKSLTSQLKDMVLKFSGSGKQYKASGSPSFRSNRFHR
SSRLAAYPGIIDESGFTSDGAGEAYSYMRTTTSAAPSSAWDRDKVNRGFRPPHVRSPSTSWIPSII
GEEEEEDDDDDADEEAVVLEEDRVPREWTAQVEPGVHITFVSIPGGAGNDLKRIRFSREMFNKCEA
QRWWGENYDRVVELYNVQTFRQQGLSTPSSSVDDAMQSFYSRGSSTRESPAPIPPPAAASSRERPP
ISRTASCKASRAACYPSSAAVPDPSDHVWAHHLSLLNSAAGASGAAAGPYDPSPRVTTSSRGDEAS
SVVSVSNASELEGAEQWVEQDEPGVHITIRELADGTRELRRVRFSRERFGEERAKVWWEQNRDRIH
AQYL*

> BdBRXL2
MLTCIACSRQPGGGGPRLHEPPEDEDAVDGGGVSDAATPSTRLAIKALTAQIKDMALKASGAYRHC
KPCAGSSAGASGRHHPYHHRGGNGFQDSETASGSDRFHYAYRRAAGGGALSSGDATPSMSARTDFP
TGDEEEEEDDEMSSGGGKEDDAKEWVAQVEPGVLITFVSLPLGGNDLKRIRFSREMFNKWQAQRWW
AENYDKVMELYNVQRFNHQSVPLPTTPKSEDESSKEDSPVTPPLDKERVPRSLNRATSGGGAMGYS
SSDSLEHHSNHYCNGLHQHQHHGHQCYDSVGLASTPKLSSISGAKTETSSMDASMRTSSSPEEVDR
SDELSVSISNASDQEREWVEEDHPGVYITIRALPGGIRELRRVRFSREKFSEMHARLWWEENRARI
HEQYL*

> BdBRXL3
MLTCIACSKQLDGGGPPLHEPPEDDDGVVVGGARGPATPSTREAIKALTAQIKDMALKASGAYRHC
KPCGGSPAAASRRHHPYSHRGAYADSEVGSGSERFHHSYRRASSSAASTPRPLSGGAVFSSDATPS
VSARTDFFAGDEEGMEGCTEVDEAKEWVAQVEPGVLITFLSLPRGGNDLKRIRFSREMFNKWQAQR
WWAENYDKVMELYNIQRFKQQTVPVPGTPRSEDESSKEDSPETPPLNNERQPRIFQRSLKSSRALG
SSSSDSLEHQSKHLGNIQHGHHEHQCYDSVGLASTPKLSSISGAKTDTSSIDASMRTSSSPEEVDR
SGELSVSVSNASDQEREWVEEDEPGVYLTIRALTGGIKELRRVRFRCKMFYNSRPTADLVSAKKLL
SAAEKDLVRRMQGYGGKRTGQGFTSSISEGRHIKLHSIAFFTAPPPPPPPPQRPMYIAIHQEYSLV
SQPWS*

> BdBRXL4
MLACIACTSKEGGDQDGSRGGAATPHSKDAVKSLTSQLKDMVLKFSGSSNKQYKPTTAGSPSFRAG
RSYRRPYPGSGFIDDATFTPTTNRPTSARAAAANSSSSATWDMTGRSNRGWPGIDEDQDRGAAREW
MAQVEPGVQITFATLPGGGNDLKRIRFSREMFNKWEAQRWWGENYDRIVELYNVQTFSGRQQGGST
PTSSVDDSHLRDSSYSRGGSARDSPVMMPPPPPSASTRDSMPRSASCKAPSYHAPQPPSSARAAYY
PSAAVPDPSDHVWAHHFNMLNSAAAGPSSSSSVMMGGSGVGAPSSYDPSRATSSSRDDASVSVSNA
SDLEATEWIEQDEPGVCLTIRELGDGTRELRRIRFSREKFGEDRAKVWWEHNKDRIQSQYL*

> BdBRXL5
MLACIACVKQEEGGGGGHGARADNGDTPTTCRPVKSLTSQLKDMVLKLSGTHRQPGGGPRRRGGSP
PPTRTTSLYRSGYYRPGVVQDDMAVPPATYLGHGHGGGASSTASSTPAWERPPGNGDAAARGEWVA
QVEPGVQITFVSLSGTGGGAGGGNDLKRIRFSREMYDKWQAQRWWAENNERIMELYNVRRFSPRHD
HVLPPSSDAGDPERESFYSQMGSTRASSPAATPSPAPETSATWAAAFARAAPPPPPSAARQHSFRG
PLSPPPPSSSNPSERAWQQQKQSQQNDGGVEPARTTTSSCRDDDASVSNASELEVTEWVIQDQPGV

YITVRELPDGARELRRVRFSREKFAELNAKLWWEENKERIHAQYL*

Sequences for Clustal Omega alignments for OPS

> AtOPS
MNPATDPVSAAAAALAPPPQPPQPHRLSTSCNRHPEERFTGFCPSCLCERLSVLDQTNNGGSSSSS
KKPPTISAAALKALFKPSGNNGVGGVNTNGNGRVKPGFFPELRRTKSFSASKNNEGFSGVFEPQRR
SCDVRLRSSLWNLFSQDEQRNLPSNVTGGEIDVEPRKSSVAEPVLEVNDEGEAESDDEELEEEEEE
DYVEAGDFEILNDSGELMREKSDEIVEVREEIEEAVKPTKGLSEEELKPIKDYIDLDSQTKKPSVR
RSFWSAASVFSKKLQKWRQNQKMKKRRNGGDHRPGSARLPVEKPIGRQLRDTQSEIADYGYGRRSC
DTDPRFSLDAGRFSLDAGRFSVDIGRISLDDPRYSFDEPRASWDGSLIGRTMFPPAARAPPPPSML
SVVEDAPPPVHRHVTRADMQFPVEEPAPPPPVVNQTNGVSDPVIIPGGSIQTRDYYTDSSSRRRKS
LDRSSSSMRKTAAAVVADMDEPKLSVSSAISIDAYSGSLRDNNNYAVETADNGSFREPAMMIGDRK
VNSNDNNKKSRRWGKWSILGLIYRKSVNKYEEEEEEEEDRYRRLNGGMVERSLSESWPELRNGGGG
GGGPRMVRSNSNVSWRSSGGGSARKVNGLDRRNKSSRYSPKNGENGMLKFYLPHMKASRRMSGTGG
AGGGGGGGWANSHGHSIARSVMRLY*

> AtOPL1
MNLSADQAPVTAVDELAPPSQPHRLSTSCDLHPEERFSGFCPSCLCDRLSVLDHNAAPPPSSSSRK
PPSISAVSLKALFKPSSSGTNNSNGNGRVRPGFFPELRRTKSFSAKNNEGFSGGFEPQRRSCDVRL
RDDERNLPINEAASVDKIEEEARESSVSEIVLEVTEEAEIEEDEENGEKDPGEIVEEKSSEIGEEE
EELKPMKDYMDLYSQTKKPSVKDFAGSFFSAASVFSKKLQKWKQKQKVKKPRNGVGGGRPQSEIGV
GRRSSDTDPRFSLDAGRFSVDIGRISMDDSRYSLDEPRASWDGHLIGRTTAARVPLPPSMLSVVEN
APLNRSDMQIPSSPSIKPISGDSDPIIIIPGGSNQTRDYYTGPPSSRRRKSLDRSNSIRKIVTELE
DVKSVSNSTTTIDSNSMETAENKGNQNGDKKSRRWGKWSILGFIYRKGKDDEEEDRYSRSNSAGMV
ERSLSESWPEMRNGEGGGPKMRRSNSNVSWRSSGGGSARNKSSRYSSKDGENGMLRFYLTPMRRSW
KTSGGSGGGGGGGGGGGWEKTAAKANSHGHSIARRVMRLY*

> AtOPL2
MVMNNPANNNPVAASSASAVALAPPPHPPQPHRPSTSCDRHPDERFTGFCPSCLFDRLSVLDITGK
NNNAVASSSKKPPSSSAALKAIFKPSSSSGSFFPELRRTKSFSASKAEAFSLGAFEPQRRSCDVRV
RNTLWSLFHEDAEHNSQTKEGLSVNCSEIDLERINSIVKSPVFEEETEIESEQDNEKDIKFETFKE
PRSVIDEIVEEEEEEETKKVEDFTMEFNPQTTAKKTNRDFKEIAGSFWSAASVFSKKLQKWRQKQK
LKKHRTGNLGAGSSALPVEKAIGRQLRDTQSEIAEYGYGRRSCDTDPRFSIDAGRFSLDAGRVSVD
DPRYSFEEPRASWDGYLIGRAAAPMRMPSMLSVVEDSPVRNHVHRSDTHIPVEKSPQVSEAVIDEI
VPGGSAQTREYYLDSSSSRRRKSLDRSSSTRKLSASVMAEIDELKLTQDREAKDLVSHSNSLRDDC
CSVENNYEMGVRENVGTIECNKKRTKKSRWSWNIFGLLHRKNGNKYEEEERRSGVDRTFSGSWNVE
PRNGFDPKMIRSNSSVSWRSSGTTGGGLQRNSVDGYISGKKKVSKAENGMLKFYLTPGKGRRRGSG
NSTAPTSRPVPASQPFGSRNVMNFY*

> AtOPL3
MANVKQTNRRRSSSSCHRHPSAKPTSGFCASCLRERLVTIEAQSSSLAAVQTPELRRIRSYSVRNA
SVSVSDQPRRRSCDVRSSASSLLDLFVDDDEERVDSSIRKPLVPDLKEEEEEEEEEEDYYDGEDIK
GFDEGKPRKIVEENKTMKEFIDLDWRNQIKKNNGKDLKEIASVLSRRLKNFTLNKRNDEKSDSRFA
GIVNGRHSSDVDPRLSFDGGRISFEKPRSSWDGCLIEKSYHKLTTLSTVTEDAKAKCGVEEEEVEE
KEKSPGGTVQTKNYYSDSRRRRSFDRSVSIKRQGLLEVDELRGISNAKVSPETVGLFHGAKLLVTE
KELRDSNWYSIKNVKPESKELVSKGKICIAAGGEGKKQDSVELKKPRKKWPKGWNIWGLIQRKNEA
KNEIKTEQILKLEGNAVEGSLAESLLKLRRVGKGETNVGVSEKLLKSYSVSARKSCDGVRSGANIV
SGFEGGRSSCDGLFHGSINSVEAGRNSCDGLVNGIEGKQNHHLLQRNANVGTCSQENLEKSMFRFY
LSPVKSHKTSKSGKSRLKN*

> AtOPL4
MTHQTHQRRRRRHSAVCHRHPSSKPTTGFCATCLRERLSTIEALSSSVSASTELRRVRSYSVRDAS
ASVLDQPRRRSCDVRSNHDDDDDDELLKSSIRFPIVPDLIEDEEEEDDEGKKLVEEEIEDGEQKTM
KELIDLESRNQQLKNNGKDSVFSRTLRKFSLKHHRKIPDSGNSLGRRSCDVDPRLSLDAGRVSFDE
PRASWDGCLIGKTYPKLIPLSSVTEDVKASPEKITGEKVEEDEKNNPGGTAQTRDYYLDSRRRRSF
DRSSRHGLLEVDELKAISNAKVSPETVGLFHGAKLLVTERELRDSNWYSIKNYKPESLELGSKGVG
CVAAGEVKKQDGFGLKKSGKNWSKGWNFWGLIQRKTDVAKNEMKTEQSLKLGGNTMEGSLAESLLK

LRRVAKGETNGDVSEKLIRSYSVSARKSCDGMLRGASIVNGFEGGRSSCDGLFHGSITGVETG
RRSLCEDGMFHGVEGKRNHLLQSDDKLGTYSPDNLRNGMVRFYLTPLNSHMTSKSGKSRLMN*

> BdOPSL1
MTLQMEPPAPPPRRSVSTSCDLHPDENFTGFCTACLRERLAGLEATAAAAAAPGRKSTSAIRSLFS
RPFAAAPSGSGSGAAPPDLRRCKSFSCGRGGAGAAVDEPQRRSCDVRGRSTTTTLWSLFHQDDRER
VRDGTAFGAFPASSSAAAAALPAEFQQQPCVPEVFLEEEIVAAECPDEITPVVEEPISAEMEAEAN
SAAREVRAMKDHIDLESRKPPPKDLKEIAGSFWLAASVFSKKWQKWRRKQKLKKEEAATGSKAAAA
AMPPSEKPSRPSFLRRSRLRGEEFAGGRRSCDTDPRFSLDAARMSVDDVGLSWDGPRASWDGYLFG
AGSGIGLGRAPLPMSRLPPILSALEDSPAGIVERSDGQIPVEDDSQPEPDGDVPGGSAQTRDYYMD
SSSSRRRRSLDRSSSSARRRSFEVPDPKPAPAAAAAITNTKDKESPLNGSSEFYHFHHAQDLLDHR
FSSNSLIEDFPASLDAAFPGPAAKKPRRLRKAWSLWGFIHRRATGRARNGGASDRAFSEPWPELRA
RGYNARMQRCSSNASARSSFSSNNCGLGSSRRSFVDGKCGGNVKRQREECVLERNRSARYSPPVHA
ADNGMLRFYLTPMGSASGRRTPGPGLPANGGRHLGSHSFTRNMLRLY*

> BdOPSL2
MSLAMDPPAPPARRSSATSCDLHPDEAFTGFCAACLRERLAGLEASAAAASAPGRKSTSAIRPFAA
AGGSGSSAPGAAEPPDLRRCKSFSCGRGGDVLSAAAAAAAARAGDEPQRRSCDVRGRSTLWALFHQ
DDRDRVRDGTAFGSFPVSSSVAAALTADVALPLPQPPPLQRPCVMEDFSEEDIPVVMECDEIMPVV
ELEPVHGVDTSGEIKEVEANVARDVKAIKDHIDLESSEPKTKPTPKDLKEIAGSFWEAASVFSKKW
QKWRRKQKLKKEAAVSKAAAAAMPPPEKPSKPSFLRRRRLRGEAGSEHALGRRSCDTDPRFSLDAG
RMSIDDAGFSWDEPRASWDGYLFGAGGGIGLGRAPPPLSRLPPILSVMEDAPAAVVERSDGQIPVE
DDADLEPPGGTFQTRDYYLDSSSRRRRSLERSSSVRRPSFEVPEPKPIPAAAAAIGNESPIAIGGS
EFYHFHHAEDLLDRGFSSNSLVEDISASLEAALSGPSSSKKPPRWRKAWSLWGFIHRRAAGRRTGG
GGGGPSDIADRSFSEPWPDLRVRGGNPKMQRCNSNLSARSSFSSNSGGLGSSRRSYVDMNGNVKLR
RGEEHAQAHALERNRSARHSPPGRVDNGMLRFYLTPMRSGGGGGGVVRRVGGGGLPGKAGRQLTSQ
SFARSVLRLY*

> BdOPSL3
MDQPPPVPSICGLHPGIAVTGFCSACLRERLAGLHPADPAELRRCKSFSYARSAAAYFEPQRRSCD
ARGAAIFHHQDLPPGHGEDELEDVPPTSTVRPMKDHISQDSSKKTTFGGGLGKKWQEWRRKSKLKK
QGPAAPAVATAAASRAAIDAHRSFRDTHSEVAIGRRSVDVDSSRLWMDAGRISVDEPPRASWQRLP
PTVEDAPIPRSDGQIPVEEEDDDAEPGGCAQTRDYYLDSSSSSRRRRSVDRSSFSSRKSFSDTNDL
PRVIAAANANARVSPAIGAEFYHYHHHAQGQSVLDHNQHWELHGPNSYSLRDDDMSGSFNSAAFQE
GVPVPLPAKKSNKWIKNIWGLIHKKSSTKESQAASIANRSFSETWPELRARGYNGQMLRCNSSVSA
RSSFSNSGAAVGAVNGRRRSNAEMHVNGLGRARKDEVLLERNFSARYSTCPVDNGVFLNPVGGSRR
HQNGMSGKGRPARSSNSLPRSALGMY*

> Bradi1g75160 (BdOPSL4)
MEVGLPGVAGRCGRHPAQLVTGVCSSCLVERLSSVRSPSHPEIVEVAATAAAQTEIVEVGTTGDSG
EGGGSVSGAGEGKLRKTLMLLFQMDDSGGDAATASPPPEAAKDPGVFEVEPGGGGGGGARGNKWKR
GSWLRSILPKRGMMRRGKKEEEEEPSRPRGEVSVDPDGGGDAQVERKASFRRSFEWMVCREPPSRG
GSLEPPRHSWDGSMVGRAFACSFACLEEPPDGVTRVRQSNAEEAAGETRAAVAESRNGGHSADMSS
GEVRRFGERSCGDTGPAMTVSGVGRRRSNRWSRVWDRSITSPLKEFVRKGEHVLDRSFSESRKETR
RCNNGETADIDGEIQPGRNGLVSGRASQVASRSSQASANGDAQNFRTDWLKNKDCKIGRSRSVHYT
SPGNMDNGMLRFYLTPMRSNRTTNRGRRRSSRLFARGLFGFV*

Sequences for Clustal Omega alignments for BRI1

> BdBRI1
MDSLRVAIAAALFVAAVAVAVAASLSGWKAADGACRFPGAACRAGRLTSLSLAGVPLNADFRAVAA
TLLQLSGVEALSLRGANVSGALAAAGGARCGGKLEALDLSGNAALRGSVADVAALADSCAGLKKLN
LSGGAVGAAKAGGGGGAGFAALDVLDLSNNKITGDAELRWMVGAGVGSVRWLDLAWNRISGELPDF
TNCSGLQYLDLSGNLIDGDVAREALSGCRSLRALNLSSNHLAGAFPPNIAGLASLTALNLSNNNFS
GEVPADAFTGLQQLKSLSLSFNHFTGSIPDSLAALPELEVLDLSSNTFTGTIPSSICQDPNSSLRV
LYLQNNFLDGGIPEAISNCSNLVSLDLSLNYINGSIPESLGELAHLQDLIMWQNSLEGEIPASLSR
IRGLEHLILDYNGLSGSIPPDLAKCTQLNWISLASNRLSGPIPSWLGKLSNLAILKLSNNSFSGRV

PPELGDCKSLVWLDLNNNQLNGSIPPELAEQSGKMSVGLIIGRPYVYLRNDELSSQCRGKGSL
LEFSSIRSEDLSRMPSKKLCNFTRVYMGSTEYTFNKNGSMIFLDLSFNQLDSEIPKELGNMFYLMI
MNLGHNLLSGPIPLELAGAKKLAVLDLSYNRLEGPIPSSFSTLSLSEINLSSNQLNGTIPELGSLA
TFPKSQYENNSGLCGFPLPPCQAHAGQSASDGHQSHRRQASLAGSVAMGLLFSLFCIFGLVIIAIE
SKKRRQKNEEASTSHDIYIDSRSHSGTMNSNWRLSGTNALSINLAAFEKPLQKLTLGDLVEATNGF
HNDSLIGSGGFGDVYKAQLKDGRIVAIKKLIHVSGQGDREFTAEMETIGKIKHRNLVPLLGYCKIG
EERLLMYDYMQFGSLEDVLHDRKKIGVKLNWPARRKIAIGAARGLAFLHHNCIPHIIHRDMKSSNV
LVDENLEARVSDFGMARMMSVVDTHLSVSTLAGTPGYVPPEYYQSFRCTTKGDVYSYGVVLLELLT
GKPPTDSADFGEDNNLVGWVKLHAKLKIIDVFDPELLKDDPSLELELLEHLKIACACLEDRPTRRP
TMLKVMTMFKEIQAGSTVDSKTSSVATGLSDDVGFGVVDMTLKEAKEEKD*

> Bradi1g72572
MTRRRRLSCGRWRTTVSSALCLAVLLLLLSPVAADGDDDDDEQLLERFKAAVPVRNRGQLEGWTRG
DGACRFPGAVCVSVSGVRTRLASLSLAGVPLDVDFRAVAGTLLRLGGVEGISLRGANVSGSLAPGG
GRCGQNLAELDLSGNPALRGSVADAGALAASCRGLRELNLSGDGDLSWMGGVRRLNLAWNRISGSL
FPAFPNCSRMESLDLFGNLISGELLPGVLSGCTALTSLNLSSNHLSGPFPPEISGLALLSYLDLSN
NNFSGELPRDAFARLPRLSLLSLSFNSFSGSLPESMDALAELRTLDLSSNLLTGAIPASLCPSTGS
KLQVLYLQNNYLTGGIPPAISNCASLESLDLSLNYINGSIPISIGSLSRLRNLIMWENELEGEIPA
SLAGARGLQNLILDYNGLTGSIPPELVNCKDLNWISLGSNQLSGSVPAWLGRLDKLAILKLSNNSF
SGPIPPELGDCKRLVWLDLNDNQLNGSIPPELAKQSGKMPVGITTGRPYVYLRNDELSSECRGKGI
LLEISGIRRGDLTRMASKKLCNFTMVYMGSTDYTSSDNGSIIFLDLSFNKLDSEIPKELGNMYYLM
IMNLAHNLLSGAIPAELGGARKLAVLDLSHNQLEGPIPGPFTSLSLSEVNLSYNRLNGSIPELGSL
ATFPESQYENNSGLCGFPLAPCGSALVPFLQRQDKSRSGNNYYVLKILLPAVAVGFGAIAICLSYL
FVRKKGEVTASVDLADPVNHQLVSHLELVRATDNFSEDNILGSGSFGKVFKGQLSNGSVVAIKVLD
MVSKRAIRSFDAECRVLRMARHRNLIRIINTCSNMDFRALMLQYMPNGNLETLLHCSQAGERQFGF
QERLEVMLGVSMAMEYLHHDYHQVVLHCDLKPSNVLFDENMIAHVADFGIARLLLQGDDSSMISAR
LHGTIGYMSPEYGSDGKASRKSDVFSYGIMLLEVFTGRRPTDAMFIGELSLRKWVHRLFPAELVNV
VDGRLLQGSSSSCCLDGGFLVPILEIGLLCSSDSPNERMRMSDVVVRLKKIKTEYTTWTTSTFGKA
GSCHMSM*

> Bradi4g27440
MAAAPTFTAAFFFLLVLLQVPAPAIASAEEAAALLAFRRVSVTADPRGALASWAPASTGANSTAPC
SWAGVSCAPSTDGRVVAVNLSGMDLAGELRLGALLALPALQRLDLRGNAFYGNLSHSASSSCALVE
VDISSNAFNATVPPAFLASCGSLQTLNLSRNSLTGGGFPFAPSLASLDLSRNRLADAGLLNYSFAG
CHGLRYLNLSANLFTGRLPEQLASCSAVTTLDVSWNLMSGALPAVLMATAPANLTYLSIAGNNFTG
DVSGYDFGRCANLTVLDWSYNGLSSTRLPPGLANCSRLEALDMSGNKLLSGSIPTFFTGFTSLRRL
ALAGNEFAGPIPGELSQLCGRIVELDLSNNGLVGALPASFAKCNSLEVLDLGGNQLSGDFVATVIS
TISSLRMLRLSFNNITGANPLPVLAAGCPLLEVIDLGSNEFNGEIMPDLCSSLPSLRKLFLPNNYL
NGTVPTLLGNCANLESIDLSFNFLVGQIPPEIITLPKLVDLVVWANGLSGKIPDILCSNGTTLETL
VISYNNFTGIIPPSITRCVNLIWVSLSGNRLTGSVPPGFAKLQKLAILQLNKNLLSGRVPAELGSC
NNLIWLDLNSNSFTGTIPSELAGQAELVPGGIASGKQFAFLRNEAGNICPGAGVLFEFFGIRPERL
AEFPAVHLCPSTRIYTGTMDYTFSKNGSMIFLDLSYNGLTGAIPGSLGNLMYLQVLNLGHNELSGT
IPEAFSSLKSIGALDLSNNQLSGGIPSGLGGLNFLADFDVSNNNLTGSIPSSGQLTTFPASRYDNN
TALCGIPLPPCGHDPGRGNGGRASPDGRRKVIGASILVGVALSVLILLLLLVTLCKLRKNQKTEEM
RTEYIESLPTSGTTSWKLSGVPEPLSINVATFEKPLRKLTFAHLLEATNGFSAETLVGSGGFGEVY
KAKLKDGSVVAIKKLIHYTGQGDREFTAEMETIGKIKHRNLVPLLGYCKIGDERLLVYEYMKHGSL
DVVLHDNDKAIVKLDWAARKKIAIGSARGLAFLHHSCIPHIIHRDMKSSNVLLDNNLDARVSDFGM
ARLMNALDTHLSVSTLAGTPGYVPPEYYQSFRCTTKGDVYSYGVVLLELLSGKKPIDPNEFGDNNL
VGWVKQMVKENRSSDIFDPTLTDTKSGEAELYQYLKIASECLDDRPIRRPTMIQVMAMFKELQLDS
DSDFLDGFSINSSTIDESAEKSS*

> Bradi3g21400
MAMDKLFLLLPIVLLLLSSVSSETDDAGALLRFKASVHKDPRNLLSSWQQAASGSGGNGNGTYYCS
WYGVSCDGDGRVSRLDLSGSGLAGRASFAALSFLEALRQLNLSGNTALTANATGDLPKLPRALETL
DLSDGGLAGALPDGDMQHRFPNLTDLRLARNNITGELSPSFASGSTTLVTLDLSGNRLTGAIPPSL
LLSGACKTLNLSYNALSGAMPEPMVSSGALEVLDVTSNRLTGAIPRSIGNLTSLRVLRASSNNISG
SIPESMSSCGALRVLELANNNVSGAIPAAVLGNLTSLESLLLSNNFISGSLPATIASCKSLRFVDL
SSNKISGSLPDELCAPGAAAALEELRMPDNLLTGAIPPGLANCTRLKVIDFSINYLSGPIPKELGR
LGDLEQLVAWFNGLDGRIPAELGQCRSLRTLILNNNFIGGDIPVELFNCTGLEWVSLTSNRISGGI

RPEFGRLSRLAVLQLANNTLSGTVPKELGNCSSLMWLDLNSNRLTGEIPLRLGRQLGSTPLSG
ILAGNTLAFVRNAGNACKGVGGLVEFAGIRPERLLEVPTLKSCDFTRLYSGAAVSGWTRYQMTLEY
LDLSYNSLNGTIPVELGDMVVLQVLDLARNKLTGEIPASLGRLHDLGVFDVSHNRLQGGIPESFSN
LSFLVQIDVSDNDLTGEIPQRGQLSTLPASQYADNPGLCGMPLLPCSDLPPRATMSGLGPAPDSRS
SNKKRSLRANVLILAALVTAGLACAAAIWAVAVRARRRDVREARMLSSLQDGTRTATTWKLGKAEK
EALSINVATFQRQLRKLTFTQLIEATNGFSAASLIGSGGFGEVFKATLKDGSCVAIKKLIPLSHQG
DREFMAEMETLGKIKHKNLVPLLGYCKIGEERLLVYEYMTHGSLEDTLHLRRHDGDGGSGAPSSLS
WEQRKKVARGAAKGLCFLHHNCIPHIIHRDMKSSNVLLDAAMEAHVADFGMARLISALDTHLSVST
LAGTPGYVPPEYYQSFRCTAKGDVYSLGVVLLELLTGRRPTDKEDFGDTNLVGWVKMKVREGTGKE
VVDPELLKAAAAVNETEKEMMMFMEIALQCVDDFPSKRPNMLQVVAVLRELDAPPQERLPAVA*

> AtBRI1
MKTFSSFFLSVTTLFFFSFFSLSFQASPSQSLYREIHQLISFKDVLPDKNLLPDWSSNKNPCTFDG
VTCRDDKVTSIDLSSKPLNVGFSAVSSSLLSLTGLESLFLSNSHINGSVSGFKCSASLTSLDLSRN
SLSGPVTTLTSLGSCSGLKFLNVSSNTLDFPGKVSGGLKLNSLEVLDLSANSISGANVVGWVLSDG
CGELKHLAISGNKISGDVDVSRCVNLEFLDVSSNNFSTGIPFLGDCSALQHLDISGNKLSGDFSRA
ISTCTELKLLNISSNQFVGPIPPLPLKSLQYLSLAENKFTGEIPDFLSGACDTLTGLDLSGNHFYG
AVPPFFGSCSLLESLALSSNNFSGELPMDTLLKMRGLKVLDLSFNEFSGELPESLTNLSASLLTLD
LSSNNFSGPILPNLCQNPKNTLQELYLQNNGFTGKIPPTLSNCSELVSLHLSFNYLSGTIPSSLGS
LSKLRDLKLWLNMLEGEIPQELMYVKTLETLILDFNDLTGEIPSGLSNCTNLNWISLSNNRLTGEI
PKWIGRLENLAILKLSNNSFSGNIPAELGDCRSLIWLDLNTNLFNGTIPAAMFKQSGKIAANFIAG
KRYVYIKNDGMKKECHGAGNLLEFQGIRSEQLNRLSTRNPCNITSRVYGGHTSPTFDNNGSMMFLD
MSYNMLSGYIPKEIGSMPYLFILNLGHNDISGSIPDEVGDLRGLNILDLSSNKLDGRIPQAMSALT
MLTEIDLSNNNLSGPIPEMGQFETFPPAKFLNNPGLCGYPLPRCDPSNADGYAHHQRSHGRRPASL
AGSVAMGLLFSFVCIFGLILVGREMRKRRRKKEAELEMYAEGHGNSGDRTANNTNWKLTGVKEALS
INLAAFEKPLRKLTFADLLQATNGFHNDSLIGSGGFGDVYKAILKDGSAVAIKKLIHVSGQGDREF
MAEMETIGKIKHRNLVPLLGYCKVGDERLLVYEFMKYGSLEDVLHDPKKAGVKLNWSTRRKIAIGS
ARGLAFLHHNCSPHIIHRDMKSSNVLLDENLEARVSDFGMARLMSAMDTHLSVSTLAGTPGYVPPE
YYQSFRCSTKGDVYSYGVVLLELLTGKRPTDSPDFGDNNLVGWVKQHAKLRISDVFDPELMKEDPA
LEIELLQHLKVAVACLDDRAWRRPTMVQVMAMFKEIQAGSGIDSQSTIRSIEDGGFSTIEMVDMSI
KEVPEGKL*

> AtBRL1
MKQRWLLVLILCFFTTSLVMGIHGKHLINDDFNETALLLAFKQNSVKSDPNNVLGNWKYESGRGSC
SWRGVSCSDDGRIVGLDLRNSGLTGTLNLVNLTALPNLQNLYLQGNYFSSGGDSSGSDCYLQVLDL
SSNSISDYSMVDYVFSKCSNLVSVNISNNKLVGKLGFAPSSLQSLTTVDLSYNILSDKIPESFISD
FPASLKYLDLTHNNLSGDFSDLSFGICGNLTFFSLSQNNLSGDKFPITLPNCKFLETLNISRNNLA
GKIPNGEYWGSFQNLKQLSLAHNRLSGEIPPELSLLCKTLVILDLSGNTFSGELPSQFTACVWLQN
LNLGNNYLSGDFLNTVVSKITGITYLYVAYNNISGSVPISLTNCSNLRVLDLSSNGFTGNVPSGFC
SLQSSPVLEKILIANNYLSGTVPMELGKCKSLKTIDLSFNELTGPIPKEIWMLPNLSDLVMWANNL
TGTIPEGVCVKGGNLETLILNNNLLTGSIPESISRCTNMIWISLSSNRLTGKIPSGIGNLSKLAIL
QLGNNSLSGNVPRQLGNCKSLIWLDLNSNNLTGDLPGELASQAGLVMPGSVSGKQFAFVRNEGGTD
CRGAGGLVEFEGIRAERLERLPMVHSCPATRIYSGMTMYTFSANGSMIYFDISYNAVSGFIPPGYG
NMGYLQVLNLGHNRITGTIPDSFGGLKAIGVLDLSHNNLQGYLPGSLGSLSFLSDLDVSNNNLTGP
IPFGGQLTTFPVSRYANNSGLCGVPLRPCGSAPRRPITSRIHAKKQTVATAVIAGIAFSFMCFVML
VMALYRVRKVQKKEQKREKYIESLPTSGSCSWKLSSVPEPLSINVATFEKPLRKLTFAHLLEATNG
FSAETMVGSGGFGEVYKAQLRDGSVVAIKKLIRITGQGDREFMAEMETIGKIKHRNLVPLLGYCKV
GEERLLVYEYMKWGSLETVLHEKSSKKGGIYLNWAARKKIAIGAARGLAFLHHSCIPHIIHRDMKS
SNVLLDEDFEARVSDFGMARLVSALDTHLSVSTLAGTPGYVPPEYYQSFRCTAKGDVYSYGVILLE
LLSGKKPIDPGEFGEDNNLVGWAKQLYREKRGAEILDPELVTDKSGDVELFHYLKIASQCLDDRPF
KRPTMIQLMAMFKEMKADTEEDESLDEFSLKETPLVEESRDKEP*

> AtBRL2
MTTSPIRVRIRTRIQISFIFLLTHLSQSSSSDQSSLKTDSLSLLSFKTMIQDDPNNILSNWSPRKS
PCQFSGVTCLGGRVTEINLSGSGLSGIVSFNAFTSLDSLSVLKLSENFFVLNSTSLLLLPLTLTHL
ELSSSGLIGTLPENFFSKYSNLISITLSYNNFTGKLPNDLFLSSKKLQTLDLSYNNITGPISGLTI
PLSSCVSMTYLDFSGNSISGYISDSLINCTNLKSLNLSYNNFDGQIPKSFGELKLLQSLDLSHNRL
TGWIPPEIGDTCRSLQNLRLSYNNFTGVIPESLSSCSWLQSLDLSNNNISGPFPNTILRSFGSLQI
LLLSNNLISGDFPTSISACKSLRIADFSSNRFSGVIPPDLCPGAASLEELRLPDNLVTGEIPPAIS

QCSELRTIDLSLNYLNGTIPPEIGNLQKLEQFIAWYNNIAGEIPPEIGKLQNLKDLILNNNQL
TGEIPPEFFNCSNIEWVSFTSNRLTGEVPKDFGILSRLAVLQLGNNNFTGEIPPELGKCTTLVWLD
LNTNHLTGEIPPRLGRQPGSKALSGLLSGNTMAFVRNVGNSCKGVGGLVEFSGIRPERLLQIPSLK
SCDFTRMYSGPILSLFTRYQTIEYLDLSYNQLRGKIPDEIGEMIALQVLELSHNQLSGEIPFTIGQ
LKNLGVFDASDNRLQGQIPESFSNLSFLVQIDLSNNELTGPIPQRGQLSTLPATQYANNPGLCGVP
LPECKNGNNQLPAGTEEGKRAKHGTRAASWANSIVLGVLISAASVCILIVWAIAVRARRRDADDAK
MLHSLQAVNSATTWKIEKEKEPLSINVATFQRQLRKLKFSQLIEATNGFSAASMIGHGGFGEVFKA
TLKDGSSVAIKKLIRLSCQGDREFMAEMETLGKIKHRNLVPLLGYCKIGEERLLVYEFMQYGSLEE
VLHGPRTGEKRRILGWEERKKIAKGAAKGLCFLHHNCIPHIIHRDMKSSNVLLDQDMEARVSDFGM
ARLISALDTHLSVSTLAGTPGYVPPEYYQSFRCTAKGDVYSIGVVMLEILSGKRPTDKEEFGDTNL
VGWSKMKAREGKHMEVIDEDLLKEGSSESLNEKEGFEGGVIVKEMLRYLEIALRCVDDFPSKRPNM
LQVVASLRELRGSENNSHSHSNSL*

> AtBRL3

MKQQWQFLILCLLVLFLTVDSRGRRLLSDDVNDTALLTAFKQTSIKSDPTNFLGNWRYGSGRDPCT
WRGVSCSSDGRVIGLDLRNGGLTGTLNLNNLTALSNLRSLYLQGNNFSSGDSSSSSGCSLEVLDLS
SNSLTDSSIVDYVFSTCLNLVSVNFSHNKLAGKLKSSPSASNKRITTVDLSNNRFSDEIPETFIAD
FPNSLKHLDLSGNNVTGDFSRLSFGLCENLTVFSLSQNSISGDRFPVSLSNCKLLETLNLSRNSLI
GKIPGDDYWGNFQNLRQLSLAHNLYSGEIPPELSLLCRTLEVLDLSGNSLTGQLPQSFTSCGSLQS
LNLGNNKLSGDFLSTVVSKLSRITNLYLPFNNISGSVPISLTNCSNLRVLDLSSNEFTGEVPSGFC
SLQSSSVLEKLLIANNYLSGTVPVELGKCKSLKTIDLSFNALTGLIPKEIWTLPKLSDLVMWANNL
TGGIPESICVDGGNLETLILNNNLLTGSLPESISKCTNMLWISLSSNLLTGEIPVGIGKLEKLAIL
QLGNNSLTGNIPSELGNCKNLIWLDLNSNNLTGNLPGELASQAGLVMPGSVSGKQFAFVRNEGGTD
CRGAGGLVEFEGIRAERLEHFPMVHSCPKTRIYSGMTMYMFSSNGSMIYLDLSYNAVSGSIPLGYG
AMGYLQVLNLGHNLLTGTIPDSFGGLKAIGVLDLSHNDLQGFLPGSLGGLSFLSDLDVSNNNLTGP
IPFGGQLTTFPLTRYANNSGLCGVPLPPCSSGSRPTRSHAHPKKQSIATGMSAGIVFSFMCIVMLI
MALYRARKVQKKEKQREKYIESLPTSGSSSWKLSSVHEPLSINVATFEKPLRKLTFAHLLEATNGF
SADSMIGSGGFGDVYKAKLADGSVVAIKKLIQVTGQGDREFMAEMETIGKIKHRNLVPLLGYCKIG
EERLLVYEYMKYGSLETVLHEKTKKGGIFLDWSARKKIAIGAARGLAFLHHSCIPHIIHRDMKSSN
VLLDQDFVARVSDFGMARLVSALDTHLSVSTLAGTPGYVPPEYYQSFRCTAKGDVYSYGVILLELL
SGKKPIDPEEFGEDNNLVGWAKQLYREKRGAEILDPELVTDKSGDVELLHYLKIASQCLDDRPFKR
PTMIQVMTMFKELVQVDTENDSLDEFLLKETPLVEESRDKEP*